

A Thesis Submitted for the Degree of PhD at the University of Warwick

Permanent WRAP URL:

<http://wrap.warwick.ac.uk/142657>

Copyright and reuse:

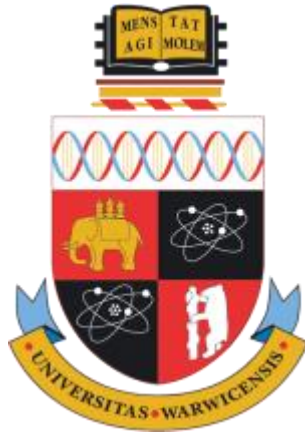
This thesis is made available online and is protected by original copyright.

Please scroll down to view the document itself.

Please refer to the repository record for this item for information to help you to cite it.

Our policy information is available from the repository home page.

For more information, please contact the WRAP Team at: wrap@warwick.ac.uk



Tumour metabolism of methylglyoxal as a target for treatment of glyoxalase1-linked multidrug resistance in cancer chemotherapy

By

Muhanad Musaad M Alhujaily

A thesis submitted in partial fulfilment of the requirements for the degree of

Doctor of Philosophy in Medical Sciences

Warwick Medical School, University of Warwick

April 2019

Contents

List of Tables.....	9
List of Figures	11
Acknowledgment	13
Dedication	14
Declaration	15
Abstract	16
Abbreviations	18
1 Introduction	22
1.1 The glyoxalase system.....	22
1.1.1 Definition and function of the glyoxalase system.....	22
1.1.2 Historical development of glyoxalase system.....	23
1.1.3 Glyoxalase 1.....	26
1.1.4 Glyoxalase 2.....	31
1.1.5 Methylglyoxal	34
1.1.6 S-D-Lactoylglutathione.....	38
1.1.7 D-Lactate.....	39
1.1.8 Non-glyoxalase detoxification of methylglyoxal.....	40
1.1.9 The critical role of glyoxalase 1 in enzymatic defence against glycation.....	41
1.2 Other aspects of glycation	42
1.2.1 Definition of glycation	42
1.2.2 Historical perspective of glycation.....	43
1.2.3 Early-stage and advanced-stage glycation	47
1.2.4 Advanced glycation endproducts	48
1.2.5 Biochemical formation and physiological effects of protein glycation.....	49

1.3	Protein oxidation	50
1.4	Protein nitration.....	50
1.5	Measurement of protein glycation, oxidation and nitration	51
1.5.1	Fluorescence.....	51
1.5.2	Immunoassay	53
1.5.3	Analysis of stable isotopic dilution liquid chromatography using tandem mass spectrometry (LC-MS/MS)	53
1.6	Proteomics	54
1.6.1	Label-free quantification.....	55
1.6.2	Sample preparation for label-free quantification	56
2	Background	65
2.1	Tumours and tumour growth.....	65
2.1.1	Definition of tumours and cancer.....	65
2.1.2	Social impact of cancer	67
2.1.3	Clinical treatment of cancer	69
2.1.4	Refractory tumour and multidrug resistance in chemotherapy	73
2.2	Role of glyoxalase system in cancer	75
2.2.1	Historical	75
2.2.2	Glyoxalase 1 and tumour growth	77
2.2.3	Glyoxalase 1 and multidrug resistance	77
2.2.4	GLO1 gene copy number in cancer	78
2.2.5	Anticancer activity of methylglyoxal.....	81
2.2.6	Cell permeable glyoxalase 1 inhibitors as anticancer agents	86
2.3	Aim and objectives of this project.....	88
2.3.1	Aim.....	88
2.3.2	Objectives.....	88

2.3.3	Study hypotheses.....	89
3	Materials and Methods.....	90
3.1	Materials.....	90
3.1.1	Cells and tissues.....	90
3.1.2	Cell culture reagents.....	90
3.1.3	Enzymes and other reagents.....	90
3.1.4	Antibodies.....	91
3.1.5	Other analytical reagents.....	91
3.1.6	Chromatographic materials.....	92
3.1.7	Instrumentation.....	93
3.1.8	Software.....	94
3.2	Bioinformatics methods.....	94
3.2.1	Cancer bioinformatics database CCLE.....	94
3.2.2	Pathway enrichment analysis tool.....	95
3.2.3	Kaplan-Meier survival analysis database.....	95
3.3	Cell Culture.....	96
3.3.1	Cell culture experiments.....	96
3.3.2	Assessment of cell viability.....	96
3.3.3	Effect of methylglyoxal on the growth and viability of HEK293 cells <i>in vitro</i> : growth curve.....	97
3.3.4	Effect of methylglyoxal on the growth and viability of HEK293 cells <i>in vitro</i> : concentration-response curve.....	97
3.4	Analytical methods.....	97
3.4.1	Bradford Assay for total protein measurements.....	97
3.4.2	BCA Assay.....	98
3.4.3	EZQ Assay.....	98

3.4.4	Enzymes activity	98
3.4.5	Western blotting for selected proteins.....	102
3.4.6	Membrane stripping	103
3.4.7	ELISA of Mitochondrial and cytosolic cytochrome c	103
3.5	Microscopy methodology	104
3.5.1	Measurement of free dsDNA using florescence microscopy.....	104
3.6	LC-MS/ MS methodology	104
3.6.1	Sample preparation, filtration and washing for glycation adduct residue content of cell protein.....	105
3.6.2	Enzymatic hydrolysis of soluble protein.....	105
3.6.3	Standards curve preparation	106
3.6.4	LC-MS/MS conditions (Xevo-TQS system).....	108
3.7	Proteomics analysis of subcellular fraction	110
3.7.1	Sample preparation.....	110
3.7.2	Protocol of tryptic digestion.....	112
3.7.3	Protocol of Lys–C/Trypsin protease digestions	112
3.7.4	Peptide separation, protein quantitation and identifications	112
3.7.5	Data analysis	114
3.7.6	Protein function and ontology	114
3.7.7	Statistical analysis	114
3.8	Other statistical analysis	118
4	Results	119
4.1	Bioinformatics analysis of glyoxalase 1 expression in tumour cell lines and clinical cancer survival	119
4.1.1	Correlation analysis of glyoxalase 1 mRNA in the cancer cell line encyclopaedia dataset CCLE.....	119
4.1.2	Study of breast cancer patients.....	122

4.2	Characterisation of the Glyoxalase system in HEK293 cell line <i>in vitro</i>	126
4.2.1	Growth and viability of HEK293 cell line <i>in vitro</i>	126
4.2.2	The activity of glyoxalase 1 and glyoxalase 2 in HEK293 cell line <i>in vitro</i>	127
4.2.3	The flux formation of D-lactate and net formation of L-lactate in HEK293 cell line <i>in vitro</i>	127
4.2.4	The effect of methylglyoxal on the growth of HEK293 cells <i>in vitro</i> : concentration-response curve.....	127
4.2.5	The effect of methylglyoxal on the growth of HEK293 cells <i>in vitro</i> : growth curve.....	128
4.2.6	Effect of exposure period in the effect of methylglyoxal on growth of HEK293 cells <i>in vitro</i>	129
4.2.7	Effect of methylglyoxal on the cytochrome c release from mitochondria to the cytosol of HEK293 cell line <i>in vitro</i>	130
4.2.8	Treatment period with methylglyoxal required to maximize the cellular protein content of methylglyoxal-derived glycation adduct MG-H1.	131
4.2.9	Investigating the potential significant proteins role from the previous proteomics study.	133
4.3	The effect of methylglyoxal on the extrachromosomal DNA secretion.	134
4.4	Analysis of fractional proteomes of HEK293 cells incubated with and without methylglyoxal	136
4.4.1	Cytoplasmic protein extract	136
4.4.2	Nuclear protein extract.....	136
4.4.3	Mitochondrial matrix and intermembrane space proteins.....	137
4.4.4	Mitochondrial membrane proteins	137

5	Discussion	162
5.1	Methylglyoxal, glyoxalase 1 and cancer – a historical and re-occurring association	162
5.2	Bioinformatics of glyoxalase 1 expression: correlation and survival analysis in human tumour cells lines and breast cancer patients, respectively	162
5.2.1	Bioinformatics of glyoxalase 1 expression: correlation analysis in human tumour cells lines	162
5.2.2	Bioinformatics of glyoxalase 1 expression and survival analysis in breast cancer patients	165
5.3	The glyoxalase system and methylglyoxal metabolism in HEK293 cell <i>in vitro</i>	167
5.4	Analysis of fractional proteomes of HEK293 cell line incubated with and without MG	169
5.4.1	Proteomic changes during methylglyoxal-induced commitment to apoptosis in HEK293 cells <i>in vitro</i>	169
5.4.2	Potential impact of the significance proteins modified by methylglyoxal in cancer chemotherapy MDR	171
5.5	The effect of methylglyoxal in free extrachromosomal DNA release in HEK293	171
5.6	Emergence of the spliceosome as a target of impairment in MG-induced commitment to apoptosis	172
6	Conclusion and future works	173
6.1	Conclusion.....	173
6.2	Future works.....	174
7	References	175
	Appendix I.....	200
	Gene expression correlating positively with glyoxalase 1 expression in tumour cell lines of the CCLE.....	200

Appendix II	211
Gene correlates negatively with Glo1mRNA	211

List of Tables

Table 1. Different fluorophores linked to oxidation glycation protein damage....	52
Table 2. Adducts marker from proteins oxidation, glycation and nitration measured by isotopic stable analysis LC-MS/MS.	54
Table 3. Anticancer drugs that target cell surface molecule and signalling intermediates..	72
Table 4. Mechanism of methylglyoxal induced cell death from.....	83
Table 5. Medium growth inhibitory concentration GC ₅₀ values of selected anticancer drugs in HEK-293 cells <i>in vitro</i>	89
Table 6. Protocol used for hydrolysis of sample protein treated with/without MG using CTC-PAL automated processor.....	106
Table 7. Calibration standard solutions preparation from mixtures of normal and stable isotopic standards for protein glycation, oxidation and nitration adduct residues of HEK293 protein extracts.	108
Table 8. Analyte content of calibration standard solutions for protein glycation, nitration and oxidation adduct residues of HEK293 protein extracts.	108
Table 9. Elution profile for stable isotopic dilution analysis liquid chromatography with tandem mass spectrometric detection analysis of protein glycation, nitration adducts and oxidation (Acquity TM -Xevo-TQS system).	109
Table 10. Chromatographic retention times and MRM detection conditions for detection of glycation, oxidation and nitration adducts by (LC-MS/MS) (Acquity TM -Xevo-TQS system).	109
Table 11. Pathways enrichment of gene expression correlating positively with glyoxalase 1 expression in tumour cell lines of the CCLE.	120
Table 12. Effect of expression of GLO1, HAGH, KDM4A, AGER, NFE2L2 and KEAP1 on survival of breast cancer patients. All patients.	124
Table 13. Effect of GLO1 expression on breast cancer patient survival: effect of genotype, intrinsic subtype, lymph node status and stage.	125
Table 14. The methylglyoxal glycation adduct MG-H1 content of cellular protein for HEK293 cells incubated with and 131 μ M MG.....	133
Table 15. Proteins in the cytoplasmic extract increased in abundance by treatment with methylglyoxal.	139

Table 16. Proteins in the cytoplasmic extract modified by methylglyoxal and increased in abundance by treatment with methylglyoxal.	142
Table 17. Proteins in the cytoplasmic extract modified by methylglyoxal and decreased in abundance by treatment with methylglyoxal.	143
Table 18. Proteins in the nuclear extract increased in abundance by treatment with methylglyoxal.....	145
Table 19. Proteins in the nuclear extract decreased in abundance by treatment with methylglyoxal.....	147
Table 20. Pathways enrichment analysis of proteins decreased in the cytoplasmic extract by treatment with methylglyoxal.....	150
Table 21. Pathways enrichment analysis of proteins decreased in the cell nucleus by treatment with methylglyoxal.	151
Table 22. Proteins of the mitochondrial matrix and intermembrane space increased by HEK293 cell treatment with methylglyoxal.	151
Table 23. Proteins of the mitochondrial matrix and intermembrane space decreased by HEK293 cell treatment with methylglyoxal.....	152
Table 24. Proteins of the mitochondrial membrane of HEK 293 cells increased by treatment with methylglyoxal.	158
Table 25. Pathways enrichment analysis of proteins of the mitochondrial membrane increased by treatment with methylglyoxal.	159
Table 26. Proteins of the mitochondrial membrane with methylglyoxal modification.	160

List of Figures

Figure 1. The glyoxalase system.	22
Figure 2. Structure of human glyoxalase 1. Solid ribbon representations of the crystal structure of human glyoxalase I (Cameron et al., 1997).	27
Figure 3. Timeline of the key discovery and development in glycation research between 1900 to 2000.	47
Figure 4. Early glycation and metabolic sources of AGEs.	48
Figure 5. Protein oxidation, glycation and nitration adducts residues in biological systems.	48
Figure 6. The hallmarks of cancer proposed by Hanahan and Weinberg	66
Figure 7. Survival rate changes from 1971-2011 for different types of cancer in the UK	68
Figure 8. Estimated number of cancer death and incidence in 2017 in the USA. .	68
Figure 9. Key discoveries of anticancer drugs (1943-2013).	71
Figure 10. Multidrug resistance types in cancer chemotherapy.	74
Figure 11. The historical timeline of the glyoxalase system: from the discovery of the glyoxalase system in the last century until the 2010.	76
Figure 12. Suggested mechanism of GLO1 gene amplification.	79
Figure 13. Mechanism of cytotoxicity of cell permeable Glo1 inhibitor through cellular accumulation of methylglyoxal in tumour cells.	85
Figure 14. Calibration curve for assay of D-lactate.	101
Figure 15. Calibration curve for assay of L-lactate.	101
Figure 16. Typical calibration curves for arginine and MG-H1 in stable isotopic dilution analysis LC-MS/MS.	107
Figure 17. Relative abundance of proteins identified in Control (left) and MG treated cells in HEK293 cells.	116
Figure 18. Missed cleavage number per peptides ions by trypsin.	116
Figure 19. The rate variation within condition in the experimental run in the mass spectrometry.	117
Figure 20. Correlation of selected genes and GLO1 CNV with Glo1 expression.	121
Figure 21. Kaplan Mier Plot of all patients with GLO1 expression.	123

Figure 22. Kaplan Mier Plot of patients treated with tamoxifen only with GLO1 expression.....	123
Figure 23. Growth curve of HEK293 cells <i>in vitro</i>	126
Figure 24. Methylglyoxal concentration-response curve for the effect on HEK293 cell growth <i>in vitro</i>	128
Figure 25. Effect of methylglyoxal on cell growth of HEK293 cells <i>in vitro</i> : effect of 131 μ M methylglyoxal.	129
Figure 26. Effect of period of exposure to methylglyoxal on growth of HEK293 cells <i>in vitro</i> . HEK293 cells were incubated with 131 μ M MG for 0, 6, 12 and 24 h.....	130
Figure 27. Cytochrome C content of the cytosol of HEK293 cells incubated with methylglyoxal <i>in vitro</i>	131
Figure 28. The methylglyoxal glycation adduct MG-H1 content of cellular protein for HEK293 cells incubated with and 131 μ M MG.....	132
Figure 29. The protein expression changes in Control and treated 131 μ M of MG in HEK293. A Glo1, B AKR1B1 and C DDX5.....	134
Figure 30. Assessment of extrachromosomal DNA in HEK293 cells incubated with and without 131 μ M MG for 6 h <i>in vitro</i>	135
Figure 31. An example of mass spectrometric detection of a peptide in the trypsin/lys-C digest: 40S Ribosomal protein S21 identified in nuclear fraction.	138



Acknowledgment

First of all, I would like to thank Allah the most beneficial and the most merciful, for all the strength, knowledge and health to complete this project.

I am tremendously grateful to the people named below, without their support, advice and help, this project would not have been completed

I would like to thank my primary supervisor, Professor Paul J Thornalley for all his advice, support, help and teaching during my time at the University of Warwick. I would like also to thank my supervisor, Dr Naila Rabbani, for all the help and advice in the proteomics work. Thanks also goes to my supervisor, Professor Dimitris Grammatopoulos, for all his advice and help. I would like to thank Dr Richard Thompson and Dr Omar Albahga for their help in the CCLE correlation analysis. Also thanks goes to Dr Andrew Bottrill For his support in the proteomics and mass spectrometry works, Thanks also goes to Dr. Cleidi Zampronio for her technical advice and help in the Mass spectrometry experiment.

I am also thankful to Dr Mingzhan Xue for all his advice in the molecular biology and cell culture work. Also I would like to thank all my colleagues in Protein Damage and Systems Biology Research Group members for shining every day with the help, smiles and support.

I would like to thank my Father Dr. Musaad Alhujaily and My lovely mother Fatimah Alsharie for all their support and prayers advice. I would like to thank the love of my life Shrouq Alharbi for all her patient during my absence from home, for taking the father responsibilities during my absence and for taking care of our children. Thank you Shrouq. I would like to thank my two little lovely boys, Musaad and Sultan, for their smile every morning before I go to work. This always give me the hidden strength.

I would like to thank the University of Bisha for its funding of this project. And I am grateful to the Saudi Embassy in London for their support in their administrative work.

Dedication

To my beloved parents Dr Musaad Alhujaily and my mother Fatimah Alsharie, my beloved wife Shrouq Alharbi and my lovely sons, Musaad and Sultan, who were, are and will always be the cause of my strength.

Declaration

I am aware of the University of Warwick regulations governing plagiarism and I declare that all the work presented in this thesis, unless otherwise specifically stated, was original research performed by myself under the supervision of Prof Paul J. Thornalley and Dr Naila Rabbani. None of this work has been previously submitted to any other degree. The work presented (including data generated and data analysis) was carried out by the author.

Muhanad Musaad M Alhujaily

Abstract

The glyoxalase system is the major pathway for metabolism of the reactive dicarbonyl metabolites, methylglyoxal (MG) in human cells. It is comprised of two enzymes, glyoxalase 1 (Glo1) and glyoxalase 2 (Glo2). These enzymes catalyse the metabolism of MG into D-lactate via intermediate called S-D-lactoylglutathione. MG is produced in glycolysis as a by-product by the trace-level degradation of triosephosphate glycolytic intermediates. The main physiological function of Glo1 is cytoprotective, suppressing the steady-state concentration of MG to low tolerable levels. Cytotoxicity of MG is linked to its reaction with cell protein and DNA, leading to activation of apoptosis. Overexpression of Glo1 in tumour cells is a mediator of multidrug resistance in cancer chemotherapy and cell permeable inhibitors of Glo1 have anticancer activity, suggesting that cytotoxicity of MG may have a key role in cancer chemotherapy. The host research suggested that increased Glo1 expression is permissive of high glycolytic rate and growth of many tumours. My project emerged from this to study evidence of Glo1 expression as a negative survival factor in cancer therapy and the proteomic mechanism of cytotoxicity of MG to human tumour cells.

I accessed databases of gene expression in the public domain: KM Plotter – gene expression with links to breast cancer patient survival; and Cancer Cell Line Encyclopaedia (CCLE) – gene expression of human tumour cell lines. Assessment between the association of Glo1 expression in cancer patients to effectiveness of treatment (progression free survival) and in human tumour cell lines to other gene expression were performed. Also investigated proteomic changes during MG-induced cytotoxicity in human HEK293 *in vitro*.

Key findings were: Glo1 is a negative survival factor in breast cancer – hazard ratio 1.37 (1.22 – 1.53), logrank $P = 2.8 \times 10^{-8}$ ($n = 3951$); applicable for all treatments, genotypes, intrinsic subtypes and stages of breast cancers. In human tumour cell lines, Glo1 expression correlated positively with GLO1 copy number and with genes enriched in spliceosome, RNA transport, and cell cycle and DNA replication pathways, and negatively with apoptosis adaptor TRADD. In proteomics analysis of MG-induced cytotoxicity, the mitochondrial apoptosis

pathway was activated and proteins of the ribosome, spliceosome, RNA transport, proteasome, respiratory electron transport, ATP formation by chemiosmotic coupling and gluconeogenesis were decreased.

It is conclude that Glo1 impacts negatively on breast cancer survival and is a potential target for improved cancer therapy with Glo1 inhibitors where associated MG-induced cytotoxicity involves impairment of multiple processes, including spliceosome function.

Abbreviations

3-DG	3-Deoxyglucosone
3DG-H	Hydroimidazolones derived from 3-DG
4-ANI	4-Amino-1,8-naphthalimide
ACTB	β -Actin gene
AGEs	Advanced glycation endproducts
AKR	Aldoketo reductase
ALDH	Aldehyde dehydrogenase
ARE	Antioxidant response element
ATP	Adenosine triphosphate
BCL2	B-cell lymphoma 2
BCL-XL	B-cell lymphoma-extra large
BCA	Bicinchoninic acid
BSA	Bovine serum albumin
CaMKII	Calmodulin-dependent protein kinase II
cAMP	Cyclic adenosine monophosphate
CDK	Cyclin dependent kinases
cDNA	Complementary deoxyribonucleic acid
CEL	N ϵ -(1-carboxyethyl)lysine
CHX	Cycloheximide
CMA	N ω -Carboxymethyl-arginine
CML	N ϵ -Carboxymethyl-lysine
CNV	Copy number variation
COX2	cyclo-oxygenase-2
CTLA4	Cytotoxic t-lymphocyte antigen 4
DAVID Discovery	Database for Annotation visualization and Integrated
DDX5	DEAD-Box helicase 5

DHAP	dihydroxyacetonephosphate
DMBA	7,12-Dimethylbenz(a)anthracene
DMEM	Dulbecco's Modified Eagle's Medium
DMSO	Dimethyl sulphoxide
EC ₅₀	Median effective concentration
ECL	Enhanced chemiluminescence
F3K	Fructosamine-3-kinase
FBS	Fetal bovine serum
FFA	Free fatty acid
FL	N _ε -Fructosyl-lysine
G6P	Glucose-6-phosphate
GA3P	Glyceraldehyde-3-phosphate
GC ₅₀	Median growth inhibitory concentration
GCS	γ-Glutamylcysteine synthetase
G-H1	Hydroimidazolone derived from glyoxal
Glo1	Glyoxalase 1
Glo2	Glyoxalase 2
GOLD	Glyoxal-lysine dimer
GR	Glutathione reductase
GSH	Reduced glutathione
GS-MS	Gas chromatography with mass spectrometric detection
GSSG	Oxidised glutathione
GST	Glutathione-S-transferase
HAGH	Hydroxyacylglutathione hydrolase (Glo1 gene)
HbA _{1C}	Glycosylated haemoglobin
HIF1 α	Hypoxia-inducible factor 1 α
HK	Hexokinase
HLA	Human leukocyte antigen

HPLC	High performance liquid chromatography
HSA	Human serum albumin
IS	Internal standard
iTRAQ	Isobaric tags for relative and absolute quantification
Keap1	Kelch-like ECH-associated protein 1
KEGG	Kyoto Encyclopedia of Genes and Genomes database
LC-MS/MS	Liquid chromatography with tandem mass spectrometric detection
LDL	Low density lipoproteins
MDR	Multidrug resistance
mDia-1	Mammalian diaphanous-1
MetSO	Methionine sulfoxide
MG	Methylglyoxal
MG-H1	Hydroimidazolones derived from MG
MOLD	MG derived lysine dimer
MRE	Metal responsive element
MRM	Multiple reaction monitoring
NER	Nucleotide excision repair
NFE2L2	Factor nuclear factor erythroid 2-related factor 2 (Nrf2 gene)
NF-kB	Nuclear factor-kB
NFK	N-Fformylkynurenine
NO	Nitric oxide
Nrf2	Nuclear erythroid factor E2 related factor-2
NSAF	Normalized spectral abundance factor
NSCLC	Non-small cell lung cancer
PBS	Phosphate buffer saline
PCA	Perchloric acid
PGC-1 α	PPAR gamma coactivator-1alpha

PTGS2	prostaglandin synthetase-2
PVDF	Polyvinyl difluoride
RAGE	Receptor of advanced glycation endproducts
RB	retinoblastoma-associated gene
ROS	Reactive oxygen species
RIPA	Radioimmunoprecipitation
RP-LC	Reversed-phase liquid chromatograph
SCLC	Small cell lung cancer
SDS-PAGE	Sodium dodecyl sulfate polyacrylamide gel electrophoresis
SOD	Superoxide dismutase
BBGCp2	S-p-bromobenzylglutathione cyclopentyl diester
TBS-T	Tris-buffered saline with Tween-20
TCA	Trichloroacetic acid
TFA	Trifluoroacetic acid
THF	Tetrahydrofuran
TNF- α	Tumour necrosis factor α
TP53	tumour suppressor P53
tRES-HESP	<i>trans</i> -resveratrol and hesperetin
UPLC	Ultra-high performance liquid chromatography
UV	Ultraviolet
WHO	World health organisation

1 Introduction

1.1 The glyoxalase system

The glyoxalase system is known as the major enzymatic defence against glycation by methylglyoxal (MG) in the physiological systems – Figure 1.

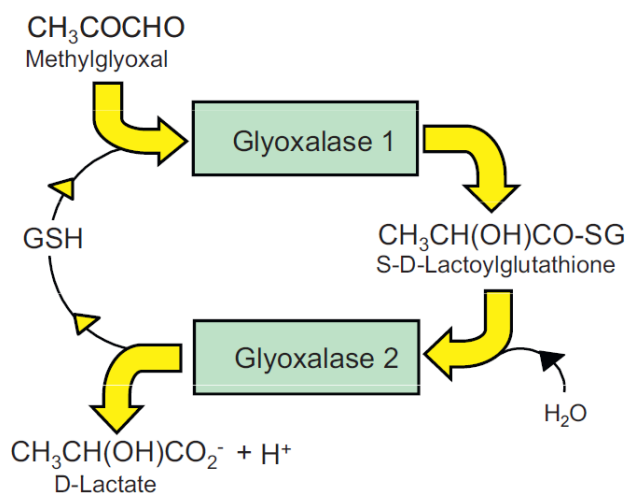


Figure 1. The glyoxalase system.

Adapted from (Xue et al., 2011)

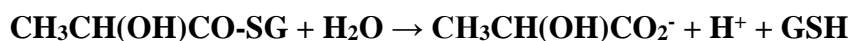
1.1.1 Definition and function of the glyoxalase system

The glyoxalase system consists of two enzymes, glyoxalase 1 (Glo1) and glyoxalase 2 (Glo2). The main function of this system is to catalyse the metabolism of MG to D-lactate through the intermediate called S-D-lactoylglutathione. This defence system is found in the cytosol of all mammalian cells (Xue et al., 2011). It is also found in bacteria, plants, animal, fungi and protocista. The process of the detoxification by the glyoxalase system can occur into two consecutive reactions. There is an initial non-enzymatic reaction of MG (CH_3COCHO) with GSH to form the hemithioacetal adduct, $\text{CH}_3\text{COCH}(\text{OH})\text{-SG}$. Glo1 catalyses isomerisation of the hemithioacetal to S-D-lactoylglutathione, $\text{CH}_3\text{CH}(\text{OH})\text{CO-SG}$.



The K_M for the methylglyoxal-glutathione hemithioacetal and Glo1 in human is approximately 71-130 μM and the k_{cat} is $7\text{-}11 \times 10^4 \text{ min}^{-1}$. The second reaction where S-D-lactoylglutathione is converted to D-lactate and GSH is

catalysed by Glo2. The GSH consumed in the Glo1 is reformed by the action of Glo2 (Xue et al., 2011) – Figure 1.



The main physiological substrate for Glo1 is MG. In events where Glo1 is suppressed *in situ* – as occurs by decrease of cellular GSH, the concentration of MG is increased. This also occurs in the presence of the cell permeable Glo1 inhibitors (Thornalley, 1998, Thornalley, 1993a, Abordo et al., 1999). There are other substrates for Glo1 such as glyoxal, hydroxypyruvaldehyde $\text{HOCH}_2\text{COCHO}$ and 4,5-doxovalerate $\text{H-COCOCH}_2\text{CH}_2\text{CO}_2^-$ (Thornalley et al., 1996, Thornalley, 1993a, Thornalley, 1998, Abordo et al., 1999). Glo1 activity metabolises these reactive α -oxoaldehydes and thereby inhibits α -oxoaldehyde-mediated glycation reaction (Shinohara et al., 1998). Thus, Glo1 is considered as one of the main anti-glycation defence enzymes (Thornalley, 2003b, Thornalley, 2003a).

1.1.2 Historical development of glyoxalase system

In the last century, scientists discovered the activity of the glyoxalase system. It was initially known that the glyoxalase system is responsible for the conversion of MG to lactate (Dakin and Dudley, 1913, Neuberg, 1913a). L-Lactate is the main metabolite involved in the metabolism of glucose through glycolysis but the product of the metabolism of MG by the glyoxalase pathway is D-lactate (Thornalley, 1990). The presence of the glyoxalase in all organisms studied suggested that this enzymatic system has a vital role in cell function (Gowland-Hopkins and Morgan, 1945). In 1951, Racker discovered that the metabolism of MG by the glyoxalase system forms D-lactate and occurred via S-D-Lactoylglutathione in two successive steps (Racker, 1951). The first discovery to show that MG and related aldehydes react with arginine residues was in 1977. However, the physiological importance of this reaction was not fully understood (Takahashi, 1977a).

In the last century, there was a several studies exploring the links between cancer and the glyoxalase system. Szent-Gyorgyi first showed that the conflict of MG and Glo1 in controlled cell growth and how it could be exploited for cancer treatment (Szent-Gyorgyi et al., 1963). It was hypothesised that MG is a growth

retarding substance and in contrast Glo1 acts as the opposite to this growth inhibition. Many other growth factors were discovered and this led to the weakness of this hypothesis. Increased levels of MG concentration were toxic to tumour cells. Vince and Wadd proposed that Glo1 inhibitors may be effective anticancer agents. Glo1 inhibitors act by increasing the accumulation of the endogenous MG (Vince and Wadd, 1969). The historical development and the link between the glyoxalase system and cancer treatment and development will be discussed further in this chapter below.

In 1970s to 1990s, scientists were able to purify glyoxalase enzymes and identified its molecular, kinetics mechanistic and structural characteristics. Mannervik and colleagues had an important contribution for mammalian and microbial Glo1, with a notable contribution of other scientists: Norton, Kimura, Principato Uotila, Thornalley and Vander Jagt (Uotila, 1973, Marmstal and Mannervik, 1979, Schimandle and Vander Jagt, 1979, Landro et al., 1992, Allen and Thornalley, 1993, Cameron et al., 1997, Cameron et al., 1999, Cordell et al., 2004). Kompf and co-worker first identified the genetic polymorphism of the human GLO1 gene and tracked inheritance patterns by detecting the related allozymes in gel electrophoresis, usually measured in red blood cells (Kompf et al., 1975).

The physiological source of the MG metabolised in the glyoxalase pathway remained unclear. Philips and Thornalley first studied the non-enzymatic degradation of triosephosphates to form MG. This study observed a minor leakage *ca.* 0.05% - 0.1% glucotriose flux from the Embden-Meyerhof pathway leading to the formation of MG in physiological systems (Phillips and Thornalley, 1993a). This low percentage flux of glucotriose represents *ca.* 3 mmol of MG formation in healthy human subjects per day (Rabbani et al., 2016b). MG has a high reactivity rate with DNA and proteins. Therefore the glyoxalase system plays a vital role to keep MG concentration at low tolerable level (Thornalley, 2003b).

In 2003, Thornalley and his colleagues found that MG-derived AGEs were one of the major endogenous types of protein damage *in vivo*. This is based on the relatively high steady-state levels of MG-derived glycation adducts and the high urinary excretion flux of the hydroimidazolone adducts (Thornalley, 2003c). In

2006, Redon *et al.* found that GLO1 gene was located in one of the copy number variation (CNV) regions and constructed a CNV map of the human genome (Redon *et al.*, 2006). In 2008 Zender *et al.* found that Glo1 is a tumour suppressor protein by investigating, in a genome-wide scan, genes with tumour suppressor activity (Zender *et al.*, 2008).

Thornalley and his colleagues found that MG-derived DNA imidazopurinone adducts are one of the major quantitative adducts of DNA damage linked to DNA instability *in vivo* (Santarius *et al.*, 2010). Cahan *et al.* showed that the non-transcribed region of the GLO1 gene is an important site of the CNV in the mouse genome giving an increase to *ca.* 4-fold changes the expression of Glo1 (Cahan *et al.*, 2009).

In 2012, Thornalley and co-worker found the presence of regulatory antioxidant response element (ARE) in exon-1 of the mammalian GLO1 gene. Transcription factor Nrf2 increases the basal and inducible expression of Glo1. Thus, they concluded that there is stress-responsive increase of Glo1 expression when MG concentration increased (Xue *et al.*, 2012). In 2016 Xue *et al.* optimized a small dietary molecule bioactive formation for activation of Nrf2-mediated ARE-linked expression of Glo1 (Xue *et al.*, 2016). This optimum induction of Glo1 expression was achieved by a combination of *trans*-resveratrol and hesperetin (tRES-HESP) combined therapy. This combination therapy was well-tolerated and in overweight and obese human subjects it increased Glo1 expression and activity in peripheral white blood cells (PBMC), decreased plasma concentration of MG, improved dysglycaemia and corrected insulin resistance. tRES-HESP also decreased in vascular inflammation - including decrease of cyclo-oxygenase-2 (COX2) or prostaglandin synthetase-2 (PTGS2). This has given the chance to develop a Glo1 inducer therapy for metabolic and vascular complications of obesity and diabetes (Xue *et al.*, 2016) – and potentially also chemoprevention of cancer through the tumour suppressor activity of Glo1 (Rabbani *et al.*, 2018).

1.1.3 Glyoxalase 1

1.1.3.1 Molecular properties

Glo1 protein of human subjects is a dimer of identical subunits in homozygotes or very similar subunits in heterozygotes held together by non-covalent bonding interactions. The molecular mass of Glo1 in human is 42 kDa by sequence, subunit mass of 23 kDa when measured by denaturing polyacrylamide gel electrophoresis and 46 kDa when determined by gel filtration. The isoelectric point pI of Glo1 is 4.8 - 5.1. Glo1 protein consists of polypeptide chains of 184 amino acid chains with one prosthetic Zn^{2+} ion per subunit (Thornalley, 2003b, Birkenmeier et al., 2010). The structure around the prosthetic Zn^{2+} ion of human Glo1 consists of two equivalent subunits which come from each domain Glu-99A, Gln-33A, His126B, Glu172B and two water molecules in octahedral configuration. In each monomer, there are two domains originating from a gene duplication and swapping of 3D domain in the N-and C-terminal domains. One domain has 124-183 residues while the other domain consists of 31-104 residues; 20 amino acid residues and long N-region link these domains together. Each of the domain there are $\beta\alpha\beta\beta$ -motif and mixed β -sheet. In the event of dimerization of the subunit, a β -parallel structure is formed which contain an active site. The individual monomers lack the enzymatic activity (Cameron et al., 1997).

The activity of Glo1 is present in all human tissues. There is *ca.* 0.2 μg Glo1 per gram protein in human tissues or *ca.* 1/5000th of total protein. There is *ca.* 2-fold increase of abundance of Glo1 protein in foetal compared to adult tissues (Larsen et al., 1985). In human fibroblasts, Glo1 was in the top 13% of proteins by abundance. Cytoprotective proteins such as Glo1 are typically found to be of high abundance (Xue et al., 2014).

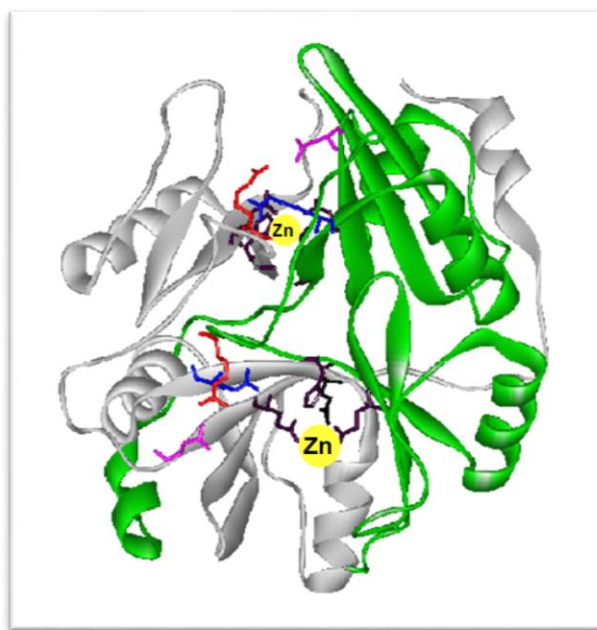


Figure 2. Structure of human glyoxalase 1. Solid ribbon representations of the crystal structure of human glyoxalase I (Cameron et al., 1997).

1.1.3.2 Kinetic characteristics

The main enzymatic role of Glo1 is to catalyse the isomerisation of the hemithioacetal formed from the non-enzymatic reaction of GSH and MG to S-D-lactoylglutathione (Thornalley, 2003b). The steady-state concentration of MG and related glycation reactions are thereby decreased in cells and tissue *in vivo*. Glo1 has a wide specificity for α -oxoaldehydes: for instance, MG (CH_3COCHO), glyoxal (CHO)₂, 4,5-dioxvaleric acid $\text{HO}_2\text{C}(\text{CH}_2)_2\text{COCHO}$ and other acyclic glyoxal derivatives. As the hydrophobicity of the side chain of the glyoxal derivative substrate increases the K_M and k_{cat} values decrease.

1.1.3.3 Regulation of expression

The GLO1 gene in human subjects has regulatory elements: insulin response element, metal response element, E2F4 and AP-2 alpha and an antioxidant response element (ARE) (Rabbani et al., 2014). Glo1 expression is increased by activation of transcription factor Nrf2 and its binding to the functional ARE. Transcriptional control of Glo1 by Nrf2 gives a stress responsive defence ability against glycation by dicarbonyls. Glo1 expression may be

decreased due to the activation of the receptor for advanced glycation end products (RAGE), although the mechanism of this response is unknown (Reiniger et al., 2010, Zeng et al., 2012) – although RAGE-activated inflammatory mechanisms countering Nrf2 regulation of Glo1 expression is a likely mechanism. Another factor which may cause Glo1 expression to be decreased comes from the activation of hypoxia inducible factor1 alpha (Zhang et al., 2012).

Once Glo1 polypeptide subunits are translated, the N-terminal Met is removed and acetylation reaction is takes place leading to the blockage of the remaining N-terminal Ala. Between the 19-20 cysteine residues there is a vicinal disulphate bridge and a mixed disulfide glutathione with cysteine-139. Cysteine-139 may also form an intra-molecular disulfide with cysteine-61. The activity of Glo1 is strongly inhibited by glutathionylation on C139 but not affected by the oxidation state of C19/C20 and the N-acetylation (Birkenmeier et al., 2010). The post-translational modification of Glo1 can lead to multiple forms of differing pI. Glo1 may also be S-nitrosylated by reaction with nitric oxide on cysteine-139. The presence of C19 and C20 are vital in the reaction of S-nitrosylation which take place on the acidic α form of Glo1 (de Hemptinne et al., 2007). The NO-responsive form of Glo1 is the basic, reduced form of Glo1 without intramolecular disulfide bonding. Glo1 is a substrate for calcium, calmodulin-dependent protein kinase II and is phosphorylated at Thr-107 preferentially but not exclusively on the basic, reduced and NO-responsive form (de Hemptinne et al., 2007, de Hemptinne et al., 2009).

A genome wide study conducted by Selbach and co-workers quantified the Glo1 expression in NIH3T3 mouse fibroblast (Schwanhausser et al., 2011). The number of copies per cell of mRNA and protein were 22 (transcriptome median 17) and 584,000 (proteome median), respectively. The half-lives of mRNA and protein of Glo1 were 7.8 h (transcriptome median 9 h) and 179 h (proteome median 46 h), respectively. The rate of transcription (molecules proteins per cell per h) was 750 (genome wide translation median *ca* 117). This suggested that Glo1 has protein abundance *ca.* 10-fold and half-life 4-fold higher than median values. This relatively high level of protein suggested that Glo1 is a highly efficient enzyme which reflect a high *in situ* activity requirement. In terms of

proteins abundance, Glo1 is detected in the top 13% of protein. Glo1 is 677 of 5028 proteins detected by abundance. Glo1 has a similar abundance to that of glycolytic enzymes such as transketolase.

There are few studies exploring the link between the levels of transcripts and the protein levels they encode in mammals. For example, genetic approach by using the natural variation to agitate both proteins and transcript level in inbred strain of mice. The study showed that mRNA of Glo1 is strongly correlated with Glo1 protein ($r=0.87$), among the quantification of 7,185 most heritable transcripts and proteins (Ghazalpour et al., 2011). In the post-transcriptional mechanisms, the conversion of mRNA Glo1 to Glo1 proteins is relatively constant, the half live of Glo1 may vary in good health state. Glo1 appears to have slight increase in proteolysis on activation of autophagy (Kristensen et al., 2008).

1.1.3.4 Genetics and polymorphism

Glo1 subunits are encoded by the gene of GLO1. GLO1 is on chromosome 6, nearby the locus of Human leukocyte Antigen-D Related (HLA-DR). GLO1 genes contains 27,250bp with six exons. The genetic locus is 6.21.2: 28751,680 - 38778,9300 (Tripodis et al., 1998, Thornalley, 1991). In the GLO1 gene there are two alleles; GLO1¹ and GLO1². The two alleles are in heterozygous inherited autosomally in a co-dominant system (Thornalley, 1991). The emergence of GLO1¹ allele is due to mutation whereas GLO1² allele is considered to be the ancestral allele. The differences between the two alleles is due to the mutation point in cDNA at position 332 (Thornalley, 2003b).

GLO1 genotypes are: GLO1 (1-1), GLO1 (1-2) and GLO1 (2-2). Mutation occurs in C419A leads to this common polymorphism which takes place in the coding region resulting to an amino acids residues polymorphism Ala111Glu (A111E) (Degaffe et al., 2007). The related allozymes may be resolved by non-denaturing gel electrophoreses and ion exchange chromatography due to the differences in molecular charge and shape densities (Kim et al., 1995). Studies have shown that in human populations, the GLO1¹ allele has the highest frequency in native tribes in Alaska with allele frequency 0.67 - 0.85. This frequency decreases geographically in south to east to Europe and South America

towards Africa, Middle East and India. The lowest allele frequency of GLO1¹ is found to be in Far East and Oceania 0 - 0.16 (Thornalley, 1991).

1.1.3.5 Mechanism of action

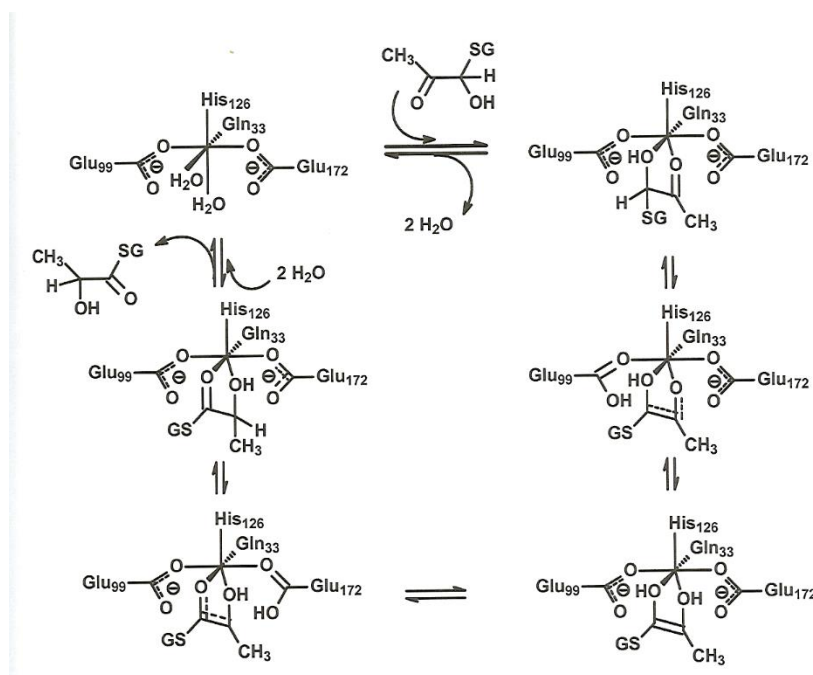


Figure 3. The catalytic mechanism of the glyoxalase I.

The catalytic mechanism of Glo1 consists of shielded proton transfer from C-1 to C-2 to the hemithioacetal to form an ene-diol intermediate and rapid ketonization to the thioester product (Thornalley, 2003b). Two stereoisomers of the hemithioacetal, R- and S-substrate diastereoisomers, are formed in the pre-equilibrium of MG reaction with GSH spontaneously. Both are accepted by Glo1. Once they are bound to the active site, an interaction between diastereoisomers with different catalytic bases: the S-diastereoisomer interacts with the conjugate base of Glu-172 and the R-diastereoisomer interacts with the conjugate base of Glu-99. It is likely that re-protonation occurs via the conjugate acid form of Glu-172 to produce the R-2-hydroxyacylglutathione product (Thornalley, 2003b).

1.1.4 Glyoxalase 2

1.1.4.1 Molecular properties and kinetic characteristics

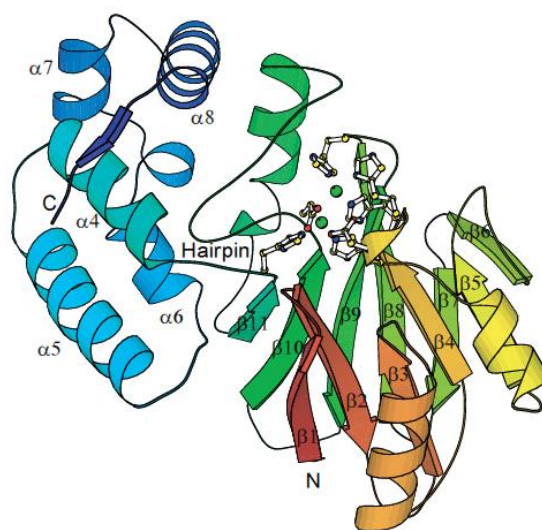


Figure 4. The structure of the human glyoxalase2. C terminus (blue)-N-terminus (red). Metal ions and coordination showed by balls and sticks. (Cameron et al., 1999).

In human subjects, Glo2 protein is a monomeric enzyme consisting of two main isoforms: mitochondrial Glo2 with molecular mass 33,806 Da and pI 8.3; and cytosolic Glo2 29,200 Da (Xue et al., 2011). In cytosolic Glo2, there are two domains: N-terminal domain comprises of 1-173 amino acids and C-terminal consist of 174-260 residues with secondary structure of five alpha-helices (Cordell et al., 2004). Glo2 in human subjects has an Fe(II)Zn(II) centre where the Fe(II) has minimal effect on the catalytic activity. The structure of Glo2 comprises metallo- β -lactamase-like and α -helical domain. The Fe(II)Zn(II) centre of the active site lies with a substrate-binding site in the 2-domain interface. A hydroxide ion coordinated to the Zn (II) ion is the base catalyst for the enzymatic reaction (Cameron et al., 1999).

The hydrolysis of S-D-lactoylglutathione to GSH and D-lactate is catalysed by Glo2. The K_m value of Glo2 is 146 μ M and k_{cat} value is 726 s^{-1} (Xue et al., 2011). Glo2 is known to be an efficient enzyme, as indicated by the k_{cat} / K_m value is near the limit of diffusion by using S-D-lactoylglutathione as substrate

(Cameron et al., 1999). Glo2 isolated from human liver had a broad optimum activity range between pH 6.8 - 7.5.

1.1.4.2 Regulation of expression

In human subjects, Glo2 is up-regulated at the transcriptional level by p63 and p73 transcription factors of the family of p53 which are involved in development. Glo2 expression is decreased in p53 knockout mice. In the intron1 of Glo2 gene HAGH there is a p53 response element which is activated when bound by p63 and p73. It was found that Glo2 is increased only in cytosol. Cells with Glo2 deficiency were hypersensitive to MG-induced apoptosis and DNA damage-induced apoptosis (Rabbani et al., 2014).

The function of Glo2 in the mitochondria is unclear. This is related to the lack of Glo1 targeting in mitochondria. However, Glo2 might be involved in GSH delivery into mitochondria with the aid of S-D-lactoylglutathione. This notion appears to be unlikely and this is due to the fact that GSH and S-D-lactoylglutathione had similar kinetics uptake of the mitochondrial and the concentration of the cytosolic S-D-lactoylglutathione is *ca.* <1% of GSH. Furthermore, other GSH derivatives can be hydrolysed by Glo2 such as S-acetyl-GSH and S-succinyl-GSH. Moreover, recent studies proposed that there is a significance non-enzymatic acetyl and succinyl transfer from acetyl-CoA and succinyl-CoA in mitochondria and this likely to be acceptor as mitochondrial GSH. Thus, Glo2 may maintain GSH by the repair of endogenous acylation where a high level of acetyl-CoA and succinyl-CoA in mitochondrial necessitate targeting of Glo2 to this part. Reviewed in- (Rabbani et al., 2014b).

1.1.4.3 Genetics and polymorphism

The human gene of Glo2 is HAGH (hydroxyacylglutathione hydrolase) (Thornalley, 1990). It is located on chromosome 16p13.3 (Xue et al., 2011). Two genotypes are known for HAGH: HAGH1 and HAGH2 (Thornalley, 1990, Allen et al., 1993a). The single gene that gives rise to two distinct mRNA species transcribed from 9 and 10 exons, respectively. The 9-exon-derived transcript encodes for both mitochondrial matrix targeted and cytosolic Glo2 whereas the 10 exon transcript encodes for only cytosolic Glo2 (Xue et al., 2011).

1.1.4.4 Mechanism of action

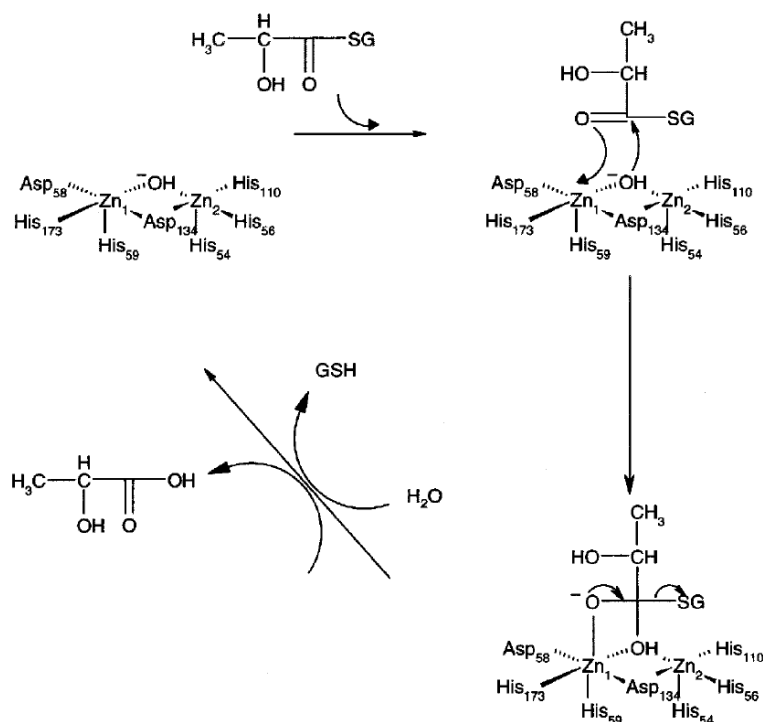


Figure 5. Catalytic mechanism of human glyoxalase 2.

Glo2 has a wide specificity for glutathione thiol ester, S-2-hydroxylacetylglutathione derivatives (Xue et al., 2011). The glutathione moiety is closely bound to the protein via cysteine and glycine residues. The γ -glutamyl is not interacting with the Glo2 protein (Xue et al., 2011). However, the same ligands are involved in hydrogen-bonding and interaction with the protein as in Glo1. The three basic residues close to the carboxyl group of glycine are: Lys-143, Lys-252 and Arg-249. Lys-252 and Arg-249 participate in the formation of α -helix of the second domain between the ranges of the hydrogen bonding interaction with protein. Asp-253 carboxylate and Cys-141 carbonyl oxygen has a major role in stabilizing and holding Arg-253 in its position (Cameron et al., 1999).

1.1.5 Methylglyoxal

1.1.5.1 Molecular characteristics, assay and physiological concentration

MG is a reactive metabolite formed by the trace-level degradation of triosephosphate glycolytic intermediates, glyceraldehyde-3-phosphate (GA3P) and dihydroxyacetonephosphate (DHAP), and is a by-product of glycolysis (Rabbani and Thornalley, 2012c). In the past, reliable estimation of MG concentration was challenging (Rabbani and Thornalley, 2014c). MG content in tissues and plasma have sometimes been overestimated by >1000-fold (Rabbani and Thornalley, 2014c). For example, published estimates of MG concentration in human plasma are in the range 123 nM to 407 μ M by different analytical methods estimates (Beisswenger et al., 1999, Scheijen and Schalkwijk, 2014). Another example is MG concentration of mouse brain in the range 1.5 μ M (Kurz et al., 2011) to 174 μ M (Hambach et al., 2010). Assays with reliable, interference-free methodologies suggest the lower estimates are the closest to the true values.

MG formation during pre-analytic processing of sample has been one of the causes of MG overestimation problem (Thornalley et al., 1999, Baba et al., 2009, McLellan et al., 1992a). During sample preparation, MG can be formed by degradation of glycated protein, monosaccharides and other samples component and derivatizing agent. This can be avoided during sample preparation. MG formation during pre-analytic processing of sample is enhanced by heating, high pH and peroxidase activity.

MG is present in aqueous solution under physiological conditions in three forms: the unhydrated form CH_3COCHO , the monohydrate $\text{CH}_3\text{COCH}(\text{OH})_2$ and the dehydrate form $\text{CH}_3\text{C}(\text{OH})_2\text{CH}(\text{OH})_2$ which under physiological conditions represent *ca.* 1%, 70% and 29% of total MG, respectively (McLellan and Thornalley, 1992b, Nemet et al., 2004). MG also has the ability to bind reversibly to peptides and proteins, mainly to cysteine residues of GSH and proteins. MG assays measure the total of free MG, MG hydrates and MG reversibly bound to proteins. MG is detached from proteins and dehydration of all hydrated forms occurs during the derivatization step in the assay procedures (Rabbani and Thornalley, 2014c).

1.1.5.2 Physiological formation of methylglyoxal

MG is produced mainly by trace-level of the degradation of GA3P and DHAP (Phillips and Thornalley, 1993b). Other minor sources of formation of MG are: formation from acetone in the metabolism of ketones bodies and aminoacetone in the catabolism of threonine (Rabbani et al., 2016a, Thornalley, 2003b). Past studies have shown that MG synthase can form MG in bacteria enzymatically but there was no evidence for MG formation enzymatically from triosephosphates in mammalian cells (Phillips and Thornalley, 1993b).

MG detoxification level by the pathway of the glyoxalase system depends mainly on the formation of GSH hemithioacetal. As discussed previously, MG can be in present in three forms: unhydrated α -oxoaldehyde, monohydrated and unhydrated forms at pH 7. The unhydrated MG has the ability to react reversibly with GSH to produce the hemithioacetal (Rabbani et al., 2016a, Thornalley, 2003b). The major abundant solution species of MG is MG-GSH hemithioacetal in cells and *in situ*. Therefore, Glo1 achieve a high catalytic activity (Rabbani et al., 2016b). Moreover, cellular protein thiols react with MG and the concentration is typically ca. 4-fold higher than concentration of GSH in cells. It is thought that protein thiols are depot storage sites of MG during excessive MG formation periods. Another factor affecting the formation of MG is the glyceraldehyde-3-phosphate dehydrogenase (GADPH). GADPH can affect the rate of MG formation by influencing the concentrations of triosephosphates in cells (Rabbani et al., 2016a).

1.1.5.3 Reactions of methylglyoxal with proteins, DNA and basic phospholipids

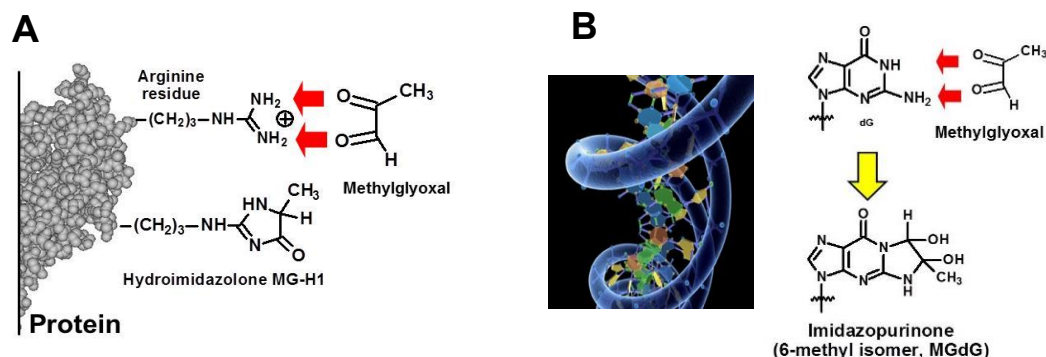


Figure 6. Schematic representation of the major protein AGEs (A) MG-H1 and Major DNA AGEs MGdG (B) produced by methylglyoxal

MG has the ability to react with nucleotides, proteins and basic phospholipids to form advanced glycation endproducts (AGEs) (Rabbani et al., 2016a). The reaction of MG with proteins leads to the formation of hydroimidazolone adducts derived from arginine residues. MG-H1 is known to be the most abundant and functionally important AGEs in physiological system (Rabbani and Thornalley, 2012a). There are other minors MG-derived AGEs such as N_ϵ (1-carboxyethyl)lysine (CEL), MG derived lysine dimer cross-link (MOLD), arginine-lysine-derived crosslinks MODIC and argpyrimidine. (Rabbani and Thornalley, 2012a). Multiple factors can influence proteins content of AGE: exposure time to MG, chemical stability of the glycation adducts, MG concentrations, protein turnover, DNA and phospholipid modification and intrinsic reactivity of the protein (Rabbani et al., 2016b).

The main nucleotide-derived AGEs formed from dicarbonyls are imidazopurinones, GdG and MGdG. The content level of MGdG in the DNA is higher when compared to the DNA oxidative damage adduct, 8-hydroxydeoxyguanosine. From glyoxal, the AGEs formed are 3-(2'-deoxyribo-5-yl)-6,7-dihydro-6,7-dihydroxyimidazo[2,3-b]purin-9(8H)-one (GdG) and N_2 -(carboxymethyl)deoxyguanosine (CMdG). However, from MG the AGEs formed are 3-(2'-deoxyribo-5-yl)-6,7-dihydro-6,7-dihydroxy-6-methylimidazo[2,3-b]purine-9(8H)-one (MGdG) and N_2 -(1-carboxyethyl)-deoxyguanosine (CEdG). MGdG and GdG are unstable at elevated temperature and pH. Imidazopurinones

are stable in the double stranded (dsDNA) and single stranded DNA (ssDNA). Formation of CEdG is related to DNA depurination (Thornalley, 2003c, Thornalley, 2008). Increases in mutation frequency, cytotoxicity and DNA strands break are linked to increased GdG and MGdG formation (Thornalley et al., 2010). Basic phospholipids can react with MG. Phospholipid glycation affects membrane interaction which leads to membrane fluidity (Pun and Murphy, 2012). Glycation of phospholipids can elevate lipid peroxidation which leads to increase oxidative damage (Pun and Murphy, 2012).

1.1.5.4 Dicarbonyl stress

Dicarbonyl stress is defined as the abnormal accumulation of α -oxoaldehyde metabolites leading to an increased DNA and protein modifications resulting in cell and tissue dysfunction. The cell and tissue dysfunction are implicated in aging and disease (Rabbani and Thornalley, 2014b). There are several examples: such as the elevation of MG-protein modification in ageing human lens, elevation of plasma and tissue concentration of MG in diabetes, the increased level of MG, glyoxal, 3-DG concentration and other dicarbonyls in renal failure (Rabbani and Thornalley, 2015). The cause of the dicarbonyl stress is the imbalance between the formation of dicarbonyl metabolites and the enzymatic metabolism of these metabolites; and also increased exposure to dicarbonyl metabolites from exogenous sources (Xue et al., 2012). Normal levels of MG, glyoxal and 3-DG range between 50 – 150 nM in human plasma and 1 – 4 μ M in plant and mammalian cells. During the increase of dicarbonyl concentration, dicarbonyl stress arises which leads to an impaired health and disease (Rabbani and Thornalley, 2015).

1.1.5.5 Clinical importance of dicarbonyl stress

Glycation adducts with proteins, nucleotides and reactive dicarbonyls have an implication clinically in ageing, disease and number of pathological process. For example, diabetes, neurodegenerative disease and tumorigenesis and multi-drug resistance in cancer chemotherapy (Rabbani and Thornalley, 2012b).

1.1.6 S-D-Lactoylglutathione

S-D-Lactoylglutathione is the physiological intermediate of metabolism of MG by the glyoxalase system. The formation of this intermediate comes from the hemithioacetal adduct of MG and GSH in a reaction catalysed by Glo1. Followed by the hydrolysis of S-D-lactoylglutathione to GSH and D-lactate in a reactions catalysed by Glo2 (McLellan et al., 1993).



The formation of S-D-lactoylglutathione occurs in the cytosol of cells and it cannot readily cross the cellular membrane. Nevertheless, S-D-lactoylglutathione can leak slowly from cells by the GSH conjugate transporter. When in the extracellular compartment, γ -glutamyltransferase present on the external surface of cellular membrane plasma cleaves S-D-lactoylglutathione to S-D-lactoylcysteinylglycine. There is then a spontaneous rearrangement of S-D-lactoylcysteinylglycine to N-D-lactoylcysteinylglycine (Tate, 1975) and cleavage of this by dipeptidase forms N-D-lactoylcysteine.

Thornalley and his co-worker made remarkable studies on the biological properties of S-D-lactoylglutathione added to cells in culture (Thornalley and Tisdale, 1988). They have shown that S-D-lactoylglutathione promote cytotoxicity and growth arrest in human cell leukaemia *in vitro* (Thornalley and Tisdale, 1988). In human neutrophils, S-D-lactoylglutathione influenced the stimulus-activated granule secretion: at low concentration (2 - 5 μ M), it potentiated secretion; and during high concentration (100 μ M – 5 mM), it inhibited secretion (Thornalley, 1990). It is found that the above effect is enhanced by N-D-lactoylcysteine which gets in the cells by passive diffusion as it has unionised solution species known. N-D-Lactoylcysteine is an inhibitor of dihydro-orotase of the *de novo* pyrimidine synthesis pathway. The ability to inhibit pyrimidine synthesis accounted for the anticancer activity of S-D-lactoylglutathione and granule secretion effects through the effect of metabolic channelling of pyrimidine metabolites into nucleotide conjugates enhancing for degranulation via cell signalling (Edwards et al., 1993, Edwards and Thornalley, 1994, Edwards et al., 1996).

1.1.7 D-Lactate

The main stereoisomer of lactate made in human intermediary metabolisms is L-lactate (Drury and Wick, 1965). D-Lactate is another enantiomer which mainly *ca.* 1 - 5% of the concentration of L-lactate in plasma. Exogenous sources of D-lactate can be found in high concentration in fermented food such as yogurt, pickles and sauerkraut. Moreover, D-lactate is absorbed from the microbial fermentation in the gut (Hove, 1998, Mortensen et al., 1991, Ewaschuk et al., 2005, de Vrese and Barth, 1991). The endogenous formation of D-lactate occurs by the glyoxalase system pathway and it is metabolised by 2-hydroxyacid dehydrogenase to pyruvate (Thornalley, 1993b). D-Lactate is well-metabolised in human subjects but it has a fractional renal clearance compared to L-lactate (Connor et al., 1983). D-lactate infusion in human subjects is at 1.0-1.3 mmol sodium D-lactate/kg/hr resulted in almost 90% of the D-lactate metabolised while the remaining 10% is secreted in urine (Oh et al., 1985). Metabolism of D-lactate dropped by almost 75% of the overall clearance with a higher rate of infusion of 3.0 - 4.6mmol/kg/hr (Oh et al., 1985). The concentration of D-lactate in blood plasma increase *ca.* 2 - 3 fold after exercising or meal consuming (Ohmori and Iwamoto, 1988, Kandoh et al., 1992a). The cell permeability of D-lactate occurs through transport mechanisms: inorganic anion exchange system, lactate specific transporter, and by non-ionic diffusion. D-lactate is excreted in urine with lower levels excreted in sweat or stool (Ohmori and Iwamoto, 1988, Kandoh et al., 1992a, Kandoh et al., 1992b).

Increased D-lactate is a sign that there is increased formation of MG, particularly where cells studied are unable to metabolise it. For instance, red blood cells, lens fibre cells and vascular endothelial cells (Thornalley, 1993a, Irshad et al., 2019). The concentration of D-lactate increases in culture media of endothelial cells and red blood cells when high glucose is used in culturing those cells (Thornalley, 1988, Karachalias et al., 2005, McLellan et al., 1994a). In healthy human subjects, the plasma level of D-lactate is *ca.* 10 μ M (Thornalley, 1988, Phillips and Thornalley, 1993, Karachalias N, 2005, McLellan et al., 1994a). D-Lactate may be overestimated if racemisation of L-lactate occurs in pre-analytic processing; this may have a marked effect as L-lactate normally exists at >100

fold higher concentration than D-lactate (de Vrese and Barth, 1991, McLellan et al., 1992a, Ohmori and Iwamoto, 1988, Brandt et al., 1980).

D-Lactate is measured using endpoint enzymatic assay with either absorbance or fluorescence detection of NADH formed in presence of D-lactic dehydrogenase. The amount of D-Lactate in the sample is equivalent to the amount of NADH formed from NAD^+ at endpoint, formed concomitantly with the oxidation of D-lactate to pyruvate (McLellan and Thornalley, 1992a). D-Lactate may also be detected from the amount of pyruvate formed in this reaction where pyruvate is detected by derivatisation with 1,2-diaminobenzene to form 2-hydroxy-3-methylquinoxaline and assay by high performance liquid chromatography (HPLC) with fluorescence detection (Ohmori and Iwamoto, 1988, Ohmori et al., 1991).

1.1.8 Non-glyoxalase detoxification of methylglyoxal.

In cases where the glyoxalase system is impaired or inhibited, glyoxal is metabolised and converted to glycolaldehyde by aldoketo reductase (AKR) isozymes 1B1 (aldose reductase), 1B3 and 1B8 may metabolise glyoxal to glycolaldehyde. In such circumstances, AKR isozymes 1A4, 1B1 and 1B3 metabolise MG to mainly hydroxyacetone (Baba et al., 2009). The majority of glyoxal and MG metabolism by AKR1B1 takes place in the renal medulla where AKR1B1 has a high expression in comparison with Glo1 (Nishimura et al., 1993, Larsen et al., 1985). Glyoxal and MG concentrations may be increased in renal failure and this is due to impaired Glo1 activity. The activity of Glo1 in vascular and renal cell may be decreased in renal failure by several factors such as the reduced concentration of GSH during oxidative stress, Glo1 expression decline and glutathionylation of Glo1. Glo1 expression may decreased due to stimulation of RAGE and suppression of Nrf2 signalling. Glo1 and AKRs 1B3, 1B1 and 1B8 are ARE-regulated genes with inducible expression controlled by Nrf2 (Xue et al., 2012, Kwak et al., 2003, MacLeod et al., 2009, Nishinaka and Yabe-Nishimura, 2005, Mercado et al., 2011).

It is thought that aldehyde dehydrogenase contributes to the degradation of MG in the event where glyoxalase system is impaired or absence. MG

dehydrogenase oxidises MG to pyruvate in a NAD⁺ - dependent reaction (Nemet et al., 2006). There are approximately more than 17 known aldehyde functional dehydrogenase genes (Vander Jagt and Hunsaker, 2003). Most significant genes: aldehyde dehydrogenase 3 (ALDH3), aldehyde dehydrogenase 1 (ALDH1) and aldehyde dehydrogenase 2 (ALDH2). These gene product enzymes detoxify many different aldehydes in human subjects (Vander Jagt and Hunsaker, 2003, Vander Jagt et al., 2001). The preferred substrates for these ALDHs are unhydrated aldehydes. MG is highly hydrated and hence is not readily oxidized by ALDH2 and ALDH1 (Vander Jagt and Hunsaker, 2003, Nemet et al., 2006, Izaguirre et al., 1998).

1.1.9 The critical role of glyoxalase 1 in enzymatic defence against glycation

Protein glycation by MG leads to the modification of protein which results in loss of side chain charge, function impairment, rearrangement of its structures and misfolding. Recent research has shown that increased MG glycation leads to activation of the cellular unfolded protein response, with downstream pro-inflammatory and pro-thrombotic cell signalling (Irshad et al., 2019) Activation of the unfolded protein response in high glucose treated endothelial cells is mediated by methylglyoxal. Increased formation of glycation adducts have been linked with chronic disease.

At physiological level, protein glycation is prevented and repaired by the enzymatic defence against glycation. In 2003, Thornalley established the concept of the enzymatic defence against glycation which prevents and repairs the glycation adduct formation (Thornalley, 2003a, Thornalley, 2003b). Enzymes involved are: fructosamine-3-kinase - which catalyses the repair of early glycation adducts; and Glo1, aldehyde reductases and aldehyde dehydrogenase – which prevent the formation of AGEs by metabolising dicarbonyl precursors. The detoxification of reactive α -oxoaldehydes, glyoxal and MG, is catalysed by Glo1. The enzymatic defence against glycation decreases endogenous glycation damage to the proteome. Nevertheless, some residual glycation of nucleotides, proteins and basic phospholipid occurs but it is reduced to a tolerable level (Thornalley, 2003a, Thornalley, 2003b). In disease conditions, such as chronic and acute renal

failure, the enzymatic defence against glycation is overcome and therefore glycation adducts rise. Glo1 expression is thought to be reduced with aging and aging linked disease (Morcos et al., 2005).

1.2 Other aspects of glycation

1.2.1 Definition of glycation

Glycation can be defined as the non-enzymatic reaction of reducing sugars and related derivatives with proteins, nucleic acids and basic phospholipids to form one or several adducts. Glycation takes place in several sequential complex and parallel reactions called the Maillard Reaction. Protein glycation by glucose occurs by initial reaction of N-terminal and lysine side chain amino group with the acyclic aldehyde form of glucose to form firstly a Schiff's base intermediate followed by slow rearrangement, called the Amadori, leading to formation of the Amadori product or ketoamine. For proteins glycated by glucose, the Amadori products are: N_α(1-deoxyfructos-1-yl) amino acids – by reaction with N-terminal amino groups, and N_ε(1-deoxyfructos-1-yl) lysine residues – by reaction with lysyl side chain amino groups. The above mentioned adducts may undergo enzymatic repair catalysed by fructosamine-3-phosphokinase, spontaneous reversal to unglycated amino groups and glucose and mannose, or may slowly degrade to form AGEs (Rabbani and Thornalley, 2012b, Rabbani and Thornalley, 2008a).

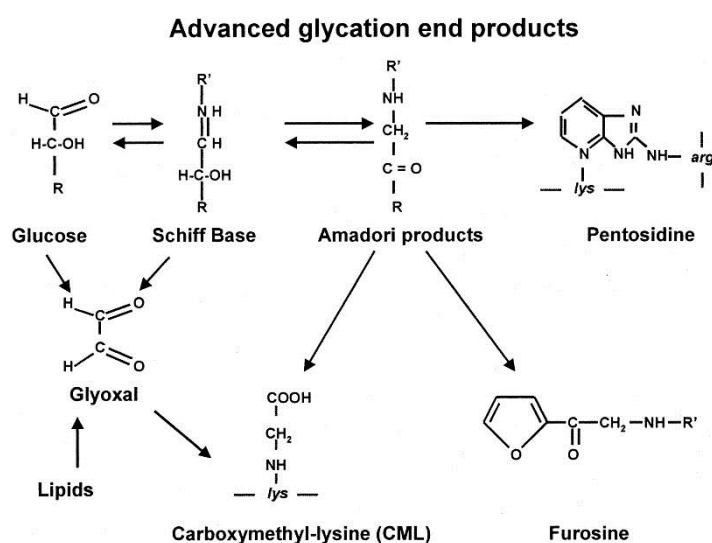


Figure 7. Chemical mechanism of Maillard reaction.

Glycation by MG, glyoxal and other reactive α -oxoaldehydes found in physiological systems and reacts with proteins to form AGEs directly (Rabbani and Thornalley, 2008c). The reaction between proteins and reactive α -oxoaldehydes occurs mainly with arginine side-chain guanidine groups to form hydroimidazolone adducts.

The normal level at steady state of protein glycation is mainly around $\leq 5\%$ of protein substrate this may have a little impact on function of protein. In cases where modified proteins assume a different pathogenic function, increase of low level may be physiologically important. Examples are: MG-modified low density lipoproteins (LDL) which has increased binding to walls of arteries; and MG-modified collagen-IV which has decreased binding of cell surface integrin proteins of endothelial cells producing cell detachment and potential initiation of thrombosis by the exposed subendothelium. Moreover, glycation could speed up the degradation of proteins, decreasing the half-life of protein substrates; and if there is no increase in synthesis of proteins, this will affect the steady state concentration of unglycated proteins. Thus, protein glycation may result in impairment of normal physiological function, tissue or cellular dysfunction production and have a major contribution towards disease. For these reasons, glycation is considered a type of protein damage (Rabbani and Thornalley, 2015).

1.2.2 Historical perspective of glycation

Arthur Robert Ling was the first investigator to develop a process involving drying proteins with sugar in 1908. This drying process produced a flavoured coloured mixture. He studied the formation of pigments by heating glucose with asparagine (Ling, 1908). This was the first time the formation of adducts between amino acids and glucose was reported. In 1912 Louise Camille Maillard, considered to be the father of glycation research, studied the reaction between glucose and glycine at high temperature (Maillard, 1912a). He concluded that the production of brown pigments, melanoidins, occurred by initial reaction between amines and saccharides which led to production of Schiff's base adducts (Maillard, 1912b). This complex process of reversible and parallel sequential reactions is called "Maillard reaction". In the same century, an important

enzymatic defence against glycation was discovered the glyoxalase system which converts MG to D-lactate systems (Dakin and Dudley, 1913, Neuberg, 1913b).

From 1925 to 1931, the condensation of D-glucose was investigated by Mario Amadori. The condensation of D-glucose with amines such as p-phentidine, or p-anisidine or p-toluidine formed two isomers which were not anomers (Amadori, 1929b). He showed that one of the isomers was more labile than the other towards hydrolysis and was also more susceptible to decomposition on standing in the solid state in air. He correctly recognised this as the N-glycosylamine but he mistakenly thought that the more stable isomer was a Schiff's base, overlooking its resistance to acid hydrolysis (Amadori, 1929a). Furthermore, Kuhn and Dansi in 1936 showed that the stability of the isomer was due to a rearrangement of Schiff's base. Kuhn and Dansi were able to confirm Amadori discovery about the labile isomers (Kuhn and Dansi, 1936). Kuhn and Weygand were the first to report the structure of the stable isomer which was an unbranched N-substituted 1-amino-1-deoxy-2-ketose (Kuhn and Weygand, 1937). In 1953, Hodge proposed that Schiff's base reaction is followed by Amadori rearrangement which involved in the starting steps of Maillard reactions. Moreover, Hodge suggested that oxidation, enolization and fragmentation reactions have a major contribution in degradation of fructosamine to glucosone and several other adducts (Hodge, 1953).

Allen and colleagues were the first investigators to study the glycation of proteins *in vivo*. They reported a type of glycated haemoglobin, HbA_{1c}, showing that it was a negatively charged variant of human blood cell haemoglobin (Allen et al., 1958). In addition, the first researchers to investigate the role of glycated haemoglobin and its elevation in diabetes were Bookchin and Gallop in 1968 (Bookchin and Gallop, 1968). In 1975, Bunn and colleagues were able to describe the reaction where glycated haemoglobin are formed (Bunn et al., 1975). Later in 1976 it was suggested by Anthony Cerami and co-worker to use HbA_{1c} as a biomarker for glycaemic control in diabetic patients (Koenig et al., 1976).

In 1960, Anet investigated fructosamine degradation (N,N-difructosylglycine) to 3-deoxyglucosone (Anet, 1960). Furthermore, Kato was able to isolate 3-DG and 3-deoxypentosone from the reaction between amines

with glucose and ribose (Kato, 1960, Shin et al., 1988). These reactive α -oxoaldehyde products of the Maillard reaction are now seen as important precursors of glycation adduct formation in biological systems.

In 1973, it was described for the first time by Bonsignore *et al.* that the triosephosphate glycolytic intermediate, glyceraldehyde-3-phosphate, degrades non-enzymatically to form MG under physiological conditions (Bonsignore et al., 1973). In 1977, Takahashi described the reaction of amino acids with glyoxal derivatives, including glyoxal and MG. Arginine was identified as the predominant amino acid modified and a hydroimidazolone was one molecular structure proposed for the adducts (Takahashi, 1977b). In 1980, Hayashi and Namiki made a remarkable contribution by finding the formation of α -oxoaldehydes by saccharide moiety fragmentation in Maillard reactions. This is termed Namiki pathway of the Maillard reaction which involves glyoxal and MG formation by saccharide fragmentation reactions (Hayashi and Namiki, 1980).

In 1980, Nakayama *et al.* reported the formation of 6-(2-formyl-5-hydroxymethylpyrrol-1-yl)-L-norleucine from 3-deoxyglucosone and lysyl residues in proteins, now commonly known as pyrroline - an AGE (Nakayama et al., 1980). In 1986, Cerami was first to use the term “advanced glycation endproducts” and refer to such compounds as “brown fluorescent pigment which crosslink proteins” (Cerami, 1986). Baynes and colleagues were the first to describe N ϵ -(carboxymethyl)lysine (CML) and erythronic acid formation from glycated protein degradation by glucose (Thorpe and Baynes, 2002). The presence of these compounds in human urine was later found (Ahmed et al., 1986). The formation of CML comes from the degradation of fructosyl-lysine and also reaction of lysine residues with glyoxal and ascorbate which is formed from peroxidation of lipids (Thorpe and Baynes, 2002).

In 1988, Thornalley made the remarkable contribution by confirming the link between hyperglycaemia in diabetes and the increased flux of MG formation and concentration and its probability as the main pathway leading to the appearance of diabetes complications (Thornalley, 1988). Thornalley reported that there is 3 - 5 fold increase in concentration of MG in blood samples of patients with T1DM and T2DM (McLellan et al., 1994b). In 1989, the discovery of an

acid-stable fluorescent compound formed from glycated collagen called pentosidine was reported by Sell and Monnier (Sell and Monnier, 1989). This compound is result of the crosslink formation by a pentose moiety and arginine and lysine residues.

Since the start of twenty first century, there has been a remarkable advancement in glycation research specifically in measuring and quantifying glycation adducts and free adducts by stable isotopic dilution analysis LC-MS/MS (Thornalley, 2003a, Thornalley and Rabbani, 2010). The application of high resolution mass spectrometry proteomics was able to identify proteins prone to glycation by glucose and reactive metabolites such as MG (Rabbani and Thornalley, 2014, Zhang et al., 2007). Mutant mouse models with increased glycation have been developed: for example, Glo1 deficient mice and F3K knockout mice (El Osta et al., 2008, Veiga-Da-Cunha et al., 2006). Transgenic mice with glycation exposure have been developed: for example, Glo1 overexpressing transgenic mice (Inagi et al., 2002). The conception of “dicarbonyl stress” has emerged: this is defined as the abnormal accumulation of dicarbonyl metabolites resulting in increased DNA and protein modification contributing to cell and tissue impairment and dysfunction in ageing and disease. The role of dicarbonyl glycation in health impairment has been described, including diabetes, renal failure, CVD, schizophrenia, Parkinson’s disease, carcinogenesis and mechanism of action of anticancer drugs including Glo1 overexpression-linked to multi-drug resistance (Rabbani and Thornalley, 2015).

The role of AGE receptors has been investigated in relation to health and disease leading to the development of receptor of advanced glycation endproducts (RAGE). Although there is thought to be involvement of RAGE in cell responses to glycated proteins, this has been questioned and the non-glycated ligands considered as a physiological agonists. The relation between RAGE and glycation was further complicated by the notion that the activation of RAGE is related to Glo1 down regulation leading to an increase in dicarbonyl sensitivity (Thornalley, 2007).

There is an important role of glycation in aging and disease. It also has an important role in specifically in carcinogenesis where Glo1 was identified as a

tumour suppressor protein (Zender et al., 2008) and cancer chemotherapy where overexpression of Glo1 is a mediator of multidrug resistance, diabetes, obesity, renal failure, Alzheimer's disease, arthritis, cirrhosis and schizophrenia (Thornalley et al., 2010, Ahmed et al., 2005, Agalou et al., 2005, Ahmed et al., 2004, Chen et al., 2004, Arai et al., 2010, Chen et al., 2013, Hambsch et al., 2010).

Dicarbonyl scavengers and inducers of Glo1 expression or “Glo1 inducers” are considered emerging therapeutic approaches to decrease dicarbonyl glycation. Currently, treatment under evaluation are small molecule Glo1 inducers and dicarbonyl scavengers such as pyridoxamine. For example *trans*-resveratrol and hesperetin (Xue et al., 2016) and sulforaphane (Xue et al., 2012). The timelines of key discoveries in glycation research is summarized in Figure 3.

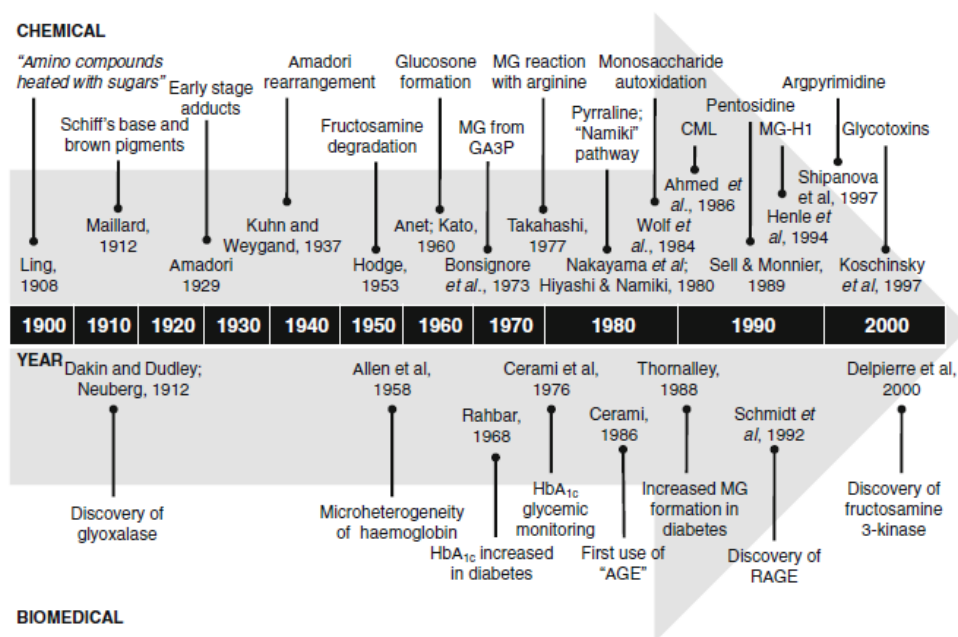


Figure 8. Timeline of the key discovery and development in glycation research between 1900 to 2000.

From (Rabbani and Thornalley, 2012b)

1.2.3 Early-stage and advanced-stage glycation

Glycation of proteins by glucose with the formation of fructosamines is considered as an early-stage glycation. Schiff's base, glycosylamine and fructosamine adducts are classified as early stage glycation adducts. In later,

advanced stages, fructosamine undergoes degradation to form end-stage adducts called advanced glycation endproducts (Rabbani and Thornalley, 2012b).

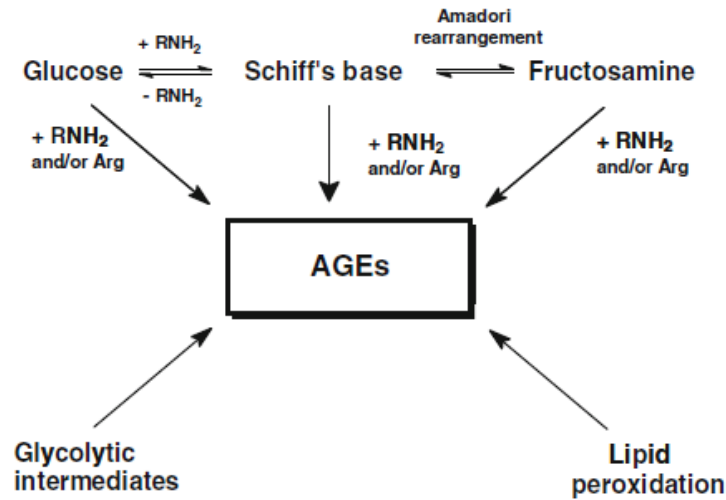


Figure 9. Early glycation and metabolic sources of AGEs.

From (Rabbani and Thornalley, 2012b)

1.2.4 Advanced glycation endproducts

AGEs compound are considered as collection of compounds with complex heterogeneous characteristics. Examples illustrated in Figure 5.

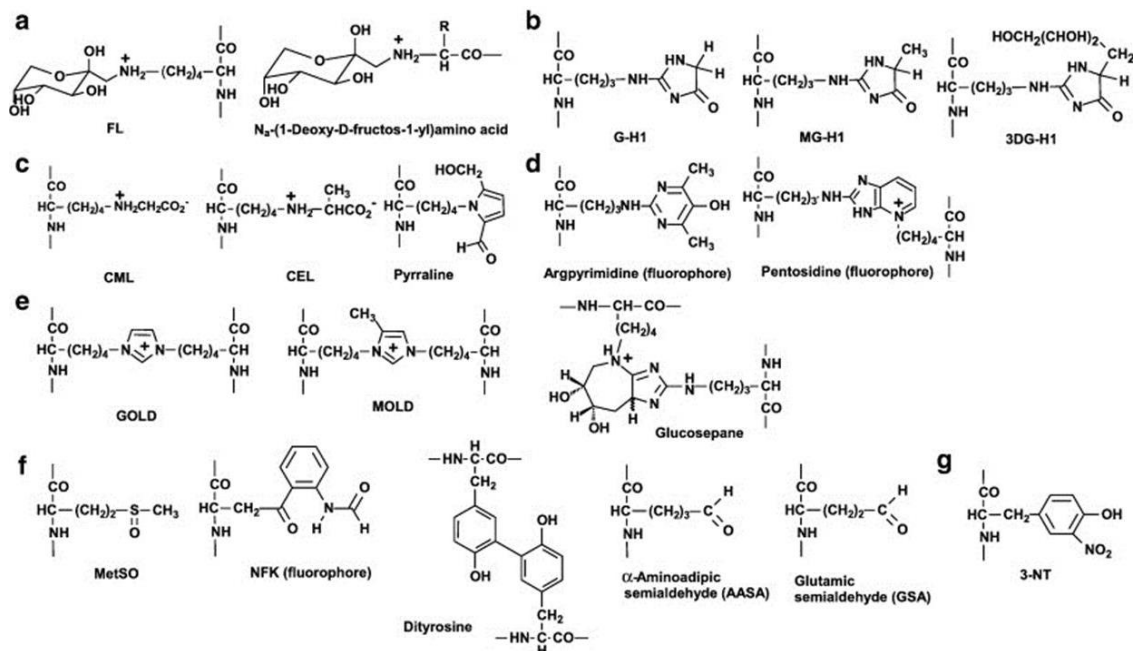


Figure 10. Protein oxidation, glycation and nitration adducts residues in biological systems.

- (a) Early glycation adducts - FL and N α -(1-deoxy-D-fructos-1-yl) amino acid residues. Advanced glycation endproducts: (b) Hydroimidazolones, (c) Monolysyl AGEs, (d) Fluorescent AGEs and (e) Non-fluorescent crosslinks. (f) Protein oxidation adducts. (g) Protein nitration adduct. Adapted from (Thornalley and Rabbani, 2014).

1.2.5 Biochemical formation and physiological effects of protein glycation

In physiological systems protein glycation is usually low; that is, ca. 0.5 - 10% of protein have one glycation adduct residue. FL residue formation enhances steric demands on the intermediate environment of the glycation site. However, there is no change in side positive charge (Roper et al., 1983). CML and CEL residues add a negative charge while preserving positive charge of the side chain. Formation of hydroimidazolones increases steric demand of the precursor Arg residue and also result in loss of positive charge. Formation of hydroimidazolones are particularly damaging because precursor Arg residues have a high probability of being in a functional domain of proteins – 42% for the human proteome and loss of positive charge on hydroimidazolone formation produces loss of functional electrostatic interactions (Rabbani and Thornalley, 2012c, Irshad et al., 2019).

Sites of lysine and arginine susceptible to glycation are thought to have activating positive and negative charge in amino acids residues close by; 3 - 4 residues distance in the primary sequence for an α -helix. However, this is yet to be confirmed experimentally (Rabbani and Thornalley, 2012c). Glycation of protein may have important functional impact. For example, AGE modification of the integrin binding sites of vascular IV collagen (Dobler et al., 2006), AGE damage of protein in mitochondrial resulting in increased ROS leakage from mitochondria (Morcos et al., 2008), neuronal voltage sodium gate modification by MG result in in diabetic neuropathy (Bierhaus et al., 2012), and modification of LDL by methylglyoxal producing atherogenic small LDL (Rabbani et al., 2011).

Protein glycation could also affect the formation of non-sulphydryl crosslink. AGE-enhanced cross linking of proteins may result in low protein solubility **and prone to enzymatic digestion** (Schnider and Kohn, 1981). This is particularly important in connective tissues and extracellular matrix where crosslinking may result in changes in structural and mechanical properties-elevated thickening and rigidity of the capillary basement membrane. Such

changes are linked with ageing (Lee et al., 1993). The formation of soluble collagen fibrils *in vitro* are inhibited by glycation. Glycation leads to an elevation of intermolecular spacing in the collagen fibril and loss of structure and expanding the molecular packing (Tanaka et al., 1988, Brownlee, 2001).

1.3 Protein oxidation

Proteins are often susceptible to oxidative damage and other oxidation-derived process. Formation of ROS occurs under normal metabolism in organelles such as mitochondria and peroxisomes and contributes to endogenous protein damage (Petropoulos and Friguet, 2005). Furthermore, environmental factors such toxins and UV radiation can increase the formation of ROS leading to increased protein oxidation. Enzymatic and non-enzymatic antioxidants suppress the levels of ROS to maintain cellular redox homeostasis. When the impairment of redox haemostasis is affected by elevated ROS formation, oxidative damage becomes excessive can significantly impair protein, DNA and lipids - resulting in accumulation of oxidized product. Accumulation of oxidized products is found in ageing and ageing related disorders (Berlett and Stadtman, 1997). Aromatic amino acid and sulphur-containing amino acids, cysteine and methionine, are more sensitive to oxidation. Protein damage caused by oxidation may be irreversible and is then only cleared through proteolysis. Degradation of oxidised proteins occurs via the proteasome for cytosolic proteins and Lon protease (Grune et al., 1997). Some oxidative damage adducts can reversed back to the unmodified precursors: for example, cystine and cysteine sulfonic acid may be reduced by thioredoxin reductase and methionine sulfoxide by methionine sulfoxide reductases (Holmgren, 2000, Bakala et al., 2003).

1.4 Protein nitration

Nitration is a chemical reaction where a nitro group ($-\text{NO}_2$) is introduced into a chemical compound. In protein nitration there are different amino acids which can be nitrated such as tyrosine, tryptophan, cysteine and methionine residues (Ischiropoulos and biophysics, 1998). The most common is tyrosine nitration with the formation of 3-nitrotyrosine. These changes will lead to marked shift of pKa

of the hydroxyl group from 10.07 in tyrosine to 7.50 in nitrotyrosine (Turko and Murad, 2002). It is thought that tyrosine nitration is a selective process but it is very low, *ca.* 0.003 mol% - reviewed in (Rabbani and Thornalley, 2008b). The site of nitration depends on protein structure, function and nitration mechanism as well as protein location. Tyrosine nitration may loss of protein function and influence phosphorylation status (Turko and Murad, 2002).

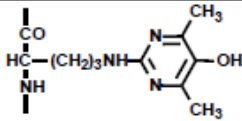
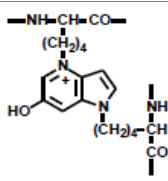
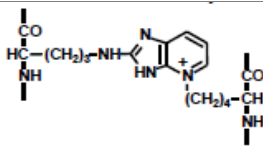
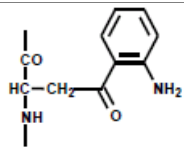
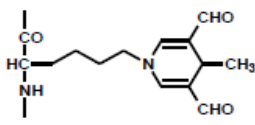
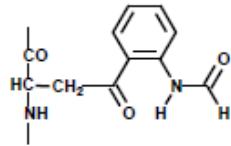
1.5 Measurement of protein glycation, oxidation and nitration

1.5.1 Fluorescence

Fluorescence can be used to measure protein glycation and oxidation. However, this method is limited to minor number of glycation and oxidation adducts analytes that are fluorescent. The use of chromatographic resolution is essential for quantitative measurement. Fluorescent AGEs are measured by determine emission and excitation wavelengths of 350nm and 450 respectively (Sebekova et al., 2001). Fluorescent AGE peptides or free adducts have also been measured (Thomas et al., 2004). This methods have several limitations and analytical difficulties: (1) Most of AGEs are not florescent and therefore cannot be detected (Rabbani and Thornalley, 2009); (2) there are multiple fluorophores related to total florescence measurement with different specific fluorescence, hence quantification cannot be performed. Table 1 shows different total AGE fluorescence estimates which provide qualitative measurement of glycation and oxidation damage.

Tryptophan oxidation can produce fluorophores NFK and kynurenine (Fukunaga et al., 1982). Protein interaction with lipid peroxidation product such as malondialdehyde may generate fluorophores such as 3,5-diformyl-1,4-dihydropyridin-4yl-pyridinium derivatives (Yamada et al., 2001) and associated crosslinks (Itakura et al., 1996).

Table 1. Different fluorophores linked to oxidation glycation protein damage.
Adapted from (Xue, 2009).

Fluorophore	Structure	Fluorescence characteristics: $\lambda_{\text{excitation}}$, $\lambda_{\text{emission}}$	Reference
Glycation			
Argpyrimidine		320 nm, 385 nm	(Kinane et al., 2011)
“AGE fluorescence	Various	350 nm, 440 nm	(Yan et al., 2009)
Vesperlysine A (LM-1)		345 nm, 405 nm	(Santos et al., 2010)
Pentosidine		335 nm, 385 nm	(Vieira Ribeiro et al., 2011)
Oxidation			
Kynurenine		365 nm, 480 nm	(Taylor et al., 2015)
2-Amino-6-(3,5-diformyl-1,4-dihydro-4-methyl-pyridin-1-yl)hexanoic Acid		387 nm, 455 nm	(Yamada et al., 2001)
NFormylkynureni Ne		325 nm, 434 nm	(Fukunaga et al., 1982)
“Fluorescent oxidation products”	Several fluorophores	360 nm, 430 nm	(Shimasaki, 1994)

Lipofuscin	Several fluorophores	340 – 390 nm, 430 – 490 nm	(Li et al., 2006, Sohal, 1981)
------------	----------------------	-------------------------------	-----------------------------------

1.5.2 Immunoassay

Immunoassays were first used for the quantification of protein glycation, oxidation and nitration adduct analysis. They have good analytical performance for high affinity binding for of peptides and proteins. Nevertheless, there are limitations in antigen specificity for detection of glycation, oxidation and nitration adducts. For instance, monoclonal antibody 6D12 was thought to bind to CML residues but it was shown later that it is bound both CML and CEL; in fact, it preferably binds to CEL rather CML (Ikeda et al., 1996, Koito et al., 2004). Several studies show that immunoassay can give variable overestimation of glycation adduct contents with the lack of reproducibility. However, immunoassay can be a good in assessing the localisation of antigen in immunohistochemical analysis and is relatively high throughput compared to other methods.

1.5.3 Analysis of stable isotopic dilution liquid chromatography using tandem mass spectrometry (LC-MS/MS)

Stable isotopic dilution liquid chromatography with tandem mass spectrometric detection (LC-MS/MS) is the best analytically performing and reference technique to quantify glycation, oxidation and nitration adducts in proteins and free adducts – reviewed in (Thornalley et al., 2003). The determination of glycation, oxidation and nitration adducts is performed after exhaustive enzymatic hydrolysis. Free adducts from protein glycation, oxidation and nitration are measured in ultrafiltrate prepared from physiological fluids by using a 3kDa or 12 kDa cut-off microspin filter. The development of this method was made in our group and it is used by several research groups around the world. Ultra-high performance liquid chromatography is now used with automated exhaustive enzymatic hydrolysis. Examples for proteins free adducts measured using isotopic dilution analysis are given in Table 2.

Table 2. Adducts marker from proteins oxidation, glycation and nitration measured by isotopic stable analysis LC-MS/MS.

Analyte group	Analyst
Early glycation adduct	FL
Advance glycation adduct AGEs	
Monolysyl AGEs	CEL, CML, pyrraline
Fluorescent AGEs	Pentosidine, argpyrimidine
Hydroimidazolones	MG-H1, G-H1, 3DG-H
Other	N _ω -Carboxymethylarginine S-Carboxymethylcysteine, ornithine
Nitration adducts	3-NT
Oxidation adducts	α-Aminoadipic semialdehyde, glutamic semialdehyde, dityrosine, NFK, MetSO

1.6 Proteomics

Proteomics can be defined as one focus of study in the science of post-genomics where all proteins in the whole or fraction of proteome are detected and post-translational modifications and protein turnover investigated. It may also include investigations of the interaction and the distribution of proteins at subcellular level (Ong and Mann, 2005).

The word “proteomics” were first used in the research to describe the use of two dimensional gel electrophoreses (2-DE) of proteins with removal of separated protein spots from gels for identification by mass spectrometry. Staining patterns of proteins in 2-DE experiments showed changes in protein abundances. However, there are several limitations using 2-DE methods. For example, the dynamic range of proteins detected are limited and it is not possible to accommodate 7 - 12 orders of magnitude within sample. More importantly, it is not possible to completely resolve of all protein into discrete spots. 2-DE has now been superseded by nanoflow liquid chromatography-high resolution mass spectrometry (MS) in proteomics research (Anderson and Anderson, 1998, Aebersold and Mann, 2003a).

The standard procedure in MS proteomics analysis includes proteolysis by Lys-C or/ and trypsin (Fang et al., 2002), partial resolution of peptides using nano-flow liquid chromatography and fragmentation and detection of peptides using positive ion electrospray ionisation mass spectrometry. Fragment ion series mass spectra and MS_n spectra are used to sequence peptides and identify related proteins. The use of bioinformatics tools is essential for data analysis. By current convention, detection of at least two unique peptides is required for protein identification. High sensitivity and high mass resolution MS can identify around 1000s proteins in each sample. The common used method for protein identification score using the Mascot algorithm (Aebersold and Mann, 2003b).

Quantitation of protein remains challenging. There are two forms of protein quantitative data: the relative change in protein amount between two conditions tested or the absolute protein amount in the sample. In absolute quantification the amount of substance of interested is measured for instance, ng ml⁻¹ of protein or protein copy number per cell. Relative quantification is measuring the ratio of the substance between two different conditions in the same sample. For examples, investigation of protein fold changes abundance caused by a chemical or drug treatment (Ong and Mann, 2005, Sadygov et al., 2004).

1.6.1 Label-free quantification

Label-free quantitation of proteins involves the quantitation of proteins without use of stable isotopic dilution analysis. There are two approaches using label-free quantitative approaches: spectral counting and peptide ion intensities. Spectral counting involves counting fragment ion spectra (MS/MS) detected for a specific protein. The number of fragment ion spectra increases as protein abundance increases (Liu et al., 2004). An alternative approach used herein is measuring the chromatographic peptide precursor ion intensities. The peak intensity is directly related to protein abundance (Bondarenko et al., 2002, Chelius and Bondarenko, 2002). This type of approach is convenient and straightforward. For reliable estimations, the raw LC-MS generated from experiments undergoes post-processing procedures – including retention time alignment and MS

intensities normalisation. In this method a typical interbatch coefficient $\geq 30\%$ (Megger et al., 2013).

1.6.2 Sample preparation for label-free quantification

Different samples can be used in proteomics analysis such as body fluids (plasma, serum, urine and bile) and cell and tissue extracts (Megger et al., 2013). This is followed by cell lysis – where applicable, protein isolation and digestion. The sample preparations and buffer of cell lysis is chosen based on whole or fractional proteome of interest. For example, nuclei protein, cytosolic protein or membrane proteins (Shevchenko et al., 2012).

Digestion methods involve the use of Lys-C or trypsin or other protease (Wiśniewski et al., 2009). The most widely used protease in mass spectrometry is trypsin. This is because it has high proteolytic activity and cleavage specificity. However, one limitation of using trypsin is incomplete digestion (Saveliev et al., 2013). Moreover, tightly folded proteins can cause resistance in trypsin activity. Lys-C has the ability to overcome this proteolytic resistance of tightly folded proteins by cleaving the lysine sites with high efficiency and specificity. One of the widely used method for sample purification is spin columns and filter digestion. Another method is in solution digestion method which is used for small sample amounts developed by Vekey and colleagues (Turiák et al., 2011).

It is important to determine the total protein concentration in samples, specifically when label-free quantification is used. Protein concentration measurement is performed after protein extraction from the sample. It is important in assessing if the protein isolation has been achieved successfully and in deducing if protease digestion has been successful (Megger et al., 2013). Several methods can be used in determining protein content: Bradford (Bradford, 1976), bicinchoninic acid (BCA) (Smith et al., 1985) and Popov assays. Amino acid analysis may also be used (Tyler, 2000).

Peptides obtained from the digestion step are partially resolved using reversed phase liquid chromatography (RP-LC) before analysis by mass spectrometry. To achieve chromatographic reproducibility using label free study, it is important to use internal standards containing stable-isotope peptides.

Retention times of the isotopic standards peptides can be used for chromatography alignment during data analysis (Burkhart et al., 2011). Nowadays, there are several mass analysers with high resolution used for free label proteomics. Predominant amongst these is the orbitrap analyser (Panchaud et al., 2008, Aebersold and Mann, 2003). This is due to its high mass resolution, relatively easy to handle output data and its applicability to different peptides fragmentation types such as electron-transfer dissociation ETD and higher energy-collisional dissociation HCD.

1.7 Introduction to mass spectrometry

1.7.1 Mass Spectrometry

Mass spectrometry is an analytical method to measure mass-to-charge ratio (m/z) of ions in the gas phase. The basic mass spectrometer is comprised of an ionisation source to produce ions, mass analyser to measure m/z and a detector to quantify ions number at specific m/z value, with the use of computer system for data processing and interpretation. Figure-11.

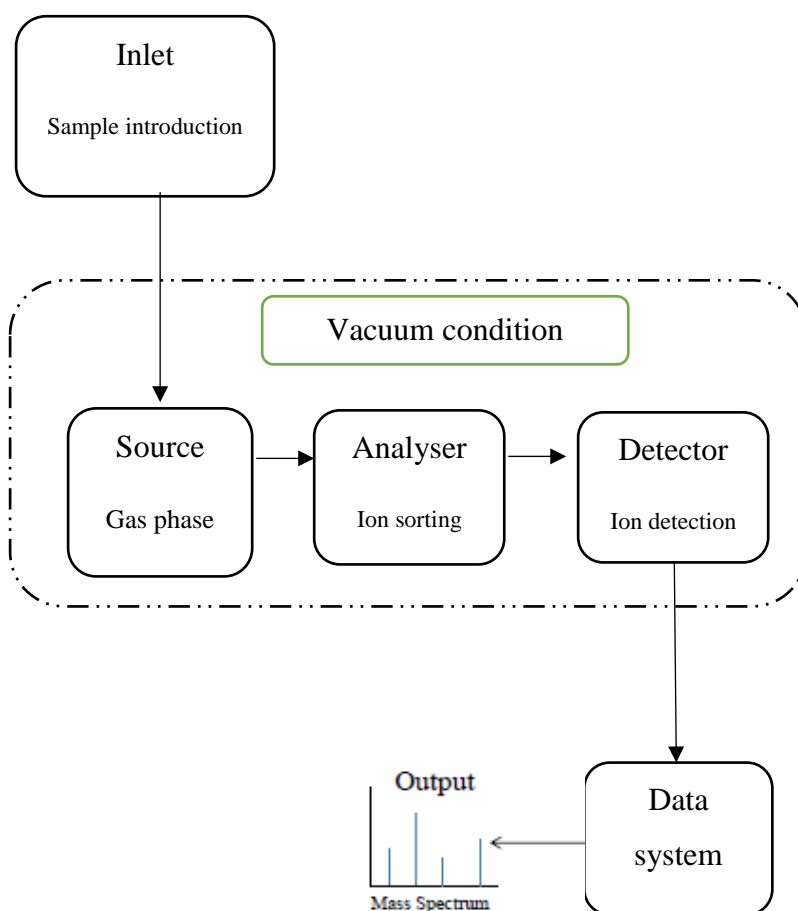


Figure11 Schematic representation of a mass spectrometer.

1.7.2 Ionisation method

There are several method can be used to ionise the sample prior the introduction to the mass spectrometer. Some of the ionisation technique is considered to be soft ionisation leaving the ion intact. Other techniques uses high energy which leads to the fragmentation of ion (de Hoffman and Stroobant 2007).

Previously, mass spectrometry instrument uses chemical ionisation, electron ionisation or field ionisation. The use of these methods require the analyte to be in a gas phase before the analysis, therefore it was unsuitable for biological sample analysis and only were used for thermally volatile stable analyte (Feng, Liu et al. 2008).

Recent development of the ionisation sources are able to transfer an analyte into the gas phase from either solid or liquid phase as part of the ionisation procedures. For example, the emergence of electrospray ionisation ESI (Wong, Meng et al. 1988, Fenn, Mann et al. 1989) and matrix-assisted laser desorption/ionisation (MALDI) (Karas, Bachmann et al. 1987, Karas and Hillenkamp 1988, Tanaka, Waki et al. 1988).

Electrospray ionisation (ESI) was first developed by John Fenn (Fenn, Mann et al. 1989). Since then, it has become the principle method for the study of biological molecules using MS. Electrospray ionisation is considered to be a soft ionisation techniques. For ESI, sample is normally introduced in aqueous solution containing organic solvent such as methanol (MeOH) or acetonitrile (ACN). For analysis of positive ions, a small acid amount is typically added to the solution in order to help the ionisation process. The solution is then sprayed through the capillary needle and high electric field is applied. Most common mechanism of ion formation by ESI is summarised in Figure12.

The charged solution inside the capillary produces a Taylor cone at the needle end which then releases small droplet with high charge. This droplet formation is aided by nebulising gas such as nitrogen. There are two mechanism suggested to describe the ion formation by ESI. These are the charge residue model (CRM) and the ion evaporation method (IEM). Both of the two models charge repulsion in the droplet surpass the surface tension leading the molecule of

solvent to evaporate. The repulsion charge leads to a Coulombic explosion and the division of the droplets. In CRM, this procedure is repeatedly occurred until multiply-charged ion is produced. In cases where ions are multiply charged at high m/z ratio, CRM is thought to be the major mechanism. In IEM, it is thought to be the model of ions with low m/z are formed. The starting process is similar however, after the Coulombic explosion ions within the droplet form are desorbed in the gas phase and entering the mass spectrometer. The ionisation produced by ESI gives the ability to be coupled with high performance liquid chromatography (HPLC) system which enable the separation of the biomolecule before MS analysis.

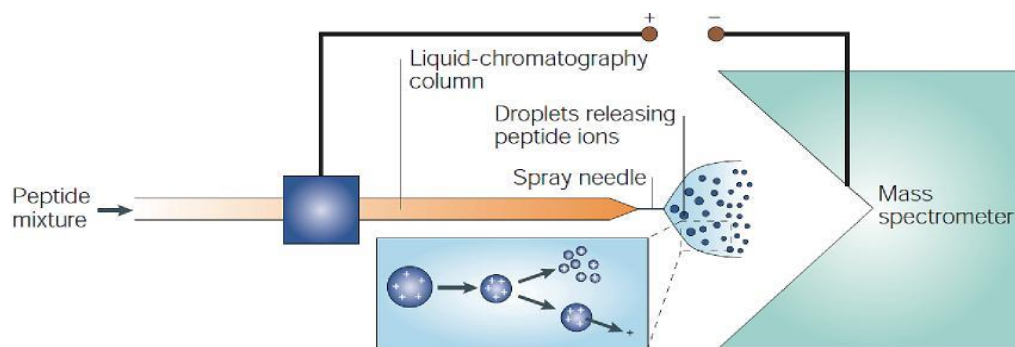


Figure 12. Electrospray ionisation. Adapted from (Steen and Mann 2004).

Another commonly used ionisation techniques is matrix laser desorption ionisation (MALDI) by Kiochi Tanaka (Tanaka, Waki et al. 1988). The process of this ionisation is taken place when the sample are embedded in a suitable matrix, mainly a small organic acid that absorbs UV radiation strongly. Under vacuum conditions, samples are focused using UV laser leading to local heating of the matrix molecule. This result in desorption of the sample and charged and neutral analyte and matrix molecule are ejected. During MALDI process, little fragmentation take place and mainly the ions formed are singly charged.

1.7.3 Mass analyser

1.7.3.1 Quadrupole

A quadrupole mass analyser compromised of four metal rods in parallel orientation. Combination of both direct current voltage and radio frequency are applied to the opposite rods pair. This will allow the quadrupole to act as mass filter. This principle were first introduced by Paul and Stienwedel (Paul and

Steinwedel 1953). Quadrupole is considered to be a low-resolution mass analyser that operate at unit mass resolution. Usually they are combined with other mass analyser. This will allow the use of quadrupole in targeted analysis of specific compounds and increase the selectivity of the experiment.

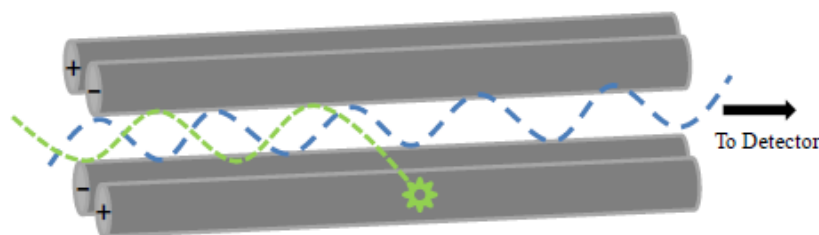


Figure13. Schematic representation of quadrupole analyser.

A quadrupole mass analyser can be performed in multiple modes. In RF-only mode, several ranges of m/z ions traverse the quadrupole (ion guide). Performed in static electric field, this will only allow a small window of ions to go through. With variable voltage applied to the quadrupole, a range of m/z ions may be detected over a relatively short period of time.

One of the methods widely used on the triple quadrupole is the selected reaction monitoring (SRM) method. In this process, samples are injected onto an LC directly coupled with the MS instrument. The elution of peptides takes place and the first quadrupole is used as a mass filter to isolate a peptide with a m/z of interest. The second quadrupole acts as a collision cell in order to break the peptide into fragments. Finally, the third quadrupole performs as a second mass filter for a particular m/z fragment from the initial parent peptide. Each of these fragment ion pairs is called a transition, and the detectors record their intensity. The total peak area shows the relative abundance of the peptide across the condition.

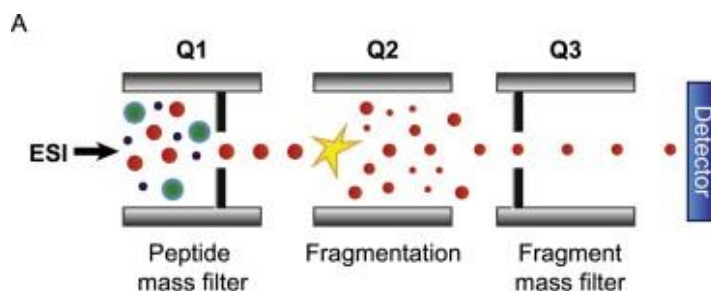


Figure14. Simplified schematic representation of triple quadrupole mass spectrometer.

Recent developments of triple quadrupole mass spectrometers allow scanning of hundreds of transitions in a single run to detect simultaneously multiple peptides. Moreover, the use of stable isotopic labelled peptides with known amount as an internal standards allows the quantification with high accuracy.

1.7.3.2 Orbitrap

Based on the design of the ion trap by Kingdon (Kingdon 1923), Alexander Makarov revealed a new mass analyser in 2000 (Makarov 2000) which is commercially known as orbitrap. Ions move in an orbital trajectory around central axis electrode in harmonic oscillation (frequency proportional to $m/z^{-1/2}$) which then can be detected by ion image current and the conversion to mass spectra is achieved using Fourier Transform (FT) techniques (Hu, Noll et al. 2005).

The orbitrap analyser can be considered as high-resolution and high mass accuracy instrument. However it should be considered that orbitrap resolution relies on both m/z and scan time. The resolution is specified at 60,000 (FWHM) at m/z and scan time of 1second. This increased as scan time increase and it could reach over 100,000. The desired resolution is inversely proportional to $(m/z)^{-1/}$. Therefore it is decreases as the range of mass is increased (de Hoffmann and Stroobant 2007).

1.7.4 Tandem Mass spectrometry

Mass spectrometers with either multiple or single mass analyser are able to perform tandem mass spectrometry (MS/MS). Generally, for mass spectrometers consisting of two mass analysers, ions are selected by the first mass analyser and fragmented into smaller ions and then measured by the second mass analyser.

The use of tandem mass spectrometry experiment is highly important for obtaining peptide ion sequence information. One of the widely used techniques involved selecting an ion of specific m/z (the precursor), colliding with an inert gas and then followed by analysing the ion formed, known as product ions. This process is called collisional induced dissociation (CID) which is first introduced by Jennings (Jennings 1968) and McLafferty (McLafferty and Bryce 1967). Once dissociation method applied to a peptide ion, fragmentation can occur at different sites. Figure 15 represent the nomenclature for the possible fragment ion that can be produced from a peptide suggested by Roepstorff, Fohlmann and Beimann (Roepstorff and Fohlman 1984), (Biemann 1992).

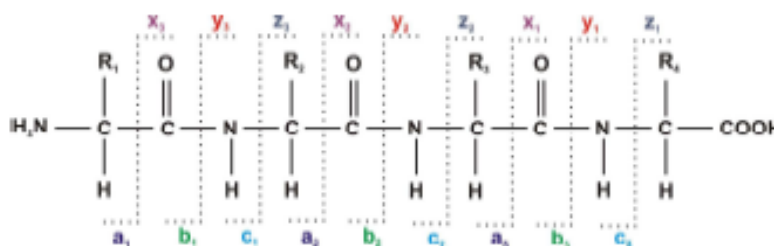


Figure 15. Peptide fragmentation nomenclature.

During low CID energy a series of *b* and *y* ions are generated from the peptide fragmented at the amide bonds of peptide backbone. These ions are produced when the charge is retained on either C- and N-terminal fragment. This process leads to a production of fragmented ions that differs in mass by a single amino acid residue which allow in theory to interpret the peptide sequence of the amino acid. This fragmentation mode can be used in various type of mass spectrometers and has reproducible fragmentation patterns. However, other labile PTMs are prone to dissociation under CID which makes them hard to analyse by

this technique. Other fragmentation techniques such as Electron capture dissociation (ECD) (Zubarev et al. 1998) and electron transfer dissociation (ETD) (Syka et al. 2004) can be used. These fragmentation method allows the PTMs to be intact and this is because it dissociates peptides in a non-ergodic manner and inducing random breakage of peptide backbone from cleavage of the C α -N bond generating *c* and *z* ions. For the ECD and ETD product to be observable, the precursor ion must hold at least two positive charges. The electron capture by singly charged ion leads in net charge of zero which cannot be detected by mass spectrometry. Several proteomics experiments uses both ETD and CID to have more comprehensive peptide sequence analysis (Kim et al. 2011; Shen et al. 2011).

Mass spectrometers can carry out several tandem mass spectrometry experiments automatically. This is vital for analysing samples with thousands of peptides. However, it is too difficult technically to sequentially select each single ion observed and perform MS/MS. Proteomics studies can be focussed on the quantification and identification of peptide/protein as many as possible. This can be done by using liquid chromatography to achieve peptide separation and collecting ion spectra on the eluting peptides by data-dependant acquisition (DDA) or by data-independent acquisitions (DIA).

Thousands of ions mass spectra are generated from proteomics works. It is essential to use bioinformatics approaches to analyse the data obtained. *In silico* digestion can be performed to generate list of peptide mass and linked fragment ions, based on the fragmentation and protease used. This is only done if the database including protein sequence is available. The database searches are performed once experimental data obtained are matched to theoretical data to infer peptide identification and protein originated from those peptide. In cases where database of an organism is not available, expermtinal data can be searched against non-specific database to find the most related sequences in other organism. Also, data can be interpreted using de novo method which work by assigning primary sequence from the MS/MS manually.

2 Background

2.1 Tumours and tumour growth

2.1.1 Definition of tumours and cancer

Tumour can be defined as cells or tissue with abnormal growth characteristics. Tumours cannot respond to growth and maturation signals or even differentiation factors. The three main types of tumour:

Benign tumours – These can be observed in any tissue. Benign tumours can grow locally but lack the ability of spreading to distant tissues. They can cause damage by obstruction or local pressure. Several types of benign tumours do not become malignant. In most cases, benign tumours are removed surgically and this is due the risk of becoming malignant in the future.

In situ tumours – These types of tumours found in the epithelium and mainly are small sized and non-invasive.

Cancers - Fully developed tumours with malignant characteristics. They have the ability to attack, evade and destroy neighbouring mesenchymal tissues. They can arise in any tissue and also have the ability to develop their own blood vessels and seeds another tumours in a process called metastasis.

The hallmarks of cancer was first proposed by Hanahan and Weinberg in 2011. (Hanahan and Weinberg, 2011). There are six biological characteristics which are essential in cancer development: (i) evading growth suppressors, (ii) sustained proliferative signalling, (iii) replicative immortality, (iv) angiogenesis, (v) invasion and metastasis and (vi) resistance of cell death. Moreover, there are further emerging hallmarks of cancer such as evading immune system and reprogramming energy metabolism.

One of the key aspects of the six hallmarks in cancer is evading growth suppressor. This relies on tumour suppressor genes actions (Hanahan and Weinberg, 2011). There are several tumour suppressor gene but the two main tumour suppressor genes are: tumour suppressor P53 (TP53) and retinoblastoma-associated (RB). These two proteins play a vital role in controlling and maintaining cell proliferation and the activation of senescence and apoptotic programmes.

Another emerging hallmark of cancer is the characteristic of reprogramming energy metabolism, with respect to non-tumour tissue (Hanahan and Weinberg, 2011). High level of metabolic energy aids and helps cell growth and division in premature tumours. Moreover, aerobic glycolysis is one of the phenomenon of tumours. In non-malignant cells, when there is low oxygen supply of hypoxia, cellular metabolism switches to high flux of anaerobic glycolysis – the conversion of D-glucose to L-lactate. Once the concentration of oxygen returns to normal, non-malignant tissues decreased anaerobic glycolysis and again utilize aerobic glycolysis – oxidation of pyruvate oxidation to CO₂. In malignant tissues, there is a high rate of conversion of glucose to L-lactate even under well-perfused and oxygenated conditions. This is referred to as tumour “aerobic glycolysis”. It was first showed by Otto Warburg and is termed as the “Warburg effect” (Warburg and Dickens, 1930). It has been suggested that this is an adjustment to intermitted hypoxia in pre-malignant lesions may confer a growth advantage (Gatenby and Gillies, 2004). Moreover, an increase in pentosephosphate pathway activity provides pentoses for nucleotide synthesis and an increased flux of NADPH for biosynthesis (Mitsuishi et al., 2012). It is thought the Warburg effect is part of a wider spectrum of metabolic reprogramming in tumour to offer growth, tissue invasion and metastasis with a varying nutrient supply (Warburg and Dickens, 1930).

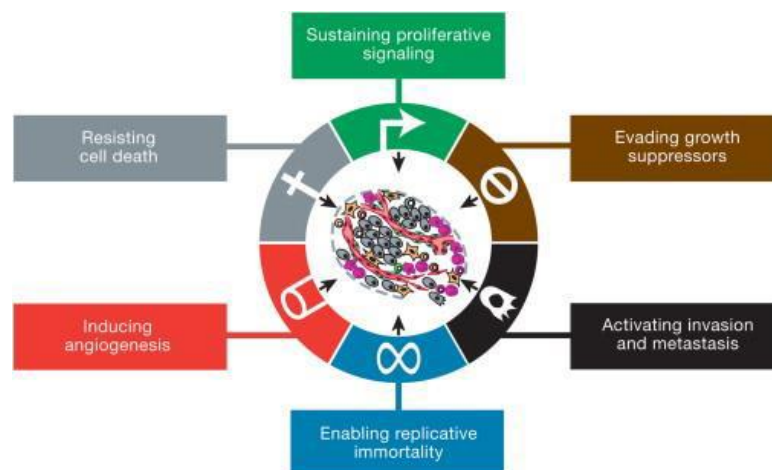


Figure 16. The hallmarks of cancer proposed by Hanahan and Weinberg (Hanahan and Weinberg, 2011).

2.1.2 Social impact of cancer

Cancer is a disease considered to be one of the major current health issues. The World Health organisation (WHO) reported in 2012 that there were 14 million new cases of cancer globally. In the same year, the estimated number of deaths globally from cancer was 4.7 million males and 3.5 million females. The most common type of cancer causing death in males is lung cancer. In contrast, breast cancer is the most common cause of death by cancer in females. The most common cancer types globally are: cancers of the lung, bowel, breast stomach and prostate cancer. In the USA, common types of cancer are: lung, prostate and colorectal cancer which occurred in 42% of all cancer in men. The most common cancer types in females are: breast, lung and colorectal (Siegel et al., 2015). In the UK, the most common cancer types in female are breast and lung cancers while in males prostate and lung cancers are the most common (Office for National Statistics, 2015). In 2014, the number of deaths caused by cancer in the UK was ca. 160,000: 53% males and 47% females. Gender differences plays a vital role in cancer death rates. Cancer is the most common cause of death in the UK.

Survival rates in cancer treatment in the UK have improved over the last 50 years – Figure 7. This is because of improved treatment and early diagnosis. Some types of cancer still poor survival rates - such as pancreatic cancer. Between 1971 to 2011, there was a minor improvement in survival rate for most cancers, except for pancreatic cancer.

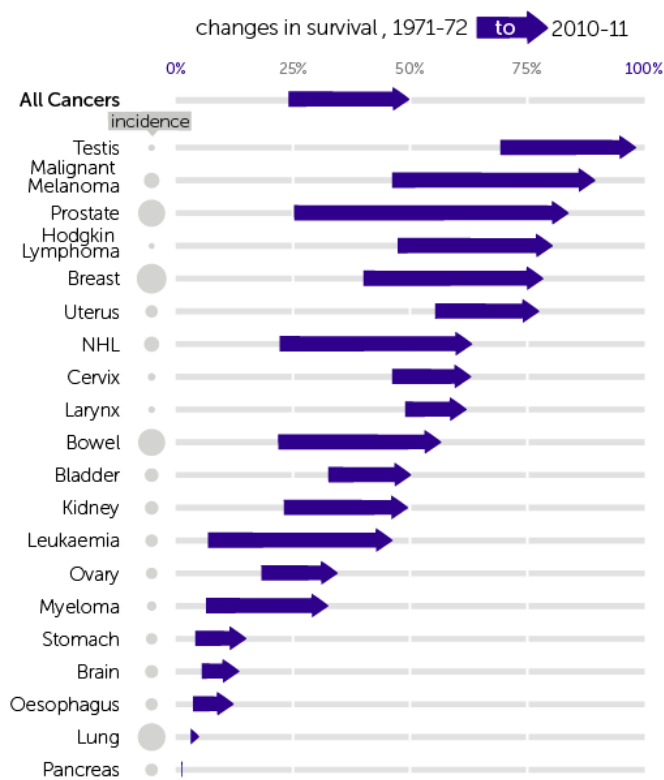


Figure 17. Survival rate changes from 1971-2011 for different types of cancer in the UK
(Quaresma et al., 2015)

Estimated New Cases					
		Males	Females		
Prostate	161,360	19%		Breast	252,710 30%
Lung & bronchus	116,990	14%		Lung & bronchus	105,510 12%
Colon & rectum	71,420	9%		Colon & rectum	64,010 8%
Urinary bladder	60,490	7%		Uterine corpus	61,380 7%
Melanoma of the skin	52,170	6%		Thyroid	42,470 5%
Kidney & renal pelvis	40,610	5%		Melanoma of the skin	34,940 4%
Non-Hodgkin lymphoma	40,080	5%		Non-Hodgkin lymphoma	32,160 4%
Leukemia	36,290	4%		Leukemia	25,840 3%
Oral cavity & pharynx	35,720	4%		Pancreas	25,700 3%
Liver & intrahepatic bile duct	29,200	3%		Kidney & renal pelvis	23,380 3%
All Sites	836,150	100%		All Sites	852,630 100%
Estimated Deaths					
		Males	Females		
Lung & bronchus	84,590	27%		Lung & bronchus	71,280 25%
Colon & rectum	27,150	9%		Breast	40,610 14%
Prostate	26,730	8%		Colon & rectum	23,110 8%
Pancreas	22,300	7%		Pancreas	20,790 7%
Liver & intrahepatic bile duct	19,610	6%		Ovary	14,080 5%
Leukemia	14,300	4%		Uterine corpus	10,920 4%
Esophagus	12,720	4%		Leukemia	10,200 4%
Urinary bladder	12,240	4%		Liver & intrahepatic bile duct	9,310 3%
Non-Hodgkin lymphoma	11,450	4%		Non-Hodgkin lymphoma	8,690 3%
Brain & other nervous system	9,620	3%		Brain & other nervous system	7,080 3%
All Sites	318,420	100%		All Sites	282,500 100%

Figure 18. Estimated number of cancer death and incidence in 2017 in the USA.
Form (Siegel et al., 2017).

2.1.3 Clinical treatment of cancer

There are three main methods for tumour treatment in clinical settings:

Surgical resections – Tumours are removed by surgery. This method is only suitable for solid mass tumour.

Radiotherapy – This type of treatments act by ionizing radiation. The current application involves the use of high energy photon (x- rays, gamma rays) and particles beams (light-ions, electrons, protons, helium and heavy ions – neon, argon , silicon ions) (Baumann et al., 2016).

Chemotherapy – tumour treatments with drugs. This includes immunological reagents. (Chabner and Roberts Jr, 2005).

Recent developments are cell-based therapy, specifically T-cells engineered to have the ability to express chimeric antigen receptor (CARs) or engineered T cell receptor to enhance host immune response to tumours (Fesnak et al., 2016).

These treatment options can be used as mono or combined therapy. In most cases, surgery is used as the first line of treatment. Radiotherapy is usually used in combination with surgery. However, certain cancer types cannot use surgery as treatments; for instance, leukaemia. Around 45% of new cancer cases are managed using radiotherapy. The number of cases where radiotherapy are used is increasing with new approaches such as the use of particle ion therapy, customised based on type and stage of tumour a precision medicine approach (Urruticoechea et al., 2010, Baumann et al., 2016). Radiotherapy is mainly used in head and neck tumours. Combination of surgery and radiotherapy are used but in a limited cases such as oesophageal and rectal carcinoma (Weichselbaum et al., 2017).

In 1940, cancer chemotherapy was first proposed to be used in cancer treatment. The historical development of cancer chemotherapy. reviewed in- (Chabner and Roberts Jr, 2005). Radiotherapy along with surgery was the common treatment method used in cancer in the 1960s. This became notable that cure rates had maximised it around 33%. This is because of the existences of unaddressed micro-metastases. Later studies suggested that combined

chemotherapy can cure patients even at advance stages. Early studies proposed the use of alkylating agents such as “nitrogen mustered” derivatives and anti-folates such as methotrexate. Development of anti-cancer agents improved remarkably in the 1970: in the period 1966 – 2000, > 28 anticancer drugs were registered for use by the USA Food & Drug Administration (FDA). The development of anti-cancer drugs has declined since then.

The historical advancement of the anticancer agents can be broadly divided into three main types (Dobbelstein and Moll, 2014) – Figure 9. Firstly, drugs targeting DNA replication and cell division blockage. For example, cancer agents act by modifying DNA or interfering with tubulin associations (Dobbelstein and Moll, 2014). The second type used drugs to target cell signalling contributing to cancer growth - primarily targeting receptors and kinases (for instance, BRAF). Recently, the third type of drug has been developed which acts by targeting cellular machineries and is not involved directly in DNA replication or cell division but it is highly important in tumour growth and survival. For instance, the proteasome, chaperones and modifier of chromatin (Dobbelstein and Moll, 2014).

In the last century, the DNA modifying agents were used to treat lymphoma in 1943 (Gilman and Philips, 1946, Goodman et al., 1946). Later, the use of such drugs developed based on clinical observation (Mukherjee, 2010). For instance, topoisomerase inhibitors and platinum derivatives are still considered to be one the most used chemotherapeutic agents. They are still used in treatment of testicular carcinoma and leukaemia in children (Travis et al., 2005). In the last two decades, several types of chemotherapy have been developed to target specific singling pathway or oncogene. Example: imatinib (Novartis) - a small molecule inhibitor of BCR-ABL used for treating Philadelphia chromosome positive myeloid leukaemia CML (Chakravarty et al., 2016). Monoclonal antibodies can be used to target cell surface receptors that are expressed specifically on cancer cells. For instance, trastuzumab (Herceptin) is a monoclonal antibody specific for HER2 and used to treat approximately 25% of breast cancer with overexpression of HER2 (Vogel et al., 2002).

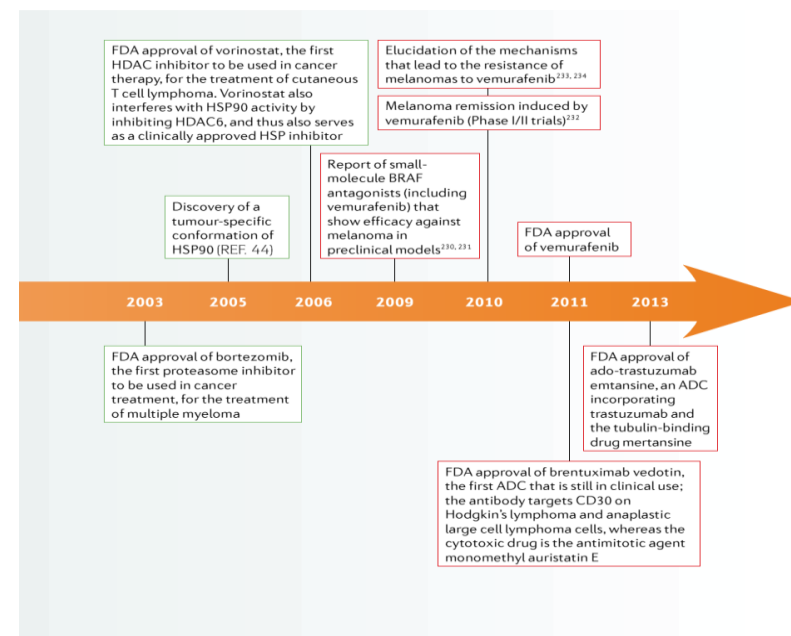
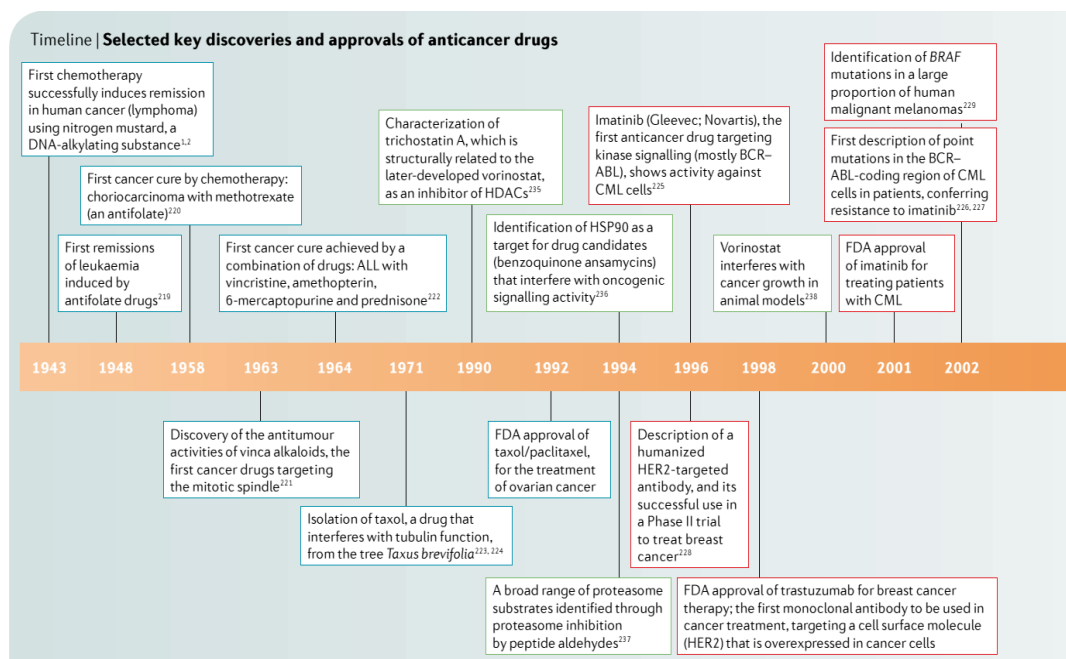


Figure 19. Key discoveries of anticancer drugs (1943-2013).
From (Dobbelstein and Moll, 2014).

Table 3. Anticancer drugs that target cell surface molecule and signalling intermediates. From (Dobbelstein and Moll, 2014).

Stress condition	Targets	Drugs
<i>Well established for clinical use</i>		
Replicative stress	Enzymes for nucleotide synthesis	Nucleoside analogues: for example, 5-fluorouracil (5-FU) and gemcitabine
	DNA polymerases	Nucleoside analogues: for example, gemcitabine or cytosine-arabinside (AraC)
	Topoisomerases	Topoisomerase inhibitors: for example, anthracyclines (doxorubicin, daunorubicin, epirubicin), camptothecin and irinotecan
Mitotic stress	Microtubules, mitotic spindle	Taxanes (paclitaxel, docetaxel), epothilones (ixabepilone, patupilone, sagopilone) and vinca alkaloids (vincristine, vinblastine)
DNA damage	DNA	Platinum compounds (cisplatin, carboplatin, oxaliplatin) and alkylating agents (cyclophosphamide, ifosfamide)
<i>More recently developed drugs</i>		
Altered chromatin dynamics	HDAC enzymes, DNA methyltransferases	SAHA (vorinostat), romidepsin LBH589 (panobinostat) azacytidine and decitabine
Proteotoxic stress: protein folding	HSP90	Geldanamycin, 17-AAG ,ganetespib and NVP-AUY922
Proteotoxic stress: protein degradation	20S core unit of the proteasome	Bortezomib and carfilzomib

2.1.4 Refractory tumour and multidrug resistance in chemotherapy

One of the main treatment approaches in cancer is the use of chemotherapy. It often has limited effectiveness due to multidrug resistance (MDR). The resistance of chemotherapy can be divided widely into two categories: acquired and intrinsic (Holohan et al., 2013). The presence of pre-existing factor in the bulk of tumour cells leading to ineffective treatment is known as intrinsic resistance. Acquired resistance is due to mutations or other changes in tumours that were originally chemotherapy sensitive. For example, increased expression of target therapeutic and alternative activation of signalling pathways. There are three levels of multidrug resistance (MDR): macroscopic level (systemic), mesoscopic level (regional) and microscopic level (local). (Alfarouk et al., 2015) – Figure 10.

MDR is influenced by both pharmacodynamics and pharmacokinetic factors. The effect of pharmacokinetic happens when drug undergoes absorption, distribution, metabolism and elimination process (ADME) resulting in limited systemic administration of drug to reach the location of tumour. The activity of anti-cancer drugs could be limited due to insufficient drug reaching the tumour by decreased influx or excessive efflux (Alfarouk et al., 2015). Decreased drug activation and increased drug inactivation may cause MDR (Holohan et al., 2013). This type of MDR can affect both molecular targeted agents and chemotherapeutic agents. For instance, glutathione can inactivate platinum drugs (Meijer et al., 1992).

One of the key roles influencing drug resistance is DNA damage repair. Several cancer chemotherapeutic agents induce DNA damage. This damage to the DNA can be indirect such as topoisomerase inhibitors or directly such as platinum-based drugs. DNA damage can also induce cell cycle arrest which has an involvement in allowing cells to repair damage. In some cancer types, regulation of cell cycle is interrupted leading to loss of function and alteration to tumour suppressor gene and gain of function alteration to oncogene. For example, mutation of p53 can affect the DNA damage. It is known that p53 has a vital role in cell cycle checkpoint and apoptosis regulation (Enoch and Norbury, 1995). p53 mutation is frequently related to MDR (Holohan et al., 2013).

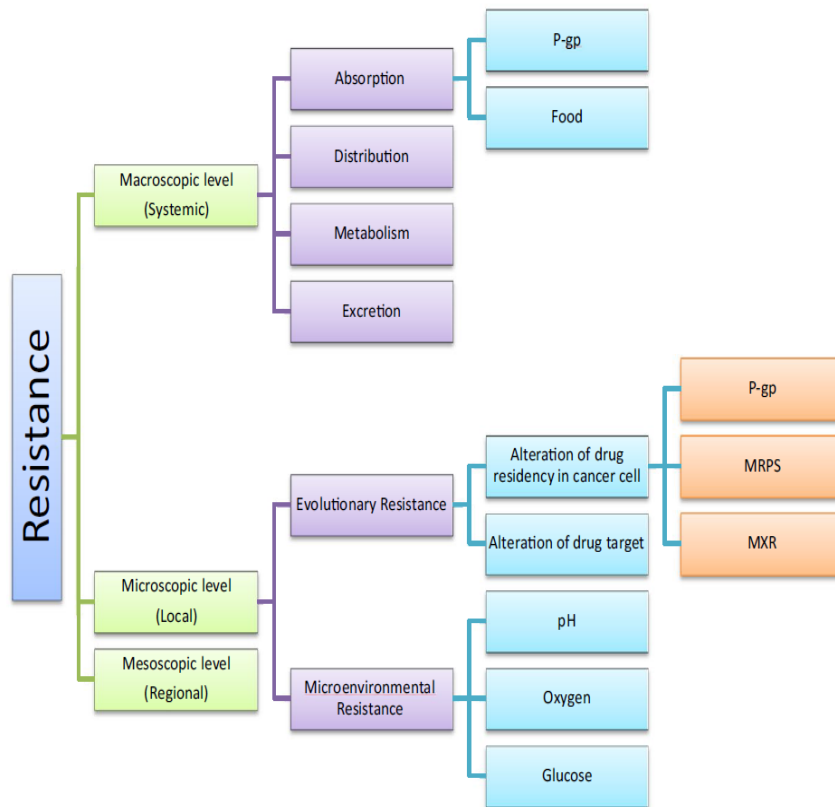


Figure 20. Multidrug resistance types in cancer chemotherapy.

P-gp is permeability glycoprotein defined as multidrug drug resistance protein. MRPs is multidrug resistance associated protein. Association of MRP and MDR identified first on lung cancer cell line. MXR is mitoxanthrone resistance protein – a protein involved in trafficking biological molecules in cell membrane (Alfarouk et al., 2015).

2.2 Role of glyoxalase system in cancer

2.2.1 Historical

In the last century, there were several studies linking the glyoxalase system with cancer treatment and development. Furthermore, in 1923 Warburg proposed that increased aerobic glycolysis is one tumour characteristics tumours (Warburg and Dickens, 1930). Although there was no clear relation to the glyoxalase system, it has an important consequences for flux differential of MG via the glyoxalase system in non-tumour and tumour tissues. Platt and Schroeder and Jowett and Quastel reported the glyoxalase activity of malignant and non-malignant in laboratory rodents (Jowett and Quastel, 1934, M. E. Platt, 1934). In 1955, McKinney and Rundles reported glyoxalase activity in human malignancies of human leukaemia (McKinney and Rundles, 1956). French and Freedlander first reported the anticancer activity of MG (Freedlander et al., 1958). The MG anti-tumour activity was investigated by Apple and Greenberg (Apple and Greenberg, 1968). Conroy showed later that MG treatment was ineffective - requiring a high dose of MG, rapid development of resistance and narrow therapeutic index (Conroy, 1979). This is due to metabolism of tumour tissue of MG by Glo1 and high capacity of non-malignant.

The development of Glo1 inhibitors suggested by Vince and Wadd (Vince and Wadd, 1969) in 1969 appeared to provide a more effective alternative. Although Glo1 inhibitor derived from glutathione thioethers was developed in 1969, it was lacking cell permeability and therefore could not reach Glo1 receptors in the cells. Lo and Thornalley later produced a Glo1 inhibitor which is a cell permeable Glo1 inhibitor prodrug, *S-p*-bromobenzylglutathione diester, which delivered the active inhibitor *S-p*-bromobenzylglutathione into cells and had potent anti-tumour activity both *in vivo* and *in vitro*. The diesterification stabilised Glo1 inhibitors from degradation by γ -glutamyl transferase and provided pro-drug modifications which aid cell permeability and entry inside the cell (Lo and Thornalley, 1992, Thornalley, 1996). Creighton and co-workers later developed more potent Glo1 inhibitors (Creighton et al., 2003). In 1974, Jerzykowski and co-workers reported that Glo2 activity was absent or had very low activity in tumours of human and laboratory rodent origin (Jerzykowski et al.,

1975), with a re-evaluation of similar conclusion published in 1978 (Jerzykowski et al., 1978).

In 2000, a notable relation between high expression of Glo1 in tumours and MDR in cancer chemotherapy was discovered by Sakamoto and colleagues. Further studies showed that tumours with high Glo1 expression are sensitive to Glo1 inhibitors (Sakamoto et al., 2001, Sakamoto et al., 2000). Furthermore, recent studies shows Glo1 gene amplification is one of the causes to increase Glo1 expression in some human tumours (Santarius et al., 2010). Recently, studies have shown that prevalence of increased GLO1 copy number and expression in human tumours negatively correlates to patient survival - reviewed in (Rabbani et al., 2018). Mechanism of elevated GLO1 copy number is thought to be through the activation of histone demethylase KDM4A/JMDJ2a in hypoxia (Shafie et al., 2016).

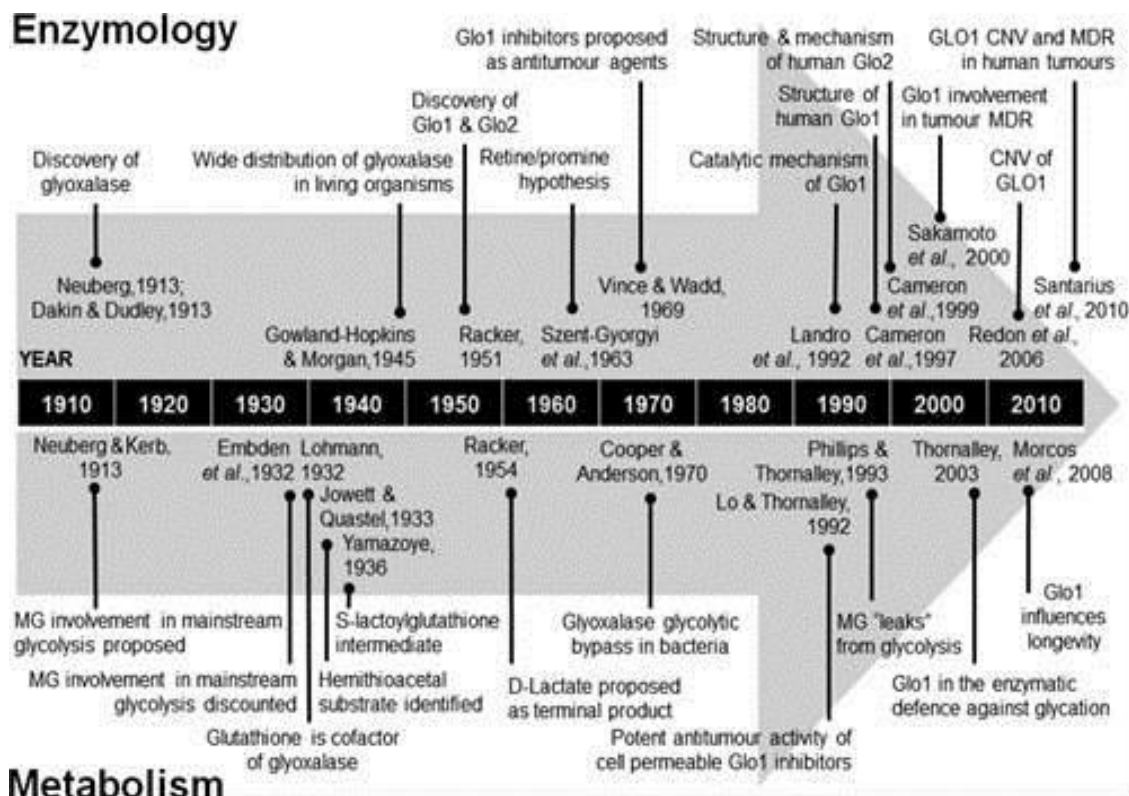


Figure 21. The historical timeline of the glyoxalase system: from the discovery of the glyoxalase system in the last century until the 2010.
From (Rabbani et al., 2018).

2.2.2 Glyoxalase 1 and tumour growth

Increased expression and activity of Glo1 in human tumours has been found in several studies – reviewed in (Thornalley and Rabbani, 2011a). It has been proposed that Glo1 is an oncogene. However, overexpression of Glo1 experimentally does not increase cell growth or malignancy *in vitro* nor *in vivo*. This suggests Glo1 is not an oncogene. In the non-malignant state, Glo1 act as tumour suppressor gene (Rabbani et al., 2018).-Glo1 is likely increased in tumours to protect against increased flux of formation of MG associated with increased tumour glycolysis. Many tumours have elevated anaerobic glycolysis (Rabbani et al., 2018).

Hypoxia is a potential threat to tumour cell survival through dicarbonyl stress. Hypoxia normally induces down regulation of Glo1 expression through a putative hypoxia response element (HRE) in the GLO1 gene and stimulation of hypoxia-inducible factor 1-alpha (HIF1 α). Hypoxia may increase the flux of formation of MG, due to switching of cells to dependence on anaerobic glycolysis. Some tumours have, however, subverted this control and increase Glo1 expression in hypoxia (Rabbani et al., 2018). This metabolic limitation may in future be exploited for therapy using cell preamble Glo1 inhibitor in hypoxia altered tumours (Hutschenreuther et al., 2016, Takeuchi et al., 2010).

2.2.3 Glyoxalase 1 and multidrug resistance

The link between elevated Glo1 expression and anticancer drug resistance was first observed by a wide transcriptome-wide study of gene expression in cell line survival (Sakamoto et al., 2000). Several anti-cancer drugs are expected to increase cellular MG concentration as part of their cytotoxic effect. Later studies revealed that the cell permeable Glo1 inhibitor, S-p-bromobenzylglutathione cyclopentyl diester (BBGCp2), offered effective treatment for tumour cell line *in vitro* and tumour bearing mice with Glo1 linked MDR (Hosoda et al., 2015, Santarius et al., 2010). Tumours with elevated Glo1 expression show a high sensitivity to short hairpin RNA knockdown of Glo1 in xenograft tumours primary culture from HCC cells. This may lead to an assumption that cell preamble Glo1 inhibitor can be used for chemotherapy treatment in HCC (Zhang

et al., 2014). The overexpression of Glo1 is likely to have a major impact on MDR in prevalent refractory tumours in clinical treatment (Rabbani et al., 2018).

Furthermore, the overexpression of Glo1 may also predict the outcome of treatment. For instance study conducted in colorectal cancer showed that the increase of Glo1 protein evaluated by immunohistochemistry IHC was linked with rapid tumour progression and poor survival (Sakellariou et al., 2016).

The overexpression of Glo1 may also contribute to ineffective treatment outcome in other type of treatment such as surgery and radiotherapy. This is due to the elevated level of Glo1 expression is permissive of increased glycolytic rate and growth of tumours. For instance, recent research on neuroendocrine tumours (NETs) showed the Glo1 expression acts as negative survival factor in patients treated by surgery (Xue et al., 2017).

2.2.4 GLO1 gene copy number in cancer

GLO1 copy number is one of the factors influencing the Glo1 expression (Santarius et al., 2010). The Thornalley group was the first to note the increased Glo1 expression and GLO1 copy number (gene copy number >2) in human tumours in 2010 (Santarius et al., 2010). In tumours, GLO1 DNA is elevated higher than gene duplication in healthy individuals (Redon et al., 2006). Furthermore, increased GLO1 copy number correlates with increased Glo1 mRNA expression and protein in clinical tumours. In 225 human tumours of variable types, the top prevalence of GLO1 copy number increase was in: breast cancer (22%), sarcomas (17%) and non-small lung cancer (11%) (Santarius et al., 2010). Additionally, several *in vitro* studies proposed that GLO1 copy number increase may play an important role in MDR (Rabbani et al., 2018).

The mechanism of increase in GLO1 copy number is not fully understood. Insights were gained from mouse embryonic stem cell studies in hypoxia suggesting that low level Glo1 copy number was induced in hypoxia conditions (Shafie et al., 2016). It is proposed that during hypoxia histone demethylase KDM4A/JMD2A may mediate the increase in copy number of GLO1. The high level of demethylation is assumed to generate more open chromatin which stimulates incorrect dwell time of mini-chromosome maintenance (MCM)

proteins and DNA polymerases at the GLO1 locus and thereby produce replication and increase of GLO1 copy number (Black et al., 2013). Hypoxia activates KDM4A demethylation to possibly increase GLO1 copy number. There is a high expression of KDM4A in multiple tumours which also involved in metabolic reprogramming of increased tumour anaerobic glycolysis (Wang et al., 2016). The high level of GLO1 copy number in early development of tumours may become dominant through clonal selection to MDR. Anticancer agents may also lead to an increase in MG concentration and enhance GLO1 copy number increase (Rabbani et al., 2018) - Figure 12.

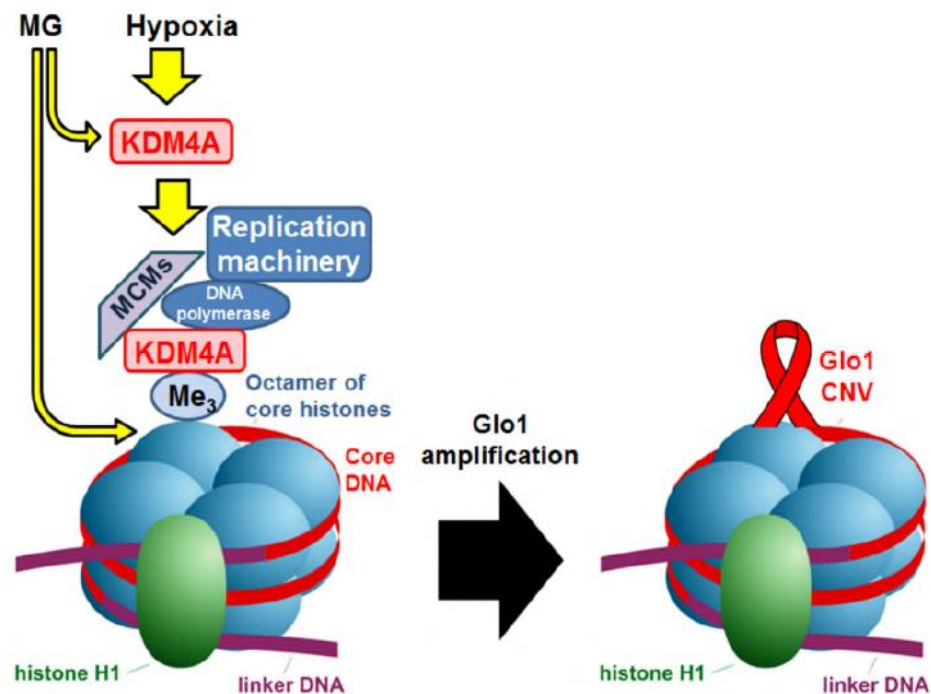


Figure 22. Suggested mechanism of GLO1 gene amplification.
From (Rabbani et al., 2018).

2.2.4.1 GLO1 copy number variation

In human subjects, GLO1 gene is found in chromosome 6 at locus 6p21.2 (Tripodis et al., 1998). Gene cloning method revealed that human GLO1 coding region comprises of 12kb with introns splitting six exons (Ranganathan et al., 1999, Gale and Grant, 2004). Copy number variation (CNV) of GLO1 was first shown by Redon *et al.* by investigating 270 subjects from different population

around the world. They found 1447 CNV regions were established covering only 12% of the human genome. There was only five subjects with copy number increase, suggesting a GLO1 duplication prevalence of approximately 2% (Redon et al., 2006). Latter studies confirmed GLO1 CNV in the human population and other primates (Wong et al., 2007, Perry et al., 2008).

In mouse, *Glo1* is found in chromosome 17 at locus 17a3.3, almost 3cM from Ss locus of the H-2 histocompatibility region (Meo et al., 1977). Murine *Glo1* was initially reported among inbred mice strains. The CNV was categorised as 475 kb tandem duplication on chromosome 17 (30174390–30651226) which involved *Glo1* copies and other gene copy partly (Williams et al., 2009). Latter reports found *Glo1* CNV as part of genome-wide study. Studying the CNV content to sub-10-kb resolution, more than 1300 regions of CNV were found in sapping 3.2% of the genome. The majority of CNVs mapped outside of the transcribed regions of genes. Approximately 600 CNVs were linked with gene expression changes with only three genes were found with high expression (Schrider and Hahn, 2010). GLO1 was one of these genes with functional CNV increase in all tissues tested – haematopoietic, hypothalamus and adipose tissue (Schrider and Hahn, 2010, Cahan et al., 2009, Xue et al., 2011).

2.2.4.2 Methods of measurement of gene copy number

CNVs discovery was one of the result of the new genomic technologies which have enabled a high resolution of Genomic DNA analysis. There are different methods can be used to detect CNVs, both at locus specific level or genome wide scale. The primary genome wide scale screening approach involves array comparative genomic hybridization (aCGH), fluorescence *in situ* hybridisation (FISH), next generation sequencing and single nucleotide polymorphism. Moreover, the primary approach in locus specific methods consist of multiplex ligation dependent probes amplification (MLPA), paralogue ratio test (PRT) and quantitative polymerase chain reaction (qPCR).

2.2.5 Anticancer activity of methylglyoxal

The cytotoxicity of increased cellular MG was investigated by inhibiting Glo1 expression by siRNA silencing of Glo1, by the addition of cell permeable Glo1 inhibitor and addition of exogenous MG (Rabbani et al., 2018). The use of exogenous MG has its drawbacks as it offers a steep negative concentration from the outside to the inside of the cells. Furthermore, commercial MG often used by some investigators contains formaldehyde and other compound contamination (Pourmotabbed and Creighton, 1986, Rabbani and Thornalley, 2014c).

Studying the changes occurring early in the time course of cytotoxicity under MG concentrations is important to understand the key process mediating MG inhibition of cell growth in tumours (Rabbani et al., 2018). Research conducted on human leukaemia 60 (HL60) cells in vitro shows their commitment to death occurs at primarily one point of cell cycle growth (Ayoub et al., 1993). Additionally, analysis of cell cycles treated with MG showed by 12 hour there is an increase formation of cells G₀-G₁, low number of S-phase and apoptosis induction. This is suggest that cells are commit to death and arrested at the S-phase entry and DNA synthesis is inhibited (Ayoub et al., 1993). Time courses experiment using [¹⁴C]MG revealed adduct formation of protein, DNA and RNA. MG adducts with DNA is elevated shortly after 2 hours (Ayoub et al., 1993).

Addition of exogenous MG, Glo1 siRNA silencing and cell preamble Glo1 inhibitor initiate tumour cells apoptosis under concentration-response limited conditions – using MG concentrations close to the median toxic concentration TC₅₀ (Kang et al., 1996, Thornalley et al., 1996, Santarius et al., 2010). High concentrations of MG induced necrosis in tumour cells (Du et al., 2000) – Table 4. Key factors are: reduction of the mitochondrial membrane potential, initiation of mitochondrial apoptotic pathway with release of cytochrome c into the cytosol; activation of cascapase-3 and cascapase-9 and decreased anti-apoptotic factors, and growth at entry into the S-phase of the cell cycle.

It is likely that MG initiate mitochondrial apoptotic pathway by modifying a high conductance channel protein known as mitochondrial permeability transition pore protein (MPTP). Elevated level of MG-H1 residues production by the increasing the cytotoxic level of MG may result in membrane depolarisation

and swelling, cytochrome c release (Speer et al., 2003). In the downstream, caspase -3 and casapase-9 are activated and interact with XIAP, Bcl-xL and BCL2 (Czabotar et al., 2014). Activation of Chk1, Chk2 and ATM kinases may be in response to DNA damage induced by MG modification (Rabbani et al., 2018). MGdG is known to be the major adducts from MG which converted DNA to a single strand breaks (ssDNA). Coating of ssDNA occurred rapidly by ssDNA-binding protein replication protein A (RPA). As result of DNA damage, Chk1/2 and other proteins intra-S-phase proteins are activated which causes replication delay (Tapia-Alveal et al., 2009). Once DNA damage is too high for repairing procedures, DNA undergoes stall replication termed as “replication catastrophe” which then initiates apoptosis or necrosis as reviewed (Dobbelstein and Sørensen, 2015).

Table 4. Mechanism of methylglyoxal induced cell death from
(Rabbani et al., 2018)

Cell type	[MG] (μ M)	Characteristics	References
HL60 (acute myeloid leukaemia)	238 33 – 524	GC ₅₀ : 282 μ M. 24 h exposure period required for growth inhibition and toxicity. Growth inhibition increased with medium serum content (growth rate). Apoptosis. Growth inhibition linked concentration-dependently to inhibition of DNA synthesis; early decrease in S-phase cells. Protein adducts maximized at 30 min and DNA adducts at 1 h.	(Taylor et al., 2015) (Dandona, 2004)
LNCaP (androgen-sensitive Prostate adenocarcinoma)	1,000	Activates mitochondrial apoptotic pathway potentiated by Glo1 silencing	(Brownlee, 2005)
HEK393 cells	400 & 800	Activation of ATM-Chk1 and Chk2 kinases, p38 kinase, MAPK and ASK1-JNK, kinase pathways.	(Preshaw et al., 2013)
Jurkat (T-cell leukaemia), MOLT-4 (T-cell leukaemia), and HeLa (cervical adenocarcinoma)	250 & 500	Apoptosis (250 μ M) with necrosis (500 μ M). JNK and caspase-3 driven apoptosis	(Paraskevas et al., 2008)
Jurkat cells	250	MG-induced activation of caspase-3 and caspase-9, release of cytochrome c, decline of mitochondrial membrane potential and JNK activation	(Preshaw et al., 2007)
SW480 colonic cancer cells	100 - 500	MG suppressed the expression of anti-apoptotic factor XIAP, survivin, cIAP1, Bcl-2, and Bcl-xL. Potentiated TRAIL apoptosis. GLO1 siRNA had the same effect.	(Salvi et al., 1997)

MCF7,MDA-MB-231,T47D	100 – 1,600	Growth inhibition, decreased invasiveness and tubule formation, MAPK activation and decreased Bcl-2 at $\geq 800 \mu\text{M}$ MG, increasing apoptosis; decreased cell migration at $400 \mu\text{M}$; decreased colony formation at $100 - 200 \mu\text{M}$. GLO1 siRNA had the same effect.	(Engbretson et al., 2004)
-----------------------------	-------------	---	---------------------------

Thus, cell death induced by MG involves both the mitochondrial and DNA damage activated apoptotic pathways. Decreased angiogenesis may also occur due to MG modification to of extracellular matrix (ECM) proteins and blockage of integrin migration (Dobler et al., 2006, Ahmed et al., 2008). MG modification of ECM protein induced cell detachment which result in cell detachment-activated cell death where apoptosis is activated extrinsic pathway termed anoikis. The missing contact of ECM results in death receptor activation and the intrinsic pathway-mitochondrial apoptotic pathway (Paoli et al., 2013).

A study by Oya and colleagues revealed the ability of MG to modify heat shock protein HSP27 (Oya et al., 1999). Heat shock protein has anti-apoptotic activity in the mitochondrial apoptotic pathway. MG modification may result in HSP27 suppression effect in the apoptotic pathway of the mitochondria. It is thought that this modification is caused by argpyrimidine but this is unlikely because argpyrimidine is minor MG derived AGE (Rabbani et al., 2018). Current study by Thornalley group suggest that MG-modified protein using direct detection with high resolution mass spectrometry, MG-H1 residues modify HSP27 at arg-188 in cell proteins incubated with exogenous MG not argpyrimidine out of 344 protein modified in the cell cytosol (Rabbani and Thornalley, 2014). Cytotoxic mechanism through MG accumulation in tumour cell are summarised in Figure13.

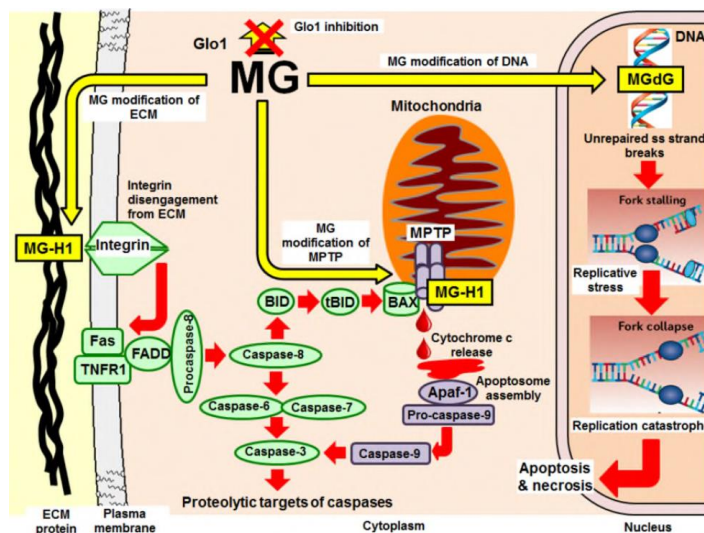


Figure 23. Mechanism of cytotoxicity of cell permeable Glo1 inhibitor through cellular accumulation of methylglyoxal in tumour cells.From (Rabbani et al., 2018)

2.2.6 Cell permeable glyoxalase 1 inhibitors as anticancer agents

Vince and Wadd was the first scientists to propose Glo1 inhibitors. This was based on substrate analogues, glutathione S-thioethers such as S-p-bromobenzylglutathione (Naguib et al., 2004, O'Connell et al., 2008). This inhibitor lacked effectiveness because it was not permeable to the plasma membrane in tumour cells and lack stability to degradation by cell surface γ -glutamyl transpeptidase. Thornalley and colleagues produced a cell permeable Glo1 inhibitor prodrug by diesterifying S-p-bromobenzylglutathione. The deesterification prevented the extracellular degradation and provided a key solution species that was membrane permeable: the unprotonated S-p-bromobenzylglutathione diester. Once inside cells, the prodrug was de-esterified by cellular non-specific esterase. This produced the active inhibitor, S-p-bromobenzylglutathione, in the cell cytosol where it can access the receptor, Glo1. To date, the most potent diester derivative is the cyclopentyl diester, BBGCp2, which can resist hydrolysis by serum of plasma esterase prior delivery into cells (Iacopino, 2001). More potent Glo1 inhibitor were developed by Creighton and co-workers (Cohen, 2002). Several studies found potent cytotoxicity to tumour cell lines by using Glo1 SiRNA silencing (Cohen, 2002). This leads to an increase in cellular and extracellular level of MG which induces apoptosis and anoikis (Dauphinee and Karsan, 2005). This suggests that the Glo1 inhibitor is likely producing antitumor activity by on-target effects.

Although BBGCp2 achieved good efficacy of treatment in tumour-bearing mice, the dose required for potent therapeutic effect were high 50 – 200 mg/kg. However, at these doses, BBGCp2 does not have toxicity other than to the tumour. Other Glo1 inhibitor diester prodrugs had off-target effects and were toxic at effective doses (Covert, 2005, Patil et al., 2006, Jönsson et al., 2011). High dose requirement is due to the rapid metabolism and excretion of inhibitors (Sakamoto et al., 2001). This may not be so in human subjects as mice have much higher plasma esterase than human subjects (Sharkey et al., 2000).

MG may also be metabolised by aldoketo reductase isozymes 1A4, (aldose reductase), 1B19 and AKR isozymes to mainly hydroxyacetone (Rabbani and Thornalley, 2008a). Nrf2 upregulated the expression of these enzymes and they

may be over-activated in some tumours. This will lead to high capacity of MG metabolism by AKR in some tumour such as squamous cell carcinomas (SCCs) adenocarcinomas that has somatic alteration in Nrf2 pathway (Rabbani and Thornalley, 2012a).

Surveying the antitumor activity of BBGCp₂ has shown that some tumour cell lines are sensitive to Glo1 inhibitor and others are resistance. The lack of a sensitivity marker for Glo1 inhibitor hinders their development for cancer treatment.

2.3 Aim and objectives of this project

2.3.1 Aim

To characterise the dicarbonyl proteome involved in MG induced cytotoxicity and its role in cancer chemotherapy.

2.3.2 Objectives

Objective 1. To study Glo1 bioinformatics cancer cell lines and primary tumours.

To achieve this objective, I will access bioinformatics databases on Glo1 expression and copy number in human tumour cell lines and primary tumours. The Cancer Cell Line Encyclopaedia (CCLE) is a database of gene expression and gene copy number estimates for 1040 human tumour cell lines (<https://portals.broadinstitute.org/ccle>). I will studied factors linked to Glo1 expression. I will access the KM plotter database of human tumour gene expression and patient survival outcomes to investigate the role of Glo1 expression on patient survival and its effect in different chemotherapy and genotypic characteristics. <http://kmplot.com/analysis/>

Objective 2. To study methylglyoxal modification of proteins involved in methylglyoxal induced tumour cell death *in vitro*.

To achieve this objective, I will study changes in MG-modified proteins and unmodified proteins in HEK293 cells exposed to cytotoxic concentrations of MG. Changes in dicarbonyl proteome and unmodified proteome critical to MG induced cell death will be identified. An example of an MG-modified proteins likely critical to MG induced cell death is mitochondrial permeability transition pore (MPTP). These MG-modified proteins will be taken as biomarkers of MG-induced cytotoxicity.

Human embryonic kidney 293 (HEK-293) cells are widely used for transfection studies for overexpression a gene of interest (Rabbani and Thornalley, 2008a, Kavsan et al., 2011). This cell line generated first by Graham *et al.* with transformation of cells produced by human adenoviruses type 5 DNA (Thornalley and Rabbani, 2011b). HEK-293 cells are tumorigenic where alteration of cancer-linked gene expression increases tumorigenicity with high

chromosome instability. They proliferate fast *in vitro*. A successful example of Glo1 transfection of HEK-239 cells to overexpress Glo1 mRNA *in vitro* was performed by Hutschenreuther *et al.* and compared to mock-transfected cells.

Table 5. Medium growth inhibitory concentration GC₅₀ values of selected anticancer drugs in HEK-293 cells *in vitro*.

Anticancer drug	GC ₅₀ HEK-293 (μM)	Reference
Mechlorethamine	300 ± 9	(Hardej and Billack, 2007)
Methotrexate	45.4 ± 6.9	(Patel and Patel, 2011)
Doxorubicin	16.7 ± 0.7	(Dakin and Dudley, 1913)
Cisplatin	5.43 ± 0.72	(Akiyode et al., 2016)

2.3.3 Study hypotheses

The hypotheses of this study are:

1. *Increased Glo1 expresion is a negative survival factor for patients with breast cancer.*
2. *Changes in protein abundance and modification by methylglyoxal linked to key pathways of cell proliferation activate the mitochondrial pathway of apoptosis to mediate MG-induced cytotoxicity.*

3 Materials and Methods

3.1 Materials

3.1.1 Cells and tissues

Human embryonic kidney – 293 (HEK-293) cell line was purchased from American Type Culture Collection (ATCC), Manassas, VA 20110, USA.

3.1.2 Cell culture reagents

Foetal bovine serum (FBS) and Dulbecco's Modified Eagles Medium (DMEM) were purchased from Thermos Fisher (Paisley, UK).

Penicillin/streptomycin solution (10,000 U/ml penicillin with 10 mg/ml streptomycin) in 0.9% (w/v) sodium chloride solution. Tissue culture grade dimethylsulphoxide (DMSO) and dimethylformamide (DMF) were purchased from Sigma-Aldrich (Poole, Dorset, UK). Cell culture grade plastic polystyrene T75, T25 and flasks was purchased from Fisher Scientific (Loughborough, UK). Trypan blue stain (cat. no. 302643) was purchased from Sigma Aldrich (Poole, Dorset, U.K.).

3.1.3 Enzymes and other reagents

Proteases, peptidases, D-lactic dehydrogenase and other enzymes were purchased from Sigma-Aldrich. D-Lactic dehydrogenase (EC 1.1.1.28), lyophilised powder, was from *Staphylococcus epidermidis* and had activity of ≥ 80 units/mg protein. Pepsin (EC 3.4.23.1) was from porcine stomach mucosa with a specific activity of 3460 units/mg protein (1 unit hydrolysed haemoglobin with an increase in A280 of 0.001 AU per min of trichloroacetic acid-soluble products, at pH 2 and 37 °C); prolidase (EC 3.4.13.9) was from porcine kidney and had a specific activity of 145 units/mg protein, where 1 unit of activity hydrolyses 1.0 μ mol of Gly-Pro per min, at pH 8 at 40 °C; leucine aminopeptidase (EC 3.4.11.2), type VI, was from porcine kidney microsomes with a specific activity of 22 units/mg protein (1 unit of activity hydrolysed 1.0 mol of L-leucine-p-nitroanilide to L-leucine and p-nitroaniline per min at pH 7.2 and 37 °C); and pronase E (EC 3.4.24.31), type XIV, was from bacterial *Streptomyces griseus* with a specific

activity of 4.4 units/mg protein (1 unit of activity hydrolysed casein forming 1.0 mmol of tyrosine per min at pH 7.5 and 37 °C).

Trypsin/ethylenediaminetetra-acetic acid (EDTA) solution (porcine pancreas-derived trypsin 0.25% w/v EDTA 0.02 w/v) was acquired from Invitrogen Life technologies (Paisley, Scotland, UK).

3.1.4 Antibodies

All the antibodies were purchased from Abcam PLC for western blotting experiments. The antibodies used are: rabbit anti- β -actin polyclonal IgG (cat. no. ab8227), rabbit anti-aldose reductase polyclonal antibody (cat. no. ab62796), rabbit anti-DEAD-Box helicase 5 (DDX5) monoclonal antibody (cat. no. ab128928), rabbit anti-Glo1 monoclonal antibody (cat. no. ab137098), rabbit anti-splicing factor U2AF 65 kDa subunit (U2AF65) polyclonal antibody (cat. no. ab37530) and goat anti-rabbit IgG, heavy and light chain, horseradish peroxidase (HRP) conjugate secondary antibody (cat. no. ab6721). Human cytochrome c ELISA kit was purchased from Oncogene Research Products (San Diego, CA, USA).

3.1.5 Other analytical reagents

All the following reagents were purchased from Fisher scientific (all HPLC grade): tetrahydrofuran (THF), acetonitrile, methanol, isopropanol (IPA) and trifluoroacetic acid (TFA, $\geq 99\%$ HPLC grade). Trifluoroacetic acid (TCA, BioUltra, $\geq 99.5\%$), formic acid (FA, $\geq 98\%$), glycine, reduced glutathione (GSH), aminoguanidine hydrochloride (cat. no. 369494), nicotinamide adenine dinucleotide, oxidised form, (NAD⁺; cat. no. N6522), pyruvate (cat. no. P2256), D-lactic acid (cat. no. L0625) were purchased from Sigma Aldrich. Methylglyoxal (MG) for cell culture was prepared by the hydrolysis of methylglyoxal dimethylacetal in dilute sulphuric acid and purified by fractional distillation under reduced pressure, as previously described (McLellan and Thornalley, 1992b). Bovine serum albumin, triton-X100, diethylenetriaminepentaacetic acid (DETAPAC), tween-20, hydrochloric acid (analytical grade, 1 N; HCl) (cat. no. H1758), mannitol, sodium phosphate monobasic (cat. no. 71505), protease

inhibitor cocktail (cat: 10720825) and HaltTM phosphatase inhibitor cocktail (cat: 10668304) were purchased from Fisher Scientific. 10 x RIPA lysis buffer (cat. no. 20-188) (0.5 M Tris-HCl, pH 7.4, 1.5 M NaCl, 2.5% deoxycholic acid, 10% NP-40, 10 mM EDTA) was purchased from Millipore, UK. The 10 x premixed electrophoresis Tris-glycine buffer (cat. no. 1610732; 1 x dilution contains 25 mM Tris, 192 mM glycine, pH 8.3), 10 x Tris-buffered-saline TBS (cat. no. 1706435 ; 1 x dilution gives 20 mM Tris, 500 mM NaCl, pH 7.4), CriterionTM TGXTM stain-free gel 4–20 % precast polyacrylamide gel (cat. no. 3450412, 3450418, 3450426), Trans-Blot® TurboTM PVDF pre-cut blotting transfer pack (cat. no. 1704157), including filter paper, buffer, polyvinyl difluoride (PVDF) membrane for use with Trans-Blot Turbo transfer system (cat. no. 1704155) were purchased from Bio-Rad (Hertfordshire, UK). Photographic film was purchased from GE Healthcare (Little Chalfont, UK). SpectroTM multicolor broad range protein ladder (10-260 kDa, for 4 – 20 % Tris-glycine SDS-PAGE), enhanced chemiluminescence (ECL) reagent kit (cat. no. 32106) and sodium dodecyl sulphate (SDS) (cat. no. 28312B) were purchased from Fisher Scientific.

BCA protein assay was purchased from Fisher Scientific. Bradford assay and dye reagents (cat. no. 5000201) were purchased from Bio-Rad. EZQTM protein quantitation kit, PicoGreenTM dsDNA quantitation reagent and ProLongTM Gold Antifade Mountant with DAPI were purchased from Invitrogen (Paisley, Scotland).

HPLC vials, caps, insets, microspin filters “Spin-X”, Microplate U bottom polystyrene 96-well SterilinTM plates were obtained from Fisher Scientific. Amicon ultrafiltration microcentrifuge tubes including filters (10k Da, 3kDa cut-off) from Merck-Millipore (Watford, UK).

3.1.6 Chromatographic materials

For the proteomics studies, an Acclaim PepMap ODS μ -precursor cartridge, 5 μ m particle size, 100 Å pore size chromatography column, 300 μ m i.d. x 5 mm, was used. For protein glycation adduct measurement by LC-MS/MS, 5 μ m particle size HypercarbTM columns (column 1, 2.1 x 50 mm; and column 2,

2.1 mm x 250 mm) were used. These were purchased from ThermoFisher Scientific (Renfrew, Scotland).

3.1.6.1 Analytical and preparative kits

3.1.6.2 Calibration standards for protein glycations nitration oxidation adducts

Protein damage adduct analytical standards were prepared in house by host research team using the methods described (Thornalley et al., 2003, Ahmed et al., 2003). 4,4,5,5-[²H₄]L-lysine, [¹³C₆]L-lysine, [*guanidino*-¹⁵N₂]-L-arginine, *ring*-[²H₄]-L-tyrosine and [*methyl*-²H₃]-L-methionine were all >98% isotopic purity obtained from Cambridge Isotope Laboratories (Andover, MA, USA). [*guanidino*-¹⁵N₂]MG-H1, [*guanidino*-¹⁵N₂]G-H1, [*guanidino*-¹⁵N₂]3DG-H were prepared by host research team from [*guanidino*-¹⁵N₂]-L-arginine as described. [¹³C₆]CML, [¹³C₆] CEL and [¹³C₆] pentosidine were prepared from [¹³C₆]-L-lysine after conversion to the N α -formyl derivative. All methods for synthesis, purification and characterisation of the AGE analytical standards have been described previously (Ahmed et al., 2003).

3.1.7 Instrumentation

Enzymatic hydrolysis was performed automatically using a CTC-PAL Automation System (CTC-Analytics, Zwingen, Switzerland). The centrifugal evaporator was a Savant Instruments SpeedVac (Thermo Scientific, Waltham MA). For (LC-MS/MS) analysis, two different instrumentation systems were used from Waters (Manchester, U.K.): 1. AcquityTM UPLC system with a Quattro Premier XE tandem mass spectrometer; 2. AcquityTM UPLC system with a Xevo-TQS tandem mass spectrometer.

For cell counting, a Neubauer haemocytometer was used (cat. no. 0630410, Marienfeld-Superior, Paul Marienfeld GmbH & Co. KG, Lauda-Königshofen, Germany). A Nikon Eclipse TE2000-S inverted microscope (Kingston-Upon-Thames Surrey, U.K.) was used to visualise and count cells. For microplate spectrophotometry and fluorimetry, a FLUOstar OPTIMA microplate reader from BMG Labtech (Aylesbury, U.K) was used. For cell sonication, a

Vibra-Cell sonicator was used to disrupt cells (Jencons Scientific, Leighton Buzzard, UK). For membrane-gel transfer and western blotting, Criterion™ Cell electrophoresis chamber (Model no. 1656020), *Trans-Blot® Turbo™* Transfer System (Model no. 170-4155) and PowerPac™ Basic Power Supply (Model no. 164-5050) were used (Bio-Rad). For visualising extrachromosomal DNA staining an EVOS M5000 Imaging System - a fully integrated digital inverted microscope for four-color fluorescence, transmitted-light and color applications, was used (ThermoFisher Scientific).

3.1.8 Software

Optima software version 2.10 R2 (BMG Labtech) were used for microplate assays. For non-linear regression of viable cell number-MG concentration data to a dose-response curve, the ENZFITTER™ program was used (Biosoft, Cambridge, U.K.). For quantification of protein bands in western blotting, ImageQuant densitometry software was used (GE Healthcare Life Sciences, Amersham, U.K.). For instrumentation control and data processing from stable isotopic dilution analysis LC-MS/MS, Masslynx™ software, version 4.1, was used (Waters, Manchester, U.K.). For the proteomics analysis, raw data was processed using Proteome Discoverer (version 1.4.0.288, Thermo Scientific), Scaffold™ version 4.4.3 (Proteome Software, Portland, Oregon, USA) and Progenesis QI™ (Nonlinear Dynamics, Newcastle upon Tyne, U.K.) SEQUEST and Mascot engine were used for Molecular ion fragmentation mass spectra, MS² search against human data proteins database. <http://www.uniprot.org>. For statistical analysis IBM SPSS were used.

3.2 Bioinformatics methods

3.2.1 Cancer bioinformatics database CCLE

Data on gene copy number and expression in human tumour cell lines were extracted from the Cancer cell line encyclopaedia (CCLE) database (<https://portals.broadinstitute.org/ccle>). The CCLE project is an effort to conduct a detailed genetic and transcriptomic characterization of a large panel of human cancer cell lines. The CCLE provides public access analysis and visualization of

DNA copy number, mRNA expression, mutation and other data for 1040 cancer cell lines. Herein the full dataset and breast cancer cell line subset are analysed. The data, log2 transformed gene copy number and RNA seq data, were downloaded. Correlation analysis was performed using the R program and Pearson correlation analysis performed on mRNA copy number expressed as Reads Per Kilobase Million (RPKM). Data for 10758 genes was available. Pearson correlation analysis was performed to assess association of Glo1 expression with genes and also GLO1 copy number with Glo1 expression. A Bonferroni correction of 10758 was applied.

3.2.2 Pathway enrichment analysis tool.

For the pathway enrichment analysis in transcriptomic and proteomic datasets, pathways analysis was performed using Database for Annotation, Visualization and Integrated Discovery (DAVID) v6.8 (<https://david.ncifcrf.gov/>). Protein ontology was evaluated using the molecular functions and biologic processes that may be impacted by changes in protein abundance and MG modification. Kyoto Encyclopedia of Genes and Genomes (KEGG) database was used <https://www.genome.jp/kegg/> and for pathways analysis and INTERPRO analysis was performed (<https://www.ebi.ac.uk/interpro/>) and for enrichment of protein domains modified by MG. Pathway and domain enrichment was considered significant with Bonferroni significant and false positive discovery rate (FDR) of <0.05.

3.2.3 Kaplan-Meier survival analysis database

The Kaplan Meier plotter analysis tool was used for the analysis of the impact of selected gene on survival from 10,461 cancer samples in the KM Plotter database of gene transcription and cancer patient survival database, classified by treatment and, for breast cancer, major genotypes (<http://kmplot.com/analysis/>). Data on 5142 breast cancer patients, treatment and survival outcomes are available to be analysed against the gene of interests. The effect of target gene expression, as judged by mRNA level, on breast cancer patient survival was analysed in 3591 patients with full datasets available. Genes of interest were: glyoxalase 1 (GLO1), glyoxalase 2 – hydroxyacylglutathione hydrolase (HAGH),

nuclear factor erythroid 2-related factor 2 or Nrf2 (NFE2L2), kelch-like ECH-associated protein 1 (KEAP1), receptor for advanced glycation endproducts (RAGE) and lysine demethylase 4A (KDM4A) – known or suspected genes functionally or regulatedly linked to Glo1. Types of cancer patient treatment and tumour genotype classification were: chemotherapy, endocrine therapy, systemic untreated, systemic treated, endocrine therapy, excluding endocrine therapy; any chemotherapy, endocrine therapy - including all chemotherapy; tamoxifen treatment only; tamoxifen including all chemotherapy; tamoxifen treatment only as adjuvant therapy; and tamoxifen only as neoadjuvant therapy. Output variables were: Number of patients, Hazard ratio and median survival (months) for low/high gene expression cohorts, and Logrank P value. Data analysis was restricted to patient sample size of ≥ 200 patients for statistical power.

3.3 Cell Culture

HEK293 cells for experiments were cultured under aseptic conditions at 37 °C, under air with 5% CO₂ and 100 % humidity. Seeding density was 1.5×10^6 cells per T75 cm² flasks containing Dulbecco's Modified Eagles Medium (DMEM) with 25 mM glucose, 4 mM L-glutamine, 10 % (v/v) FBS and 100 U/ml penicillin/0.1 mg/ml streptomycin. Cells were cultured until 80 - 90% confluent for approximately 3 - 4 days incubated. All cells culture experimentations were performed after passage 3, unless stated otherwise. For cell passage, cultured cells were trypsinized, sedimentation by centrifugation and cell viability assessed by the Trypan blue exclusion method and cell number counted.

3.3.1 Cell culture experiments

3.3.2 Assessment of cell viability

HEK293 cells were seeded in 6-well plates (20,000 cells/cm²) in triplicate in DMEM media containing 25 mM of glucose and cultured for four days. Total viable cells number was counted and cell viability assessed using the Trypan blue exclusion method. Growth curves were then constructed.

3.3.3 Effect of methylglyoxal on the growth and viability of HEK293 cells *in vitro*: growth curve

HEK293 cells were cultured in 12 well plates containing DMEM media with 25 mM glucose concentration; seeding density 20,000 cells/cm². Cells were incubated for 24 hours for cells to adhere then 200 µM MG was added. Viable cell number and cell viability of control and MG-treated cultures was determined every day for 4 days.

3.3.4 Effect of methylglyoxal on the growth and viability of HEK293 cells *in vitro*: concentration-response curve

HEK293 cells were cultured in 12 well plates containing DMEM media with 25 mM glucose concentration; seeding density 20,000 cells/cm². Cells were incubated for 24 hours for cells to adhere then MG, 15, 50, 100, 150, 300 and 400 µM added; cells were incubated without added MG for control. Cells were cultured for 2 days and then viable cell number and cell viability determined. Data were fitted to a concentration response curve:

$$V = 100 \times GC_{50}^n / (GC_{50}^n + [MG]^n)$$

where V is viable cell number (% of control), [MG] the concentration of added exogenous MG, GC₅₀ - the median growth inhibitory concentration value of MG; and n - the logistic regression coefficient. Experimental data of V and [MG] were fitted by non-linear regression of V on [MG] using ENZFITTER software to solve for GC₅₀ and n the logistic regression coefficient.

3.4 Analytical methods

3.4.1 Bradford Assay for total protein measurements

Protein concentration of cell lysate were measured using Bradford protein assay (Bradford, 1976, Compton and Jones, 1985). Bovine serum albumin stock solution calibrated using UV absorption spectrophotometry at wavelength 279 nm using the extinction coefficient for a 1% (10 mg/ml) solution; ε₂₇₉ (1%) = 6.9 cm⁻¹ (Peters, 1962). Aliquots BSA standards and tests samples (20 µl) were loaded in 96 well plates mixed with 200 µl Bradford reagent. Samples and standards were

measured at 595 nm absorbance and the concentration in tests samples was deduced by interpolation on calibration curves.

3.4.2 BCA Assay

For western blotting studies, the detergent compatible BCA assay were used to measure protein concentrations in extracts of HEK293 cells containing RIPA buffer. It is a colorimetric assay for proteins solubilised in detergents based on similar chemistry to the Lowry protein assay.

3.4.3 EZQ Assay

The EZQ protein assay is used for high sensitivity protein assay in solutions containing detergents. It was used herein to assay protein content in mitochondrial fractions prior to proteomics analysis. In the commercial kit provided the calibration standard is ovalbumin. The standards were prepared in a range of 0.02–5 mg/ml. Volumes of 1 µl of both standards (0.05 – 5 µg protein) and samples were spotted in the EZQ microplate and fluorescence measured at wavelength 450 nm. Protein concentration was deduced by interpolation on calibration curves plotted from measurement of calibration standards.

3.4.4 Enzyme activity

3.4.4.1 Sample preparation

HEK293 cells were cultured as described above. Followed by trypsinisation, cells were counted and sedimented by centrifugation (250g, 5 min). Cell pellets (*ca.* 1.5×10^6 cells) were washed three times with phosphate-buffered saline (PBS; 10 mM, pH 7.0, 200 µl). Cells were then sonicated on ice (110 W, 30 s). Cell membranes were then sedimented by centrifugation (20,000 g, 30 min, 4 °C). The supernatant was retained and stored at -80 °C for later use as lysate in enzymatic activity assays.

3.4.4.2 Glyoxalase 1

Glo1 activity is determined by measuring the initial rate of formation of S-D-lactoylglutathione from MG-GSH hemithioacetal prepared by pre-incubation of

MG and GSH. The reaction is followed spectrophotometrically at 240 nm; $\Delta\epsilon_{240} = 2.86 \text{ mM}^{-1}\text{cm}^{-1}$ (Allen et al., 1993b).



The preparation of hemithioacetal was made using the pre-incubation of MG (2 μmol) with GSH (2 μmol) at 37 °C for 10 min in sodium phosphate buffer (50 mM, pH 6.6, 980 μl). An aliquot of cell lysate (20 μl) was added and absorbance were measured at 240 nm over the initial 5 min. Glo1 activity were deduced from the initial increase in absorbance, corrected for the blank change using lysate buffer only. Glo1 activity is measured in units per mg protein where one unit of Glo1 activity catalyses the formation of 1 μmol S-D-lactoylglutathione from the hemithioacetal substrate per minute under assay conditions (Allen et al., 1993b). It is possible to assay Glo1 activity in the presence of Glo2 because the high concentration of MG-GSH hemithioacetal used inhibits the activity of Glo2 in the assay solution mixture (Uotila, 1973).

3.4.4.3 Glyoxalase 2

Glo2 activity is determined by measuring the initial rate of S-D-lactoylglutathione hydrolysis to GSH and D-lactate. This hydrolysis reaction is followed spectrophotometrically at 240 nm for which $\Delta\epsilon_{240} = -3.10 \text{ mM}^{-1}\text{cm}^{-1}$ (Clelland and Thornalley, 1991, Allen et al., 1993a). The S-D-lactoylglutathione is incubated in Tris/HCl (50 mM, pH 7.4, 850 μl) at 37 °C. An aliquot of cell lysate is added (50 μl) and the absorbance followed at 240 nm for 5 min at 37 °C. The initial rate of change in absorbance is deduced and activity of Glo1 calculated in units where one unit of the Glo2 activity is the amount of enzyme required to hydrolyse 1 μmol of S-D-lactoylglutathione per minute under assay conditions (Allen et al., 1993b).

3.4.4.4 Assay of D-lactate

The determination of the flux of formation of D-lactate by HEK293 cells line is performed by measuring the concentration of D-lactate in culture media at the baseline and the end of the culture time. D-Lactate equilibrates across the cell plasma membrane by the inorganic anion exchange system, specific lactate

transporter and by non-ionic passive diffusion (McLellan and Thornalley, 1992a) and therefore cellular flux of D-lactate may be estimated from measurement of D-lactate in the culture medium. The measurement used is an end-point enzymatic assay with fluorometric detection (McLellan et al., 1992b). The conversion of D-lactate to pyruvate is catalysed by added D-lactic dehydrogenase enzyme during the assay reaction incubation time at 37 °C. The formation of NADH is determined by fluorescence ($\lambda_{\text{excitation}} = 340 \text{ nm}$, $\lambda_{\text{emission}} = 460 \text{ nm}$).



Samples are initially deproteinized by adding ice-cold perchloric acid (PCA; 1 ml, 0.6 M) to the culture medium. Samples are vortex mixed and incubated on ice for 10 min to achieve complete precipitation. Samples are then centrifuged (7000 g, 4 °C, 5 min) to sediment the protein precipitate. Afterwards, the supernatant is removed and neutralised to pH 7 with potassium bicarbonate (200 μl , 2 M), mixed and centrifuged again (7000 g, 4 °C, 10 min) to sediment the precipitate of potassium perchlorate. The resulting supernatant is removed and has become saturated with CO_2 formed in the neutralisation reaction. Samples are degassed using a centrifugal evaporator at room temperature, applying reduced pressure (20 mmHg) for 5 min. For D-lactate assay, aliquots of degassed extract (100 μl) are added to wells of black 96-well microplates for both assay and blank correction (assay mixture without added D-lactic dehydrogenase). Calibration standards D-lactate are prepared similarly. The assay mixtures contain NAD^+ (4 mM, 25 μl) and glycine hydrazine buffer (100 μl ; 1.2 M glycine, 0.5 M hydrazine hydrate, 2.5 mM DETAPAC, pH 9.2). The reaction is initiated with the addition of D-lactic dehydrogenase enzyme to test samples (25 μl , 250 units per ml) and water to blanks, followed by an incubation of 2 h at 37 °C in the dark. NADH fluorescence is then measured at $\lambda_{\text{excitation}} 340 \text{ nm}$ and $\lambda_{\text{emission}} 460 \text{ nm}$. A standard curve for calibration was constructed in the range of 0 – 6 nmol D-lactate/ well.

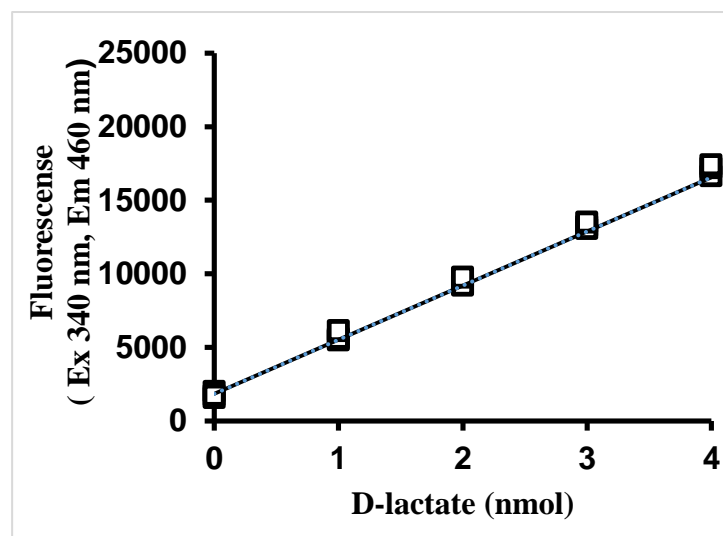


Figure 24. Calibration curve for assay of D-lactate.

Calibration equation: Fluorescence = $(3662 \pm 374) \times [\text{D-lactate (nmol)}] + 2048.5 \pm 393$ (N= 18); $R^2 = 0.998$.

3.4.4.5 Assay of L-lactate

Net formation of L-lactate in HEK293 cultures was measured similarly to D-lactate – see above. L-Lactate standards was used to generate the standard curve and instead of using D-lactic dehydrogenase, L-lactic dehydrogenase was used for this assay. The L-lactate concentration in culture medium is higher than D-lactate and therefore samples were diluted 10 time to ensure sample response was within the range of the calibration curve.

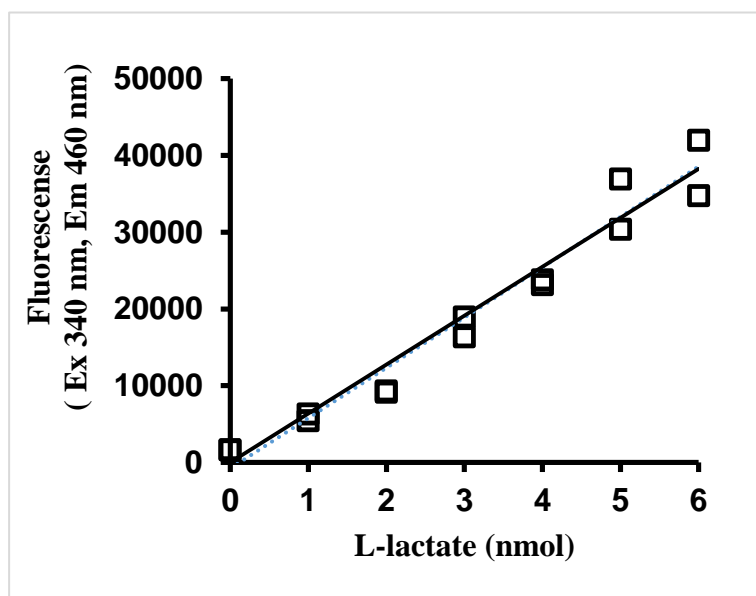


Figure 25. Calibration curve for assay of L-lactate.

Calibration equation: Fluorescence = $(6255 \pm 399) \times [\text{L-lactate (nmol)}]$ (n= 12); $R^2 = 0.98$.

3.4.5 Western blotting for selected proteins

Selected proteins found to be up-regulated and downregulated by MG from proteomics studies were investigated for attempted corroboration of change by western blotting.

3.4.5.1 Sample preparation

HEK293 cells were cultured in medium containing 25 mM glucose with and without added exogenous MG. HEK293 were left first to adhere for 24 h and incubated with and without 131 μM MG for 6 h. Following this incubation, cells were trypsinised and sedimented by centrifugation. Cell pellets are then washed 3 times with ice-cold PBS. The cell pellets were resuspended in RIPA buffer containing phosphatase inhibitor and protease inhibitors, mixed well and left on ice for 10 min. Cell membranes were then sedimented by centrifugation (20,000g, 30 min, 4 °C) and the supernatant collected and stored at -80 until further analysis. Protein concentration were measured using BCA assay. Aliquots of samples were then loaded onto SDS-PAGE gels. The loading buffer contained β -mercaptoethanol (4x Laemmli sample buffer, Bio-rad) and the protein samples were mixed to make the total concentration 20 μg . Samples were heated at 95 °C for 5 min to denature the protein and loaded onto the gel.

3.4.5.2 Western blotting

The separation of cell protein extracts was performed using 4 – 20% precast polyacrylamide gels (4 - 20% criterion™ TGX stain-free™ gel), followed by the insertion of the gel into Criterion electrophoresis cell (Bio-rad). Electrophoresis premixed buffer containing 25 mM Tris, 192 mM glycine, 0.1% SDS, pH 8.3 was poured into the cells in order to separate proteins by SDS-PAGE. An aliquot of prestained protein ladder (10 μl) and test samples were loaded into the gel samples were then electrophoresed at 120 V for 1 h. For electrophoretic transfer of proteins onto nitrocellulose membranes, the semi-dry sandwich layer compromise of gel, paper and membrane was arranged by using pre-cutting blotting transfer pack.

Trans-Blot Turbo transfer system was used to transfer proteins from the gel into membrane. The semi-dry membrane transfer conditions were: 2.5A, constant 25 V for 15 min.

Following the membrane transfer, membranes were initially blocked with 5% (w/v) dried semi-skimmed milk protein diluted in Tris-buffer saline contains tween-20 (TBS-T buffer; 150 mM NaCl, 10 mM Tris/HCl pH 7.6 and 0.05% Tween-20). Membranes were probed according to the manufactures with pre-determinant dilution concentrations of primary antibodies. Membranes were incubated overnight in 1% dried milk protein in TBST buffer (w/v) at 4 °C, followed by washing of the membrane with TBST buffer for 10 min for 3 cycles. Membranes were incubated then with secondary antibody, 1/5000 dilution anti-rabbit IgG-HRP conjugate at room temperature for 1 h followed by TBST washing and developed using ECL reagents. Images were taken using G-BOX chemi system (syngene). Protein band intensities were normalised to β -actin (protein loading control). ImageQuants software were used for quantifying.

3.4.6 Membrane stripping

Membrane stripping were used to probe membranes with different primary antibody. Membranes were firstly incubated with stripping buffer at 37 °C on a shaker for 45 min. Then, the membranes were washed with water and TBST buffer wash for 10 min for three times. The membranes were then blocked with 5% of dried milk protein in TBST with incubation for 1 h. Membranes were then incubated with the primary antibody of interest and western blotting procedures performed as described above.

3.4.7 ELISA of Mitochondrial and cytosolic cytochrome c

A commercial ELISA was used to measure cytochrome c content of mitochondrial and cytosolic fractions of HEK293 cells incubated with and without MG. HEK293 cells (1×10^6) were incubated with and without MG 131 μ M for 1, 3, 6 and 12 h, harvested and washed three times with ice-cold PBS. Cells were re-suspended in isotonic buffer A (10 mM HEPES, 0.3 M mannitol and 0.1% BSA, pH 7.4 supplemented with 0.1 mM digitonin; 0.67 ml), left on ice for 5 min, and

immediately centrifuged (8500g, 5 min, 4 °C). The collected supernatant was used as the cytosolic fraction. The pellet was resuspended in sonication buffer (50 mM Tris/HCl, pH 7.4, 150 mM NaCl, 2 mM EDTA, 1 mM PMSF and 0.5% Tween 20), sonicated three times (20 s each) on ice, and centrifuged (10,000g, 30 min, 4 °C). The resulting supernatant was used as the mitochondrial fraction. The amount of cytochrome c in mitochondrial and cytosolic fractions was measured with a commercially available cytochrome c ELISA kit according to the manufacturer's instructions, after appropriate dilution.

3.5 Microscopy methodology

3.5.1 Measurement of free dsDNA using florescence microscopy

HEK293 cells were cultured in DMEM media containing 25 mM glucose. Cells were seeded at density of 20,000 cells/cm² in 6-well plates. Cells were incubated at 37 °C, 5 % CO² and 100 % humidity for 24 h. Cell were then treated with 131 µM MG and incubated for 6 h.

Following MG incubation, the medium containing MG was carefully removed and 4 µg/ml Pico-green reagent diluted in DMEM media was added to the cells and incubated for 2 h. Media containing picogreen reagent were removed and cells were covered with Prolonged gold DAPI reagent. Cells were then fixed with 4% formaldehyde. Cells were visualised and image were extracted at different cellular location using EVOSE florescence microscope.

3.6 LC-MS/ MS methodology

Adducts residues from protein glycation in cellular proteins were measured using the gold standard method of stable isotopic dilution analysis liquid chromatography with tandem mass spectrometric detection (LC-MS/MS) following exhaustive enzymatic hydrolysis. Analytes determined were: N_ε-carboxymethyl-lysine (CML), MG-H1, N_ε-(1-carboxyethyl)lysine (CEL), 3-DG-H and N_ω-carboxymethyl-arginine (CMA). MG adducts measurements were performed using stable isotopic dilution analysis LC-MS/MS (Rabbani et al., 2014, Thornalley et al., 2003).

3.6.1 Sample preparation, filtration and washing for glycation adduct residue content of cell protein

HEK293 cell lysate was washed ultrafiltration: 4 cycles of dilution to 500 µl with water and concentration to 50 µl over microspin ultrafilter (10 kDa cut-off) at 4 °C. Protein concentration in the final concentrate was assayed by the Bradford assay. Aliquots of protein (100 µg) were loaded in glass vials and diluted to 20 µl with water followed by degassing with argon and then used for exhaustive enzymatic hydrolysis.

3.6.2 Enzymatic hydrolysis of soluble protein

Samples and reagents were placed in an automated CTC PAL Analytics sample autoprocessor for enzymatic hydrolysis. All procedures were performed under argon in order to prevent oxidative degradation of protein substrate. The CTC PAL autoprocessor is programmed to perform an automated sequential addition of: aliquots of 100 mM HCl (10 µl), pepsin solution (2 mg/ml in 20 mM HCl; 5 µl), and thymol solution (2 mg/ml in 20 mM HCl; 5 µl), followed by sample incubation for 24 h at 37 °C. Neutralization of the samples to pH 7.4 was then performed by addition of 12.5 µl 100 mM potassium phosphate buffer, pH 7.4, and 5 µl 260 mM KOH. Pronase E solution (2 mg/ml in 10 mM KH₂PO₄, pH 7.4; 5 µl) and penicillin/streptomycin (1000 units/ml and 1 mg/ml in order; 5 µl) was then added and samples then incubated for 24 h at 37 °C. Lastly, addition was made of both aminopeptidase solution (2 mg/ml in 10 mM KH₂PO₄, pH 7.4; 5 µl) and prolidase solution (2 mg/ml in 10 mM KH₂PO₄, pH 7.4; 5 µl). Samples were then incubated for 48 h at 37 °C. It is vital to consider the order of the addition of these reagents and this is due to the avoidance of pH overshooting. Aliquots of exhaustive digest (5 µl) were then mixed with 20 µl of water and 25 µl of internal standards in HPLC vials and analysis of glycation adduct contents was performed using LC-/MS-MS. The protocol used is summarized in Table 6.

Table 6. Protocol used for hydrolysis of sample protein treated with/without MG using CTC-PAL automated processor.

Addition	Volume added (μl)
Day 0	
100 mM HCl	10.0
Pepsin solution (2 mg/ ml)	5.0
Thymol (1 mg/ml)	5.0
Incubate for 24 hours at 37 °C	
Day 1	
100 mM KH ₂ PO ₄ /K ₂ HPO ₄ buffer, pH 7.4	12.5
260 mM KOH	5.0
Pronase E solution (2 mg/ml)	5.0
Penicillin (100 units/ml) and streptomycin (1 mg/ml)	5.0
Incubate for 24 h at 37 °C	
Day 2	
Aminopeptidase solution (2 mg/ml)	5.0
Prolidase solution (2 mg/ml)	5.0
Incubate for 48 h at 37 °C	

Modified from (Rabbani et al., 2014).

3.6.3 Standards curve preparation

LC-MS/MS standards curve analysis were prepared as described in Table 7. A mixture of normal and isotopic standards were prepared by host research team summarised in Table 8. There were 7 calibration standards used ranging from calibrants 0 to 6 using water and stock solution. Each analytes solution (50 μl) were applied directly to the LC-MS/MS. Typical calibration curve of arginine and MG-H1 is shown in Figure 16.

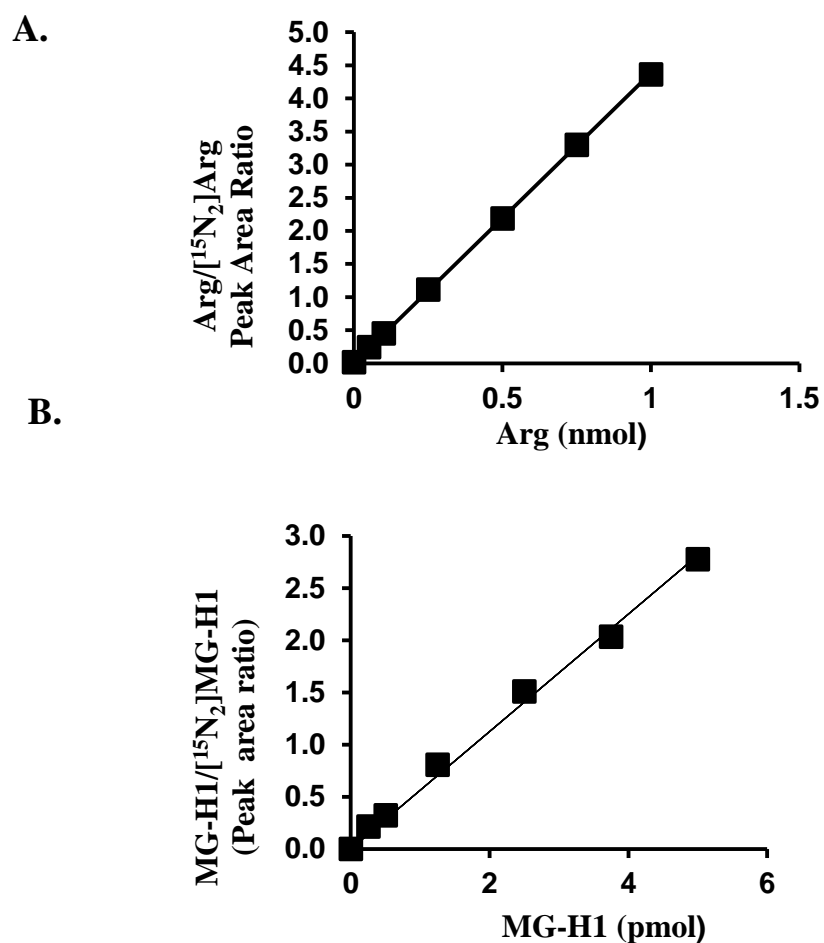


Figure 26. Typical calibration curves for arginine and MG-H1 in stable isotopic dilution analysis LC-MS/MS.

Linear regression equation: $\text{arg}/[^{15}\text{N}_2]\text{arg peak area ratio} = (4.35 \pm 0.0104) \times \text{arg (nmol)} + (0.02 \pm 0.0054)$; $R^2 = 0.994$ ($n = 7$). B. Calibration curve of MG-H1. Linear regression equation: $\text{MG-H1}/[^{15}\text{N}_2]\text{MG-H1 peak area ratio} = (0.542 \pm 0.0137) \times \text{MG-H1 (pmol)} + (0.07 \pm 0.03)$; $R^2 = 0.994$ ($n = 7$).

Table 7. Calibration standard solutions preparation from mixtures of normal and stable isotopic standards for protein glycation, oxidation and nitration adduct residues of HEK293 protein extracts.

Cal no	Normal standards solution (μl)	Water (μl)		Stable isotopic standard solution (μl)	Total volume (μl)
0	0.00	25.00		25	50
1	1.25	23.75		25	50
2	2.50	22.75		25	50
3	6.25	18.75		25	50
4	12.50	12.50		25	50
5	18.75	6.25		25	50
6	25.00	0.00		25	50

Table 8. Analyte content of calibration standard solutions for protein glycation, nitration and oxidation adduct residues of HEK293 protein extracts.

Analytical standard (nmol)								Internal standard	
Cal no	0	1	2	3	4	5	6	(nmol)	
Lys	0	0.05	0.10	0.25	0.50	0.75	1.00	[¹³ C ₆]Lys	0.25
Arg	0	0.05	0.10	0.25	0.50	0.75	1.00	[¹⁵ N ₂]Arg	0.25
Analytical standard (pmol)								Internal standard	
Cal no	0	1	2	3	4	5	6	(pmol)	
MG-H1	0	0.125	0.25	0.625	1.25	1.875	2.50	[¹⁵ N ₂]MG-H1	1.25
3DG-H	0	0.125	0.25	0.625	1.25	1.875	2.50	[¹⁵ N ₂]3DG-H	1.25

3.6.4 LC-MS/MS conditions (Xevo-TQS system)

The conditions used for the chromatographic LC-MS/MS analysis are as follows: two 5 μm particle size Hypercarb columns were used in series (column 1: 2.1 x 50 mm; and column 2: 2.1 mm x 250 mm) For the mobile phase: Solvent A contained 0.1% TFA in water; and solvent B, 0.1% TFA in 50% acetonitrile (ACN). For the post run method solvents, Solvent A used for column washing contained 0.1% TFA in water, and solvent C - 0.1% TFA in 50% tetrahydrofuran (THF). Elution profiles for the assay run and washing re-equilibration of the column are summarised in Table 9. The flow from column to the MS/MS detector was directed from 4 to 35 min interval. The detection of protein damage analytes was performed using electrospray ionisation mass spectrometric multiple reaction monitoring (MRM). The temperature of the ionisation source was 120 °C and that

of the desolvation gas was 350 °C. The gas flow in the cone gas were 991/h and for the desolvation gas was 901 1/h. Fragment ion masses, collision energies and optimised molecular ion are summarised in Table 10. Chromatographic peaks integration was performed using Masslynx software.

Table 9. Elution profile for stable isotopic dilution analysis liquid chromatography with tandem mass spectrometric detection analysis of protein glycation, nitration adducts and oxidation (Acquity™-Xevo-TQS system).

Time (min)	Flow rate (ml/min)	Solvent A (%)	Solvent B (%)	Gradient
0	0.2	100	0	----
5	0.2	100	0	Isocratic
8	0.2	97	3	Linear
12	0.2	97	3	Isocratic
15	0.2	83	17	Linear
18	0.2	83	17	Isocratic
24	0.2	20	80	Linear
24	0.2	97	3	Immediate
35	0.2	97	3	Isocratic
Post-run				
0	0.4	0	100	-----
10	0.4	0	100	Isocratic
20	0.2	0	100	Isocratic
20	0.2	100	0	Immediate
25	0.2	100	0	Isocratic
40	0.4	100	0	Isocratic

Table 10. Chromatographic retention times and MRM detection conditions for detection of glycation, oxidation and nitration adducts by (LC-MS/MS) (Acquity™-Xevo-TQS system).

Analyte	Rt (min)	Molecular ion (Da)	Fragment ion (Da)
Lys	5.6	147.1	84.1
[¹³ C ₆]Lys	5.6	153.1	89.1
3DG-H	11.7	319.1	70.1
[¹⁵ N ₂]3DG-H	11.7	321.1	70.1
MG-H1	11.9	229.2	114.1
[¹⁵ N ₂]MG-H1	11.9	231.2	116.1
[¹³ C ₆]CEL	32.2	225.2	136.0
Arg	32.2	176.2	70.1
[¹⁵ N ₂]Arg	32.2	178.2	70.1

3.7 Proteomics analysis of subcellular fraction

Approximately 3×10^6 HEK293 cells were cultured as described above to 80 - 70% confluence. Cells were incubated with 131 μ M MG for 6 h. Cells were then collected after trypsinisation, sedimentation and washed with PBS as described previously. Each subcellular fraction isolation described further below.

3.7.1 Sample preparation

3.7.1.1 Cytosolic sample preparation and isolation

After the incubation with and without MG, cell pellets were suspended in 10 mM sodium phosphate buffer, pH 7.0, sonicated on ice (110 W, 30s, 4 °C), and membranes sedimented by centrifugation (20,000g, 30 min, 4°C). The supernatant was then removed and stored at -80 °C until further analysis. Protein concentrations of samples were measured using Bradford assay, as described above. An aliquot of protein (300 μ g) was washed with argon-purged water by ultradialfiltration in 4 consecutive cycles of dilution and concentration over a 10 kDa cut-off membrane filter and then centrifuged (14,000g, 20 min, 4°C). Protein concentration were measured again using the Bradford assay and aliquot (100 μ g) digested by the trypsin/lys-C digestion method described below.

3.7.1.2 Mitochondrial membrane and inner matrix isolation and preparation

For mitochondrial subcellular fraction isolation, cells were re-suspended in isotonic buffer (25 M sucrose, 5 mM Tris/HCl, pH 7.5, and 0.1 mM phenylmethylsulfonylfluoride PMSF]; 1 ml) and homogenized using a glass Teflon homogeniser. Unbroken cells and nuclei are pelleted by centrifugation (600g, 15 min, 4 °C). Supernatants are centrifuged (10,000g, 25 min, 4 °C). The resulting supernatant was isolated as the cytoplasmic fraction and the pellet as the mitochondrial fraction. The pellet was washed once with isotonic buffer containing 1 mM EDTA, pH 7.5; 1 ml.

For the extraction of the mitochondrial soluble matrix and intermembrane space, samples were thawed on ice and 200 μ l lysis buffer (1 mM DTT and 10

mM HEPES pH 7.4) was added and incubated on ice for 30 min. Samples were sonicated 3 times for 30s on ice and centrifuged (1 h, 120,000g, 4°C). Supernatant was transferred to 3 kDa cut-off filter and washed by ultrafiltration by 3 cycles of concentration to 50 µl and dilution with 0.45 ml ice-cold water at 14,000g at 4°C; concentrating the samples finally to 25 µl. Protein content was quantified with Bradford assay.

For the mitochondrial membrane isolation protein was extracted by addition of 0.2 ml membrane extraction buffer ME (20 mM Tris-HCl, pH 7.4; 0.4 M NaCl, 15% glycerol, 1 mM DTT, and 1.5% Triton-X-100) to membranes pellets and samples shaken gently at 4 °C for 1 h. Samples were then centrifuged (20,000g, 4 °C, 1 h). The supernatant was retained and protein was washed by ultrafiltration by 3 cycles of concentration to 50 µl and dilution with 0.45 ml ice-cold water containing 1.5% Triton-X-100; concentrating finally to 25 µl. Protein was quantified with EZQ-protein quantification kit according to the manufacturer's instructions. Protein solutions were extracted 5 times with 20 volumes of water-saturated HPLC grade ethyl acetate to remove the Triton-X-100. Residual ethyl acetate was evaporated by vacuum centrifugation at room temperature for 5 min.

3.7.1.3 Nuclear isolation and preparation

For the nuclear isolation, cells were washed in PBS and re-suspended in homogenization buffer [0.3 M sucrose, 10 mM MgCl₂, 50 mM Tris-HCl, pH 7.8 and 0.1 mM phenylmethylsulfonylfluoride (PMSF)]; 1 ml. Cells are homogenized at 0 °C in a Teflon-Glass homogenizer at 1200 rpm with 10 down-up cycles. The homogenate was centrifuged (1000g, 10 min, 4°C) and the pellet retained as the crude nuclear extract. The pellet was suspended in NF buffer [0.3 M sucrose, 10 mM MgCl₂, 50 mM Tris-HCl, pH 7.8]; 0.1 ml. The suspension was layered onto a 'sucrose cushion' consisting of 2 M sucrose in the same buffer; 1 ml. After centrifugation (16,000g, 20 min, 4°C) the supernatant was discarded and the pellet containing purified nuclei was washed twice with phosphate-buffered saline. Purified nuclei then re-suspended in 25 µl NE buffer (20 mM HEPES, pH 7.9, 1.5 mM MgCl₂, 0.5 M NaCl, 0.2 mM EDTA and 20% glycerol) and incubated for 30

min with gentle rocking at 4°C. Nuclei were then lysed with 10 passages through an 18-gauge needle. Lysate were then centrifuged at (9,000g, 30 min 4 °C). Protein content was measured using Bradford assay and the supernatant were then used for proteomic analysis.

3.7.2 Protocol of tryptic digestion

Following the subcellular protein isolation, 100 µg protein extract was dissolved in dithiothreitol (6 µl, 6 mM) and incubated in the dark for 30 min at 37 °C. Iodoacetamide solution (5.9 µl, 10.8 mM) was then added and samples incubated at 37 °C in the dark for 30 min. Residual iodoacetamide was then quenched by further addition of dithiothreitol (5.9 µl, 6 mM) and incubated at 37 °C in the dark for 30 min. Then, TPCK-treated trypsin was added (1 mg/ml, 5 µl) in 1 mM calcium chloride/500 mM ammonium bicarbonate, pH 8.0 and incubated for 5 h in the dark at 37 °C. An aliquot of 10% TFA in water (5 µl) was addition to stop the reaction. Samples were then lyophilised to dryness for removal of volatile salts and re-suspended in 0.1% formic acid in water. Sample analysis was made by nanoflow liquid-chromatography-Orbitrap mass spectrometry.

3.7.3 Protocol of Lys-C/Trypsin protease digestions

A Lys-C protease digestion protocol similar to the previous one for tryptic digestion was used; instead of adding TPCK-treated trypsin to the cytosolic protein, an aliquot of Lys-C protease (1 mg/ml, 5 µl) in 500 mM ammonium bicarbonate, pH 8.0, was added and incubated for 1 h at 37°C. Then TPCK-treated trypsin (1 mg/ml, 5 µl) in 1 mM calcium chloride/500 mM ammonium bicarbonate, pH 8.0, was added and samples were incubated at 37°C for 5 h in the dark.

3.7.4 Peptide separation, protein quantitation and identifications

The processed cell lysate samples were submitted to the Mass Spectrometry and Proteomics Facility at Warwick University for a label-free proteomic quantitation analysis. Reversed phase nanoflow liquid chromatography-mass spectrometry for global protein identification was performed on an Orbitrap

mass spectrometer equipped with a microspray source operating in positive ion mode. For proteomics analysis, the column used was: an Acclaim PepMap μ -pre-column cartridge (trap), 300 μm i.d. x 5 mm, 5 μm particle size, 100 Å pore size, fitted to an Acclaim PepMap RSLC 75 μm i.d. x 50 cm, 2 μm particle size, 100 Å pore size main column (Thermo Scientific). It was installed on an Ultimate 3000 RSLCnano system (Dionex). An aliquot (5 μl) of each sample was injected. After injection, the peptides were eluted off of the trap onto the analytical column. Mobile phases were: A - 0.1 % formic acid in water, and B - 0.1 % formic acid in acetonitrile. The flow rate was programmed at 0.3 $\mu\text{l}/\text{min}$. Mobile phase B was increased from 3 % to 35 % in 125 to 220 min, depending on the complexity of the sample, in order to separate the peptides. Mobile phase B was then increased from 35 % to 80 % in 5 min before being brought back quickly to 3 % in 1 min. The column was equilibrated at 3 % of mobile phase B for 15 min before the next sample. Peptides were eluted directly (300 nl min^{-1}) via a Triversa Nanomate nanospray source (Advion Biosciences, NY) into a Thermo Orbitrap Fusion (Q-OT-qIT, Thermo Scientific) mass spectrometer. Survey scans of peptide precursors from 350 to 1500 m/z were performed at 120K resolution (at 200 m/z) with automatic gain control (AGC) 4×10^5 . Precursor ions with charge state 2 - 7 were isolated (isolation at 1.6 Th [Thomson units; $m/z = 1$] in the quadrupole) and subjected to high energy collision dissociation (HCD) fragmentation. The collision-induced dissociation fragmentation energy was programmed to 35 %. It was used rapid scan MS analysis in the ion trap, the AGC was set to 1×10^4 and the max injection time was 200 ms. Dynamic exclusion duration was set to 45 s with a 10 ppm tolerance around the selected precursor and its isotopes. Monoisotopic precursor selection was turned on. The instrument was run in top speed mode with 2 s cycles. Sequence information from the MS/MS data was managed by converting the raw (.raw) files into a merged file (.mgf) using MSConvert in ProteoWizard Toolkit (version 3.0.5759) (Kessner et al., 2008). The resulting .mgf files were searched, and the database was searched against protein sequence databases.

3.7.5 Data analysis

For the data search, Mascot engine were used for searching Matrix Science, version 2.5.0) against *Homo sapiens* database (<http://www.uniprot.org/>). The search set up in the mascot assumed the digestion enzyme trypsin, in order to identify false positive peptide identification. The search parameter used for product ions and precursor mass: ± 5 ppm and ± 0.8 Da, with allowance made for six trypsin missed cleavages, fixed modification of cysteine through carbamidomethylation, MG-H1 and methionine oxidation. Only fully tryptic peptide matches were included. For validation, we used Scaffold (version Scaffold 4.3.2, Proteome Software Inc.). The software was used for validating MS/MS based peptides and protein identification. It is only accepted if peptides could achieve 95% probability false discovery rate FDR provided by the software logarithms. This is also similar to protein identification 95% of probability or higher are only accepted which contains at least 2 peptides. The probabilities of proteins were assigned using protein prophet algorithms (Nesvizhskii et al., 2003).

3.7.6 Protein function and ontology

The evaluation of protein ontology was performed using literature reports of proteins roles and website tool (<http://www.reactome.org/>). This tool able to identify the functional annotation for characterisation biological process and molecular functions.

3.7.7 Statistical analysis

All the statistical analysis such as mean, confidence score, standards deviation, ANOVA were performed using the dataset of the matched HEK293 cells replicates using statistical programme analysis provided in Progenies QI (QIP) for proteomics 2.0(Nonlinear Dynamics, Newcastle upon Tyne). Protein probabilities calculating from peptide probabilities were performed using Progenies. Relative protein concentration quantification was measured using non-conflicting peptides in Progenies described in details (see <http://www.nonlinear.com/progenesis/qi-for-proteomics/v2.0/faq/which-quantitation-method-should-i-choose-for-my-experiment.aspx#relative-all>) In

summary, the method recognises non-conflicting peptides found as part of protein for quantification.

For the statistical analysis performed on the proteomics data generated from the QIP. Data were only included if they have a P-value >0.05 produced by the software. The Q value, power analysis, peptide number and unique peptide number of the significant proteins by the software were included in Appendix III.

The following figures is the experimental metrics of the cytoplasmic subcellular fraction as an example, visualised and calculated using QIP. The relative abundance of peptides identified finds in each groups are shown in yellow – Figure17. The levels of peptide identification was similar in both test and control conditions. The biological replicate used in each subcellular fraction experiment were three replicate for each condition. In order to assess the reproducibility of the replicate of the samples, Power analysis were performed using algorithmic by QIP. For all the significant protein power analysis were listed in Appendix III. The power analysis performed can be defined as the probability of showing a true differences between the two conditions. 0.8 Or 80% is acceptable value for the power. This is performed independently for each compound, considering variance of abundance and the size of the difference wanted to be detected. Nevertheless, the power analysis can give an initial thought of how many replicate is required to ensure the differences are exist between the two conditions.

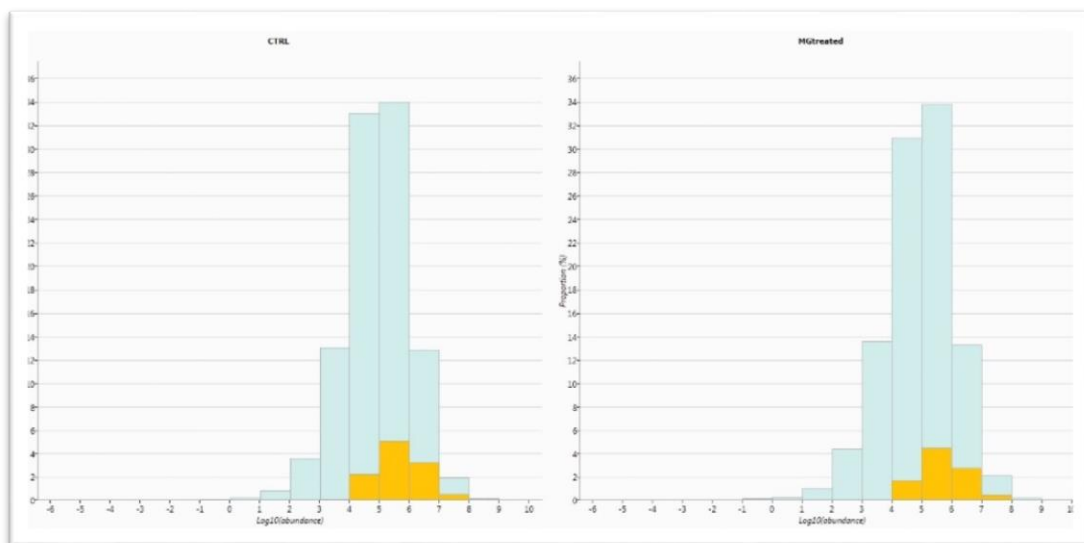


Figure 27. Relative abundance of proteins identified in Control (left) and MG treated cells in HEK293 cells.

Data are mean \pm SD, n = 3.

Tryptic digestion efficiency was high with approximately 70% rate of proteins were digested. However, ca. 22% peptides contains 1 missed cleavage and ca.3% were 2 missed cleavage-figure18.

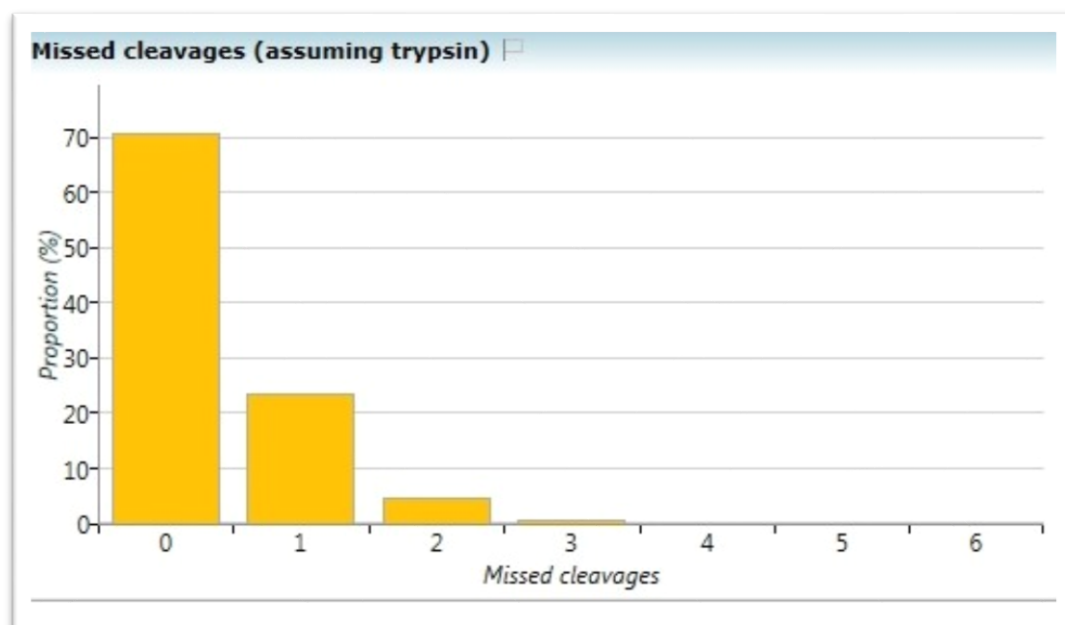
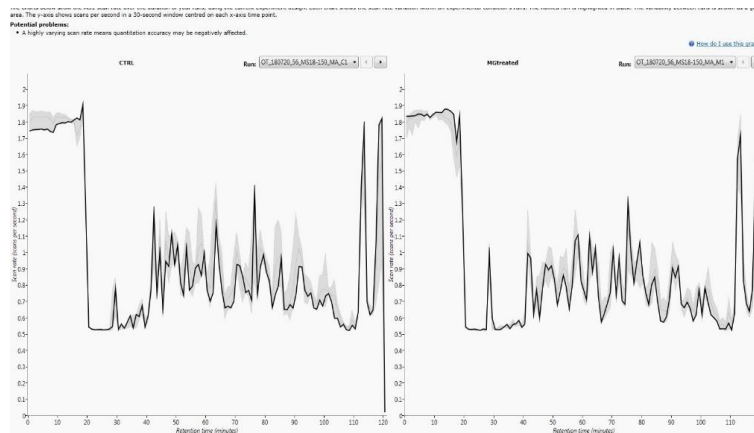
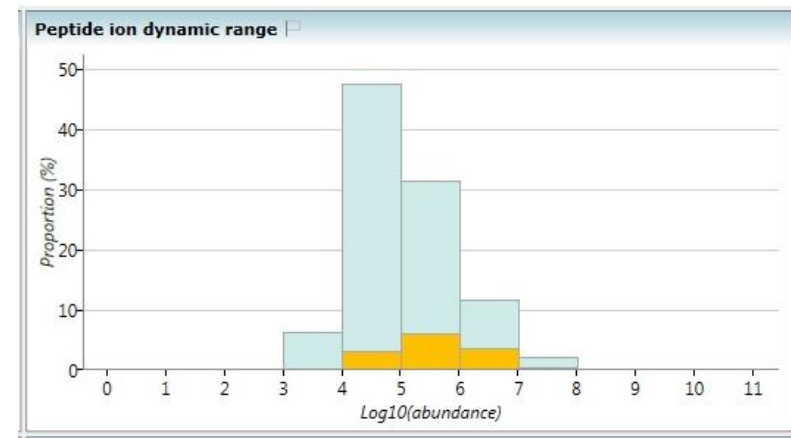


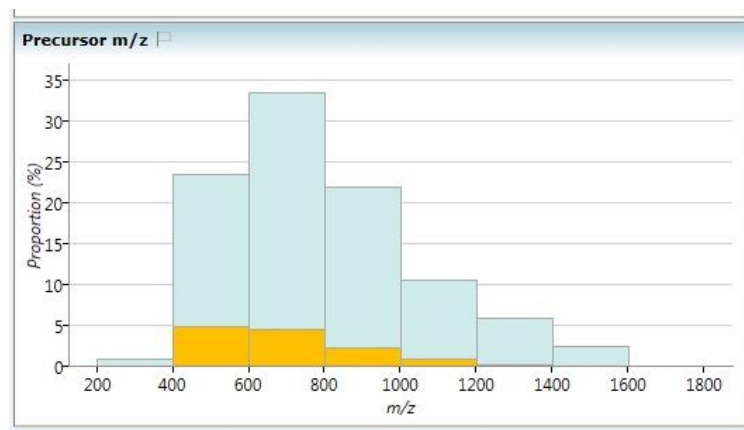
Figure 28. Missed cleavage number per peptides ions by trypsin.



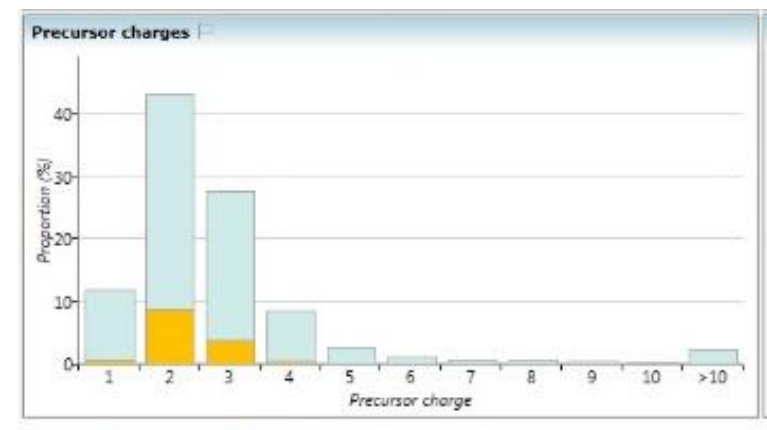
A. Dynamic range of abundance



B. precursor m/z



C. Precusour m/z



D. Precursor charge

Figure 29.The rate variation within condition in the experimental run in the mass spectrometry.

3.8 Other statistical analysis

All experimental work was performed in triplicate or greater. Student's t-test were used to assess the significance of difference between means, assuming normally distributed data where the F-test was used to determine where data sets had unequal or equal variances and appropriate t-test procedures applied. Significance was assumed for $p < 0.05$.

4 Results

4.1 Bioinformatics analysis of glyoxalase 1 expression in tumour cell lines and clinical cancer survival

4.1.1 Correlation analysis of glyoxalase 1 mRNA in the cancer cell line encyclopaedia dataset CCLE

In this section, I describe examination of gene expression correlation with expression of Glo1 in the cancer cell line encyclopaedia (CCLE). Correlation was performed of mRNA copy number from RNA-seq analysis data downloaded from the CCLE website. mRNA copy number was normally distributed and hence Pearson correlation analysis was performed with data from 1010 tumour cell lines for 10,758 genes, applying a Bonferroni correction of 10,758. Genes correlated with Glo1 positively and negatively listed - Appendix I. There were 4,021 genes correlating significantly with expression of Glo1: 3,032 correlated positively with Glo1 with correlation coefficients 0.134 – 0.568 and 989 genes correlated negatively with Glo1 with correlation coefficients from - 0.535 - - 0.134. For breast cancer cell lines ($n = 60$), the analysis had markedly less power and only 3 significant correlations were found: RP11.312J18.5, $r = 0.633$; FBXO9, $r = 0.619$; and SMS, $r = 0.605$.

Genes significantly correlated with Glo1 in the complete CCLE collection were analysed for pathways enrichment analysis ($r^2 \geq 0.10$, threshold criteria: Bonferroni corrected P-value < 0.05 ; FDR < 0.05). Only limited genes for which $r^2 \geq 0.10$ so that included genes were accounting for $\geq 10\%$ variation in Glo1 expression. For the 340 genes submitted for analysis by the DAVID bioinformatics pathways enrichment analysis using the Kyoto Encyclopaedia of Genes and Genomes (KEGG) database. Three hundred and twenty-three genes were recognised; seventeen were unrecognised. Unrecognised genes in pathways analysis were: pseudogene (2), antisense RNA (7), microRNA (2), long non-coding RNA (4), other intronic RNA (1) and uncharacterized proteins (1). Recognised genes were enriched in 4 pathways (ranked ordered by statistical significance, most significant first): spliceosome, RNA transport, cell cycle and DNA replication – Table 11.

Table 11. Pathways enrichment of gene expression correlating positively with glyoxalase 1 expression in tumour cell lines of the CCLE.

Pathway	Count	Fold enrichment	Bonferroni corrected P-value	FDR	Genes
Spliceosome	22	7.5	7.9×10^{-11}	6.9×10^{-10}	CDC5L, HNRNPA1, HNRNPA3, HNRNPC, HNRNPK, LSM2, LSM3, LSM5, MAGOH, MAGOHB, PPIL1, PRPF4, RBMXL1, SF3B6, SNRNP40, SNRPB, SNRPC, SNRPD1, SNRPD2, SNRPE, SNRPG, SRSF3
RNA transport	22	5.8	1.3×10^{-8}	1.1×10^{-7}	DDX20, EIF1AX, EIF2S1, EIF4E, GEMIN5, GEMIN6, KPNB1, MAGOH, MAGOHB, NDC1, NUP107, NUP153, NUP155, NUP35, NUP37, NUP43, NUP54, RPP40, SUMO1, SUMO2, XPO1, XPO5
Cell cycle	19	7.0	1.7×10^{-8}	1.5×10^{-7}	CCNB1, CCNB2, CCNE2, CDC25C, CDC27, CDC7, CDK1, DBF4, HDAC2, MAD2L1, MCM3, ORC2, ORC3, ORC4, PTTG1, SKP1, SKP2, SMC3, TTK
DNA replication	10	12.7	6.7×10^{-6}	5.9×10^{-5}	DNA2, MCM3, POLA1, POLE2, PRIM2, RFC2, RFC3, RFC4, RFC5, RPA2

Enrichment analysis was performed by the DAVID bioinformatics site using the Kyoto Encyclopaedia of Genes and Genomes (KEGG) database. Statistical threshold criteria were: Bonferroni-corrected P-value <0.05 and FDR <0.05.

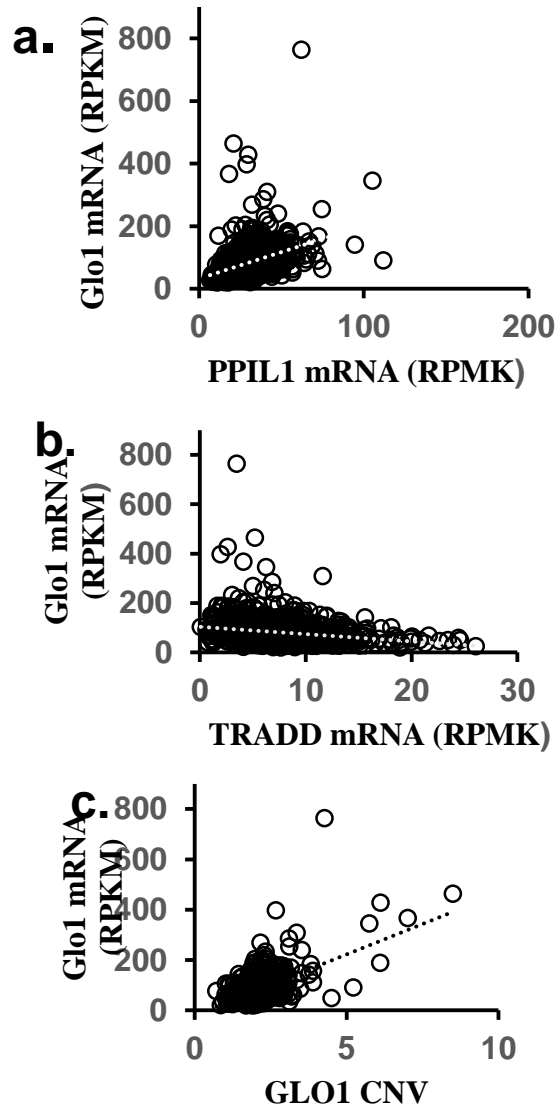


Figure 30. Correlation of selected genes and GLO1 CNV with Glo1 expression. a. Correlation on Glo1 mRNA on PPIL1 mRNA ($r = 0.568$ – the highest correlation coefficient found), b. Correlation on Glo1 mRNA on TRADD mRNA ($r = -0.353$ - the lowest correlation coefficient found). c. Correlation on Glo1 mRNA on GLO1 CNV ($r = 0.530$. Significance: $P < 0.001$).

4.1.2 Study of breast cancer patients

Over 3951 breast cancer patients were tested in this study using Kaplan-Meier (KM) plotter analysis tool for survival. The survival impact of expression of the following genes were studied (detected oligonucleotide probe-sets): GLO1 (200681_at); HAGH or Glo2 (205012_s_at), KDM4A (203205_at); AGER or RAGE (217046_s_at), NFE2L2 or Nrf2 (201146_at) and MGC9454 or KEAP1 (202417_at) of breast cancer patients. Data fitting optimised the best gene expression cut-off for low and high expression, relapse-free survival (RFS) was the clinical endpoint, and JetSetTM best probe set was used for mRNA detection. The maximum number of patients with breast cancer used in the data fitting was 3951.

In all breast cancer patients included in the analysis, increased GLO1 expression was a negative survival factor while HAGH was not linked to survival and KDM4A and AGER were linked positively to survival. Expression of NFE2L2 was linked negatively survival with a slightly lower hazard ratio and lower significance than GLO1, and KEAP1 expression was linked positively to survival, consistent with a positive and negative regulation of Glo1 expression in breast cancer. These relationships were maintained for KDM4A in systemically untreated patients, for GLO1 in systemic endocrine therapy – including systemic endocrine therapy with tamoxifen only, and for KEAP1 in patients treated with chemotherapy - Table 12.

The effect of tumour genotype, intrinsic subtype, lymph node status and stage on the association of GLO1 expression to patient survival was explored. Of the common breast cancer genotypes, ER, PR and HER2, there was only a negative association of GLO1 expression and patient survival for ER positive tumours. There were insufficient data in the KM Plotter database to form a judgement on the triple negative genotype. There were also negative associations of GLO1 expression and patient survival for luminal A and luminal B intrinsic subtypes, and lymph node negative status patients. The association with lymph node negative status patients was maintained in systemically untreated patients and the association with luminal A intrinsic type was maintained in patients

treated with systemic endocrine therapy – Table 13. Kaplan- Meier plots are given for all patient associations in Figures 21 - 22.

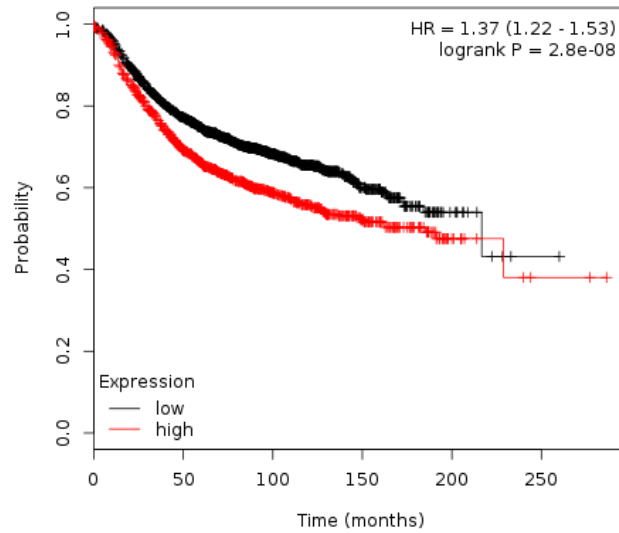


Figure 31. Kaplan Mier Plot of all patients with GLO1 expression.

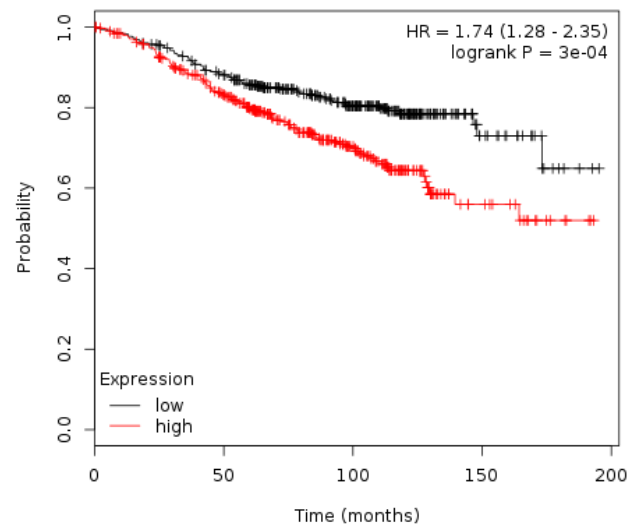


Figure 32. Kaplan Mier Plot of patients treated with tamoxifen only with GLO1 expression

Table 12. Effect of expression of GLO1, HAGH, KDM4A, AGER, NFE2L2 and KEAP1 on survival of breast cancer patients. All patients.

Patient criteria (patient number)	Gene	Hazard ratio	Logrank P	FDR	Low expression survival (months)	High expression survival (months)
All (3951)	GLO1	1.37 (1.22 – 1.53)	2.8×10^{-8}	0.01	217	185
	KDM4A	0.64 (0.57 – 0.72)	3.0×10^{-14}	0.01	140	217
	AGER	0.64 (0.57 – 0.72)	9.3×10^{-14}	0.01	145	217
	NFE2L2	1.30 (1.16 – 1.45)	3.1×10^{-6}	0.01	229	184
	KEAP1	0.8 (0.71 - 0.89)	8.4×10^{-5}	0.02	37	57
Systemically untreated (1010)	KDM4A	0.68 (0.54 – 0.84)	4.7×10^{-4}	0.05	51	912
Systemic endocrine therapy (1873)	GLO1	1.42 (1.19 – 1.88)	6.4×10^{-5}	0.02	217	191
Endocrine therapy - Tamoxifen only (733)	GLO1	1.74 (1.28 – 2.35)	3.0×10^{-4}	0.05	138	76
Chemotherapy – any (1616)	KEAP1	0.70 (0.59 – 0.84)	1.2×10^{-4}	0.05	42	80

Survival analysis: association of breast cancer patient survival analysis with expression of GLO1, HAGH, KDM4A, AGER, NFE2L2 and KEAP1. Where no data are shown there was no significant association. Significance criteria: Logrank P <0.05 and FDR ≤0.05

Table 13. Effect of GLO1 expression on breast cancer patient survival: effect of genotype, intrinsic subtype, lymph node status and stage.

Treatment	Genotype, intrinsic subtype, lymph node status and stage (patient number)	Hazard ratio	Logrank P	FDR	Low Glo1 expression survival (months)	High Glo1 expression survival (months)
All	ER positive (n = 2061)	1.65 (1.37 – 1.92)	1.7 x 10 ⁻⁸	0.01	217	163
	Luminal A (1933)	1.54 (1.29 – 1.84)	1.1 x 10 ⁻⁶	0.01	217	185
	Luminal B (1149)	1.53 (1.26 – 1.85)	1.3 x 10 ⁻⁵	0.01	171	122
	Lymph node negative (n = 2020)	1.39 (1.17 – 1.65)	1.6 x 10 ⁻⁴	0.05	228	217
Systemically untreated	Lymph node negative (n = 956)	1.39 (1.17 – 1.65)	1.6 x 10 ⁻⁴	0.05	228	217
Systemic endocrine therapy	Luminal A (1093)	1.57 (1.23 – 2.00)	2.3 x 10 ⁻⁴	0.01	217	191

Survival analysis: association of breast cancer patient survival analysis with expression of GLO1, HAGH, KDM4A, AGER, NFE2L2 and KEAP1. Where no data are shown there was no significant association. Significance criteria: Logrank P <0.05 and FDR ≤0.05

4.2 Characterisation of the Glyoxalase system in HEK293 cell line *in vitro*

4.2.1 Growth and viability of HEK293 cell line *in vitro*

The growth and viability of HEK293 cells *in vitro* were investigated. HEK293 Cells, 76,000 per well in 12-well plates, were cultured incubated in DMEM medium containing 25 mM glucose for four days. There is an increase in viable cell number throughout the culture time. At day one, viable cell number had increased to an average of $98,700 \pm 18,100$ cells per well ($n=3$). It was then exponential growth with marked increase in viable cell number to $1.07 \pm 0.03 \times 10^6$ cells per well at day 3. The rate of cell growth then decreased to day four and reaching a final viable cell number of $1.24 \pm 0.13 \times 10^6$ cells per well. Cell viability were determined by Trypan blue exclusion test. The related growth curve is given - Figure 23.

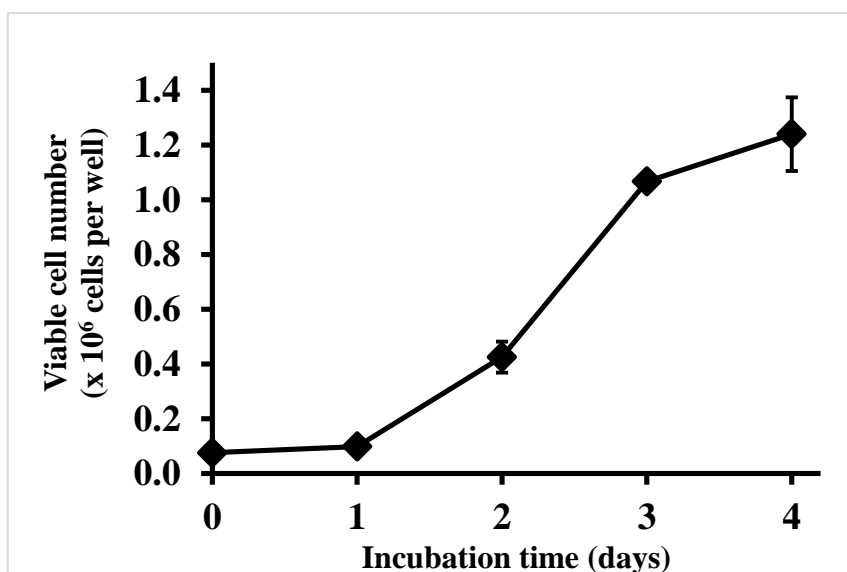


Figure 33. Growth curve of HEK293 cells *in vitro*.

HEK293 cells (seeding density $20,000 \text{ cells/cm}^2$) were cultured for four days. Data are mean \pm SD ($n=3$).

4.2.2 The activity of glyoxalase 1 and glyoxalase 2 in HEK293 cell line *in vitro*.

The activity of Glo1 and Glo2 was measured in HEK293 cells cultured in DMEM medium containing 25 mM glucose. The activity of Glo1 was 2018 ± 577 units per million cells ($n = 3$). The activity of Glo2 was 20.78 ± 6.35 units per million cells.

4.2.3 The flux formation of D-lactate and net formation of L-lactate in HEK293 cell line *in vitro*

D-Lactate is very slowly metabolised in HEK 293 cells and the activity of other enzymes metabolising MG, MG reductase and MG dehydrogenase, is very low in HEK 293 cells such that the main metabolic fate of MG is conversion to D-lactate. The rate of formation of D-lactate is, therefore, a surrogate measure of the flux of formation of MG. This was estimated by measuring the concentration of D-lactate in cultures at baseline and end of culture and deducing the rate of formation of D-lactate. The rate of formation of D-lactate in HEK293 cells over four days was 37.6 ± 2.0 nmol/day/million cells.

L-Lactate is formed and metabolized in HEK293 cells and so the net flux of formation of L-lactate may be measured. The net flux of formation of L-lactate in HEK293 cells incubated for 4 days was $2,470 \pm 90$ nmol/day/million cells.

4.2.4 The effect of methylglyoxal on the growth of HEK293 cells *in vitro*: concentration-response curve

HEK293 cells (seeding density 20,000 cells/cm²) were incubated with MG 20 -400 μ M for 48 h and viable cell number determined. There was a progressive decrease in viable cell number of HEK293 cells with increase in MG concentration over this range of MG concentration. A MG concentration - response curve was produced by plotting viable cell number (percentage of control - untreated HEK293 cells) against MG concentration - Figure 24. The median growth inhibitory concentration GC₅₀ value of MG for HEK293 cells *in vitro* was deduced by non-linear regression fitting of data to a dose-response curve, solving for GC₅₀ and logistic regression coefficient. The GC₅₀ of MG was $131 \mu\text{M} \pm 19.1$ where the logistic regression coefficient $n = 0.702 \pm 0.05$.

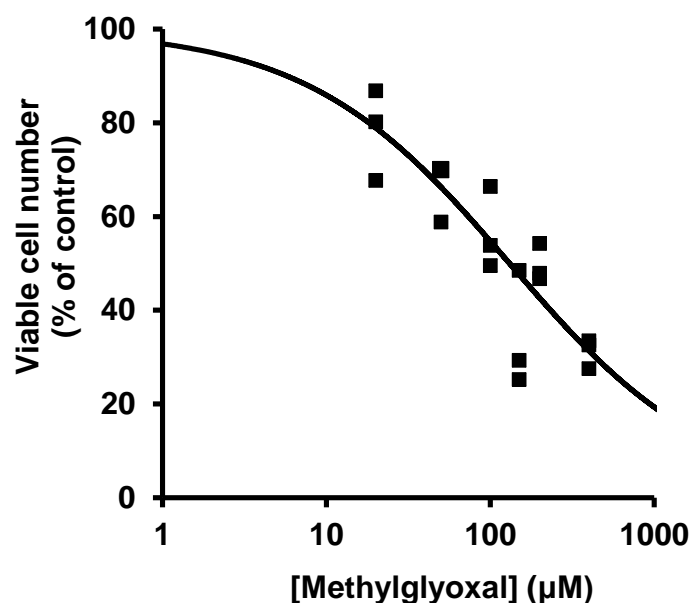


Figure 34. Methylglyoxal concentration-response curve for the effect on HEK293 cell growth *in vitro*.

HEK293 cells were incubated with and without 20 -400 μM for 48 h and viable cell number determined. $\text{GC}_{50} = 131 \pm 19.1 \mu\text{M}$, $n = 0.702 \pm 0.05$ ($N = 18$).

4.2.5 The effect of methylglyoxal on the growth of HEK293 cells *in vitro*: growth curve

Following the dose response study, the effect of the 131 μM MG on the growth and viability of HEK293 cells was investigated *in vitro*. HEK293 cells were incubated for 3 days with and without MG. Cells incubated with 131 μM MG showed a decreased rate of cell growth – Figure 25.

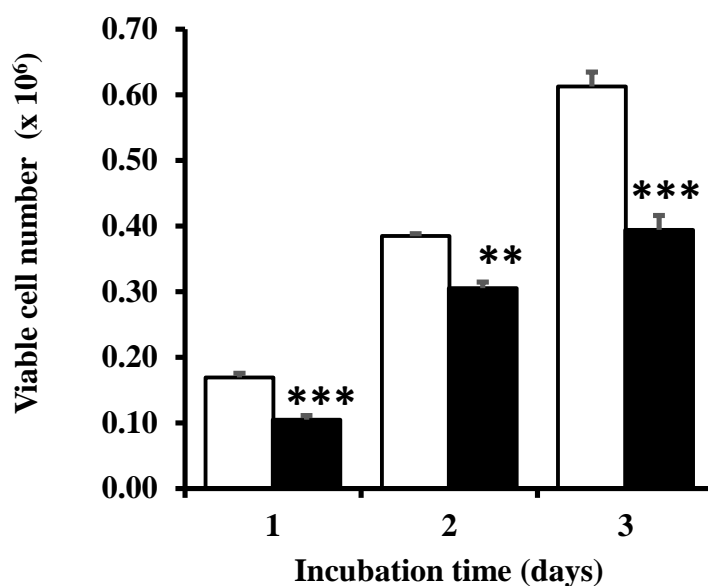


Figure 35. Effect of methylglyoxal on cell growth of HEK293 cells *in vitro*: effect of 131 μM methylglyoxal.

Key: open bars, control; solid bars, + 131 μM MG. Data are mean ± SD (n = 3). Significance: ** and ***, P<0.05 and P<0.001, respectively (*t*-test)

4.2.6 Effect of exposure period in the effect of methylglyoxal on growth of HEK293 cells *in vitro*

MG induces cytotoxicity under concentration-limiting conditions, as applies for the GC₅₀ concentration, by activation of apoptosis (Kang et al., 1996). The minimum period of exposure of HEK293 cells to MG required to induce growth arrest and cytotoxicity will inform on the culture period when processes leading to commitment to apoptosis occur. To identify the minimum period of exposure to MG required to induce growth and toxicity to HEK293 cells *in vitro*, HEK293 cells were incubated with 131 μM MG for 6, 12 and 24 h, cell culture medium then changed and cultures continued for a total of 48. There is a progressive decrease in viable cell number for exposure of HEK293 cells for 6 and 12 h. Thereafter, no further decrease in viable cell number was achieved. This indicates that commitment of HEK293 cells to apoptosis was achieved fully at 12 h.

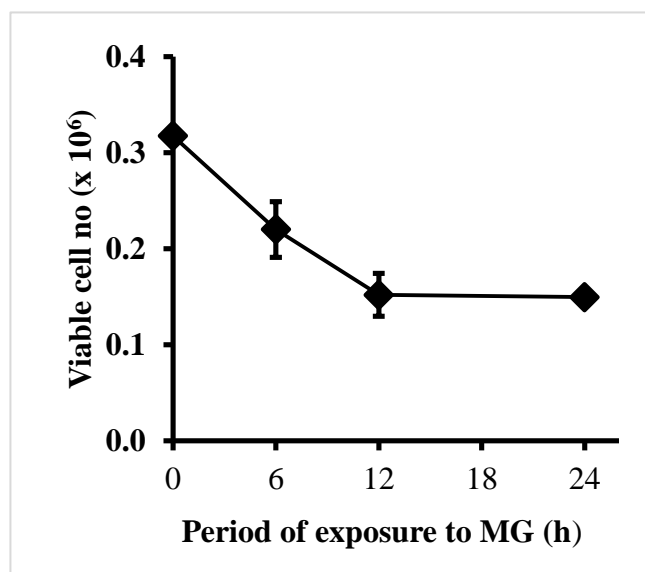


Figure 36. Effect of period of exposure to methylglyoxal on growth of HEK293 cells *in vitro*. HEK293 cells were incubated with 131 μ M MG for 0, 6, 12 and 24 h.

Data are mean and \pm SD (n = 3).

4.2.7 Effect of methylglyoxal on the cytochrome c release from mitochondria to the cytosol of HEK293 cell line *in vitro*

MG is considered to induce apoptosis by activation of the mitochondrial apoptotic pathway (Kang et al., 1996, Thornalley et al., 1996, Santarius et al., 2010). An indicator of this is release of cytochrome c from mitochondria to the cytosol (Matsura et al., 2002). The release of cytochrome c from the mitochondrial to cytosolic compartments were investigated by incubating HEK293 cells with 131 μ M MG for 1.5, 3, 6 and 12 h and preparing cytosolic extracts for assay of cytochrome c by commercial ELISA. Data are presented as ng/million cells. There was a marked increase in the cytosolic content of cytochrome c at 3 h and 6 h. Thereafter, there was a sharp decline at 12 h – the period where cells are beginning to develop apoptosis.

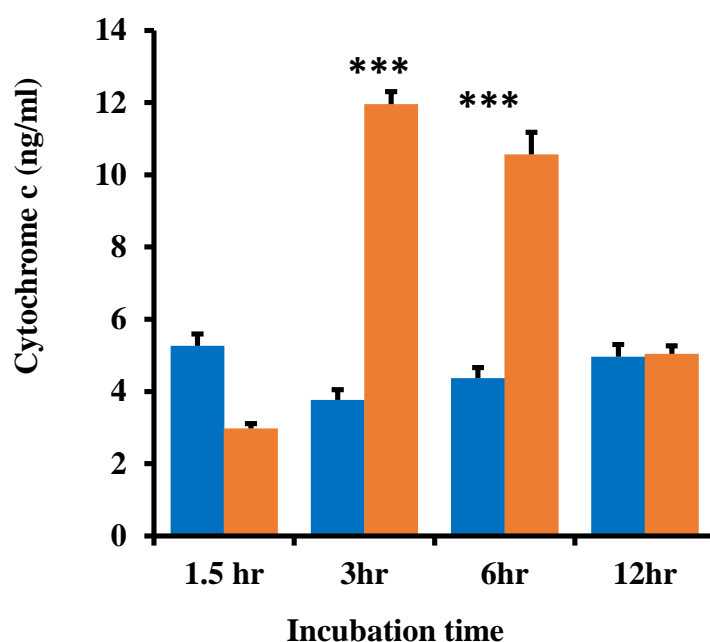


Figure 37. Cytochrome C content of the cytosol of HEK293 cells incubated with methylglyoxal *in vitro*.

Data are mean \pm SD (n = 3), (Blue) control, (Red) MG treated cells.

4.2.8 Treatment period with methylglyoxal required to maximize the cellular protein content of methylglyoxal-derived glycation adduct MG-H1.

Modification of cellular proteins by MG is an early-stage event in MG-induced cytotoxicity and likely contributes critically to the activation of apoptosis under MG concentration-limited conditions (Kang et al., 1996). To detect and identify cellular proteins modified by MG and possibly involved in the apoptotic process, it is important to identify the period of treatment with MG yielding the maximum total modification by MG. The major adduct formed by the modification of proteins by MG is the hydroimidazolone MG-H1. Hence, I incubated HEK293 cells from 0 – 12 h – the early-stage period of exposure to MG when commitment to apoptosis occurs, to identify when MG-H1 adduct content of cell protein is maximised. HEK293 cells were incubated with 131 μ M MG for 1.5 h, 3 h, 6 h and 12 h. Thereafter cell protein extracts were prepared and content of MG-H1 and for comparison the 3DG-derived hydroimidazolone isomers, 3DG-H, by stable isotopic dilution analysis LC-MS/MS. In the time course of MG-H1 content of cell protein, cellular protein content of MG-H1 increased markedly at

1.5 – 6 h and then declined thereafter at 12 h. The highest content of MG-H1 was achieved at 6 h: 2.78 ± 1.21 mmol/mol arg (n = 3; $P < 0.001$). The decline in MG-H1 content of cell protein at 12 h may be due to increased cellular proteolysis as commitment to apoptosis sets in– Figure 28 and Table 14.

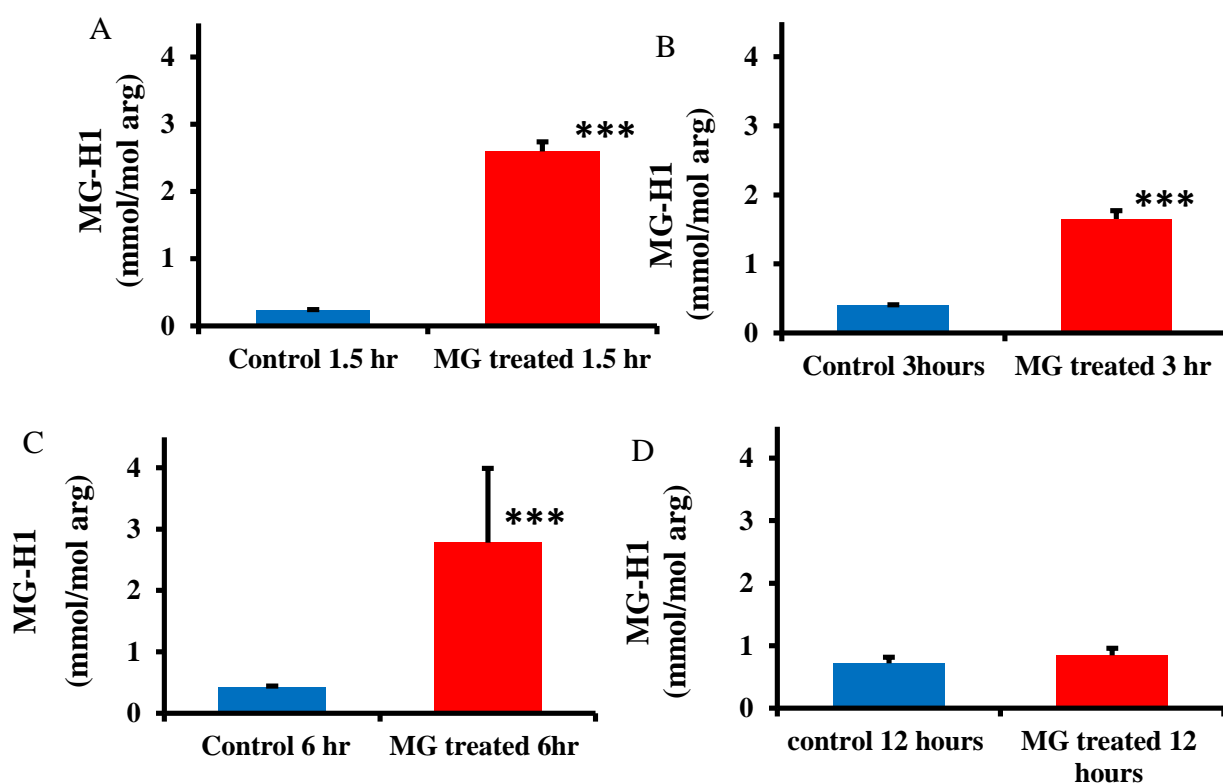


Figure 38. The methylglyoxal glycation adduct MG-H1 content of cellular protein for HEK293 cells incubated with and 131 μ M MG.

Key: blue bar, control; red bar, + MG. Treatment period: A., 1.5 h; B, 3 h; C, 6 h; and D, 12 h. Data are mean \pm SD (n = 3). Significance: ***, $P < 0.001$; Student's t-test.

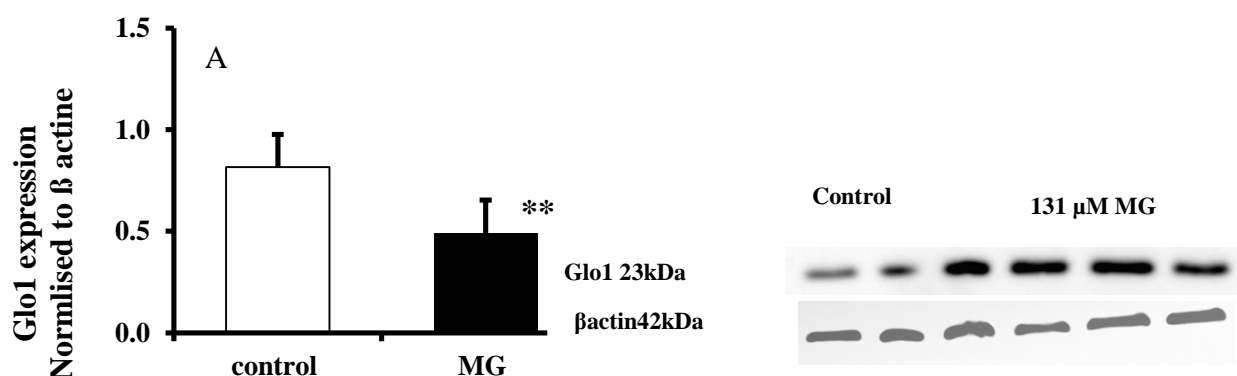
Table 14. The methylglyoxal glycation adduct MG-H1 content of cellular protein for HEK293 cells incubated with and 131 μ M MG.

Treatment period (h)	MG-H1 (mmol/mol arg)	
	Control	MG treated
1.5	0.23 \pm 0.02	2.60 \pm 0.14***
3	0.40 \pm 0.01	1.65 \pm 0.12***
6	0.42 \pm 0.02	2.78 \pm 1.21***
12	0.23 \pm 0.1	0.84 \pm 0.12

Data are mean \pm SD (n = 3). Significance: ***, P<0.001; Student's t-test.

4.2.9 Investigating the potential significant proteins role from the previous proteomics study.

an investigation of the content of Glo1, AKR1B1 and DDX5 at the protein level in HEK293 cell line incubated with 131 μ M of MG for 6 h were performed. There was a decrease in Glo1 protein expression in MG-treated cells: -45% (P< 0.01). There was also an increase of aldose reductase AKR1B1 but the increase was not statistically significant. For the DDX5, there was a significant increase in MG treated cells in comparison to control: + 18% (P<0.01).



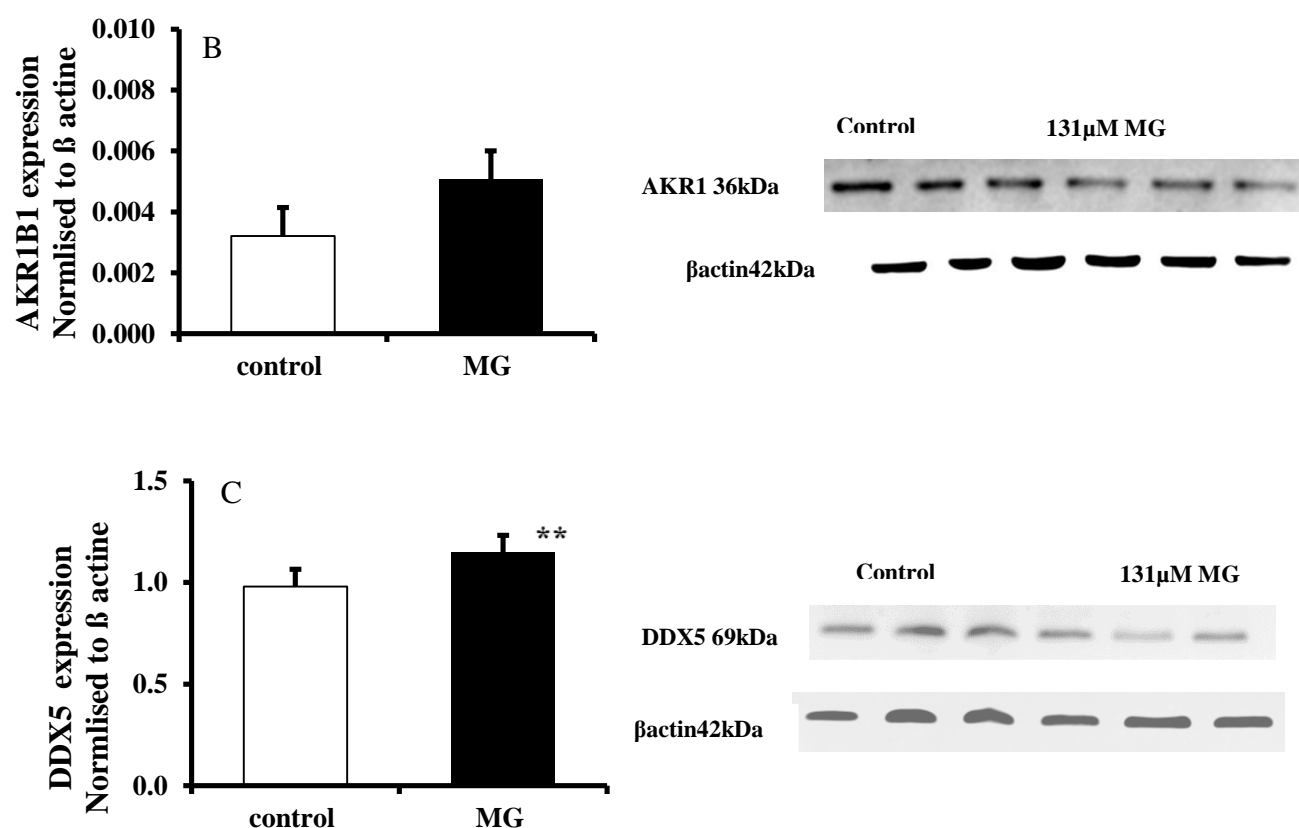


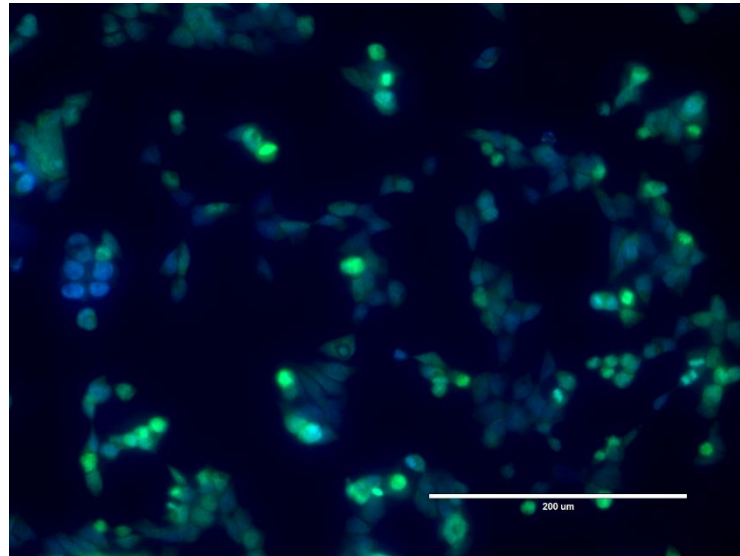
Figure 39. The protein expression changes in Control and treated 131 μ M of MG in HEK293. A Glo1, B AKR1B1 and C DDX5.

Data are mean \pm SD, n = 3. Significance: *, P<0.05, **, P<0.01.

4.3 The effect of methylglyoxal on the extrachromosomal DNA secretion.

For the extrachromosomal DNA release analysis, HEK293 cell line were treated with 131 μ M MG to investigate the secretion of the extrachromosomal DNA by staining the nuclei and the backbone of the DNA as explained in section 3.5.1. In treating cells there was remarkable increase in DNA secretion from the nuclei suggesting that treating with MG also induces the secretion of the free dsDNA - see Figure 30.

Control



MG treated

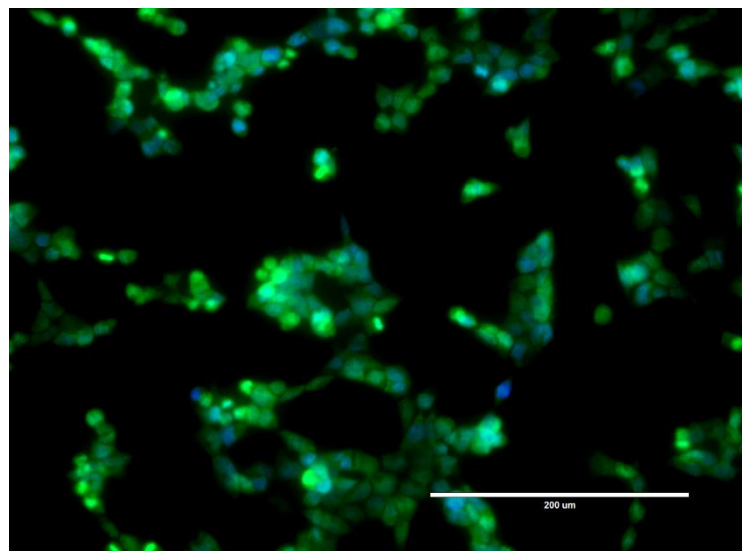


Figure 40. Assessment of extrachromosomal DNA in HEK293 cells incubated with and without 131 μ M MG for 6 h *in vitro*.

Increase can be observed in the MG-treated cells. Key: green, extrachromosomal free dsDNA; blue, cell, cell nuclei stain.

4.4 Analysis of fractional proteomes of HEK293 cells incubated with and without methylglyoxal

HEK293 cells were incubated with and without 131 μ M MG for 6 hr reaches to produce the maximum of MG-H1 adduct content of cell protein immediately prior to the commitment of cells to apoptosis. Cell extracts were then prepared for analysis of fractional proteomes: soluble proteins of the cytoplasm; cell nucleus; mitochondrial matrix with intermembrane space; and mitochondrial membranes.

4.4.1 Cytoplasmic protein extract

Four thousand and seventy proteins were detected in all replicates of cytoplasmic protein extract of control and MG-treated cells. There were abundance changes of 1365 proteins with MG treatment: 121 proteins were increased in abundance and 1244 decreased in abundance. For the proteins increased in abundance, the abundance change ranged from 1.2 to 30 fold – Table 15. The highest increase, 30-fold, was of the calcium activated cation channel CSC1-like protein 2 (TMEM63B). Overexpression of TMEM63B promotes migration in HEK293T cells (Marques et al., 2019). There was also increase in abundance of the MG metabolizing enzyme aldo-keto reductase 1B1 (aldose reductase); + 21%. For the proteins of decreased abundance, abundance decreases ranged from 7 – 95%. Pathways analysis showed of protein with decreased abundance with MG treatment showed enrichment or overrepresentation of proteins in the ribosome, spliceosome, RNA transport and proteasome metabolic pathways – Table 20. Four hundred and eighty-one proteins were detected with MG-H1 modification: 42 of these increased with MG treatment and 71 decreased with MG treatment – Table 16 and Table 17. MG-H1 modified proteins were not significantly enriched to any metabolic pathways.

4.4.2 Nuclear protein extract

Two thousand and forty-four proteins were detected in the nuclear fractions of HEK293 cells in all replicates of control and test samples. Only 107 proteins were changed in abundance by treatment with MG: 49 proteins were

increased and 58 proteins were decreased. Proteins increased were not enriched in any pathway whereas the proteins decreased were enriched in the major mRNA splicing pathway – Table 21. One hundred and nineteen proteins were detected with MG-H1 modification but only 6 were changed in abundance with MG treatment. Five were increased: carbohydrate-responsive element-binding protein, 263 fold; Protachykinin-1, 21 fold; 3-ketoacyl-CoA thiolase, mitochondrial, 15-fold; Diphthamide biosynthesis protein 1, 7-fold; and Enoyl-CoA hydratase, mitochondrial, 2-fold. The MG-H1 modified protein decreased was protein ABHD14A; decreased - 91%.

4.4.3 Mitochondrial matrix and intermembrane space proteins

One thousand, nine hundred and twenty-eight proteins were detected in the mitochondrial matrix and intermembrane space. Only 150 proteins were changed in abundance by treatment with MG: 16 were increased and 134 were decreased – Table 22 and Table 23. Proteins increases were in the range 1.4 – 49 fold. One of the proteins increased was caspase-14, increased *ca.* 3-fold. Decreases in abundances of proteins was from 21% to 98%. Forty-two proteins were detected with MG-H1 modification. Only two MG-H1 modified proteins were increased in MG-treated cells: scaffold attachment factor, increased 8-fold; and metastasis suppressor protein 1, increased 7-fold. One MG-H1 modified proteins was decreased in MG-treated wells: B-cell CLL/lymphoma 9-like protein, - 98%.

4.4.4 Mitochondrial membrane proteins

One hundred and 168 proteins were detected in all samples for mitochondrial membrane proteins. Treatment with MG increased the abundance of 9 proteins. Two proteins are linked to mitochondrial stress responses and intrinsic apoptotic pathway: CREB-regulated transcription coactivator 3 and prohibitin, respectively – Table 24. One hundred and sixteen proteins were decreased in abundance by MG treatment: decreases ranging from 79 – 99%. Pathways analysis of these proteins revealed enrichment in 4 pathways: respiratory electron transport, mRNA splicing - major pathway, gluconeogenesis and formation of ATP by chemiosmotic coupling – Table 25. There were 26

proteins detected with MG-H1 modification: 9 were decreased with MG-H1 treatment and 2 were increased – Table 26.

a.

Uniprot accession no: P63220

Molecular mass: 9.111.6 Da

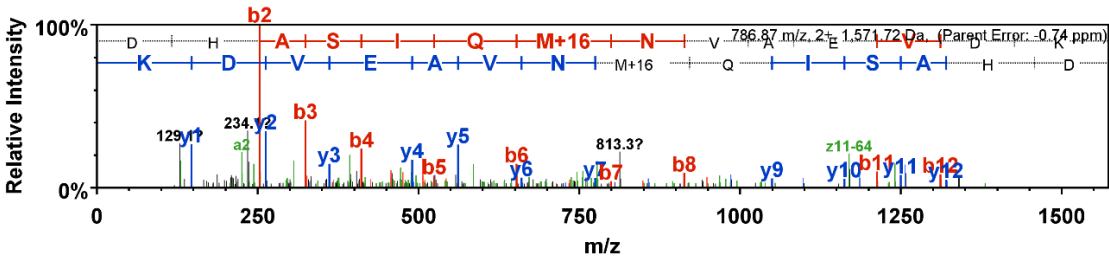
Protein name: 40 Ribosomal protein S21

Gene name: RPS21

5 exclusive unique peptides, 6 exclusive unique spectra, 14 total spectra, 44/83 amino acids (53% coverage)

MQNDAGEFVD **LYVPRK**CSAS NRILGAK**DHA** **SIQMNVAEVD** **K**VTGRFNGQF
KTYAICGAIR **RMGESDDSL** **RLAK**ADGIVS KNF

b.



c.

B	B Ions	B+2H	B-NH3	B-H2O	AA	Y Ions	Y+2H	Y-NH3	Y-H2O	Y
1	116.0			98.0	D	1,572.7	786.9	1,555.7	1,554.7	14
2	253.1	127.1		235.1	H	1,457.7	729.4	1,440.7	1,439.7	13
3	324.1	162.6		306.1	A	1,320.6	660.8	1,303.6	1,302.6	12
4	411.2	206.1		393.2	S	1,249.6	625.3	1,232.6	1,231.6	11
5	524.2	262.6		506.2	I	1,162.6	581.8	1,145.6	1,144.6	10
6	652.3	326.7	635.3	634.3	Q	1,049.5	525.3	1,032.5	1,031.5	9
7	799.3	400.2	782.3	781.3	M...	921.4	461.2	904.4	903.4	8
8	913.4	457.2	896.4	895.4	N	774.4	387.7	757.4	756.4	7
9	1,012.5	506.7	995.4	994.4	V	660.4	330.7	643.3	642.3	6
10	1,083.5	542.2	1,066.5	1,065.5	A	561.3		544.3	543.3	5
11	1,212.5	606.8	1,195.5	1,194.5	E	490.3		473.2	472.2	4
12	1,311.6	656.3	1,294.6	1,293.6	V	361.2		344.2	343.2	3
13	1,426.6	713.8	1,409.6	1,408.6	D	262.1		245.1	244.1	2
14	1,572.7	786.9	1,555.7	1,554.7	K	147.1		130.1		1

Figure 41. An example of mass spectrometric detection of a peptide in the trypsin/lys-C digest: 40S Ribosomal protein S21 identified in nuclear fraction.

a. Protein information and sequence coverage. Key: yellow highlighting – sequence detected; green shading – M detected as methionine sulfoxide (+16 Da).

b. Peptide fragmentation ion mass scan of peptide 28 - 41. **c.** Fragment ion assignment table. Ions detected are colour coded in the mass spectrum assignments with colour shading in the table. m/z ion values unshaded were not detected and blank spaces in the table indicate ions are not expected chemically.

Table 15. Proteins in the cytoplasmic extract increased in abundance by treatment with methylglyoxal.

Uniprot accession no	Name of protein(gene)	Fold increase
H0YCP6	transmembrane protein 63B(TM63B)	30.53
A0A087WT97	multiple EGF like domains 11(MEGF11)	13.99
U3KQQ5	transmembrane protein 259 (TMEM259)	8.22
A0A0J9YX13	tissue specific transplantation antigen P35B (TSTA3)	5.69
F8VRE9	coronin 1C(CORO1C)	5.24
D6RBW1	eukaryotic translation initiation factor 4E (EIF4E)	5.10
A0A087X2I5	LSM7 homolog, U6 small nuclear RNA and mRNA degradation associated(LSM7)	4.89
Q14DG7	transmembrane protein 132B(TM6132B)	4.79
H0YDJ4	ninein(NIN)	4.77
Q9BZL1	ubiquitin like 5(UBL5)	4.40
A0A0G2JLQ8	NLR family pyrin domain containing 2(NLRP2)	4.13
E9PQR4	tubby bipartite transcription factor(TUB)	3.93
Q9H2G4	TSPY like 2(TSPYL2)	3.76
Q96A61	tripartite motif containing 52(TRIM52)	3.59
M0QXX8	charged multivesicular body protein 2A(CHMP2A)	3.48
D6RBJ7	GC, vitamin D binding protein(GC)	3.47
P01031	complement C5(C5)	3.45
Q8TDV5	G protein-coupled receptor 119(GPR119)	3.45
P35527	keratin 9(KRT9)	3.25
Q7Z5M8	abhydrolase domain containing 12B(ABHD12B)	3.24
H3BMW6	calcium voltage-gated channel subunit alpha1 H(CACNA1H)	3.23
Q7L1I2	synaptic vesicle glycoprotein 2B(SV2B)	3.18
Q7RTV0	PHD finger protein 5A(PHF5A)	2.95
P07858	cathepsin B(CTSB)	2.88
Q9UKX7	nucleoporin 50(NUP50)	2.83
H3BNC9	Uncharacterized protein	2.77
P10827	thyroid hormone receptor, alpha(THRA)	2.68
A0A0G2JQ76	KIAA0355(KIAA0355)	2.62
H3BNT2	coenzyme Q9(COQ9)	2.61
H7C3A6	Fanconi anemia core complex associated protein 20(FAAP20)	2.57
H0YGR4	RNA exonuclease 2(REXO2)	2.41
A0A087X2I7	class II major histocompatibility complex transactivator(CIITA)	2.37
H0YB67	drosha ribonuclease III(DROSHA)	2.37
K7EM19	vesicle amine transport 1(VAT1)	2.31
H7C202	mitotic spindle organizing protein 2A(MZT2A)	2.26

Q03181	peroxisome proliferator activated receptor delta(PPARD)	2.21
P33552	CDC28 protein kinase regulatory subunit 2(CKS2)	2.16
Q9BYD6	mitochondrial ribosomal protein L1(MRPL1)	2.15
Q3ZCX4	zinc finger protein 568(ZNF568)	2.14
P51587	BRCA2, DNA repair associated(BRCA2)	2.13
Q6ZR64	matrix remodeling associated 7(MXRA7)	2.11
H7BZL2	3-hydroxyisobutyrate dehydrogenase(HIBADH)	2.10
A0A0A0MSD7	protein tyrosine phosphatase, receptor type N2(PTPRN2)	2.09
F8W9Q7	solute carrier family 25 member 37(SLC25A37)	2.09
H0Y903	methionyl aminopeptidase 1(METAP1)	2.08
H3BPB0	S-phase cyclin A associated protein in the ER(SCAPER)	2.08
D6RFM5	succinate dehydrogenase complex flavoprotein subunit A(SDHA)	2.07
A0A0B4J1Y4	gamma-glutamylcyclotransferase(GGCT)	2.06
Q6KC79	NIPBL, cohesin loading factor(NIPBL)	2.05
E7EQL8	tubulin gamma complex associated protein 6(TUBGCP6)	2.03
F5GYA2	uracil DNA glycosylase(UNG)	2.03
P53420	collagen type IV alpha 4 chain(COL4A4)	2.03
A0A087WZY0	ceroid-lipofuscinosis, neuronal 5(CLN5)	2.03
H0Y390	microtubule-actin crosslinking factor 1(MACF1)	2.02
P29373	cellular retinoic acid binding protein 2(CRABP2)	2.02
P43897	Ts translation elongation factor, mitochondrial(TSFM)	2.01
Q5T1U7	collagen type XXVII alpha 1 chain(COL27A1)	1.98
P51608	methyl-CpG binding protein 2(MECP2)	1.93
H3BQA6	cyclin D1 binding protein 1(CCNDBP1)	1.93
A0A087WT80	phospholipase C beta 1(PLCB1)	1.93
P05543	serpin family A member 7(SERPINA7)	1.90
A0A087WWL5	chromosome 19 open reading frame 68(C19orf68)	1.90
A0A1C7CYZ2	ceroid-lipofuscinosis, neuronal 5(CLN5)	1.89
Q9H0W5	coiled-coil domain containing 8(CCDC8)	1.89
Q96ST2	IWS1, SUPT6H interacting protein(IWS1)	1.85
P02549	spectrin alpha, erythrocytic 1(SPTA1)	1.85
J3KNP4	semaphorin 4B(SEMA4B)	1.83
A0A024R214	cytoplasmic polyadenylation element binding protein 1(CPEB1)	1.83
A6PWM2	cysteine rich with EGF like domains 2(CRELD2)	1.83
A0A1B0GUS7	unc-13 homolog B(UNC13B)	1.82
K7ENL0	septin 9(SEPT9)	1.81
P01023	alpha-2-macroglobulin(A2M)	1.79
A0A087WWW8	calcineurin binding protein 1(CABIN1)	1.79

Q969S3	zinc finger protein 622(ZNF622)	1.78
H0YHS6	tyrosyl-tRNA synthetase 2(YARS2)	1.78
Q96N66	membrane bound O-acyltransferase domain containing 7(MBOAT7)	1.76
H0Y9N9	LPS responsive beige-like anchor protein(LRBA)	1.74
E9PJ65	solute carrier family 6 member 9(SLC6A9)	1.73
Q5T2E8	chromosome 10 open reading frame 76(C10orf76)	1.73
E9PJF9	aminopeptidase puromycin sensitive(NPEPPS)	1.73
A0A087WUT0	myelin expression factor 2(MYEF2)	1.70
Q86T26	transmembrane protease, serine 11B(TMPPRSS11B)	1.70
Q14676	mediator of DNA damage checkpoint 1(MDC1)	1.64
H0YEZ9	ubiquilin 1(UBQLN1)	1.63
A0A0G2JQF3	mucin 20, cell surface associated(MUC20)	1.62
Q7Z698	sprouty related EVH1 domain containing 2(SPRED2)	1.62
P41223	BUD31 homolog(BUD31)	1.62
A0A087WX24	sterile alpha motif domain containing 11(SAMD11)	1.59
Q9BV73	centrosomal protein 250(CEP250)	1.56
Q9C0J8	WD repeat domain 33(WDR33)	1.56
Q99832	chaperonin containing TCP1 subunit 7(CCT7)	1.54
P08579	small nuclear ribonucleoprotein polypeptide B2(SNRPB2)	1.52
A0A087WWT1	succinate dehydrogenase complex iron sulfur subunit B(SDHB)	1.49
Q9P1A2	protein phosphatase 4 regulatory subunit 1 like (pseudogene)(PPP4R1L)	1.48
A0A087WZL3	anaplastic lymphoma receptor tyrosine kinase(ALK)	1.47
A0A0G2JS85	syntrophin gamma 2(SNTG2)	1.47
Q9GZN8	chromosome 20 open reading frame 27(C20orf27)	1.47
A8MUM1	tumor suppressing subtransferable candidate 1(TSSC1)	1.47
V9GYA7	death associated protein 3(DAP3)	1.46
H0YL19	WD repeat domain 61(WDR61)	1.46
H7C440	DIS3 like 3'-5' exoribonuclease 2(DIS3L2)	1.45
J3QRD1	aldehyde dehydrogenase 3 family member A2(ALDH3A2)	1.43
P14921	ETS proto-oncogene 1, transcription factor(ETS1)	1.43
A0A0J9YYF7	dishevelled associated activator of morphogenesis 2(DAAM2)	1.42
A0A087WYK2	WNK lysine deficient protein kinase 3(WNK3)	1.41
H3BPN4	enhancer of mRNA decapping 3(EDC3)	1.41
Q9NZ56	formin 2(FMN2)	1.41
P00390	glutathione-disulfide reductase(GSR)	1.35
Q08E93	family with sequence similarity 27 member E3(FAM27E3)	1.33

P82933	mitochondrial ribosomal protein S9(MRPS9)	1.32
A0A0A0MQX8	muscleblind like splicing regulator 1(MBNL1)	1.30
P02545	lamin A/C(LMNA)	1.30
Q9Y2W2	WW domain binding protein 11(WBP11)	1.29
	SMG6, nonsense mediated mRNA decay	
Q86US8	factor(SMG6)	1.28
Q01469	fatty acid binding protein 5(FABP5)	1.23
Q96PK6	RNA binding motif protein 14(RBM14)	1.23
A0A075B7F8	POM121 transmembrane nucleoporin C(POM121C)	1.22
H7C537	NFU1 iron-sulfur cluster scaffold(NFU1)	1.22
P15121	aldo-keto reductase family 1 member B(AKR1B1)	1.21
P62995	transformer 2 beta homolog (Drosophila)(TRA2B)	1.17
E9PNB5	nuclear autoantigenic sperm protein(NASP)	1.15

Table 16. Proteins in the cytoplasmic extract modified by methylglyoxal and increased in abundance by treatment with methylglyoxal.

Protein (Gene)	Fold change
Multiple epidermal growth factor-like domains protein 11 (MEGF11)	13.99
GDP-L-fucose synthase (TSTA3)	5.69
NACHT, LRR and PYD domains-containing protein 2 (NLRP2)	4.13
Tripartite motif-containing protein 52 (TRIM52)	3.59
Charged multivesicular body protein 2a (CHMP2A)	3.48
Glucose-dependent insulinotropic receptor (GPR119)	3.45
Keratin, type I cytoskeletal 9 (KRT9)	3.25
Protein ABHD12B (ABHD12B)	3.24
Voltage-dependent T-type calcium channel subunit alpha-1H (CACNA1H)	3.23
Synaptic vesicle glycoprotein 2B (SV2B)	3.18
Thyroid hormone receptor alpha (THRA)	2.68
Uncharacterized protein KIAA0355 (KIAA0355)	2.62
Fanconi anemia core complex-associated protein 20 (FAAP20)	2.57
Oligoribonuclease, mitochondrial (REXO2)	2.41
MHC class II transactivator (CIITA)	2.37
Mitotic-spindle organizing protein 2A (MZT2A)	2.26
Receptor-type tyrosine-protein phosphatase N2 (PTPRN2)	2.09
Mitoferrin-1 (SLC25A37)	2.09
Gamma-tubulin complex component 6 (TUBGCP6)	2.03
Ceroid-lipofuscinosis neuronal protein 5 (CLN5)	2.03

Microtubule-actin cross-linking factor 1, isoforms 1/2/3/5 (MACF1)	2.02
Collagen alpha-1(XXVII) chain (COL27A1)	1.98
Phosphoinositide phospholipase C (PLCB1)	1.93
Uncharacterized protein C19orf68 (C19orf68)	1.90
Ceroid-lipofuscinosis neuronal protein 5 (CLN5)	1.89
Semaphorin-4B OS=Homo sapiens (SEMA4B)	1.83
Calcineurin-binding protein cabin-1 (CABIN1)	1.79
Transporter (SLC6A9)	1.73
Myelin expression factor 2 (MYEF2)	1.70
Mucin-20 (MUC20)	1.62
Sterile alpha motif domain-containing protein 11 (SAMD11)	1.59
Centrosome-associated protein CEP250 (CEP250)	1.56
pre-mRNA 3' end processing protein WDR33 (WDR33)	1.56
Putative serine/threonine-protein phosphatase 4 regulatory subunit 1-like (PPP4R1L)	1.48
Gamma-2-syntrophin (SNTG2)	1.47
28S ribosomal protein S29, mitochondrial (DAP3)	1.46
Serine/threonine-protein kinase WNK3 (WNK3)	1.41
Enhancer of mRNA-decapping protein 3 (EDC3)	1.41
Protein FAM27E3 (FAM27E3)	1.33
Telomerase-binding protein EST1A (SMG6)	1.28
Nuclear envelope pore membrane protein POM 121C (POM121C)	1.22
Nuclear autoantigenic sperm protein (NASP)	1.15

Table 17. Proteins in the cytoplasmic extract modified by methylglyoxal and decreased in abundance by treatment with methylglyoxal.

Protein (Gene)	Fold change
heterogeneous nuclear ribonucleoprotein K(HNRNPK)	0.91
heterogeneous nuclear ribonucleoprotein K(HNRNPK)	0.88
FUS RNA binding protein(FUS)	0.86
zinc finger CCHC-type containing 2(ZCCHC2)	0.84
DEAH-box helicase 15(DHX15)	0.82
tripartite motif containing 46(TRIM46)	0.81
casein kinase 2 alpha 2(CSNK2A2)	0.81
heterogeneous nuclear ribonucleoprotein M(HNRNPM)	0.81
heterogeneous nuclear ribonucleoprotein M(HNRNPM)	0.81
EWS RNA binding protein 1(EWSR1)	0.81
KRI1 homolog(KRI1)	0.79

lactate dehydrogenase A(LDHA)	0.79
espin-like(ESPNL)	0.78
mutS homolog 6(MSH6)	0.78
interleukin enhancer binding factor 2(ILF2)	0.76
peroxiredoxin 1(PRDX1)	0.76
MAK16 homolog(MAK16)	0.76
heterogeneous nuclear ribonucleoprotein U(HNRNPU)	0.75
RecQ like helicase 5(RECQL5)	0.75
eukaryotic translation elongation factor 2(EEF2)	0.73
histone cluster 1 H2B family member n(HIST1H2BN)	0.73
bromodomain adjacent to zinc finger domain 1B(BAZ1B)	0.71
ataxin 10(ATXN10)	0.71
PH domain and leucine rich repeat protein phosphatase 1(PHLPP1)	0.70
SPT6 homolog, histone chaperone(SUPT6H)	0.68
potassium channel tetramerization domain containing 9(KCTD9)	0.67
carboxypeptidase X, M14 family member 2(CPXM2)	0.67
ubiquitin specific peptidase 5(USP5)	0.66
zinc finger RNA binding protein(ZFR)	0.66
nuclear pore complex interacting protein family member A3(NPIPA3)	0.64
myosin XVA(MYO15A)	0.62
ATP/GTP binding protein like 4(AGBL4)	0.62
hydroxyacylglutathione hydrolase(HAGH)	0.62
zinc finger protein 513(ZNF513)	0.62
zinc finger protein 345(ZNF345)	0.61
signal recognition particle 54(SRP54)	0.61
ubiquitin A-52 residue ribosomal protein fusion product 1(UBA52)	0.61
myeloid differentiation primary response 88(MYD88)	0.61
uncharacterized LOC105372343(LOC105372343)	0.61
RNA pseudouridylate synthase domain containing 3(RPUSD3)	0.60
dedicator of cytokinesis 2(DOCK2)	0.60
tRNA isopentenyltransferase 1(TRIT1)	0.58
spen family transcriptional repressor(SPEN)	0.56
desmoplakin(DSP)	0.55
ankyrin repeat domain 1(ANKRD1)	0.54
RNA polymerase I subunit A(POLR1A)	0.53
myosin XVIII A(MYO18A)	0.53
A-kinase anchoring protein 6(AKAP6)	0.52
par-3 family cell polarity regulator beta(PARD3B)	0.51
intraflagellar transport 172(IFT172)	0.51
topoisomerase (DNA) II beta(TOP2B)	0.50

kelch like family member 33(KLHL33)	0.50
ankyrin repeat and sterile alpha motif domain containing 3(ANKS3)	0.49
atypical chemokine receptor 2(ACKR2)	0.47
carboxypeptidase E(CPE)	0.46
glycerol-3-phosphate dehydrogenase 2(GPD2)	0.46
chromodomain helicase DNA binding protein 3(CHD3)	0.42
solute carrier family 39 member 11(SLC39A11)	0.39
testis expressed 33(TEX33)	0.39
MAP3K12 binding inhibitory protein 1(MBIP)	0.38
periaxin(PRX)	0.38
microtubule associated protein 7(MAP7)	0.35
V-set and transmembrane domain containing 2A(VSTM2A)	0.25
mitochondrial ribosomal protein S21(MRPS21)	0.24
tripartite motif containing 21(TRIM21)	0.24
KIAA0556(KIAA0556)	0.21
ciliary rootlet coiled-coil, rootletin(CROCC)	0.18
lipase E, hormone sensitive type(LIPE)	0.17
TATA-box binding protein associated factor 3(TAF3)	0.13
F-box and WD repeat domain containing 8(FBXW8)	0.10
olfactory receptor family 4 subfamily A member 15(OR4A15)	0.05

Table 18. Proteins in the nuclear extract increased in abundance by treatment with methylglyoxal.

Uniprot Accession	Name of protein (Gene)	Fold increase
A0A0C4DG 26	Carbohydrate-responsive element-binding protein (MLXIPL)	262.60
P02775	Platelet basic protein (PPBP)	48.34
P01859	Immunoglobulin heavy constant gamma (IGHG2)	23.81
P20366	Protachykinin-1 (TAC1)	20.60
Q5T7N2	LINE-1 type transposase domain-containing protein 1 (L1TD1)	19.54
A0A0A0M R66	RNA binding motif protein 10, (RBM10)	19.14
P01042	Kininogen-1 GN=(KNG1)	17.30

A0A0B4J2	3-ketoacyl-CoA thiolase, mitochondrial (ACAA2)	14.74
A4		
Q9BS19	HPX protein (HPX)	13.93
P04196	Histidine-rich glycoprotein (HRG)	11.31
P02776	Platelet factor 4 (PF4)	10.92
F8W696	Apolipoprotein (APOA1)	9.56
P01860	Immunoglobulin heavy constant gamma (IGHG3)	7.77
P01023	Alpha-2-macroglobulin (A2M)	6.28
Q96M27	Protein PRRC1 (PRRC1)	6.22
Q13541	Eukaryotic translation initiation factor 4E-binding protein 1 (EIF4EBP1)	5.41
P19878	Neutrophil cytosol factor (NCF2)	4.02
Q8TBY9	WD repeat-containing protein 66 (WDR66)	2.94
Q9BT09	Protein canopy homolog 3 (CNPY3)	2.79
X6R700	Chromatin target of PRMT1 protein (CHTOP)	2.73
E9PDQ8	Succinate--CoA ligase [GDP-forming] subunit beta, mitochondrial (SUCLG2)	2.28
O14828	Secretory carrier-associated membrane protein 3 (SCAMP3)	2.16
Q5M9N0	Coiled-coil domain-containing protein (CCDC158)	2.07
P30084	Enoyl-CoA hydratase, mitochondrial (ECHS1)	2.01
O14745	Na(+)/H(+) exchange regulatory cofactor NHE-RF1 (SLC9A3R1)	1.90
Q6S8J3	POTE ankyrin domain family member (POTEE)	1.77
Q9UMX5	Neudesin (NENF)	1.64
P60709	Actin, cytoplasmic 1 (ACTB)	1.56
Q562R1	Beta-actin-like protein 2 (ACTBL2)	1.55
P14735	Insulin-degrading enzyme (IDE)	1.54
P52907	F-actin-capping protein subunit alpha-1 (CAPZA1)	1.53
P680325	Actin, alpha cardiac muscle 1 (ACTC1)	1.51
B4DSN5	Tyrosine-protein phosphatase non-receptor type (PTPN1)	1.47

A8K7Q2	Heat shock cognate 71 kDa protein (HSPA8)	1.37
C9JIZ6	Prosaposin OS=Homo sapiens (PSAP)	1.33
O43923	Matrix metalloproteinase (mmp20)	1.31
C9J8T6	Cytochrome c oxidase copper chaperone (COX17)	1.25
P10253	Lysosomal alpha-glucosidase (GAA)	1.20

Table 19. Proteins in the nuclear extract decreased in abundance by treatment with methylglyoxal.

Gene	Name of protein	Fold increase
P13010+	X-ray repair cross-complementing protein 5 (XRCC5)	0.78
A0A087WZR9	Pyrroline-5-carboxylate reductase (PYCR2 PE)	0.77
F5H6P7	Protein mago nashi homolog 2(MAGOHB)	0.72
Q10570	Cleavage and polyadenylation specificity factor subunit 1 (CPSF1)	0.71
A0A0A0MRA53	Heterogeneous nuclear ribonucleoprotein U-like protein 1 (HNRNPUL1)	0.67
Q14011	Cold-inducible RNA-binding protein (CIRBP)	0.67
P09661	U2 small nuclear ribonucleoprotein A (SNRPA10)	0.66
F8VZX2	Poly(rC)-binding protein 2 (PCBP2)	0.63
E7EQY1	Protein FAM136A (FAM136A)	0.61
H0Y5B4	60S ribosomal protein L36a (RPL36A)	0.60
Q96KR1	Zinc finger RNA-binding protein (ZFR)	0.60
A0A0A0MSI2	Polyhomeotic-like protein 2 (PHC2)	0.59
J3QLW7	60S ribosome subunit biogenesis protein NIP7 homolog (NIP7)	0.58
Q9BXT5	Testis-expressed protein 15 (TEX15)	0.57
Q04760	Lactoylglutathione lyase (GLO1)	0.56
P62314	Small nuclear ribonucleoprotein D1 (SNRPD1)	0.56

A0A0U1R	Polypyrimidine tract-binding protein 1 (PTBP1)	0.55
RM4		
P32322	Pyrroline-5-carboxylate reductase 1, mitochondrial (PYCR1)	0.50
A0A087X1		
W2	Protein arginine N-methyltransferase 1 (PRMT1)	0.50
Q3SX64	Outer dense fiber protein 3-like protein 2 (ODF3L2)	0.50
H0YKD8	60S ribosomal protein L28 (RPL28)	0.49
A0A087W		
WR2	Myc-associated zinc finger protein (MAZ)	0.47
P53999	Activated RNA polymerase II transcriptional coactivator p15 (SUB1)	0.47
F8WBM4	Follicle-stimulating hormone receptor (FSHR)	0.47
F5H1S9	tRNA pseudouridine synthase (PUS1)	0.46
O60832	H/ACA ribonucleoprotein complex subunit 4 (DKC1)	0.44
Q9H0A0	RNA cytidine acetyltransferase (NAT10)	0.43
Q15427	Splicing factor 3B subunit 4 (SF3B4)	0.42
A0A0A0M		
SE2	Hydroxyacyl-coenzyme A dehydrogenase, mitochondrial (HADH)	0.42
Q9Y2H1	Serine/threonine-protein kinase 38-like (STK38L)	0.42
E7EVA0	Microtubule-associated protein (MAP4)	0.41
P21953	2-oxoisovalerate dehydrogenase subunit beta, mitochondrial (BCKDHB)	0.40
P41208	Centrin-2 (CETN20)	0.39
Q5JSZ5	Protein PRRC2B (PRRC2B)	0.38
A0A024R3	Ngg1 interacting factor 3 like 1 binding protein 1, isoform CRA_b (NIF3L1BP1)	0.37
41		
D6RAV8	Carbonyl reductase family member 4 (CBR4)	0.36
Q9UNZ5	Leydig cell tumor 10 kDa protein homolog (C19)	0.36
A0A0A0M		
RZ6	Lysosomal-trafficking regulator LYST	0.34
Q8IXW0	Lamin tail domain-containing protein 2 (LMNTD2)	0.31

Q9NYB0	Telomeric repeat-binding factor 2-interacting protein 1 (TERF2IP)	0.30
Q9UII2;	ATPase inhibitor, mitochondrial (ATPIF1)	0.29
H0YMV8	40S ribosomal protein S27 (RPS27L)	0.26
F5H2A4	High mobility group protein (HMGA2)	0.20
Q9UK45	U6 snRNA-associated Sm-like protein LSm7 (LSM7)	0.18
F8WAH1	Alpha-aminoadipic semialdehyde synthase, mitochondrial (AASS)	0.17
P29084	Transcription initiation factor IIE subunit beta (GTF2E2)	0.17
P13807	Glycogen [starch] synthase, muscle (GYS1)	0.16
A0A087X2 I5	U6 snRNA-associated Sm-like protein LSm7 (LSM7)	0.13
Q92947	Glutaryl-CoA dehydrogenase, mitochondrial (GCDH)	0.13
H3BNT7	26S proteasome non-ATPase regulatory subunit 7 (PSMD7)	
P98179	RNA-binding protein 3 (RBM3)	0.02

Table 20. Pathways enrichment analysis of proteins decreased in the cytoplasmic extract by treatment with methylglyoxal.

Pathway	Count	Fold Enrichment	Bonferroni P-values	FDR	Genes
Ribosome	51	4.4	4.2×10^{-18}	2.2×10^{-17}	RPL18, RPL17, RPL13, RPS10, NUDT3, RPLP2, RPS27L, RPL22L1, RPS3, RPL10, FAU, RPL11, RPL12, MRPL1, MRPL3, MRPS5, RPS18, RPS19, RPS16, RPS14, RPS13, RPS11, UBA52, MRPS11, RPL35, RPL36, RPL38, MRPL11, RPS25, MRPL13, RPS27, RPS28, RPL32, RPL7, RPS29, RPL6, RPL31, RPL34, RPL8, RPS20, RPSA, RPL26, RPL23A, MRPS21, RPS6, RPS8, RPL29, RPL23, RPL22, MRPL27, RPL13A, RPL21
Spliceosome	43	3.8	3.3×10^{-12}	1.7×10^{-11}	SRSF1, CCDC12, TRA2B, U2AF2, LSM7, SF3B6, SF3B5, BUD31, SF3B3, SF3B2, CTNNBL1, PRPF19, HNRNPM, SF3B1, HNRNPK, DDX23, DHX15, DHX16, MAGOHB, SNRNP70, PRPF40A, MAGOH, EFTUD2, DDX39B, SNW1, PRPF3, SF3A2, DDX5, RBMX, PRPF4, SF3A1, HNRNPU, PRPF6, PPIE, EIF4A3, PPIH, SRSF5, SRSF4, SRSF6, SNRNP200, THOC3, PRPF38B, RBM17 NUP98, ELAC2, XPO5, PABPC4, RANGAP1, PNN, SUMO3, EIF3C, SUMO2, EIF3D, EIF3CL, SUMO1, EIF4EBP1, EIF3G, RAE1, EIF3H, EIF3E, RPP30, MAGOHB, EIF3I, EIF1, PABPC1, EIF3J, TPR, GEMIN4, NMD3, GEMIN5, NUP133, EEF1A1, RGPDP8, UPF1, RAN, MAGOH, EEF1A2, DDX39B, TACC3, TRNT1, EIF4G1, EIF4A3, UPF3B, NUP205, EIF2S1, THOC6, POP1, CYFIP1, THOC3
RNA transport	46	3.1	6.8×10^{-10}	3.5×10^{-9}	PSMC5, PSMB6, PSMD12, PSME1, PSMB1, PSMA6, PSMD11, PSME2, PSMA4, PSMB2, PSMA3, PSMD3, PSME3, PSMD4, PSMD7, PSMD8
Proteasome	16	4.3	4.1×10^{-4}	2.1×10^{-3}	

Threshold criterion for significance: Bonferroni-corrected $P < 0.05$ and $FDR < 0.05$.

Table 21. Pathways enrichment analysis of proteins decreased in the cell nucleus by treatment with methylglyoxal.

Pathway	Fold change	Count	Fold Enrichment	Genes
mRNA Splicing - Major Pathway	0.52 ± 0.21	9	12.1	CPSF1, HNRNPUL1, LSM7, MAGOHB, PCBP2, PTBP1, SF3B4, SNRPA1, SNRPD1

Significance: Bonferroni corrected P-value, 5.11×10^{-5} ; FDR, 5×10^{-4} .

Threshold criterion for significance: Bonferroni-corrected $P < 0.05$ and $FDR < 0.05$.

Table 22. Proteins of the mitochondrial matrix and intermembrane space increased by HEK293 cell treatment with methylglyoxal.

Uniprot accession no	Fold change	Protein
A0A024R3B9	49.3	crystallin alpha B (CRYAB)
Q15554	27.3	telomeric repeat binding factor 2 (TERF2)
A8MYB8	20.6	aldehyde dehydrogenase 3 family member A1 (ALDH3A1)
P13647	18.4	keratin 5 (KRT5)
A0A1B0GVP8	10.7	solute carrier family 26 member 10 (SLC26A10)
Q14151	8.0	scaffold attachment factor B2 (SAFB2)
H0YBL3	6.8	MTSS1, I-BAR domain containing (MTSS1)
Q9NWZ3	6.6	interleukin 1 receptor associated kinase 4 (IRAK4)
Q9NZT1	4.1	calmodulin like 5 (CALML5)
P31944	3.0	caspase 14 (CASP14)
G3V1V0	2.0	myosin light chain 6 (MYL6)
P46778	1.9	ribosomal protein L21 (RPL21)
G5E9G0	1.7	ribosomal protein L3 (RPL3)
H3BMM9	1.7	RNA binding protein with serine rich domain 1 (RNPS1)
P39023	1.6	ribosomal protein L3 (RPL3)
P00441	1.4	superoxide dismutase 1, soluble (SOD1)

Table 23. Proteins of the mitochondrial matrix and intermembrane space decreased by HEK293 cell treatment with methylglyoxal.

Uniprot accession no.	Name of protein (gene)
J3KRC4	5', 3'-nucleotidase, cytosolic(NT5C)
F5GZY1	acidic residue methyltransferase 1(ARMT1)
G3V2E7	kinesin light chain 1(KLC1)
A0A087X060	E2F associated phosphoprotein(EAPP)
Q9BV57	acireductone dioxygenase 1(ADI1)
E7ER27	hydroxysteroid 17-beta dehydrogenase 4(HSD17B4)
P50990	chaperonin containing TCP1 subunit 8(CCT8)
G3V1C3	apoptosis inhibitor 5(API5)
Q96GX2	ataxin 7 like 3B(ATXN7L3B)
Q13257	MAD2 mitotic arrest deficient-like 1 (yeast)(MAD2L1)
F8VQZ7	methionyl aminopeptidase 2(METAP2)
Q96JG6	VPS50, EARP/GARPII complex subunit(VPS50)
P36871	phosphoglucomutase 1(PGM1)
E7ENV7	copine 8(CPNE8)
P62937	peptidylprolyl isomerase A(PPIA)
Q96CT7	coiled-coil domain containing 124(CCDC124)
Q86WV7	coiled-coil domain containing 43(CCDC43)
F2Z2Y4	pyridoxal (pyridoxine, vitamin B6) kinase(PDXK)
O15067	phosphoribosylformylglycinamide synthase(PFAS)
Q6P2E9	enhancer of mRNA decapping 4(EDC4)
M0R0Y2	NSF attachment protein alpha(NAPA)
O15160	RNA polymerase I subunit C(POLR1C)
Q14980	nuclear mitotic apparatus protein 1(NUMA1)
A0A087WY61	nuclear mitotic apparatus protein 1(NUMA1)
P46108	CRK proto-oncogene, adaptor protein(CRK)
A0A0A0MTN3	glutathione S-transferase mu 3(GSTM3)
Q15527	surfeit 2(SURF2)
A0A087WTP3	KH-type splicing regulatory protein(KHSRP)

Q4G0X9	coiled-coil domain containing 40(CCDC40)
K7EJX8	dihydrouridine synthase 3 like(DUS3L)
Q8WU90	zinc finger CCCH-type containing 15(ZC3H15)
O15455	toll like receptor 3(TLR3)
P24666	acid phosphatase 1, soluble(ACP1)
H7C170	Williams-Beuren syndrome chromosome region 22(WBSCR22)
Q99543	DnaJ heat shock protein family (Hsp40) member C2(DNAJC2)
Q7Z4Q2	HEAT repeat containing 3(HEATR3)
E5RGS4	prefoldin subunit 1(PFDN1)
H0YIV4	nucleosome assembly protein 1 like 1(NAP1L1)
F8VV59	nucleosome assembly protein 1 like 1(NAP1L1)
A0A087WTB8	ubiquitin C-terminal hydrolase L3(UCHL3)

Table 23. Proteins of the mitochondrial matrix and intermembrane space decreased by HEK293 cell treatment with methylglyoxal (cont'd).

Uniprot accession no.	Name of protein (gene)
Q99956	dual specificity phosphatase 9(DUSP9)
O00178	GTP binding protein 1(GTPBP1)
P62487	RNA polymerase II subunit G(POLR2G)
H7C0X7	methionine adenosyltransferase 2B(MAT2B)
A0A087WY 55	vesicle trafficking 1(VTA1)
Q99733	nucleosome assembly protein 1 like 4(NAP1L4)
Q14691	GIN5 complex subunit 1(GINS1)
E9PCB6	neurolysin(NLN)
A0A087W WE2	RNA polymerase II subunit A(POLR2A)

P43487	RAN binding protein 1(RANBP1)
P15924	desmoplakin(DSP)
A0A0D9SG E8	PHD finger protein 6(PHF6)
P02647	apolipoprotein A1(APOA1)
P0DN79	cystathionine-beta-synthase(CBS)
Q6Y7W6	GRB10 interacting GYF protein 2(GIGYF2)
P35609	actinin alpha 2(ACTN2)
P17480	upstream binding transcription factor, RNA polymerase I(UBTF)
O14776	transcription elongation regulator 1(TCERG1)
F5H6C2	intraflagellar transport 88(IFT88)
Q9Y5J1	UTP18, small subunit processome component(UTP18)
Q5VYK3	KIAA0368(KIAA0368)
A0A087WZ T3	bolA family member 2(BOLA2)
Q92922	SWI/SNF related, matrix associated, actin dependent regulator of chromatin subfamily c member 1(SMARCC1)
H0YJH9	poly(A) binding protein nuclear 1(PABPN1)
H3BPJ9	NADH:ubiquinone oxidoreductase subunit B10(NDUFB10)
I3L2H7	ubiquitin conjugating enzyme E2 G1(UBE2G1)
A0A087WS W9	thioredoxin reductase 1(TXNRD1)
Q96GX9	APAF1 interacting protein(APIP)
Q5T7U1	general transcription factor IIIC subunit 5(GTF3C5)
P36404	ADP ribosylation factor like GTPase 2(ARL2)
P13797	plastin 3(PLS3)
C9JA08	NMD3 ribosome export adaptor(NMD3)
Q8TDD1	DEAD-box helicase 54(DDX54)
Q14247	cortactin(CTTN)
P22059	oxysterol binding protein(OSBP)
Q9UJA5	tRNA methyltransferase 6(TRMT6)

A0A0C4DG	ADP ribosylation factor like GTPase 6 interacting protein
62	4(ARL6IP4)
J3KTF8	Rho GDP dissociation inhibitor alpha(ARHGDIA)
O95433	activator of Hsp90 ATPase activity 1(AHSA1)
F6TLX2	glyoxalase domain containing 4(GLOD4)

Table 23. Proteins of the mitochondrial matrix and intermembrane space decreased by HEK293 cell treatment with methylglyoxal (cont'd).

Uniprot accession no.	Name of protein (gene)
Q3YEC7	RAB, member RAS oncogene family-like 6(RABL6)
E7EVX8	pre-mRNA processing factor 31(PRPF31)
Q16762	thiosulfate sulfurtransferase(TST)
Q16513	protein kinase N2(PKN2)
P43652	afamin(AFM)
M0R389	platelet activating factor acetylhydrolase 1b catalytic subunit 3(PAFAH1B3)
P53004	biliverdin reductase A(BLVRA)
P31942	heterogeneous nuclear ribonucleoprotein H3(HNRNPH3)
B2WTI3	arginine demethylase and lysine hydroxylase(JMJD6)
Q9Y224	chromosome 14 open reading frame 166(C14orf166)
D6RGE2	isochorismatase domain containing 1(ISOC1)
Q9Y5X3	sorting nexin 5(SNX5)
C9JJP5	TRK-fused gene(TFG)
I3L397	eukaryotic translation initiation factor 5A(EIF5A)
E7EPN9	proline rich coiled-coil 2C(PRRC2C)
Q5T4U8	Rab geranylgeranyltransferase beta subunit(RABGGTB)
F5H5U2	DEAD-box helicase 55(DDX55)
F5GZQ9	purinergic receptor P2X 4(P2RX4)
Q9BQC6	mitochondrial ribosomal protein L57(MRPL57)
H0Y9N5	TROVE domain family member 2(TROVE2)

O75794	cell division cycle 123(CDC123)
A0A087WZX0	B-cell CLL/lymphoma 9-like(BCL9L)
Q15056	eukaryotic translation initiation factor 4H(EIF4H)
P18615	negative elongation factor complex member E(NELFE)
Q06124	protein tyrosine phosphatase, non-receptor type 11(PTPN11)
P49770	eukaryotic translation initiation factor 2B subunit beta(EIF2B2)
K7EM18	eukaryotic translation initiation factor 1(EIF1)
A6NIR2	heat shock protein family B (small) member 11(HSPB11)
O43172	pre-mRNA processing factor 4(PRPF4)
P78362	SRSF protein kinase 2(SRPK2)
E9PEB5	far upstream element binding protein 1(FUBP1)
P48147	prolyl endopeptidase(PREP)
Q13564	NEDD8 activating enzyme E1 subunit 1(NAE1)
Q8WUM0	nucleoporin 133(NUP133)
O75792	ribonuclease H2 subunit A(RNASEH2A)
J3KPM9	signal transducer and activator of transcription 1(STAT1)
Q96KP4	CNDP dipeptidase 2 (metallopeptidase M20 family)(CNDP2)
P62993	growth factor receptor bound protein 2(GRB2)
H7BYN3	transcription factor A, mitochondrial(TFAM)
P08670	vimentin(VIM)

Table 23. Proteins of the mitochondrial matrix and intermembrane space decreased by HEK293 cell treatment with methylglyoxal (cont'd).

Uniprot accession no.	Name of protein (gene)
Q9GZL7	WD repeat domain 12(WDR12)
A0A087X1A5	staufen double-stranded RNA binding protein 1(STAU1)
Q9NVN8	G protein nucleolar 3 like(GNL3L)

Q92688	acidic nuclear phosphoprotein 32 family member B(ANP32B)
F8VXU5	VPS29, retromer complex component(VPS29)
I3L2B0	clustered mitochondria homolog(CLUH)
O75153	clustered mitochondria homolog(CLUH)
B5MBZ8	protein phosphatase 1 regulatory subunit 7(PPP1R7)
Q8IXS0	family with sequence similarity 217 member A(FAM217A)
Q9Y5X1	sorting nexin 9(SNX9)
D6REK3	CWC27 spliceosome associated protein homolog(CWC27)
Q9BRS2	RIO kinase 1(RIOK1)
Q5VZU9	tripeptidyl peptidase 2(TPP2)
B4E1Z4	highly similar to Complement factor B

Table 24. Proteins of the mitochondrial membrane of HEK 293 cells increased by treatment with methylglyoxal.

Gene	Protein	Fold change	Comment on function	References
RPS5	Ribosomal protein S5	9.6	Involved in malignant cell differentiation	(Vizirianakis et al., 1999)
YLPM1	YLP motif-containing protein 1	9.4		
CRTC3	CREB-regulated transcription coactivator 3	5.0	Mitochondrial biogenesis and stress response	(Than et al., 2011)
GRIN2D	Glutamate receptor ionotropic, NMDA 2D	4.4		
RPS23	40S ribosomal protein S23	4.0		
STATH	Statherin	3.2		
GRM6	Metabotropic glutamate receptor 6	2.7		
PHB	Prohibitin	2.5	Stabilizes the mitochondrial genome and modulate mitochondrial dynamics, morphology, biogenesis, and the mitochondrial intrinsic apoptotic pathway	(Peng et al., 2015)
UFSP1	Inactive Ufm1-specific protease 1	2.1		

Table 25. Pathways enrichment analysis of proteins of the mitochondrial membrane increased by treatment with methylglyoxal.

Pathway	Count	Fold Enrichment	Bonferroni P-value	FDR	Genes
Respiratory electron transport	10	12.1	2.3×10^{-5}	1.3×10^{-4}	COX5A, UQCR10, CYCS, COX7C, UQCRB, NDUFB10, NDUFA5, COX5B, NDUFA4, SDHB
mRNA Splicing - Major Pathway	12	7.0	2.0×10^{-4}	1.1×10^{-3}	HNRNPH, RBMX, HNRNPA1, HNRNPC, DDX5, SRSF3, ALYREF, SNRPC, HSPA8, YBX1, SRSF1, PTBP1
Gluconeogenesis	6	19.3	2.6×10^{-3}	1.5×10^{-2}	SLC25A11, GAPDH, GOT2, MDH2, ENO1, ENO2
Formation of ATP by chemiosmotic coupling	5	28.6	4.8×10^{-3}	2.8×10^{-2}	ATP5F1D, ATP5F1B, ATP5H, ATP5PO, ATP5F1A

Threshold criterion for significance: Bonferroni-corrected $P < 0.05$ and $FDR < 0.05$.

Table 26. Proteins of the mitochondrial membrane with methylglyoxal modification.

Protein	Gene	Fold change
Toll/interleukin-1 receptor domain-containing adapter protein	TIRAP	0.007
Synaptonemal complex protein 2	SYCP2	0.050
Dedicator of cytokinesis protein 8	DOCK8	0.055
Coiled-coil domain-containing protein 74A	CCDC7 4A	0.136
Steroidogenic acute regulatory protein, mitochondrial	STAR	0.181
Gamma-enolase	ENO2	0.181
Protein FAM71E1	FAM71 E1	0.211
Polyhomeotic-like protein 3	PHC3	0.237
Very long-chain-specific acyl-CoA dehydrogenase, mitochondrial	ACADV L	0.284
Testis- and ovary-specific PAZ domain-containing protein 1	TOPAZ 1	0.528
Heterogeneous nuclear ribonucleoprotein M	HNRNP M	
Potassium voltage-gated channel subfamily KQT member 2	KCNQ2	
Adenomatous polyposis coli protein	APC	
Vacuolar protein sorting-associated protein 72	VPS72	
Putative uncharacterized protein UNQ6190	UNQ619 0	
40S ribosomal protein S15	RPS15	

Neurogenic locus notch homolog protein 4	NOTCH 4	
RNA-binding protein 42	RBM42	
Rho-related BTB domain-containing protein 2	RHOB T B2	
Cytosolic carboxypeptidase 1	AGTPB P1	
Eukaryotic translation initiation factor 3 subunit A	EIF3A	
Coiled-coil domain-containing protein 17	CCDC1 7	
Kelch-like protein 40	KLHL40	
Calmodulin-like protein 3	CALML 3	
Glutamate receptor ionotropic, NMDA 2D	GRIN2D	4.4
Metabotropic glutamate receptor 6	GRM6	2.7

“Fold change” is the change of protein abundance in MG-treated cells compared to control

5 Discussion

5.1 Methylglyoxal, glyoxalase 1 and cancer – a historical and re-occurring association

MG and Glo1 have long been associated with control of cell growth and cancer therapy. They were initially thought to be key controllers of cell growth and then discounted with discovered of other more potent and well-evidenced growth factors (Apple and Greenberg, 1968). MG was initially proposed as a cancer treatment but discounted due to poor efficacy (Conroy, 1979). Recent research has seen the emergence of high Glo1 expression as permissive of rapid tumour growth – rather than mediator of growth – through metabolism of MG and thereby facilitating tumours to develop high glycolytic activity to sustain high tumour growth (Rabbani et al., 2018). The latter effect has suggested that MG-induced cytotoxicity has an unrecognised role in the mechanism of action of several clinical anticancer drugs. The association of MG and Glo1 with cancer and cancer chemotherapy is historical yet recurring with improved scientific evidence and qualified yet critical mechanistic insights in tumour development and treatment responses emerging. It is not certain but is becoming increasingly likely that treatment of cancer – particularly breast cancer – may be improved with better understanding of this system and a Glo1 inhibitor available for clinical evaluation.

5.2 Bioinformatics of glyoxalase 1 expression: correlation and survival analysis in human tumour cells lines and breast cancer patients, respectively

5.2.1 Bioinformatics of glyoxalase 1 expression: correlation analysis in human tumour cells lines

To my knowledge this study is the first to examine and identify the genes that correlate with Glo1 mRNA expression in human tumour cell lines. In this section, I investigated gene expression correlation with Glo1 expression from data available in the cancer cell line encyclopaedia (CCLE). Data analysis was performed in on the mRNA copy number from RNA-seq analysis data (Reads Per

Kilobase Million or RPKM). Data were normally distributed therefore Pearson correlation was used.

The findings produced new insights into Glo1 and cell growth. Glo1 expression correlated positively with genes enriched in spliceosome, RNA transport cell cycle and DNA replication pathways. Two of the top four genes rank-ordered by correlation coefficient, high r value first, were genes of the spliceosome - PPIL1 (first) and CDC5L (fourth). To my knowledge, this is the first association of the Glo1 to the spliceosome – the high enrichment, 7.5 fold, and extremely strong statistical association (Bonferroni-corrected P-value = 7.9×10^{-11} , FDR = 6.9×10^{-10}) making it of likely importance and highly unlikely to be a chance observation. I suspect this association reflects a high level of importance for the spliceosome to be protected against MG modification to work effectively. Indeed, the spliceosome function depends on a family of the serine- and arginine-rich proteins (SR proteins) which are involved in spliceosome assembly and interactions with RNA regulatory sequences on the pre-mRNA and with multiple cofactors.(Bourgeois et al., 2004). Genes involved in RNA transport were also strongly correlated – particularly of the nuclear core complex (NUP107, NUP153, NUP155, NUP35, NUP37, NUP43, NUP54, SUMO1 and SUMO2). This may not be arginine-rich itself but its carrier substrate, **α -importin, binds carried molecular cargo** via arginine-rich nuclear localization sequences (McLane and Corbett, 2009, Kosugi et al., 2009). There are also critical functional arginine residues in the origin recognition complex proteins, ORC2, ORC3 and ORC4, for initiation of DNA replication (Bleichert et al., 2015) and arginine finger sensors of RFC2, RFC3, RFC4, and RFC5 proteins to drive DNA binding and proliferating cell nuclear antigen loading for multiprotein ATP-driven DNA replicase to duplicate chromosomal DNA prior to cell division (Johnson et al., 2006). Protection of these proteins from MG modification and inactivation may underly the enrichment of genes of cell cycle regulation and DNA replication with positive correlates of Glo1 expression in human tumor cell lines. A link between Glo1 activity and tumour cell proliferation, cell cycle changes and differentiation status system was examined previously by the Thornalley team (Thornalley, 1990). The study have shown that cells such as Raji(+) had increased Glo1

activity during growth arrest which is consistent with increased Glo1 activity on entry of cells into G₀–G₁ phase of the cells cycle. (Hooper et al., 1988b). There is no evidence of Glo1 interacting directly with components of the spliceosome, RNA transport cell cycle and DNA replication pathways. The spliceosome is involved in pre-RNA processing, mRNA metabolism and splicing. This positive correlation with Glo1 suggest a stronger links in between the Glo1 expression and the pre-mRNA splicing. In cancer, evidence is accumulating to suggest that aberrant splicing events play a role in cancer chemotherapy. Multiple cancer-related genes have been shown to be associated with this: such as tumour suppressor, p53, apoptosis regulator *BCL2L1*, *HRAS*, *CD44* and others (Wang and Lee, 2018, El Marabti and Younis, 2018).

For the negative correlation, eight genes found to be correlated with Glo1 expression: 3 pseudogenes, 2 long non-coding RNAs, N-acetylglucosamine-1-phosphate transferase subunit gamma (GNTPG) – part of aTop of Form complex involved in targeting of lysosomal hydrolases to the lysosome, Tapasin binding protein like (TAPBPL) – involved in antigen processing in the endoplasmic reticulum, and tumor necrosis factor receptor type 1 (TNFR1)-associated death domain protein (TRADD). TRADD is an adaptor protein for multiple receptor-mediated pathways of apoptosis: TNFR1, TNF receptor-associated factor 2 (TRAF2), recruitment of inhibitor-of-apoptosis proteins and tumor necrosis factor receptor superfamily member 6/FAS cell death receptor (TNFRSF6/FAS) and adaptor protein Fas-associated protein with death domain (FADD/MORT1) (Pobezinskaya and Liu, 2012). This negative correlation between Glo1 expression and TRADD may indicate that tumour cells with high Glo1 expression have decreased propensity to undergo apoptosis.

For GLO1 gene copy number, normal GLO1 copy number was assumed for the range 2.39 - 1.61, mean 2.00, which reflects the precision with which GLO1 copy number may be measured (range of mean \pm 3SD) (Shafie et al., 2014). GLO1 copy number correlated positively and strongly with Glo1 expression: $r = 0.53$ ($P = 9 \times 10^{-68}$). This suggests that increase of GLO1 copy number is a major determinant of increased Glo1 expression is often, but not always, functional and gives rise to proportionate change in Glo1 expression

(Redon et al., 2006, Santarius et al., 2010). These findings compare well with previous studies showed that GLO1 DNA increased in clinical tumors. Glo1 expression in tumour cell lines. Increased GLO1 copy number is also highly prevalent and correlates with increased Glo1 expression in some clinical tumours – reviewed in (Rabbani et al., 2018).

5.2.2 Bioinformatics of glyoxalase 1 expression and survival analysis in breast cancer patients

For the impact of Glo1 expression on cancer patient survival, I performed Kaplan-Meier survival analysis using Glo1 expression and cancer patient survival data in the KM-Plotter database. Most data available was for breast cancer patients – 3951 patients, and hence analysis was performed for this cancer type with progression-free survival as the clinical endpoint. The results showed that Glo1 is a negative survival impact on breast cancer patients regardless of the treatment type, common genotype variants (ER, PR and HER2), intrinsic type and stage. The hazard ratio (HR) of 1.37 compares well with outcomes of algorithm-selected multivariate analysis. For example, in a recent study 88 genes with HRs >1.22 were combined in an algorithm but only produced an overall HR of *ca.* 1.26 (Zhang et al., 2018). Assessment of Glo1 expression alone is performing better than this. Glo1 expression was suggested previously in a small, under-powered study of 121 cancer patients (Peng et al., 2017).

The negative survival impact appears not linked to AGE receptor signaling via RAGE as increased AGER expression was a positive survival factor; nor to KDM4A – considered a potential mediator of GLO1 copy number increase (Rabbani et al., 2018), as increased KDM4A expression was a positive survival factor. The effect may be linked to increased expression of Glo1 through the functional antioxidant response element by binding of Nrf2 and suppression of Glo1 expression by the antagonist of Nrf2, Keap1, as NFE2L2 and KEAP1 had HRs of 1.30 and 0.80, respectively (Xue et al., 2012). Nrf2 is thought to be hyperactivated by HER2 in breast cancer (Kang et al., 2014). However, the negative and positive survival associations with NFE2L2 and KEAP1 found herein applied to all cancer genotypes.

The HR of GLO1 was particularly high in patients treated with tamoxifen; 1.74. This impacted markedly on median survival: high Glo1 expression, 75 months; low Glo1 expression, 138 months. Tamoxifen is an oestrogen receptor modulator. It competes with oestrogen for binding to the ligand binding domain of ER and is used for treatment of both pre- and postmenopausal patients. Tamoxifen-bound ER binds to the same genomic binding sites as oestrogen-bound ER but target genes are counter-regulated, with the downstream effect decreased tumour cell proliferation or antagonism at ERs (Johnston et al., 2018). Tamoxifen was found to increase Glo1 expression in breast cancer cell lines although there is no classical oestrogen response element in the GLO1 promoter (Rulli et al., 2006). This effect and the high HR for Glo1 in Tamoxifen-treated breast cancer patients may be explained by activation of Nrf2 by Tamoxifen and induction of Glo1 expression and related increase breast cancer cell proliferation. Tamoxifen is an activator of Nrf2 and this may explain these effects (Feng et al., 2017).

The effect of breast cancer genotypes, lymph node status and intrinsic subtype were further investigated with Glo1 expression. GLO1 had a slightly higher and significant HR of 1.65 in ER positive breast cancer may be due to estrogen signalling activating Nrf2 and increasing Glo1 expression in these patients (Wu et al., 2014). The negative survival impact of Glo1 expression was found in tumours of intrinsic subtypes luminal A and luminal B which account for 24% and 39% of breast cancers, respectively. Luminal subtypes usually have a good prognosis, with luminal B tumours having worse prognosis than the luminal A subtype. Luminal tumours respond well to hormone therapy but poorly to conventional chemotherapy. Glo1-linked MDR may contribute to this (Györfy et al., 2010, Dai et al., 2015). The negative survival impact of high Glo1 expression was maintained in lymph node negative breast cancer, suggesting that the impact of Glo1 overexpression is experienced at least from primary, pre-metastatic breast tumours. The link between GLO1 expression and the molecular subtypes in cancer patients needs to be investigated further in order to understand the impact of Glo1 in these subtypes in preclinical studies. I was unable to explore the link of so-called triple negative breast cancer patient survival to GLO1 copy number as there are insufficient data in the public databases for reliable analysis. However,

increased GLO1 copy number was found at high prevalence in triple negative breast cancer and this may contribute to increased Glo1 expression in this genotype of clinical breast cancer and negative survival impact (Santarius et al., 2010).

5.3 The glyoxalase system and methylglyoxal metabolism in HEK293 cell *in vitro*

HEK293 cell line is widely used in cancer research studies. Here I have characterised the glyoxalase system by measuring the Glo1 and Glo2 activity in order to have in depth understanding of activity of the major enzymes that metabolised MG. I also measured the flux of formation of D-lactate and the net formation of L-lactate. D-Lactate is little metabolised in HEK293 cells and the glyoxalase pathway accounts for >99% of MG metabolism (Abbas, H. and Thornalley, P.J., unpublished observation) and so the flux of D-lactate is approximately equivalent to the flux of formation of MG. The net formation of L-lactate is a measure of glycolytic activity of HEK293 cells. Both of these estimates were relatively high compared to corresponding fluxes found in cultures of corresponding non-malignant cells – renal proximal tubular epithelial cells (Al-Gambdi, O. and Thornalley, P.J., unpublished observations).

I found exogenous MG induced growth arrest and toxicity of HEK293 cells *in vitro*. The GC_{50} of MG was 131 μ M. The normal cellular concentration of in HEK293 cells was 4.3 ± 2.6 pmol per 10^6 cells, equivalent to a cellular concentration of *ca.* 2 μ M (Abbas, H. and Thornalley, P.J., unpublished observations). Therefore, with an active glyoxalase system, a high concentration of exogenous MG is required to induce cytotoxicity. From mathematical modelling studies of MG metabolism and the effect of a cell permeable Glo1 inhibitor, it was estimated that a cellular concentration of MG of *ca.* 12 fold higher than in control, or *ca.* 24 μ M, for 24 h is required to induce effective cytotoxicity. Without the Glo1 inhibitor, a higher concentration of exogenous MG is required as most of the dose is metabolised to D-lactate.

Cytotoxicity of MG develops in human tumour cells treated with MG after 24 h and under concentration limiting conditions – such as at the GC_{50}

concentration, cells die by apoptosis. From previous studies, we know that under limiting concentration condition such as GC_{50} of MG may induce growth arrest and cell growth which leads to cell death via apoptosis (Kang et al., 1996, Thornalley et al., 1996, Santarius et al., 2010) and under high concentration of MG cause cell death via necrosis (Du et al., 2000). Commitment to apoptosis occurs earlier. Previous studies in the human leukaemia 60 (HL60) cell line showed that commitment to cell death begins after 6 h, and is maximised after 24 h (Ayoub et al., 1993). It is likely, therefore, that if we wish to identify processes leading to commitment to apoptosis we need to analyse cells after ca. 6 – 12 h exposure. In HEK293 cells I found that the maximum decrease in viable cell number was produced by exposure to 131 μ M MG for 12 h and ca. 50% of the effect was achieved at 6 h exposure. I reasoned that the effects of MG were produced by modification of cell protein and I measured the time course of increase of the steady-state concentration of MG-derived adducts, MG-H1, in HEK293 cells protein extracts. This maximised at 6 h and so this was the chosen time point for analysis of fractional cell proteomes to assess changes in protein abundances and MG modification with MG treatment.

Several studies have shown that MG include cell death via apoptosis. It is thought that MG initiates the mitochondrial apoptotic pathway by the modification of mitochondrial permeability transition pore. High levels of MG-H1 formation may lead to depolarisation of membrane, release of the cytochrome c and activation of caspase-3 and caspase-9 (Czabotar et al., 2014). Alternative way of MG activating apoptosis is by the activation of Chk1, Chk2 and ATM kinases. This activation due to response to DNA damage caused by MG modification (Rabbani et al., 2018). MGdG is one of the major adducts are known to convert DNA to single strands break (ssDNA). In cases where DNA damage is too high for repair, DNA undergoes stall replication which may results in activation of apoptosis or necrosis (Dobbelstein and Sørensen, 2015).

Herein I measured the release of cytochrome c from mitochondria into the cytosol by ELISA and I could confirm that cytochrome c was released by treatment of cells with 131 μ M MG at both 3 - 6 h. This suggests that HEK293 cells commit to cell death via the mitochondrial apoptotic pathway at these time

points. In 1.5 h of treatment there was no change in the cytochrome c level when treating with MG; nevertheless, by this time protein adducts of MG-H1 had increased. It is likely that protein modification by MG preceding activation of apoptosis leads to the commitment to cell death.

5.4 Analysis of fractional proteomes of HEK293 cell line incubated with and without MG

I adapted pre-analytic processing methods for proteomics to avoid sample heating and high pH to avoid loss of MG-H1 adducts and migration between protein sites. Protocols had been optimised in a previous study by the host team applied to endothelial cells (Irshad et al., 2019). In this study, I have investigated MG-induced abundance changes and protein modification in HEK293 cells with 131 μ M MG after treatment for 6 h. This was done to investigate the proteomic changes at the time when cells are undergoing MG-induced commitment to apoptosis. As far as I am aware, this is the first study to show the modification of MG at the subcellular level in cytoplasm, nuclear and mitochondrial membrane and matrix in HEK293 cell line *in vitro*. Moreover, there have been no studies prior to this one attempting to measure protein abundances and MG-modified proteins in fractional proteomes at the period when cells undergoing MG-induced commitment to apoptosis.

5.4.1 Proteomic changes during methylglyoxal-induced commitment to apoptosis in HEK293 cells *in vitro*.

I detected 4391 proteins in the cytoplasmic extract. Since the extract was prepared by sonicating cells, it is expected to contain soluble protein from both cytosol and organelles. The highest increase abundance change induced by MG was a 30-fold, increase of calcium activated cation channel CSC1-like protein 2 (TMEM63B). Overexpression of TMEM63B promotes migration in HEK293T cells (Marques et al., 2019). There was also increase in abundance of the MG metabolizing enzyme aldo-keto reductase 1B1 (aldose reductase), which may be a stress responsive induction to support metabolism of MG along with that occurring by the glyoxalase system. The major effect was decrease of protein

abundances ranging from 7 – 95%. Proteins with decreased abundances were enriched or overrepresented in the ribosome, spliceosome, RNA transport and proteasome metabolic pathways. There are two main causes of cellular decreased protein in apoptosis: proteasome degradation and proteolysis by caspases and other proteases. As subunits of the proteasome were decreased (mean \pm SD fraction: 0.70 ± 0.06), the likely mechanism driving the decrease of these proteins is proteolysis other than by the proteasome. In apoptosis this is mediated by caspases and other proteases (Julien et al., 2017). An example is decrease of spliceosome subunit SF3B1 (Wiita et al., 2013). This may also account for decrease of proteasome subunits at least 20 proteasome subunits are cleaved by the caspases during apoptosis (Gray et al., 2010). Some of the proteins decreased were also detected with MG-H1 modification: for example, heterogeneous nuclear ribonucleoproteins K (HNRNPK) and M (HNRNPM). In such cases, increased MG modification may drive the degradation through increased targeting for proteolysis. Decrease of the spliceosome was confirmed by selective study of the nuclear proteome where components of the found in pathways enrichment had a mean decrease in abundance of 48% - similar to the decrease in viable cell number of 50% with 131 μ M used. Interestingly, components of the nuclear spliceosome are imported into mitochondria for splicing of mitochondria RNA, mtRNA (Herai et al., 2017). During MG-induced commitment to apoptosis I detected decrease in components of both the nuclear and mitochondrial splice machinery. Decreases common to both were decreased of RBMX, DDX5, SRSF1 and PTBP1. This suggest that impaired splicing of RNA is a target for MG-induced commitment to apoptosis in both nuclear and mitochondrial compartments.

A further profound effect of MG-induced commitment to apoptosis was the decrease of key proteins of energy production in cells: respiratory electron transport and formation of ATP by chemiosmotic coupling. The mean decreases in abundance of these components was: respiratory electron transport, $82 \pm 8\%$; and formation of ATP by chemiosmotic coupling, $76 \pm 12\%$. Clearly, during the commitment to apoptosis induced by MG, HEK293 cells are being starved of ATP. Collapse of oxidative phosphorylation as well as release of ATP has been

observed previously in apoptosis (Ricci et al., 2004)) but this is first time it has been implicated in MG-induced commitment to apoptosis. The depletion of ATP in MG-induced apoptosis of human tumour cells in vitro has been reported previously (He et al., 2016).

5.4.2 Potential impact of the significance proteins modified by methylglyoxal in cancer chemotherapy MDR

In order to validate the finding from the proteomics works. Western blot were in DEAD (Asp-Glu-Ala-Asp) box polypeptide 5 DDX5, AKR1B1 and Glo1. Cells were incubated with the same GC₅₀ and time point which is 6 hours. DDX5 has vital role in cell growth and in cancer several studies have shown its link in different multiple dysregulation of cellular process (Hashemi et al., 2019). Komori showed that Silencing DDX5 inhibit proliferation of four different breast cancer cell line (Komori, 2010). From the western blot data, we found that in MG treated cells there is a significant increase in DDX5 expression in comparison with control. This is suggesting that MG may play roles in DDX5 expression and further validation needed to be confirmed.

Measurement of the Glo1 protein were significantly increased in MG treated cells this is expected to be seen as Glo1 metabolising MG therefore there is high expression of protein in MG treated cell. There is no significant found when looking at the AKR1B1 protein by Western blotting. Experimental errors on Western blotting estimates were large, however, and further optimisation of procedures may produce data that corroborate the proteomics analysis.

5.5 The effect of methylglyoxal in free extrachromosomal DNA release in HEK293

In order to investigate the DNA damage caused by MG, Cells were incubated with MG at the same GC₅₀ and the time point. This was done to see the effect of MG on the extrachromosomal DNA secretion caused by MG. From the data obtained, there is a remarkable increase in ssDNA released by MG. this is agrees with the notion that MG caused DNA damage within 2 hours of exposure (Dobbelstein and Sørensen, 2015). There is a persistence in increase of DNA in

MG treated cell in comparison to control. The staining of picogreen showed the level of DNA secreted by MG.

5.6 Emergence of the spliceosome as a target of impairment in MG-induced commitment to apoptosis

The emergence of the spliceosome as a target of impairment in MG-induced commitment to apoptosis is, perhaps, one of the most interesting findings of my work. If important in MG-induced cytotoxicity clinically, we might expect the spliceosome to be impaired by anticancer drugs that increase cellular MG and are susceptible to Glo1-linked MDR – such as doxorubicin and mitomycin C (Abbas, H. and Thornalley, P.J., unpublished observations). These drugs do induce changes in the spliceosome, leading to alternative splicing that contributes to cytotoxicity (Dutertre et al., 2011). It might also be expected that there is impairment of the spliceosome in other clinical conditions where MG concentration is increased and linked to pathobiological processes: such as the chronic vascular complications of diabetes – for example, peripheral diabetic neuropathy (Bierhaus et al., 2012). Evidence from the literature suggests that there is impairment of the spliceosome in peripheral diabetic neuropathy (Kobayashi et al., 2017). So this research may open a new aspect of the mechanism of MG-linked pathogenesis and cytotoxicity with applications for cancer survival and treatment, vascular complications of diabetes and possibly others.

6 Conclusion and future works

6.1 Conclusion

The main aim of this project is to characterise the dicarbonyl proteome involved in MG induced cytotoxicity and its role in cancer chemotherapy. In order to achieve this aim, I have studied the bioinformatics cancer cell line and the survival analysis of mRNA Glo1 to investigate the role of Glo1 expression in linked in Cancer MDR. The results shown that Glo1 mRNA correlated positively with one of the causes of its expression GLO1 CNV. Nevertheless, we have shown that Glo1 correlated with several genes positively and negatively. These genes showed an interesting pathway enrichment outcome such as spliceosome, RNA transport, and cell cycle and DNA replication positively.

In this project, I investigated methylglyoxal of protein involved in methylglyoxal induced cell death. This was performed by studying the modified protein in HEK293 in vitro. I have characterised the glyoxalase system by measuring the Glo1 and Glo2 activity. Nevertheless, I measured the D-lactate and L-lactate in HEK293 cells in order to have in depth understanding of how MG are metabolised and secreted in this cell line. Time course study were also performed to confirm the time point needed for MG to initiate cell death in HEK293 cell line. Measurement of the cytosolic cytochrome c were performed in order to confirm the cell death pathway caused by MG which was agreed with previous study via apoptosis. Moreover, we have quantify the major protein adducts caused by MG which is MG-H1 by LC-MS/MS at different time point to gain more understanding of the modification caused by MG. The level MG-H1 were found to be maximum at 6 hr points in comparison to other time points.

Proteomics analysis were performed on four subcellular fraction to see the protein abundance change caused by MG and the protein modification by MG-H1. The data have shown for the first time the role of MG in the spliceosome assembly which may linked to anti-cancer drug resistance. The data for the proteomics also showed several pathway analysis which also agrees with the findings from the bioinformatics such as the mRNA major pathway and other cell cycle related pathway.

Finally, we have shown the MG ability to induce cell death via the secretion of extrachromosomal DNA released from the nucleus when treated with MG. This is confirming the previous finding that showed MG induce DNA damage leading to cell death via apoptosis.

6.2 Future works

In this project, I have analysed the role MG in modification and change of abundance in subcellular protein. I also have investigated the role of GLO1 on the database of cancer cell line and the impact of GLO1 in the survival analysis in cancer patient. Several pathway analysis enrichments were performed to investigate the role Glo1 expression and its metabolites MG in inducing cell death. However, I did not test the role of Glo1 inhibitor in modifying protein by inducing endogenous level of MG. it would highly interesting to see the role of endogenous MG to see the modified protein which may linked to Glo1 MDR chemotherapy resistance.

Nevertheless, the study was performed in cell line and it would be highly valuable to examine the role of inducing the concentration of MG in primary tumour cells to see the modification of MG occurs. Nevertheless, Other MG adducts should be tested to see what further information could be extracted.

Along with this bioinformatics finding about the increased GLO1 copy number changes which results in overexpression of Glo1 it is highly important to measure the GLO1 copy number in primary tumour to see changes may linked Glo1 expression MDR linked. from the data obtained in the impact of negative survival the role of Glo1 in endocrine therapy could be further investigated in animal model which may give more understanding of how GLO1 expression have an impact negatively on those patients.

All the data generated from this work will be soon published in scinfiftic journal articles, after the submission of the thesis.

7 References

- ABORDO, E. A., MINHAS, H. S. & THORNALLEY, P. J. 1999. Accumulation of α -oxoaldehydes during oxidative stress. A role in cytotoxicity. *Biochem.Pharmacol.*, 58, 641-648.
- AEBERSOLD, R. & MANN, M. 2003. Mass spectrometry-based proteomics. *Nature*, 422, 198-207.
- AGALOU, S., AHMED, N., THORNALLEY, P. J. & DAWNAY, A. 2005. Advanced glycation endproduct free adducts are cleared by dialysis. *Ann.N.Y.Acad.Sci.*
- AHMED, M. U., THORPE, S. R. & BAYNES, J. W. 1986. Identification of N^ε-carboxymethyl-lysine as a degradation product of fructoselysine in glycated protein. *J.Biol.Chem.*, 261, 4889-4894.
- AHMED, N., BABAEI-JADIDI, R., HOWELL, S. K., BEISSWENGER, P. J. & THORNALLEY, P. J. 2005. Degradation products of proteins damaged by glycation, oxidation and nitration in clinical type 1 diabetes. *Diabetologia*, 48, 1590-1603.
- AHMED, N., THORNALLEY, P. J., DAWCZYNSKI, J., FRANKE, S., STROBEL, J., STEIN, G. & HAIK, G. M. 2003. Methylglyoxal-derived hydroimidazolone advanced glycation end-products of human lens proteins. *Invest Ophthalmol Vis Sci*, 44, 5287-92.
- AHMED, N., THORNALLEY, P. J., LUTHEN, R., HAUSSINGER, D., SEBEKOVA, K., SCHINZEL, R., VOELKER, W. & HEIDLAND, A. 2004. Processing of protein glycation, oxidation and nitrosation adducts in the liver and the effect of cirrhosis. *J.Hepatol.*, 41, 913-919.
- AHMED, U., DOBLER, D., LARKIN, S. J., RABBANI, N. & THORNALLEY, P. J. 2008. Reversal of Hyperglycemia- Induced Angiogenesis Deficit of Human Endothelial Cells by Overexpression of Glyoxalase 1In Vitro. *Annals of the New York Academy of Sciences*, 1126, 262-264.
- AKIYODE, O., GEORGE, D., GETTI, G. & BOATENG, J. 2016. Systematic comparison of the functional physico-chemical characteristics and biocidal activity of microbial derived biosurfactants on blood-derived and breast cancer cells. *J Colloid Interface Sci*, 479, 221-33.
- ALFAROUC, K. O., STOCK, C. M., TAYLOR, S., WALSH, M., MUDDATHIR, A. K., VERDUZCO, D., BASHIR, A. H., MOHAMMED, O. Y., ELHASSAN, G. O., HARGUINDEY, S., RESHKIN, S. J., IBRAHIM, M. E. & RAUCH, C. 2015. Resistance to cancer chemotherapy: failure in drug response from ADME to P-gp. *Cancer Cell Int*, 15, 71.
- ALLEN, D. W., SCHROEDER, W. A. & BALOG, J. 1958. Observations on the Chromatographic Heterogeneity of Normal Adult and Fetal Human Hemoglobin: A Study of the Effects of Crystallization and Chromatography on the Heterogeneity and Isoleucine Content. *J.Am.Chem.Soc.*, 80, 1628-1634.
- ALLEN, R. E., LO, T. W. & THORNALLEY, P. J. 1993a. Purification and characterisation of glyoxalase II from human red blood cells. *Eur J Biochem*, 213, 1261-7.

- ALLEN, R. E., LO, T. W. & THORNALLEY, P. J. 1993b. A simplified method for the purification of human red blood cell glyoxalase. I. Characteristics, immunoblotting, and inhibitor studies. *J Protein Chem*, 12, 111-9.
- ALLEN, R. E. & THORNALLEY, P. J. 1993. The effect of S-D-lactoylglutathione on the movement of neutrophils. *Biochem.Soc.Trans.*, 21, 161S-161S.
- AMADORI, M. 1929a. The condensation product of glucose and p -anisidine. *Atti Reale Accad.Nazl.Lincei*, 9, 226-230.
- AMADORI, M. 1929b. The product of the condensation of glucose and p -phenetidine. *Atti Reale Accad.Nazl.Lincei*, 9, 68-73.
- ANDERSON, N. L. & ANDERSON, N. G. 1998. Proteome and proteomics: New technologies, new concepts, and new words. *ELECTROPHORESIS*, 19, 1853-1861.
- ANET, E. F. L. J. 1960. Degradation of carbohydrates. I. Isolation of 3-deoxyhexosones. *Australian J.Chem.*, 13, 396-403.
- APPLE, M. & GREENBERG, D. 1968. Arrest of cancer in mice by therapy with normal metabolites. II. Indefinite survivors among mice treated with mixtures of 2-oxopropanal (NSC-79019) and 2, 3-dihydroxypropanal (NSC67934). *Cancer chemotherapy reports*, 52, 687.
- ARAI, M., YUZAWA, H., NOHARA, I., OHNISHI, T., OBATA, N., IWAYAMA, Y., HAGA, S., TOYOTA, T., UJIKE, H., ARAI, M., ICHIKAWA, T., NISHIDA, A., TANAKA, Y., FURUKAWA, A., AIKAWA, Y., KURODA, O., NIIZATO, K., IZAWA, R., NAKAMURA, K., MORI, N., MATSUZAWA, D., HASHIMOTO, K., IYO, M., SORA, I., MATSUSHITA, M., OKAZAKI, Y., YOSHIKAWA, T., MIYATA, T. & ITOKAWA, M. 2010. Enhanced Carbonyl Stress in a Subpopulation of Schizophrenia. *Archives of General Psychiatry*, 67, 589-597.
- AYOUB, F. M., ALLEN, R. E. & THORNALLEY, P. J. 1993. Inhibition of proliferation of human leukaemia 60 cells by methylglyoxal in vitro. *Leukemia research*, 17, 397-401.
- BABA, S. P., BARSKI, O. A., AHMED, Y., O'TOOLE, T. E., CONKLIN, D. J., BHATNAGAR, A. & SRIVASTAVA, S. 2009. Reductive metabolism of AGE precursors: a metabolic route for preventing AGE accumulation in cardiovascular tissue. *Diabetes*, 58, 2486-2497.
- BAKALA, H., DELAVAL, E., HAMELIN, M., BISMUTH, J., BOROT-LALOI, C., CORMAN, B. & FRIGUET, B. 2003. Changes in rat liver mitochondria with aging. Lon protease-like reactivity and N(epsilon)-carboxymethyllysine accumulation in the matrix. *Eur J Biochem*, 270, 2295-302.
- BAUMANN, M., KRAUSE, M., OVERGAARD, J., DEBUS, J., BENTZEN, S. M., DAARTZ, J., RICHTER, C., ZIPS, D. & BORTFELD, T. J. N. R. C. 2016. Radiation oncology in the era of precision medicine. 16, 234.
- BIEMANN, K. 1992. Mass spectrometry of peptides and proteins. *Annual review of biochemistry*, 61, 977-1010.
- BEISSWENGER, P. J., HOWELL, S. K., TOUCHETTE, A., LAL, S. & SZWERGOLD, B. S. 1999. Metformin reduces systemic methylglyoxal levels in type 2 diabetes. *Diabetes*, 48, 198-202.

- BERLETT, B. S. & STADTMAN, E. R. 1997. Protein oxidation in aging, disease, and oxidative stress. *J Biol Chem*, 272, 20313-6.
- BIERHAUS, A., FLEMING, T., STOYANOV, S., LEFFLER, A., BABES, A., NEACSU, C., SAUER, S. K., EBERHARDT, M., SCHNOLZER, M., LASISCHKA, F., NEUHUBER, W. L., KICHKO, T. I., KONRADE, I., ELVERT, R., MIER, W., PIRAGS, V., LUKIC, I. K., MORCOS, M., DEHMER, T., RABBANI, N., THORNALLEY, P. J., EDELSTEIN, D., NAU, C., FORBES, J., HUMPERT, P. M., SCHWANINGER, M., ZIEGLER, D., STERN, D. M., COOPER, M. E., HABERKORN, U., BROWNLEE, M., REEH, P. W. & NAWROTH, P. P. 2012. Methylglyoxal modification of Nav1.8 facilitates nociceptive neuron firing and causes hyperalgesia in diabetic neuropathy. *Nature Med*, 18, 926-933.
- BIRKENMEIER, G., STEGEMANN, C., HOFFMANN, R., GUNTHER, R., HUSE, K. & BIRKEMEYER, C. 2010. Posttranslational modification of human glyoxalase 1 indicates redox-dependent regulation. *PLoS ONE*, 5, e10399.
- BLACK, J. C., MANNING, A. L., VAN RECHEM, C., KIM, J., LADD, B., CHO, J., PINEDA, C. M., MURPHY, N., DANIELS, D. L. & MONTAGNA, C. 2013. KDM4A lysine demethylase induces site-specific copy gain and rereplication of regions amplified in tumors. *Cell*, 154, 541-555.
- BLEICHERT, F., BOTCHAN, M. R. & BERGER, J. M. J. N. 2015. Crystal structure of the eukaryotic origin recognition complex. 519, 321.
- BONDARENKO, P. V., CHELIUS, D. & SHALER, T. A. 2002. Identification and relative quantitation of protein mixtures by enzymatic digestion followed by capillary reversed-phase liquid chromatography-tandem mass spectrometry. *Analytical chemistry*, 74, 4741-4749.
- BONSIGNORE, A., LEONCINI, G., SIRI, A. & RICCI, D. 1973. Kinetic behaviour of glyceraldehyde 3-phosphate conversion into methylglyoxal. *Ital.J.Biochem.*, 22, 131-140.
- BOOKCHIN, R. M. & GALLOP, P. M. 1968. Structure of hemoglobin A 1c : nature of the N -terminal β -chain blocking group. *Biochem.Biophys.Res.Com.*, 32, 86-93.
- BOURGEOIS, C. F., LEJEUNE, F., STÉVENIN, J. J. P. I. N. A. R. & BIOLOGY, M. 2004. Broad specificity of SR (serine/arginine) proteins in the regulation of alternative splicing of pre-messenger RNA. 78, 37-88.
- BRADFORD, M. 1976. A Rapid and Sensitive Method for the Quantitation of Microgram Quantities of Protein Utilizing the Principle of Protein-Dye Binding. *Analytical Biochemistry*, 72, 248-254.
- BRANDT, R. B., SIEGEL, S. A., WATERS, M. G. & BLOCH, M. H. 1980. Spectrophotometric assay for D-(-)-lactate in plasma. *Anal.Biochem.*, 102, 39-46.
- BROWNLEE, M. 2001. Biochemistry and molecular cell biology of diabetic complications. *Nature*, 414, 813-820.
- BROWNLEE, M. 2005. The pathobiology of diabetic complications: a unifying mechanism. *Diabetes*, 54, 1615-25.
- BUNN, H. F., HANEY, D. N., GABBAY, K. H. & GALLOP, P. M. 1975. Further identification of the nature and linkage of the carbohydrate in

- hemoglobin A1c. *Biochemical and Biophysical Research Communications*, 67, 103-109.
- BURKHART, J. M., PREMSLER, T. & SICKMANN, A. 2011. Quality control of nano- LC- MS systems using stable isotope- coded peptides. *Proteomics*, 11, 1049-1057.
- CAHAN, P., LI, Y., IZUMI, M. & GRAUBERT, T. A. 2009. The impact of copy number variation on local gene expression in mouse hematopoietic stem and progenitor cells. *Nat Genet*, 41, 430-437.
- CAMERON, A. D., OLIN, B., RIDDERSTROM, M., MANNERVIK, B. & JONES, T. A. 1997. Crystal structure of human glyoxalase I - evidence from gene duplication and 3D domain swapping. *The EMBO Journal*, 16, 3386-3395.
- CAMERON, A. D., RIDDERSTROM, M., OLIN, B. & MANNERVIK, B. 1999. Crystal structure of human glyoxalase II and its complex with a glutathione thiolester substrate analogue. *Structure*, 7, 1067-1078.
- CERAMI, A. 1986. Aging of proteins and nucleic acids: what is the role of glucose? *TIBS*, 11, 311-314.
- CHABNER, B. A. & ROBERTS JR, T. G. J. N. R. C. 2005. Chemotherapy and the war on cancer. 5, 65.
- CHAKRAVARTY, G., MATHUR, A., MALLADE, P., GERLACH, S., WILLIS, J., DATTA, A., SRIVASTAV, S., ABDEL-MAGEED, A. B. & MONDAL, D. 2016. Nelfinavir targets multiple drug resistance mechanisms to increase the efficacy of doxorubicin in MCF-7/Dox breast cancer cells. *Biochimie*, 124, 53-64.
- CHELIUS, D. & BONDARENKO, P. V. 2002. Quantitative profiling of proteins in complex mixtures using liquid chromatography and mass spectrometry. *Journal of proteome research*, 1, 317-323.
- CHEN, B.-G., LIN, C., CHEN, C., HAMBSCH, B. & CHERN, C.-L. 2013. Quantitation by GC-MS of Methylglyoxal as a Marker in Anxiety-Related Studies. *Chromatographia*, 76, 571-576.
- CHEN, F., WOLLMER, M. A., HOERNDLI, F., MUNCH, G., KUHLA, B., ROGAEV, E. I., TSOLAKI, M., PAPASSOTIROPOULOS, A. & GOTZ, J. 2004. Role for glyoxalase I in Alzheimer's disease. *Proc.Natl.Acad.Sci.USA*, 101, 7687-7692.
- CLELLAND, J. D. & THORNALLEY, P. J. 1991. S-2-hydroxyacylglutathione-derivatives: enzymatic preparation, purification and characterisation. *J. Chem. Soc., Perkin Trans. 1*, 3009-3015.
- COHEN, J. 2002. The immunopathogenesis of sepsis. *Nature*, 420, 885-891.
- COMPTON, S. J. & JONES, C. G. 1985. Mechanism of dye response and interference in the Bradford protein assay. *Anal Biochem*, 151, 369-74.
- CONNOR, H., WOODS, H., LEDINGHAM, J. J. A. O. N. & METABOLISM 1983. Comparison of the kinetics and utilisation of D (-)-and L (+)-sodium lactate in normal man. 27, 481-487.
- CONROY, P. J. Carcinostatic activity of methylglyoxal and related substances in tumour-bearing mice. Submolecular Biology and Cancer: Ciba Foundation Symposium, 1979. 271-298.
- CORDELL, P. A., FUTERS, T. S., GRANT, P. J. & PEASE, R. J. 2004. The human hydroxyacylglutathione hydrolase (HAGH) gene encodes both

- cytosolic and mitochondrial forms of glyoxalase II. *Journal of Biological Chemistry*, 279, 28653-28661.
- COVERT, M. W. 2005. Achieving Stability of Lipopolysaccharide-Induced NF- B Activation. *Science*, 309, 1854-1857.
- CREIGHTON, D., ZHENG, Z.-B., HOLEWINSKI, R., HAMILTON, D. & EISEMAN, J. 2003. Glyoxalase I inhibitors in cancer chemotherapy. Portland Press Limited.
- CZABOTAR, P. E., LESSENE, G., STRASSER, A. & ADAMS, J. M. 2014. Control of apoptosis by the BCL-2 protein family: implications for physiology and therapy. *Nature reviews. Molecular cell biology*, 15, 49.
- DAI, X., LI, T., BAI, Z., YANG, Y., LIU, X., ZHAN, J. & SHI, B. J. A. J. O. C. R. 2015. Breast cancer intrinsic subtype classification, clinical use and future trends. 5, 2929.
- DAKIN, H. & DUDLEY, H. 1913. An enzyme concerned with the formation of hydroxy acids from ketonic aldehydes. *Journal of Biological Chemistry*, 14, 155-157.
- DANDONA, P. 2004. Inflammation: the link between insulin resistance, obesity and diabetes. *Trends in Immunology*, 25, 4-7.
- DAUPHINEE, S. M. & KARSAN, A. 2005. Lipopolysaccharide signaling in endothelial cells. *Lab Invest*, 86, 9-22.
- DE HEMPTINNE, V., RONDAS, D., TOEPOEL, M. & VANCOMPERNOLLE, K. 2009. Phosphorylation on Thr-106 and NO-modification of glyoxalase I suppress the TNF-induced transcriptional activity of NF-kappa B. *Molecular and Cellular Biochemistry*, 325, 169-178.
- DE HEMPTINNE, V., RONDAS, D., VANDEKERCKHOVE, J. & VANCOMPERNOLLE, K. 2007. Tumour necrosis factor induces phosphorylation primarily of the nitric-oxide-responsive form of glyoxalase I. *Biochemical Journal*, 407, 121-128.
- DE HOFFMAN, E. & STROOBANT, V. 2007. Tandem mass spectrometry. *Mass spectrometry principles and applications, 3rd Edition, John Wiley & Sons Ltd., West Sussex, England*, 189-215.
- DE VRESE, M. & BARTH, C. A. 1991. Postprandial plasma D-lactate concentrations after yogurt ingestion. *Z Ernährungswiss*, 30, 131-7.
- DEGAFFE, G. H., VANDER JAGT, D. L., BOBELU, A., BOBELU, J., NEHA, D., WAIKANIWA, M., ZAGER, P. & SHAH, V. O. 2007. Distribution of glyoxalase I polymorphism among Zuni Indians: the Zuni Kidney Project. *Journal of Diabetes and Its Complications*, 22, 267-272.
- DOBBELSTEIN, M. & MOLL, U. 2014. Targeting tumour-supportive cellular machineries in anticancer drug development. *Nat Rev Drug Discov*, 13, 179-96.
- DOBBELSTEIN, M. & SØRENSEN, C. S. 2015. Exploiting replicative stress to treat cancer. *Nature reviews. Drug discovery*, 14, 405.
- DOBLER, D., AHMED, N., SONG, L., EBOIGBODIN, K. E. & THORNALLEY, P. J. 2006. Increased dicarbonyl metabolism in endothelial cells in hyperglycemia induces anoikis and impairs angiogenesis by RGD and GFOGER motif modification. *Diabetes*, 55, 1961-9.

- DRURY, D. R. & WICK, A. N. J. A. O. T. N. Y. A. O. S. 1965. Chemistry and metabolism of L (+) and D (-) lactic acids. 119, 1061-1069.
- DU, J., SUZUKI, H., NAGASE, F., AKHAND, A. A., YOKOYAMA, T., MIYATA, T., KUROKAWA, K. & NAKASHIMA, I. 2000. Methylglyoxal induces apoptosis in Jurkat leukemia T cells by activating c- Jun N- Terminal kinase. *Journal of cellular biochemistry*, 77, 333-344.
- DUTERTRE, M., SANCHEZ, G., BARBIER, J., CORCOS, L. & AUBOEUF, D. J. R. B. 2011. The emerging role of pre-messenger RNA splicing in stress responses: sending alternative messages and silent messengers. 8, 740-747.
- EDWARDS, L. G., ADESIDA, A. & THORNALLEY, P. J. 1996. Inhibition of human leukaemia 60 cell growth by S -D-lactoylglutathione in vitro . Mediation by metabolism to N -D-lactoylcysteine and induction of apoptosis. *Leuk.Res.*, 20, 17-26.
- EDWARDS, L. G., CLELLAND, J. D. & THORNALLEY, P. J. 1993. Characteristics of the inhibition of human promyelocytic leukaemia HL60 cell growth by S- D-lactoylglutathione in vitro *Leuk Res.*, 17, 305-310.
- EDWARDS, L. G. & THORNALLEY, P. J. 1994. Prevention of S-D- Lactoylglutathione-induced inhibition of Human Leukemia 60 Cells Growth by Uridine. *Leukemia Research*, 118, 717-722.
- EL MARABTI, E. & YOUNIS, I. J. F. I. M. B. 2018. The Cancer Spliceome: reprogramming of alternative splicing in cancer. 5.
- EL OSTA, A., BRASACCHIO, D., YAO, D., POCAI, A., JONES, P. L., ROEDER, R. G., COOPER, M. E. & BROWNLEE, M. 2008. Transient high glucose causes persistent epigenetic changes and altered gene expression during subsequent normoglycemia. *The Journal of Experimental Medicine*, jem.
- ENGBRETSON, S. P., HEY-HADAVI, J., EHRHARDT, F. J., HSU, D., CELENTI, R. S., GRBIC, J. T. & LAMSTER, I. B. 2004. Gingival Crevicular Fluid Levels of Interleukin-1 β and Glycemic Control in Patients With Chronic Periodontitis and Type 2 Diabetes. *Journal of Periodontology*, 75, 1203-1208.
- ENOCH, T. & NORBURY, C. J. T. I. B. S. 1995. Cellular responses to DNA damage: cell-cycle checkpoints, apoptosis and the roles of p53 and ATM. 20, 426-430.
- EWASCHUK, J. B., NAYLOR, J. M. & ZELLO, G. A. 2005. d-Lactate in Human and Ruminant Metabolism. *The Journal of Nutrition*, 135, 1619-1625.
- FANG, X., SCHUMMER, M., MAO, M., YU, S., TABASSAM, F. H., SWABY, R., HASEGAWA, Y., TANYI, J. L., LAPUSHIN, R., EDER, A., JAFFE, R., ERICKSON, J. & MILLS, G. B. 2002. Lysophosphatidic acid is a bioactive mediator in ovarian cancer. *Biochimica et Biophysica Acta (BBA) - Molecular and Cell Biology of Lipids*, 1582, 257-264.
- FENG, L., LI, J., YANG, L., ZHU, L., HUANG, X., ZHANG, S., LUO, L., JIANG, Z., JIANG, T. & XU, W. J. T. 2017. Tamoxifen activates Nrf2-dependent SQSTM1 transcription to promote endometrial hyperplasia. 7, 1890.
- FENG, X., LIU, X., LUO, Q. & LIU, B. F. 2008. Mass spectrometry in systems biology: an overview. *Mass spectrometry reviews*, 27, 635-660.

- FENN, J. B., MANN, M., MENG, C. K., WONG, S. F. & WHITEHOUSE, C. M. 1989. Electrospray ionization for mass spectrometry of large biomolecules. *Science*, 246, 64-71.
- FESNAK, A. D., JUNE, C. H. & LEVINE, B. L. J. N. R. C. 2016. Engineered T cells: the promise and challenges of cancer immunotherapy. 16, 566.
- FREEDLANDER, B., FRENCH, F. A., HOSKING, A. & FRENCH, J. 1958. Carcinostatic action of polycarbonyl compounds and their derivatives. *Cancer research*, 18, 1286-1289.
- FUKUNAGA, Y., KATSURAGI, Y., IZUMI, T. & SAKIYAMA, F. 1982. Fluorescence characteristics of kynurenine and N'-formylkynurenine. Their use as reporters of the environment of tryptophan 62 in hen egg-white lysozyme. *J.Biochem.*, 92, 129-141.
- GALE, C. P. & GRANT, P. J. 2004. The characterisation and functional analysis of the human glyoxalase-1 gene using methods of bioinformatics. *Gene*, 340, 251-260.
- GATENBY, R. A. & GILLIES, R. J. 2004. Why do cancers have high aerobic glycolysis? *Nat Rev Cancer*, 4, 891-9.
- GHAZALPOUR, A., BENNETT, B., PETYUK, V. A., OROZCO, L., HAGOPIAN, R., MUNGRUE, I. N., FARBER, C. R., SINSHEIMER, J., KANG, H. M., FURLOTTE, N., PARK, C. C., WEN, P. Z., BREWER, H., WEITZ, K., CAMP, D. G., PAN, C., YORDANOVA, R., NEUHAUS, I., TILFORD, C., SIEMERS, N., GARGALOVIC, P., ESKIN, E., KIRCHGESSNER, T., SMITH, D. J., SMITH, R. D. & LUSIS, A. J. 2011. Comparative Analysis of Proteome and Transcriptome Variation in Mouse. *PLoS Genet*, 7, e1001393.
- GILMAN, A. & PHILIPS, F. S. 1946. The biological actions and therapeutic applications of the B-chloroethyl amines and sulfides. *Science*, 103, 409-436.
- GOODMAN, L. S., WINTROBE, M. M., DAMESHEK, W., GOODMAN, M. J., GILMAN, A. & MCLENNAN, M. T. 1946. Nitrogen mustard therapy: Use of methyl-bis (beta-chloroethyl) amine hydrochloride and tris (beta-chloroethyl) amine hydrochloride for Hodgkin's disease, lymphosarcoma, leukemia and certain allied and miscellaneous disorders. *Journal of the American Medical Association*, 132, 126-132.
- GOWLAND-HOPKINS, F. G. & MORGAN, E. J. 1945. On the distribution of glyoxalase and glutathione. *Biochem.J.*, 39, 320-324.
- GRAY, D. C., MAHRUS, S. & WELLS, J. A. J. C. 2010. Activation of specific apoptotic caspases with an engineered small-molecule-activated protease. 142, 637-646.
- GRUNE, T., REINHECKEL, T. & DAVIES, K. J. T. F. J. 1997. Degradation of oxidized proteins in mammalian cells. 11, 526-534.
- GYÖRFFY, B., LANCZKY, A., EKLUND, A. C., DENKERT, C., BUDCZIES, J., LI, Q. & SZALLASI, Z. 2010. An online survival analysis tool to rapidly assess the effect of 22,277 genes on breast cancer prognosis using microarray data of 1,809 patients. *Breast cancer research and treatment*, 123, 725-731.
- HAMBSCH, B., CHEN, B. G., BRENNENDORFER, J., MEYER, M., AVRABOS, C., MACCARRONE, G., LIU, R. H., EDER, M., TURCK, C. W. &

- LANDGRAF, R. 2010. Methylglyoxal-mediated anxiolysis involves increased protein modification and elevated expression of glyoxalase 1 in the brain. *Journal of Neurochemistry*, 113, 1240-1251.
- HANAHAN, D. & WEINBERG, R. A. 2011. Hallmarks of cancer: the next generation. *Cell*, 144, 646-74.
- HARDEJ, D. & BILLACK, B. 2007. Ebselen protects brain, skin, lung and blood cells from mechlorethamine toxicity. *Toxicol Ind Health*, 23, 209-21.
- HASHEMI, V., MASJEDI, A., HAZHIR- KARZAR, B., TANOMAND, A., SHOTORBANI, S. S., HOJJAT- FARSANGI, M., GHALAMFARSA, G., AZIZI, G., ANVARI, E. & BARADARAN, B. 2019. The role of DEAD- box RNA helicase p68 (DDX5) in the development and treatment of breast cancer. *Journal of cellular physiology*, 234, 5478-5487.
- HAYASHI, T. & NAMIKI, M. 1980. Formation of two-carbon sugar fragments at an early stage of the browning reaction of sugar and amine. *Agric.Biol.Chem.*, 44, 2575-2580.
- HE, T., ZHOU, H., LI, C., CHEN, Y., CHEN, X., LI, C., MAO, J., LYU, J., MENG, Q. H. J. C. B. & THERAPY 2016. Methylglyoxal suppresses human colon cancer cell lines and tumor growth in a mouse model by impairing glycolytic metabolism of cancer cells associated with down-regulation of c-Myc expression. 17, 955-965.
- HERAI, R. H., NEGRAES, P. D. & MUOTRI, A. R. J. H. M. G. 2017. Evidence of nuclei-encoded spliceosome mediating splicing of mitochondrial RNA. 26, 2472-2479.
- HODGE, J. E. 1953. Dehydrated foods: chemistry of browning reactions in model systems. *J.Agric.Food Chem.*, 1, 928-943.
- HOLMGREN, A. 2000. Antioxidant function of thioredoxin and glutaredoxin systems. *Antioxid Redox Signal*, 2, 811-20.
- HOLOHAN, C., VAN SCHAEYBROECK, S., LONGLEY, D. B. & JOHNSTON, P. G. 2013. Cancer drug resistance: an evolving paradigm. *Nat Rev Cancer*, 13, 714-726.
- HOSODA, F., ARAI, Y., OKADA, N., SHIMIZU, H., MIYAMOTO, M., KITAGAWA, N., KATAI, H., TANIGUCHI, H., YANAGIHARA, K. & IMOTO, I. 2015. Integrated genomic and functional analyses reveal glyoxalase I as a novel metabolic oncogene in human gastric cancer. *Oncogene*, 34, 1196.
- HOVE, H. 1998. Lactate and short chain fatty acid production in the human colon: implications for D-lactic acidosis, short-bowel syndrome, antibiotic-associated diarrhoea, colonic cancer, and inflammatory bowel disease. *Dan Med Bull*, 45, 15-33.
- HU, C., NOLL, B. C., SCHULZ, C. E. & SCHEIDT, W. R. 2005. Proton-mediated electron configuration change in high-spin iron (II) porphyrinates. *Journal of the American Chemical Society*, 127, 15018-15019.
- HUTSCHENREUTHER, A., BIGL, M., HEMDAN, N. Y., DEBEBE, T., GAUNITZ, F. & BIRKENMEIER, G. 2016. Modulation of GLO1 expression affects malignant properties of cells. *International journal of molecular sciences*, 17, 2133.

- IACOPINO, A. M. 2001. Periodontitis and Diabetes Interrelationships: Role of Inflammation. *Annals of Periodontology*, 6, 125-137.
- IKEDA, K., HIGASHI, T., SANO, H., JINNOUCHI, Y., YOSHIDA, M., ARAKI, T., UEDA, S. & HORIUCHI, S. 1996. N ϵ -(carboxymethyl) lysine protein adduct is a major immunological epitope in proteins modified with advanced glycation end products of the Maillard reaction. *Biochemistry*, 35, 8075-8083.
- INAGI, R., MIYATA, T., UEDA, Y., YOSHINO, A., NANGAKU, M., DE STRIHO, C. V. & KUROKAWA, K. 2002. Efficient in vitro lowering of carbonyl stress by the glyoxalase system in conventional glucose peritoneal dialysis fluid. *Kidney International*, 62, 679-687.
- IRSHAD, Z., XUE, M., ASHOUR, A., LARKIN, J. R., THORNALLEY, P. J. & RABBANI, N. J. S. R. 2019. Activation of the unfolded protein response in high glucose treated endothelial cells is mediated by methylglyoxal. 9, 7889.
- ISCHIROPOULOS, H. J. A. O. B. & BIOPHYSICS 1998. Biological tyrosine nitration: a pathophysiological function of nitric oxide and reactive oxygen species. 356, 1-11.
- ITAKURA, K., UCHIDA, K. & OSAWA, T. 1996. A novel fluorescent malondialdehyde-lysine adduct. *Chemistry and Physics of Lipids*, 84, 75-79.
- IZAGUIRRE, G., KIKONYOGO, A. & PIETRUSZKO, R. 1998. Methylglyoxal as substrate and inhibitor of human aldehyde dehydrogenase: Comparison of kinetic properties among the three isozymes. *Comparative Biochemistry and Physiology B-Biochemistry & Molecular Biology*, 119, 747-754.
- JERZYKOWSKI, T., WINTER, R., MATUSZEWSKI, W. & PISKORSKA, D. 1978. A re-evaluation of studies on the distribution of glyoxalases in animal and tumour tissues. *International Journal of Biochemistry*, 9, 853-860.
- JERZYKOWSKI, T., WINTER, R., MATUSZEWSKI, W. & SZCZUREK, Z. 1975. Glyoxalase II activity in tumours. *Cellular and Molecular Life Sciences*, 31, 32-33.
- JOHNSON, A., YAO, N. Y., BOWMAN, G. D., KURIYAN, J. & O'DONNELL, M. J. J. O. B. C. 2006. The replication factor C clamp loader requires arginine finger sensors to drive DNA binding and proliferating cell nuclear antigen loading. 281, 35531-35543.
- JOHNSTON, S. J., CHEUNG, K.-L. J. O. & THERAPY 2018. Endocrine therapy for breast cancer: a model of hormonal manipulation. 6, 141-156.
- JÖNSSON, D., NEBEL, D., BRATTHALL, G. & NILSSON, B. O. 2011. The human periodontal ligament cell: a fibroblast- like cell acting as an immune cell. *Journal of periodontal research*, 46, 153-157.
- JOWETT, M. & QUASTEL, J. H. 1934. The glyoxalase activity of tissues. *Biochemical Journal*, 28, 162.
- JULIEN, O., WELLS, J. A. J. C. D. & DIFFERENTIATION 2017. Caspases and their substrates. 24, 1380.
- KANDOH, Y., KAWASE, M. & KAWAKAMI, Y. 1992a. Concentration of D-lactate and it's related metabolic intermediates in liver, blood and muscle of diabetic and starved rats. *Res.Exp.Med.*, 192, 407-414.

- KANDOH, Y., KAWASE, M. & OHMORI, S. 1992b. D-Lactate concentration in blood, urine and sweat before and after exercise. *Eur.J.Appl.Physiol.*, 65, 88-93.
- KANG, H. J., YI, Y. W., HONG, Y. B., KIM, H. J., JANG, Y.-J., SEONG, Y.-S. & BAE, I. J. S. R. 2014. HER2 confers drug resistance of human breast cancer cells through activation of NRF2 by direct interaction. 4, 7201.
- KANG, Y., EDWARDS, L. G. & THORNALLEY, P. J. 1996. Effect of methylglyoxal on human leukaemia 60 cell growth: modification of DNA, G1 growth arrest and induction of apoptosis. *Leukemia research*, 20, 397-405.
- KARACHALIAS, N., BABAEI-JADIDI, R., AHMED, N., BAYNES, K. & THORNALLEY, P. J. 2005. Urinary D-lactate as a marker of biochemical dysfunction linked to the development of diabetic microvascular complications. *Diabetic Med.*, 22, Suppl.2, 21-21.
- KARAS, M., BACHMANN, D., BAHR, U. & HILLENKAMP, F. 1987. Matrix-assisted ultraviolet laser desorption of non-volatile compounds. *International journal of mass spectrometry and ion processes*, 78, 53-68.
- KARAS, M. & HILLENKAMP, F. 1988. Laser desorption ionization of proteins with molecular masses exceeding 10,000 daltons. *Analytical chemistry*, 60, 2299-2301
- KATO, H. 1960. Studies on browning reactions between sugars and amino compounds. V. Isolation and characterisation of new carbonyl compounds, 3-deoxyglucosones formed from N -glycosides and their significance for browning reaction. *Bull.Agric.Chem.Soc.Japan*, 24, 1-12.
- KAVSAN, V. M., IERSHOV, A. V. & BALYNSKA, O. V. 2011. Immortalized cells and one oncogene in malignant transformation: old insights on new explanation. *BMC Cell Biol*, 12, 23.
- KESSNER, D., CHAMBERS, M., BURKE, R., AGUS, D. & MALLICK, P. 2008. ProteoWizard: open source software for rapid proteomics tools development. *Bioinformatics*, 24, 2534-2536.
- KIM, N. S., SEKINE, S., KIUCHI, N. & KATO, S. 1995. cDNA Cloning and characterisation of human glyoxalase I isoforms from HT-1080 cells. *J.Biochem.*, 117, 359-361.
- KINANE, D. F., PRESHAW, P. M. & LOOS, B. G. 2011. Host-response: understanding the cellular and molecular mechanisms of host-microbial interactions - Consensus of the Seventh European Workshop on Periodontology. *Journal of Clinical Periodontology*, 38, 44-48.
- KINGDON, K. 1923. A method for the neutralization of electron space charge by positive ionization at very low gas pressures. *Physical Review*, 21, 408.
- KOBAYASHI, M., CHANDRASEKHAR, A., CHENG, C., MARTINEZ, J. A., NG, H., DE LA HOZ, C., ZOCHODNE, D. W. J. D. M. & MECHANISMS 2017. Diabetic polyneuropathy, sensory neurons, nuclear structure and spliceosome alterations: a role for CWC22. 10, 215-224.
- KOENIG, R. J., PETERSON, C. M., JONES, R. L., SAUDEK, C., LEHRMAN, M. & CERAMI, A. 1976. A correlation of glucose regulation and Hemoglobin A1c in diabetes mellitus. *New Engl.J.Med.*, 295, 417-420.
- KOITO, W., ARAKI, T., HORIUCHI, S. & NAGAI, R. 2004. Conventional antibody against Nε-(carboxymethyl) lysine (CML) shows cross-reaction

- to N ϵ -(carboxyethyl) lysine (CEL): immunochemical quantification of CML with a specific antibody. *Journal of biochemistry*, 136, 831-837.
- KOMORI, T. 2010. Regulation of bone development and extracellular matrix protein genes by RUNX2. *Cell and tissue research*, 339, 189.
- KOMPF, J., BISSBORT, S. & RITTER, H. 1975. Red cell glyoxalase I (EC 4.4.1.5): formal genetics and linkage relations. *Humangenetik*, 28, 248-251.
- KOSUGI, S., HASEBE, M., MATSUMURA, N., TAKASHIMA, H., MIYAMOTO-SATO, E., TOMITA, M. & YANAGAWA, H. J. J. O. B. C. 2009. Six classes of nuclear localization signals specific to different binding grooves of importin α . 284, 478-485.
- KRISTENSEN, A. R., SCHANDORFF, S., HOYER-HANSEN, M., NIELSEN, M. O., JAATTELA, M., DENGJEL, J. & ANDERSEN, J. S. 2008. Ordered Organelle Degradation during Starvation-induced Autophagy. *Molecular & Cellular Proteomics*, 7, 2419-2428.
- KUHN, R. & DANSI, A. 1936. A molecular rearrangement of N -glucosides. *Ber.*, 69B, 1745-1754.
- KUHN, R. & WEYGAND, F. 1937. The Amadori rearrangement. *Ber.*, 70B, 769-772.
- KURZ, A., RABBANI, N., WALTER, M., BONIN, M., THORNALLEY, P. J., AUBURGER, G. & GISPert, S. 2011. Alpha-synuclein deficiency leads to increased glyoxalase I expression and glycation stress. *Cell and Molecular Life Sci*, 68, 721-733.
- KWAK, M. K., WAKABAYASHI, N., ITOH, K., MOTOHASHI, H., YAMAMOTO, M. & KENSLER, T. W. 2003. Modulation of gene expression by cancer chemopreventive dithiolethiones through the Keap1-Nrf2 pathway. Identification of novel gene clusters for cell survival. *J.Biol.Chem.*, 278, 8135-8145.
- LANDRO, J. A., BRUSH, E. J. & KOZARICH, J. W. 1992. Isomerization of (R)- and (S)- glutathiolactaldehyde by glyoxalase I: The case of dichotomous stereochemical behaviour in a single active site. *Biochemistry*, 31, 6096-6077.
- LARSEN, K., ARONSSON, A. C., MARMSTAL, E. & MANNERVIK, B. 1985. Immunological comparison of glyoxalase I from yeast and mammals with quantitative determination of the enzyme in human tissues by radioimmunoassay. *Comp.Biochem.Physiol.*, 82, 625-638.
- LEE, W. K., BELL, J., KILPATRICK, E., HAYES, M., LINDOP, G. B. M. & DOMINICZAK, M. H. 1993. Collagen linked fluorescence in human atherosclerotic plaques. *Atherosclerosis*, 98, 219-227.
- LI, G., LIAO, Y., WANG, X., SHENG, S. & YIN, D. 2006. In situ estimation of the entire color and spectra of age pigment-like materials: Application of a front-surface 3D-fluorescence technique. *Experimental gerontology*, 41, 328-336.
- LING, A. R. 1908. Malting. *J.Inst.Brewing*, 14, 521.
- LIU, H., SADYGOV, R. G. & YATES, J. R. 2004. A model for random sampling and estimation of relative protein abundance in shotgun proteomics. *Analytical chemistry*, 76, 4193-4201.

- LO, T. W. & THORNALLEY, P. J. 1992. Inhibition of proliferation of human leukaemia 60 cells by diethyl esters of glyoxalase inhibitors in vitro. *Biochemical pharmacology*, 44, 2357-2363.
- M. E. PLATT, E. F. S. 1934. Glyoxalase: II. The distribution of glyoxalase in tissues of normal and cancerous albino rats. *Journal of Biological Chemistry. Journal of Biological Chemistry*, 106, 179-90.
- MACLEOD, A. K., MCMAHON, M., PLUMMER, S. M., HIGGINS, L. G., PENNING, T. M., IGARASHI, K. & HAYES, J. D. 2009. Characterization of the cancer chemopreventive NRF2-dependent gene battery in human keratinocytes: demonstration that the KEAP1-NRF2 pathway, and not the BACH1-NRF2 pathway, controls cytoprotection against electrophiles as well as redox-cycling compounds. *Carcinogenesis*, 30, 1571-1580.
- MAILLARD, L. C. 1912a. Action des acides amines sur les sucres: Formation des melanoidines par voie methodique. *Compt.Rend.Hebd.Seances Acad.Sci.*, 154, 66-68.
- MAILLARD, L. C. 1912b. Formation d'humus et de combustibles mineraux sans intervention de l'oxygene atmospherique des microorganismes, des hautes temperatures, ou des fortes pressions. *Compt.Rend.Hebd.Seances Acad.Sci.*, 155, 1554-1556.
- MAKAROV, A. 2000. Electrostatic axially harmonic orbital trapping: a high-performance technique of mass analysis. *Analytical chemistry*, 72, 1156-1162.
- MARMSTAL, E. & MANNERNVIK, B. 1979. Purification, characterization and kinetic studies of glyoxalase I from rat liver. *Biochim.Biophys.Acta*, 566, 362-370.
- MARQUES, M. C., ALBUQUERQUE, I. S., VAZ, S. H. & BERNARDES, G. J. L. 2019. Overexpression of osmosensitive Ca²⁺-activated channel TMEM63B promotes migration in HEK293T cells. *bioRxiv*, 626010.
- MATSURA, T., SERINKAN, B. F., JIANG, J. & KAGAN, V. E. J. F. L. 2002. Phosphatidylserine peroxidation/externalization during staurosporine-induced apoptosis in HL- 60 cells. 524, 25-30.
- MCKINNEY, G. R. & RUNDLES, R. W. 1956. Lactate formation and glyoxalase activity in normal and leukemic human leukocytes in vitro. *Cancer research*, 16, 67-69.
- MCLAFFERTY, F. & BRYCE, T. 1967. Metastable-ion characteristics: characterization of isomeric molecules. *Chemical Communications (London)*, 1215-1217.
- MCLANE, L. M. & CORBETT, A. H. J. I. L. 2009. Nuclear localization signals and human disease. 61, 697-706.
- MCLELLAN, A. C., PHILLIPS, S. A. & THORNALLEY, P. J. 1992a. The assay of methylglyoxal in biological systems by derivatization with 1,2-diamino-4,5-dimethoxybenzene. *Anal.Biochem.*, 206, 17-23.
- MCLELLAN, A. C., PHILLIPS, S. A. & THORNALLEY, P. J. 1992b. Fluorimetric assay of D-lactate. *Anal Biochem*, 206, 12-6.

- MCLELLAN, A. C., PHILLIPS, S. A. & THORNALLEY, P. J. 1993. The assay of S -D-lactoylglutathione in biological systems. *Anal.Biochem.*, 211, 37-43.
- MCLELLAN, A. C. & THORNALLEY, P. J. 1992a. Electrophoretic analysis of isoforms of glyoxalase II in clinical blood samples. *Eur.J.Clin.Chem.Clin.Biochem.*, 30, 7-10.
- MCLELLAN, A. C. & THORNALLEY, P. J. 1992b. Synthesis and chromatography of 1,2-diamino-4,5-dimethoxybenzene, 6,7-dimethoxy-2-methylquinoxaline and 6,7-dimethoxy-2,3-dimethylquinoxaline for use in a liquid chromatographic fluorimetric assay of methylglyoxal. *Anal.Chim.Acta*, 263, 137-142.
- MCLELLAN, A. C., THORNALLEY, P. J., BENN, J. & SONKSEN, P. H. 1994a. The glyoxalase system in clinical diabetes mellitus and correlation with diabetic complications. *Clin.Sci.*, 87, 21-29.
- MCLELLAN, A. C., THORNALLEY, P. J., BENN, J. & SONKSEN, P. H. 1994b. Population genetics of human glyoxalases and the development of diabetic complications. *Biochem.Soc.Trans.*
- MEGGER, D. A., BRACHT, T., MEYER, H. E. & SITEK, B. 2013. Label-free quantification in clinical proteomics. *Biochimica et Biophysica Acta (BBA) - Proteins and Proteomics*, 1834, 1581-1590.
- MEIJER, C., MULDER, N. H., TIMMER-BOSSCHA, H., SLUITER, W. J., MEERSMA, G. J. & DE VRIES, E. G. 1992. Relationship of cellular glutathione to the cytotoxicity and resistance of seven platinum compounds. *Cancer Res*, 52, 6885-9.
- MEO, T., DOUGLAS, T. & RIJNBEEK, A. M. 1977. Glyoxalase-I polymorphism in mouse - new genetic-marker linked to H-2. *Science*, 198, 311-313.
- MERCADO, N., THIMMULAPPA, R., THOMAS, C. M. R., FENWICK, P. S., CHANA, K. K., DONNELLY, L. E., BISWAL, S., ITO, K. & BARNES, P. J. 2011. Decreased histone deacetylase 2 impairs Nrf2 activation by oxidative stress. *Biochem Biophys Res Commun*, 406, 292-298.
- MITSUISHI, Y., TAGUCHI, K., KAWATANI, Y., SHIBATA, T., NUKIWA, T., ABURATANI, H., YAMAMOTO, M. & MOTOHASHI, H. 2012. Nrf2 redirects glucose and glutamine into anabolic pathways in metabolic reprogramming. *Cancer Cell*, 22, 66-79.
- MORCOS, M., DU, X., PFISTERER, F., HUTTER, H., SAYED, A. A. R., THORNALLEY, P., AHMED, N., BAYNES, J., THORPE, S., KUKUDOV, G., SCHLOTTERER, A., BOZORGMEHR, F., EL BAKI, R. A., STERN, D., MOEHRLEN, F., IBRAHIM, Y., OIKONOMOU, D., HAMANN, A., BECKER, C., ZEIER, M., SCHWENGER, V., MIFTARI, N., HUMPERT, P., HAMMES, H. P., BUECHLER, M., BIERHAUS, A., BROWNLEE, M. & NAWROTH, P. P. 2008. Glyoxalase-1 prevents mitochondrial protein modification and enhances lifespan in *Caenorhabditis elegans*. *Aging Cell*, 7, 260-269.
- MORCOS, M., DU, X. L., HUTTER, A. A. S. H., PFISTERER, F., THORNALLEY, P. J., BAYNES, J., THORPE, S., EL BAKI, R. A., AHMED, N., MIFTARI, N., STERN, D., SCHLOTTERER, A., MOHRLEN, F., HAMANN, A., BECKER, C., HUMPERT, P.,

- HAMMES, H. P., BUCHLER, M., BIERHAUS, A., BROWNLEE, M. & NAWROTH, P. P. 2005. Life extension in *Caenorhabditis elegans* by overexpression of glyoxalase I - The connection to protein damage by glycation, oxidation and nitration. *Free Radical Research*, 39, S43-S43.
- MORTENSEN, P. B., HOVE, H., CLAUSEN, M. R. & HOLTUG, K. 1991. Fermentation to short-chain fatty acids and lactate in human faecal batch cultures. Intra- and inter-individual variations versus variations caused by changes in fermented saccharides. *Scand J Gastroenterol*, 26, 1285-94.
- MUKHERJEE, S. 2010. *The emperor of all maladies: a biography of cancer*, Simon and Schuster.
- NAGUIB, G., AL-MASHAT, H., DESTA, T. & GRAVES, D. T. 2004. Diabetes Prolongs the Inflammatory Response to a Bacterial Stimulus Through Cytokine Dysregulation. *J Invest Dermatol*, 123, 87-92.
- NAKAYAMA, T., HAYASE, F. & KATO, H. 1980. Formation of N^ε-(2-formyl-5-hydroxy-methyl-pyrrol-1-yl)-L-norleucine in the Maillard reaction between D-glucose and L-lysine. *Agric.Biol.Chem.*, 44, 1201-1202.
- NEMET, I., VARGA-DEFTERDAROVIC, L. & TURK, Z. 2006. Methylglyoxal in food and living organisms. *Mol Nutr Food Res*, 50, 1105-17.
- NEMET, I., VIKIC-TOPIĆ, D. & VARGA-DEFTERDAROVIC, L. 2004. Spectroscopic studies of methylglyoxal in water and dimethylsulfoxide. *Bioorganic Chemistry*, 32, 560-570.
- NESVIZHSHKII, A. I., KELLER, A., KOLKER, E. & AEBERSOLD, R. 2003. A statistical model for identifying proteins by tandem mass spectrometry. *Analytical chemistry*, 75, 4646-4658.
- NEUBERG, C. 1913a. Der Zuckerumsatz der Zelle. *Handbuch der Biochemie des Menschen und der Tiere*, 581-582.
- NEUBERG, C. 1913b. The destruction of lactic aldehyde and methylglyoxal by animal organs. *Biochem Z*, 49, 502-506.
- NISHIMURA, C., FURUE, M., ITO, T., OHMORI, Y. & TANIMOTO, T. 1993. Quantitative determination of human aldose reductase by enzyme-linked immunosorbent assay. *Biochem.Pharmac*, 46, 21-28.
- NISHINAKA, T. & YABE-NISHIMURA, C. 2005. Transcription Factor Nrf2 Regulates Promoter Activity of Mouse Aldose Reductase (AKR1B3) Gene. *Journal of Pharmacological Sciences*, 97, 43-51.
- O'CONNELL, P. A. A., TABA, M., NOMIZO, A., FOSS FREITAS, M. C., SUAID, F. A., UYEMURA, S. A., TREVISAN, G. L., NOVAES, A. B., SOUZA, S. L. S., PALIOTO, D. B. & GRISI, M. F. M. 2008. Effects of Periodontal Therapy on Glycemic Control and Inflammatory Markers. *Journal of Periodontology*, 79, 774-783.
- OH, M. S., URIBARRI, J., ALVERANGA, D., LAZAR, I., BAZILINSKI, N. & CARROLL, H. J. 1985. Metabolic utilisation and renal handling of D-lactate in man. *Met.Clin.Exp.*, 34, 621-625.
- OHMORI, S. & IWAMOTO, T. 1988. Sensitive determination of D-lactic acid in biological samples by high performance chromatography. *J.Chromatogr.*, 431, 239-247.
- OHMORI, S., NOSE, Y., OGAWA, H., TSUYAMA, K. & HIROTA, T. 1991. Fluorimetric and high-performance liquid chromatographic determination of D-lactate in biological samples. *J.Chromatogr.*, 566, 1-8.

- ONG, S.-E. & MANN, M. 2005. Mass spectrometry-based proteomics turns quantitative. *Nat Chem Biol*, 1, 252-262.
- OYA, T., HATTORI, N., MIZUNO, Y., MIYATA, S., MAEDA, S., OSAWA, T. & UCHIDA, K. 1999. Methylglyoxal Modification of Protein Chemical and Immunochemical Characterization of Methylglyoxal-Arginine Adducts. *Journal of Biological Chemistry*, 274, 18492-18502.
- PANCHAUD, A., AFFOLTER, M., MOREILLON, P. & KUSSMANN, M. 2008. Experimental and computational approaches to quantitative proteomics: status quo and outlook. *Journal of proteomics*, 71, 19-33.
- PAOLI, P., GIANNONI, E. & CHIARUGI, P. 2013. Anoikis molecular pathways and its role in cancer progression. *Biochimica et Biophysica Acta (BBA)-Molecular Cell Research*, 1833, 3481-3498.
- PARASKEVAS, S., HUIZINGA, J. D. & LOOS, B. G. 2008. A systematic review and meta-analyses on C-reactive protein in relation to periodontitis. *J Clin Periodontol*, 35, 277-290.
- PATEL, R. M. & PATEL, S. K. 2011. Cytotoxic activity of methanolic extract of *Artocarpus heterophyllus* against A549, Hela and MCF-7 cell lines.
- PATIL, C., ROSSA, C. & KIRKWOOD, K. L. 2006. *Actinobacillus actinomycetemcomitans* lipopolysaccharide induces interleukin-6 expression through multiple mitogen-activated protein kinase pathways in periodontal ligament fibroblasts. *Oral Microbiology and Immunology*, 21, 392-398.
- PENG, H.-T., CHEN, J., LIU, T.-Y., WU, Y.-Q., LIN, X.-H., LAI, Y.-H. & HUANG, Y.-F. J. I. J. C. E. P. 2017. Up-regulation of the tumor promoter Glyoxalase-1 indicates poor prognosis in breast cancer. 10, 10852-10862.
- PENG, Y.-T., CHEN, P., OUYANG, R.-Y. & SONG, L. 2015. Multifaceted role of prohibitin in cell survival and apoptosis. *Apoptosis : an international journal on programmed cell death*, 20, 1135-1149.
- PERRY, G. H., YANG, F., MARQUES-BONET, T., MURPHY, C., FITZGERALD, T., LEE, A. S., HYLAND, C., STONE, A. C., HURLES, M. E. & TYLER-SMITH, C. 2008. Copy number variation and evolution in humans and chimpanzees. *Genome research*, 18, 1698-1710.
- PETERS, T., JR. 1962. The biosynthesis of rat serum albumin. I. Properties of rat albumin and its occurrence in liver cell fractions. *J Biol Chem*, 237, 1181-5.
- PETROPOULOS, I. & FRIGUET, B. 2005. Protein maintenance in aging and replicative senescence: a role for the peptide methionine sulfoxide reductases. *Biochimica et Biophysica Acta-Proteins and Proteomics*, 1703, 261-266.
- PHILLIPS, S. A. & THORNALLEY, P. J. 1993a. Formation of methylglyoxal and D-lactate in human red blood cells in vitro *Biochem.Soc.Trans.*, 21, 163-163.
- PHILLIPS, S. A. & THORNALLEY, P. J. 1993b. The formation of methylglyoxal from triose phosphates. Investigation using a specific assay for methylglyoxal. *Eur.J.Biochem.*, 212, 101-105.
- POBEZINSKAYA, Y. L. & LIU, Z. J. C. C. 2012. The role of TRADD in death receptor signaling. 11, 871-876.

- POURMOTABBED, T. & CREIGHTON, D. 1986. Substrate specificity of bovine liver formaldehyde dehydrogenase. *Journal of Biological Chemistry*, 261, 14240-14244.
- PRESHAW, P. M., ALBA, A. L., HERRERA, D., JEPSEN, S., KONSTANTINIDIS, A., MAKRILAKIS, K. & TAYLOR, R. 2013. Periodontitis and diabetes: a two-way relationship. *Diabetologia*, 55, 21-31.
- PRESHAW, P. M., FOSTER, N. & TAYLOR, J. J. 2007. Cross-susceptibility between periodontal disease and type 2 diabetes mellitus: an immunobiological perspective. *Periodontol 2000*, 45, 138-157.
- PUN, P. B. & MURPHY, M. P. 2012. Pathological significance of mitochondrial glycation. *Int J Cell Biol*, 2012, 843505.
- RABBANI, N., GODFREY, L., XUE, M., SHAHEEN, F., GEOFFRION, M., MILNE, R. & THORNALLEY, P. J. 2011. Glycation of LDL by Methylglyoxal Increases Arterial Atherogenicity A Possible Contributor to Increased Risk of Cardiovascular Disease in Diabetes. *Diabetes*, 60, 1973-1980.
- RABBANI, N., SHAHEEN, F., ANWAR, A., MASANIA, J. & THORNALLEY, P. J. 2014. Assay of methylglyoxal-derived protein and nucleotide AGEs. *Biochem. Soc. Trans*, 42, 511-517.
- RABBANI, N. & THORNALLEY, P. 2008a. Dicarbonyls linked to damage in the powerhouse: glycation of mitochondrial proteins and oxidative stress. *Biochem Soc Trans*, 36, 1045-50.
- RABBANI, N. & THORNALLEY, P. J. 2008b. Assay of 3-Nitrotyrosine in Tissues and Body Fluids by Liquid Chromatography with Tandem Mass Spectrometric Detection. *Methods in Enzymology*, 440, 337-359.
- RABBANI, N. & THORNALLEY, P. J. 2008c. The Dicarbonyl Proteome: Proteins Susceptible to Dicarbonyl Glycation at Functional Sites in Health, Aging, and Disease. *Annals of the New York Academy of Sciences*, 1126, 124-127.
- RABBANI, N. & THORNALLEY, P. J. 2009. Quantitation of Markers of Protein Damage by Glycation, Oxidation, and Nitration in Peritoneal Dialysis. *Peritoneal Dialysis International*, 29, S51-S56.
- RABBANI, N. & THORNALLEY, P. J. 2012a. Dicarbonyls (Glyoxal, Methylglyoxal, and 3-Deoxyglucosone). *Uremic Toxins*. John Wiley & Sons, Inc.
- RABBANI, N. & THORNALLEY, P. J. 2012b. Glycation research in Amino Acids: a place to call home. *Amino Acids*, 42, 1087-1096.
- RABBANI, N. & THORNALLEY, P. J. 2012c. Methylglyoxal, glyoxalase 1 and the dicarbonyl proteome. *Amino Acids*, 42, 1133-1142.
- RABBANI, N. & THORNALLEY, P. J. 2014a. Dicarbonyl proteome and genome damage in metabolic and vascular disease. Portland Press Limited.
- RABBANI, N. & THORNALLEY, P. J. 2014b. Glyoxalase Centennial conference: introduction, history of research on the glyoxalase system and future prospects. *Biochem.Soc.Trans.*, 42, 413-418.
- RABBANI, N. & THORNALLEY, P. J. 2014c. Measurement of methylglyoxal by stable isotopic dilution analysis LC-MS/MS with corroborative prediction in physiological samples. *Nat. Protocols*, 9, 1969-1979.

- RABBANI, N. & THORNALLEY, P. J. 2015. Dicarbonyl stress in cell and tissue dysfunction contributing to ageing and disease. *Biochem Biophys Res Commun*, 458, 221-6.
- RABBANI, N., XUE, M. & THORNALLEY, P. J. 2014. Activity, regulation, copy number and function in the glyoxalase system. *Biochem. Soc. Trans*, 42, 419-424.
- RABBANI, N., XUE, M. & THORNALLEY, P. J. 2016a. Dicarbonyls and glyoxalase in disease mechanisms and clinical therapeutics. *Glycoconj J*, 33, 513-25.
- RABBANI, N., XUE, M. & THORNALLEY, P. J. J. C. S. 2016b. Methylglyoxal-induced dicarbonyl stress in aging and disease: first steps towards glyoxalase 1-based treatments. 130, 1677-1696.
- RABBANI, N., XUE, M., WEICKERT, M. O. & THORNALLEY, P. J. Multiple roles of glyoxalase 1-mediated suppression of methylglyoxal glycation in cancer biology—Involvement in tumour suppression, tumour growth, multidrug resistance and target for chemotherapy. *Seminars in cancer biology*, 2018. Elsevier, 83-93.
- RACKER, E. 1951. The mechanism of action of glyoxalase. *J.Biol.Chem.*, 190, 685-696.
- RANGANATHAN, S., CIACCIO, P. J., WALSH, E. S. & TEW, K. D. 1999. Genomic sequence of human glyoxalase-I: analysis of promoter activity and its regulation. *Gene*, 240, 149-155.
- REDON, R., ISHIKAWA, S., FITCH, K. R., FEUK, L., PERRY, G. H., ANDREWS, T. D., FIEGLER, H., SHAPERO, M. H., CARSON, A. R., CHEN, W., CHO, E. K., DALLAIRE, S., FREEMAN, J. L., GONZALEZ, J. R., GRATACOS, M., HUANG, J., KALAITZOPOULOS, D., KOMURA, D., MACDONALD, J. R., MARSHALL, C. R., MEI, R., MONTGOMERY, L., NISHIMURA, K., OKAMURA, K., SHEN, F., SOMERVILLE, M. J., TCHINDA, J., VALSESIA, A., WOODWARK, C., YANG, F., ZHANG, J., ZERJAL, T., ZHANG, J., ARMENGOL, L., CONRAD, D. F., ESTIVILL, X., TYLER-SMITH, C., CARTER, N. P., ABURATANI, H., LEE, C., JONES, K. W., SCHERER, S. W. & HURLES, M. E. 2006. Global variation in copy number in the human genome. *Nature*, 444, 444-454.
- REINIGER, N., LAU, K., MCCALLA, D., EBY, B., CHENG, B., LU, Y., QU, W., QUADRI, N., ANANTHAKRISHNAN, R., FURMANSKY, M., ROSARIO, R., SONG, F., RAI, V., WEINBERG, A., FRIEDMAN, R., RAMASAMY, R., D'AGATI, V. & SCHMIDT, A. M. 2010. Deletion of the Receptor for Advanced Glycation End Products Reduces Glomerulosclerosis and Preserves Renal Function in the Diabetic OVE26 Mouse. *Diabetes*, 59, 2043-2054.
- RICCI, J.-E., MUÑOZ-PINEDO, C., FITZGERALD, P., BAILLY-MAITRE, B., PERKINS, G. A., YADAVA, N., SCHEFFLER, I. E., ELLISMAN, M. H. & GREEN, D. R. J. C. 2004. Disruption of mitochondrial function during apoptosis is mediated by caspase cleavage of the p75 subunit of complex I of the electron transport chain. 117, 773-786.

- ROEPSTORFF, P. & FOHLMAN, J. 1984. Proposal for a common nomenclature for sequence ions in mass spectra of peptides. *Biomedical mass spectrometry*, 11, 601-601.
- ROPER, H., ROPER, S. & HEYNS, K. 1983. N.M.R. spectroscopy of N-(1-deoxy-D-fructos-1-yl)-L-amino acids ("fructose-amino acids"). *Carbohydr.Res.*, 116, 183-195.
- RULLI, A., ANTOGNELLI, C., PREZZI, E., BALDRACCHINI, F., PIVA, F., GIOVANNINI, E. & TALESA, V. 2006. A possible regulatory role of 17beta-estradiol and tamoxifen on glyoxalase I and glyoxalase II genes expression in MCF7 and BT20 human breast cancer cells. *Breast Cancer Research and Treatment*, 96, 187-196.
- SADYGOV, R. G., COCIORVA, D. & YATES, J. R. 2004. Large-scale database searching using tandem mass spectra: Looking up the answer in the back of the book. *Nat Meth*, 1, 195-202.
- SAKAMOTO, H., MASHIMA, T., KIZAKI, A., DAN, S., HASHIMOTO, Y., NAITO, M. & TSURUO, T. 2000. Glyoxalase I is involved in resistance of human leukemia cells to antitumor agent-induced apoptosis. *Blood*, 95, 3214-3218.
- SAKAMOTO, H., MASHIMA, T., SATO, S., HASHIMOTO, Y., YAMORI, T. & TSURUO, T. 2001. Selective activation of apoptosis program by Sp-bromobenzylglutathione cyclopentyl diester in glyoxalase I-overexpressing human lung cancer cells. *Clinical Cancer Research*, 7, 2513-2518.
- SAKELLARIOU, S., FRAGKOU, P., LEVIDOU, G., GARGALIONIS, A. N., PIPERI, C., DALAGIORGOU, G., ADAMOPOULOS, C., SAETTA, A., AGROGIANNIS, G. & THEOHARI, I. 2016. Clinical significance of AGE-RAGE axis in colorectal cancer: associations with glyoxalase-I, adiponectin receptor expression and prognosis. *BMC cancer*, 16, 174.
- SALVI, G. E., YALDA, B., COLLINS, J. G., JONES, B. H., SMITH, F. W., ARNOLD, R. R. & OFFENBACHER, S. 1997. Inflammatory Mediator Response as a Potential Risk Marker for Periodontal Diseases in Insulin-Dependent Diabetes Mellitus Patients. *Journal of Periodontology*, 68, 127-135.
- SANTARIUS, T., BIGNELL, G. R., GREENAN, C. D., WIDAA, S., CHEN, L., MAHONEY, C. L., BUTLER, A., EDKINS, S., WARIS, S., THORNALLEY, P. J., FUTREAL, P. A. & STRATTON, M. R. 2010. GLO1 - A novel amplified gene in human cancer. *Genes, Chromosomes and Cancer*, 49, 711-725.
- SANTOS, V. R., LIMA, J. A., GONÇALVES, T. E. D., BASTOS, M. F., FIGUEIREDO, L. C., SHIBLI, J. A. & DUARTE, P. M. 2010. Receptor activator of nuclear factor-kappa B ligand/osteoprotegerin ratio in sites of chronic periodontitis of subjects with poorly and well-controlled type 2 diabetes. *Journal of periodontology*, 81, 1455-1465.
- SAVELIEV, S., BRATZ, M., ZUBAREV, R., SZAPACS, M., BUDAMGUNTA, H. & URH, M. 2013. Trypsin/Lys-C protease mix for enhanced protein mass spectrometry analysis. *Nature Methods*, 10.
- SCHEIJEN, J. & SCHALKWIJK, C. G. 2014. Quantification of glyoxal, methylglyoxal and 3-deoxyglucosone in blood and plasma by ultra

- performance liquid chromatography tandem mass spectrometry: evaluation of blood specimen. *Clinical Chemistry and Laboratory Medicine*, 52, 85-91.
- SCHIMANDLE, C. M. & VANDER JAGT, D. L. 1979. Isolation and kinetic analysis of multiple forms of glyoxalase I from human erythrocytes. *Arch.Biochem.Biophys.*, 195, 261-268.
- SCHNIDER, V. M. & KOHN, R. R. 1981. Effects of age and diabetes-mellitus on the solubility and non- enzymatic glycosylation of human skin collagen. *J.Clin.Invest.*, 67, 1630-1635.
- SCHRIDER, D. R. & HAHN, M. W. 2010. Gene copy-number polymorphism in nature. *Proceedings of the Royal Society B: Biological Sciences*, 277, 3213-3221.
- SCHWANHAUSSER, B., BUSSE, D., LI, N., DITTMAR, G., SCHUCHHARDT, J., WOLF, J., CHEN, W. & SELBACH, M. 2011. Global quantification of mammalian gene expression control. *Nature*, 473, 337-342.
- SEBEKOVA, K., BLAZICEK, P., SYROVA, D., KRIVOSIKOVA, Z., SPUSTOVA, V., HEIDLAND, A. & SCHINZEL, R. 2001. Circulating advanced glycation end product levels in rats rapidly increase with acute renal failure. *Kidney International*, 59, S58-S62.
- SELL, D. R. & MONNIER, V. M. 1989. Structure elucidation of a senescence crosslink from human extracellular matrix. Implication of pentoses in the aging process. *J.Biol.Chem.*, 264, 21597-21602.
- SHAFIE, A., XUE, M., BARKER, G., ZEHNDER, D., THORNALLEY, P. J. & RABBANI, N. 2016. Reappraisal of putative glyoxalase 1-deficient mouse and dicarbonyl stress on embryonic stem cells in vitro. *Biochem J*, 473, 4255-4270.
- SHARKEY, E. M., O'NEILL, H. B., KAVARANA, M. J., WANG, H., CREIGHTON, D. J., SENTZ, D. L., EISEMAN, J. L. J. C. C. & PHARMACOLOGY 2000. Pharmacokinetics and antitumor properties in tumor-bearing mice of an enediol analogue inhibitor of glyoxalase I. 46, 156-166.
- SHEVCHENKO, G., MUSUNURI, S., WETTERHALL, M. & BERGQUIST, J. 2012. Comparison of extraction methods for the comprehensive analysis of mouse brain proteome using shotgun-based mass spectrometry. *Journal of proteome research*, 11, 2441-2451.
- SHIMASAKI, H. 1994. Assay of fluorescent lipid peroxidation products. *Methods in enzymology*, 233, 338.
- SHIN, D. B., HAYASE, F. & KATO, H. 1988. Polymerization of proteins caused by reaction with sugars and the formation of 3-deoxyglucosone under physiological conditions. *Agric.Biol.Chem.*, 52, 1451-1458.
- SHINOHARA, M., THORNALLEY, P. J., GIARDINO, I., BEISSWENGER, P. J., THORPE, S. R., ONORATO, J. & BROWNLEE, M. 1998. Overexpression of glyoxalase I in bovine endothelial cells inhibits intracellular advanced glycation endproduct formation and prevents hyperglycaemia-induced increases in macromolecular endocytosis. *J.Clin.Invest.*, 101, 1142-1147.

- SIEGEL, R. L., MILLER, K. D. & JEMAL, A. J. C. A. C. J. F. C. 2015. Cancer statistics, 2015. 65, 5-29.
- SMITH, P. K., KROHN, R. I., HERMANSON, G. T., MALLIA, A. K., GARTNER, F. H., PROVENZANO, M. D., FUJIMOTO, E. K., GOEKE, N. M., OLSON, B. J. & KLENK, D. C. 1985. Measurement of protein using bicinchoninic acid. *Analytical Biochemistry*, 150, 76-85.
- SOHAL, R. 1981. *Age pigments*, Elsevier/North-Holland Biomedical Press Amsterdam.
- SPEER, O., MORKUNAITE-HAIMI, S., LIObIKAS, J., FRANCK, M., HENSBO, L., LINDER, M. D., KINNUNEN, P. K., WALLIMANN, T. & ERIKSSON, O. 2003. Rapid Suppression of Mitochondrial Permeability Transition by Methylglyoxal ROLE OF REVERSIBLE ARGININE MODIFICATION. *Journal of Biological Chemistry*, 278, 34757-34763.
- SYKA, J. E., COON, J. J., SCHROEDER, M. J., SHABANOWITZ, J. & HUNT, D. F. 2004. Peptide and protein sequence analysis by electron transfer dissociation mass spectrometry. *Proceedings of the National Academy of Sciences*, 101, 9528-9533.
- SZENT-GYORGYI, A., HEGYELI, A. & MCLAUGHLIN, J. A. 1963. Cancer therapy: a possible new approach. *Science (New York, N.Y.)*, 140, 1391-1392.
- TAKAHASHI, K. 1977a. Further studies on the reactions of phenylglyoxal and related reagents with proteins. *Biochem.J.*, 81, 403-414.
- TAKAHASHI, K. 1977b. The reactions of phenylglyoxal and related reagents with amino acids. *J.Biochem.*, 81, 395-402.
- TAKEUCHI, M., KIMURA, S., KURODA, J., ASHIHARA, E., KAWATANI, M., OSADA, H., UMEZAWA, K., YASUI, E., IMOTO, M. & TSURUO, T. 2010. Glyoxalase-I is a novel target against Bcr-Abl+ leukemic cells acquiring stem-like characteristics in a hypoxic environment. *Cell death and differentiation*, 17, 1211.
- TANAKA, M., GROSSNIKLAUS, U., HERR, W. & HERNANDEZ, N. 1988. Activation of the U2 snRNA promoter by the octamer motif defines a new class of RNA polymerase II enhancer elements. *Genes & Development*, 2, 1764-1778.
- TANAKA, K., WAKI, H., IDO, Y., AKITA, S., YOSHIDA, Y., YOSHIDA, T. & MATSUO, T. 1988. Protein and polymer analyses up to m/z 100 000 by laser ionization time- of- flight mass spectrometry. *Rapid communications in mass spectrometry*, 2, 151-153.
- TAPIA-ALVEAL, C., CALONGE, T. M. & O'CONNELL, M. J. 2009. Regulation of chk1. *Cell division*, 4, 8.
- TATE, S. S. 1975. Interaction of γ -glutamyltranspeptidase with S -acyl derivatives of glutathione. *FEBS Lett.*, 54, 319-322.
- TAYLOR, J. J., PRESRAW, P. M. & LALLA, E. 2015. A review of the evidence for pathogenic mechanisms that may link periodontitis and diabetes. *Journal of clinical periodontology*, 40, S113-S134.
- THAN, T. A., LOU, H., JI, C., WIN, S. & KAPLOWITZ, N. 2011. Role of cAMP-responsive Element-binding Protein (CREB)-regulated Transcription Coactivator 3 (CRTC3) in the Initiation of Mitochondrial

- Biogenesis and Stress Response in Liver Cells. *Journal of Biological Chemistry*, 286, 22047-22054.
- THOMAS, M. C., TSALAMANDRIS, C., MACISAAC, R., MEDLEY, T., KINGWELL, B., COOPER, M. E. & JERUMS, G. 2004. Low-molecular-weight AGEs are associated with GFR and anemia in patients with type 2 diabetes. *Kidney International*, 66, 1167-1172.
- THORNALLEY, P. J. 1988. Modification of the glyoxalase system in human red blood cells by glucose in vitro *Biochem.J.*, 254, 751-755.
- THORNALLEY, P. J. 1990. The glyoxalase system: new developments towards functional characterization of a metabolic pathway fundamental to biological life. *Biochemical Journal*, 269, 1.
- THORNALLEY, P. J. 1991. Population genetics of human glyoxalases. *Heredity*, 67, 139-142.
- THORNALLEY, P. J. 1993a. The glyoxalase system in health and disease. *Molecular Aspects of Medicine*, 14, 287-371.
- THORNALLEY, P. J. 1993b. Modification of the glyoxalase system in disease processes and prospects for therapeutic strategies. *Biochem.Soc.Trans.*, 21, 531-534.
- THORNALLEY, P. J. 1996. Pharmacology of methylglyoxal: formation, modification of proteins and nucleic acids, and enzymatic detoxification-a role in pathogenesis and antiproliferative chemotherapy. *General Pharmacology: The Vascular System*, 27, 565-573.
- THORNALLEY, P. J. 1998. Glutathione-dependent detoxification of α -oxoaldehydes by the glyoxalase system: involvement in disease mechanisms and antiproliferative activity of glyoxalase I inhibitors. *Chem.-Biol.Interact.*, 111-112, 137-151.
- THORNALLEY, P. J. 2003a. The enzymatic defence against glycation in health, disease and therapeutics: a symposium to examine the concept. *Biochem.Soc.Trans.*, 31, 1343-1348.
- THORNALLEY, P. J. 2003b. Glyoxalase I - structure, function and a critical role in the enzymatic defence against glycation. *Biochemical Society Transactions*, 31, 1343-1348.
- THORNALLEY, P. J. 2003c. Protecting the genome: defence against nucleotide glycation and emerging role of glyoxalase I over expression in multidrug resistance in cancer chemotherapy. *Biochem.Soc.Trans.*, 31, 1372-1377.
- THORNALLEY, P. J. 2007. Dietary AGEs and ALEs and risk to human health by their interaction with the receptor for advanced glycation endproducts (RAGE) - an introduction. *Molec.Nutrit.and Food Res*, 51, 1107-1110.
- THORNALLEY, P. J. 2008. Protein and nucleotide damage by glyoxal and methylglyoxal in physiological systems - role in ageing and disease. *Drug Metab & Drug Interact*, 23, 125-150.
- THORNALLEY, P. J., BATTAH, S., AHMED, N., KARACHALIAS, N., AGALOU, S., BABAEI-JADIDI, R. & DAWNAY, A. 2003. Quantitative screening of advanced glycation endproducts in cellular and extracellular proteins by tandem mass spectrometry. *Biochem J*, 375, 581-92.
- THORNALLEY, P. J., EDWARDS, L. G., KANG, Y., WYATT, C., DAVIES, N., LADAN, M. J. & DOUBLE, J. 1996. Antitumour activity of S-p-bromobenzylglutathione cyclopentyl diester in vitro and in vivo.

- Inhibition of glyoxalase I and induction of apoptosis. *Biochem.Pharmacol.*, 51, 1365-1372.
- THORNALLEY, P. J., LANGBORG, A. & MINHAS, H. S. 1999. Formation of glyoxal, methylglyoxal and 3-deoxyglucosone in the glycation of proteins by glucose. *Biochem.J.*, 344, 109-116.
- THORNALLEY, P. J. & RABBANI, N. 2010. Protein damage in diabetes and uremia - identifying hotspots of proteome damage where minimal modification is amplified to marked pathophysiological effect. *Free Radical Research*, 45, 89-100.
- THORNALLEY, P. J. & RABBANI, N. Glyoxalase in tumourigenesis and multidrug resistance. *Seminars in cell & developmental biology*, 2011a. Elsevier, 318-325.
- THORNALLEY, P. J. & RABBANI, N. 2011b. Protein damage in diabetes and uremia-identifying hotspots of proteome damage where minimal modification is amplified to marked pathophysiological effect. *Free Radical Research*, 45, 89-100.
- THORNALLEY, P. J. & RABBANI, N. 2014. Detection of oxidized and glycated proteins in clinical samples using mass spectrometry - A user's perspective. *Biochim. Biophys. Acta*, 1840, 818-829.
- THORNALLEY, P. J. & TISDALE, M. J. 1988. Inhibition of proliferation of human promyelocytic leukaemia HL60 cells by S- D-lactoylglutathione in vitro *Leuk Res.*, 12, 897-904.
- THORNALLEY, P. J., WARIS, S., FLEMING, T., SANTARIUS, T., LARKIN, S. J., WINKLHOFFER-ROOB, B. M., STRATTON, M. R. & RABBANI, N. 2010. Imidazopurinones are markers of physiological genomic damage linked to DNA instability and glyoxalase 1-associated tumour multidrug resistance. *Nucleic Acids Research*, 138, 5432-5442.
- THORPE, S. R. & BAYNES, J. W. CML: a brief history. *International Congress Series*, 2002. Elsevier, 91-99.
- TRAVIS, L. B., FOSSA, S. D., SCHONFELD, S. J., MCMASTER, M. L., LYNCH, C. F., STORM, H., HALL, P., HOLOWATY, E., ANDERSEN, A., PUKKALA, E., ANDERSSON, M., KAIJSER, M., GOSPODAROWICZ, M., JOENSUU, T., COHEN, R. J., BOICE, J. D., JR., DORES, G. M. & GILBERT, E. S. 2005. Second cancers among 40,576 testicular cancer patients: focus on long-term survivors. *J Natl Cancer Inst*, 97, 1354-65.
- TRIPODIS, N., MASON, R., HUMPHRAY, S. J., DAVIES, A. F., HERBERG, J. A., TROWSDALE, J., NIZETIC, D., SENGER, G. & RAGOISSIS, J. 1998. Physical Map of Human 6p21.2–6p21.3: Region Flanking the Centromeric End of the Major Histocompatibility Complex. *Genome Research*, 8, 631-643.
- TURIÁK, L., OZOHANICS, O., MARINO, F., DRAHOS, L. & VÉKEY, K. 2011. Digestion protocol for small protein amounts for nano-HPLC-MS (MS) analysis. *Journal of proteomics*, 74, 942-947.
- TURKO, I. V. & MURAD, F. J. P. R. 2002. Protein nitration in cardiovascular diseases. 54, 619-634.
- TYLER, M. I. 2000. Amino acid analysis. *Amino Acid Analysis Protocols*. Springer.

- UOTILA, L. 1973. Purification and characterization of S-2-hydroxyacylglutathione hydrolase (glyoxalase II) from human liver. *Biochemistry*, 12, 3944-3951.
- URRUTICOECHEA, A., ALEMANY, R., BALART, J., VILLANUEVA, A., VIÑALS, F. & CAPELLA, G. J. C. P. D. 2010. Recent advances in cancer therapy: an overview. 16, 3-10.
- VANDER JAGT, D. L., HASSEBROOK, R. K., HUNSAKER, L. A., BROWN, W. M. & ROYER, R. E. 2001. Metabolism of the 2-oxoaldehyde methylglyoxal by aldose reductase and by glyoxalase-I: roles for glutathione in both enzymes and implications for diabetic complications. *Chem Biol Interact*, 130-132, 549-62.
- VANDER JAGT, D. L. & HUNSAKER, L. A. 2003. Methylglyoxal metabolism and diabetic complications: roles of aldose reductase, glyoxalase-I, betaine aldehyde dehydrogenase and 2-oxoaldehyde dehydrogenase. *Chem Biol Interact*, 143-144, 341-51.
- VEIGA-DA-CUNHA, M., JACQUEMIN, P., DELPIERRE, G., GODFRAIND, C., THEATE, I., VERTOMMEN, D., CLOTMAN, F., LEMAIGRE, F., DEVUYST, O. & VAN SCHAFTINGEN, E. 2006. Increased protein glycation in fructosamine 3-kinase-deficient mice. *Biochemical Journal*, 399, 257-264.
- VIEIRA RIBEIRO, F., DE MENDONÇA, A. C., SANTOS, V. R., BASTOS, M. F., FIGUEIREDO, L. C. & DUARTE, P. M. 2011. Cytokines and bone-related factors in systemically healthy patients with chronic periodontitis and patients with type 2 diabetes and chronic periodontitis. *Journal of periodontology*, 82, 1187-1196.
- VINCE, R. & WADD, W. B. 1969. Glyoxalase inhibitors as potential anticancer agents. *Biochemical and biophysical research communications*, 35, 593-598.
- VIZIRIANAKIS, I. S., PAPPAS, I. S., GOUGOUMAS, D. & TSIFTSOGLU, A. S. 1999. Expression of ribosomal protein S5 cloned gene during differentiation and apoptosis in murine erythroleukemia (MEL) cells. *Oncology research*, 11, 409-19.
- VOGEL, C. L., COBLEIGH, M. A., TRIPATHY, D., GUTHEIL, J. C., HARRIS, L. N., FEHRENBACHER, L., SLAMON, D. J., MURPHY, M., NOVOTNY, W. F. & BURCHMORE, M. 2002. Efficacy and safety of trastuzumab as a single agent in first-line treatment of HER2-overexpressing metastatic breast cancer. *Journal of Clinical Oncology*, 20, 719-726.
- WANG, B.-D. & LEE, N. 2018. Aberrant RNA splicing in cancer and drug resistance. *Cancers*, 10, 458.
- WANG, L.-Y., HUNG, C.-L., CHEN, Y.-R., YANG, J. C., WANG, J., CAMPBELL, M., IZUMIYA, Y., CHEN, H.-W., WANG, W.-C. & ANN, D. K. 2016. KDM4A coactivates E2F1 to regulate the PDK-dependent metabolic switch between mitochondrial oxidation and glycolysis. *Cell reports*, 16, 3016-3027.
- WARBURG, O. H. & DICKENS, F. 1930. Metabolism of tumours.
- WEICHSELBAUM, R. R., LIANG, H., DENG, L. & FU, Y.-X. J. N. R. C. O. 2017. Radiotherapy and immunotherapy: a beneficial liaison? 14, 365.

- WIITA, A. P., ZIV, E., WIITA, P. J., URISMAN, A., JULIEN, O., BURLINGAME, A. L., WEISSMAN, J. S. & WELLS, J. A. J. E. 2013. Global cellular response to chemotherapy-induced apoptosis. 2, e01236.
- WILLIAMS, R., LIM, J. E., HARR, B., WING, C., WALTERS, R., DISTLER, M. G., TESCHKE, M., WU, C., WILTSHIRE, T., SU, A. I., SOKOLOFF, G., TARANTINO, L. M., BOREVITZ, J. O. & PALMER, A. A. 2009. A Common and Unstable Copy Number Variant Is Associated with Differences in Glo1 Expression and Anxiety-Like Behavior. *PLoS ONE*, 4, e4649.
- WIŚNIEWSKI, J. R., ZOUGMAN, A., NAGARAJ, N. & MANN, M. 2009. Universal sample preparation method for proteome analysis. *Nature methods*, 6, 359-362.
- WONG, K. K., DELEEuw, R. J., DOSANJH, N. S., KIMM, L. R., CHENG, Z., HORSMAN, D. E., MACAULAY, C., NG, R. T., BROWN, C. J. & EICHLER, E. E. 2007. A comprehensive analysis of common copy-number variations in the human genome. *The American Journal of Human Genetics*, 80, 91-104.
- WONG, S., MENG, C. & FENN, J. 1988. Multiple charging in electrospray ionization of poly (ethylene glycols). *The Journal of Physical Chemistry*, 92, 546-550.
- WU, J., WILLIAMS, D., WALTER, G. A., THOMPSON, W. E. & SIDELL, N. J. E. C. R. 2014. Estrogen increases Nrf2 activity through activation of the PI3K pathway in MCF-7 breast cancer cells. 328, 351-360.
- XUE, M., ANTONYSUNIL, A., RABBANI, NAILA AND THORNALLEY, PAUL J 2009. Protein damage in the ageing process : advances in quantitation and the importance of enzymatic defences. *Redox metabolism and longevity relationships in animals and plants*. New York ; Abingdon [England]: Taylor & Francis Group.
- XUE, M., MOMIJI, H., RABBANI, N., BARKER, G., BRETSCHNEIDER, T., SHMYGOL, A., RAND, D. A. & THORNALLEY, P. J. 2014. Frequency modulated translocational oscillations of Nrf2 mediate the ARE cytoprotective transcriptional response *Antioxidants & Redox Signaling*, in press.
- XUE, M., RABBANI, N., MOMIJI, H., IMBASI, P., ANWAR, M. M., KITTERINGHAM, N. R., PARK, B. K., SOUMA, T., MORIGUCHI, T., YAMAMOTO, M. & THORNALLEY, P. J. 2012. Transcriptional control of glyoxalase 1 by Nrf2 provides a stress responsive defence against dicarbonyl glycation. *Biochem J*, 443, 213-222.
- XUE, M., RABBANI, N. & THORNALLEY, P. J. 2011. Glyoxalase in ageing. *Semin Cell Dev Biol*, 22, 293-301.
- XUE, M., SHAFIE, A., KAISER, T., RAJPOOT, N. M., KALTSAS, G., GOPALAKRISHNAN, K., FISK, A., DIMITRIADIS, G. K., GRAMMATOPOULOS, D. K. & RABBANI, N. 2017. Glyoxalase 1 copy number variation in patients with well differentiated gastroenteropancreatic neuroendocrine tumours (GEP-NET). *Oncotarget*.
- XUE, M., WEICKERT, M. O., QURESHI, S., KANDALA, N.-B., ANWAR, A., WALDRON, M., SHAFIE, A., MESSENGER, D., FOWLER, M. & JENKINS, G. J. D. 2016. Improved glycemic control and vascular

- function in overweight and obese subjects by glyoxalase 1 inducer formulation. 65, 2282-2294.
- YAMADA, S., KUMAZAWA, S., ISHII, T., NAKAYAMA, T., ITAKURA, K., SHIBATA, N., KOBAYASHI, M., SAKAI, K., OSAWA, T. & UCHIDA, K. 2001. Immunochemical detection of a lipofuscin-like fluorophore derived from malondialdehyde and lysine. *Journal of lipid research*, 42, 1187-1196.
- YAN, S. F., RAMASAMY, R. & SCHMIDT, A. M. 2009. Receptor for AGE (RAGE) and its ligands—cast into leading roles in diabetes and the inflammatory response. *Journal of Molecular Medicine*, 87, 235-247.
- ZENDER, L., XUE, W., ZUBER, J., SEMIGHINI, C. P., KRASNITZ, A., MA, B., ZENDER, P., KUBICKA, S., LUK, J. M. & SCHIRMACHER, P. J. C. 2008. An oncogenomics-based in vivo RNAi screen identifies tumor suppressors in liver cancer. 135, 852-864.
- ZENG, S., ZHANG, Q. Y., HUANG, J. Z., VEDANTHAM, S., ROSARIO, R., ANANTHAKRISHNAN, R., YAN, S. F., RAMASAMY, R., DEMATTEO, R. P., EMOND, J. C., FRIEDMAN, R. A. & SCHMIDT, A. M. 2012. Opposing roles of RAGE and Myd88 signaling in extensive liver resection. *Faseb Journal*, 26, 882-893.
- ZHANG, H., LI, H., XI, H. S. & LI, S. 2012. HIF1 α is required for survival maintenance of chronic myeloid leukemia stem cells. *Blood*, 119, 2595-2607.
- ZHANG, Q. B., FROLOV, A., TANG, N., HOFFMANN, R., VAN DE GOOR, T., METZ, T. O. & SMITH, R. D. 2007. Application of electron transfer dissociation mass spectrometry in analyses of non-enzymatically glycated peptides. *Rapid Communications in Mass Spectrometry*, 21, 661-666.
- ZHANG, S., LIANG, X., ZHENG, X., HUANG, H., CHEN, X., WU, K., WANG, B. & MA, S. 2014. Glo1 genetic amplification as a potential therapeutic target in hepatocellular carcinoma. *International Journal of Clinical and Experimental Pathology*, 7, 2079-2090.
- ZHANG, Y., YANG, W., LI, D., YANG, J. Y., GUAN, R. & YANG, M. Q. J. B. M. G. 2018. Toward the precision breast cancer survival prediction utilizing combined whole genome-wide expression and somatic mutation analysis. 11, 104.
- ZUBAREV, R. A., KELLEHER, N. L. & MCLAFFERTY, F. W. 1998. Electron capture dissociation of multiply charged protein cations. A nonergodic process. *Journal of the American Chemical Society*, 120, 3265-3266.

Appendix

Appendix I

Gene expression correlating positively with glyoxalase 1 expression in tumour cell lines of the CCLE.

Gene	Correlation	r-squared
PPIL1	0.567545	0.322108
RPL7L1	0.566208	0.320592
PRIM2	0.530774	0.281722
CDC5L	0.516734	0.267014
CCT4	0.506131	0.256169
CENPQ	0.489336	0.239449
SF3B14	0.481207	0.231561
SNRPC	0.479415	0.229838
CSE1L	0.462649	0.214045
AC107081.5	0.458086	0.209842
GPN3	0.453936	0.206058
TAF11	0.448653	0.20129
TTK	0.446596	0.199448
RPS10	0.445359	0.198344
RAD54B	0.444554	0.197629
LSM12	0.442879	0.196141
LSM2	0.438242	0.192056
CDK1	0.435797	0.189919
RNF8	0.433665	0.188066
XPO1	0.43065	0.18546
RRP36	0.427866	0.183069
RP11.355B11.2	0.426225	0.181668
SRSF3	0.423585	0.179425
MRPL19	0.422789	0.178751

MTERFD1	0.418466	0.175114
GMPS	0.418388	0.175049
GMNN	0.417197	0.174053
SRP9	0.414003	0.171399
LRRC40	0.413508	0.170989
MAD2L1	0.41329	0.170808
PAK1IP1	0.41325	0.170775
ERCC6L	0.411538	0.169363
SUMO1	0.411418	0.169264
HSP90AB1	0.409958	0.168066
ORC3	0.409653	0.167816
OLA1	0.409551	0.167732
MIR3917	0.406777	0.165468
HDAC2	0.405805	0.164678
LIN9	0.405622	0.164529
NDC1	0.40302	0.162425
HNRNPC	0.401117	0.160895
PPP2R5D	0.400303	0.160243
NUP54	0.400119	0.160095
MRPL42	0.398823	0.15906
NUDCD1	0.396837	0.157479
UQCC2	0.396464	0.157183
MRPS10	0.396004	0.156819
RPF2	0.395558	0.156466
NUP155	0.394869	0.155922
SPC25	0.392642	0.154168
BTF3L4	0.392399	0.153977
NOL11	0.392286	0.153889
SKA2	0.391183	0.153024
PTGES3	0.38984	0.151975
CCDC138	0.389302	0.151556
MRPL47	0.388757	0.151132

CCT8	0.38867	0.151064
RRM1.AS1	0.388225	0.150719
NUP43	0.387986	0.150533
MATR3	0.386567	0.149434
PCNP	0.386379	0.149288
DFFA	0.386315	0.149239
ZBTB9	0.386147	0.149109
NUP35	0.385811	0.14885
RPP40	0.385452	0.148574
SUV39H2	0.385132	0.148327
KHDRBS1	0.385127	0.148323
CCT7	0.384426	0.147784
GLMN	0.384118	0.147547
MELK	0.38403	0.147479
SGOL2	0.38391	0.147387
DHFR	0.382527	0.146327
UTP11L	0.382435	0.146257
TRMT10C	0.382143	0.146034
METTL2A	0.382	0.145924
IPO11	0.381548	0.145579
PSMC1	0.380882	0.145071
KNSTRN	0.380855	0.145051
CKS1B	0.380595	0.144853
USP1	0.380386	0.144693
MAD2L1BP	0.38007	0.144453
MRPL13	0.37814	0.14299
NPM1	0.377748	0.142693
CENPI	0.377435	0.142457
RP11.342K6.1	0.37637	0.141654
PSMD12	0.375945	0.141335
VTA1	0.375643	0.141108
PCGF6	0.375113	0.14071

KPNA2	0.374707	0.140405
CDC25C	0.374658	0.140368
RP11.138C9.1	0.373966	0.139851
HSPA4	0.373836	0.139753
BYSL	0.373821	0.139742
XPO5	0.373752	0.139691
NAE1	0.373504	0.139505
KIF11	0.373117	0.139217
TCP1	0.372856	0.139022
COQ3	0.372765	0.138954
APOO	0.371972	0.138363
KIAA0101	0.370923	0.137584
CHAF1B	0.369814	0.136763
XRCC5	0.369546	0.136564
HAT1	0.369089	0.136227
PAICS	0.368967	0.136137
PNO1	0.368742	0.135971
COIL	0.367958	0.135393
GTF3C4	0.367925	0.135368
TPRKB	0.367726	0.135222
UTP18	0.367525	0.135074
DCLRE1B	0.366908	0.134621
MLF1IP	0.366574	0.134377
MTBP	0.366371	0.134228
CEP78	0.366345	0.134209
NAA15	0.366222	0.134119
CTD.2510F5.4	0.366098	0.134028
CDC27	0.364614	0.132944
TAF9B	0.364088	0.13256
TIPIN	0.363943	0.132454
NUSAP1	0.363603	0.132207
PARPBP	0.363306	0.131991

MRPL14	0.362652	0.131516
AHCTF1	0.361475	0.130664
FKBPL	0.361227	0.130485
AMD1	0.361188	0.130457
RP11.360L9.7	0.361186	0.130456
MMS22L	0.360674	0.130086
SNRNP40	0.360272	0.129796
SSB	0.360039	0.129628
MRPL22	0.359602	0.129314
RFC5	0.359601	0.129313
DEK	0.359367	0.129144
FAM98B	0.358777	0.128721
RAD51AP1	0.358529	0.128543
NCAPG	0.358293	0.128374
PSMB1	0.35805	0.1282
SNRPE	0.357179	0.127577
HNRNPK	0.356906	0.127382
VDAC2	0.356821	0.127321
DYNC1LI1	0.356783	0.127294
CCNB1	0.356646	0.127196
VBP1	0.356227	0.126897
EEF1E1	0.355735	0.126548
HSPD1P1	0.355118	0.126108
RP11.303E16.8	0.35461	0.125748
SNRPD1	0.354388	0.125591
PBK	0.354004	0.125319
GEMIN6	0.353957	0.125286
FBXO5	0.353586	0.125023
CACYBP	0.353429	0.124912
SLC25A17	0.353374	0.124873
HBS1L	0.353136	0.124705
RFC4	0.35258	0.124313

UBE2N	0.351936	0.123859
RP11.15L13.4	0.351908	0.12384
CDC7	0.351901	0.123834
NUF2	0.351842	0.123793
TOP2A	0.351702	0.123694
EIF4E	0.350993	0.123196
IPO7	0.35082	0.123075
RP11.342K6.2	0.350367	0.122757
SMIM13	0.349928	0.12245
PFDN6	0.349802	0.122362
RRM1	0.349767	0.122337
AL590762.1	0.34975	0.122325
GCFC2	0.34938	0.122066
PTTG1	0.34927	0.12199
ESCO2	0.349211	0.121948
CCT5	0.348798	0.12166
XRCC6	0.348713	0.121601
NUP37	0.348626	0.12154
TUBD1	0.348619	0.121535
RPF1	0.348375	0.121365
ZWILCH	0.34814	0.121201
DSCC1	0.347946	0.121066
KPNB1	0.347806	0.120969
MCM10	0.3478	0.120965
ISCA1	0.347717	0.120907
ST13	0.34756	0.120798
GCSH	0.347457	0.120726
CEP57L1	0.347329	0.120638
STIL	0.34701	0.120416
PDCL3	0.346891	0.120333
BRIX1	0.34675	0.120235
BCCIP	0.346567	0.120109

OSGEPL1	0.346479	0.120048
HSF2	0.346333	0.119946
PPP1CC	0.346173	0.119836
RMI1	0.345936	0.119671
CSNK2B	0.34586	0.119619
NSL1	0.345477	0.119354
CENPW	0.345058	0.119065
VDAC3	0.34473	0.118839
SERBP1	0.344652	0.118785
RPAP3	0.344563	0.118724
CTB.43P18.1	0.344227	0.118492
UBE2T	0.344141	0.118433
UCHL5	0.343252	0.117822
GINS4	0.34314	0.117745
SET	0.342985	0.117639
LSM5	0.342246	0.117132
AUNIP	0.342134	0.117056
PSMB3	0.34199	0.116957
LSM3	0.341823	0.116843
CCDC58	0.341822	0.116842
ZW10	0.340986	0.116272
TRIP13	0.340958	0.116253
TFAM	0.340904	0.116216
PSMD14	0.340814	0.116154
POLR1C	0.340613	0.116017
SGOL1	0.340463	0.115915
STMN1	0.340382	0.11586
ATP5F1	0.340256	0.115774
DLGAP5	0.340134	0.115691
PPP2CA	0.339739	0.115423
DDX20	0.339588	0.11532
ILF2	0.339443	0.115222

DNA2	0.339411	0.1152
DEPDC1	0.339297	0.115123
COPS2	0.339122	0.115004
SUMO2	0.339079	0.114975
GEMIN5	0.339015	0.114932
CCT2	0.338997	0.114919
POLE2	0.338899	0.114852
KIFC1	0.338234	0.114402
RP5.1113E3.3	0.33791	0.114183
DHX9	0.337014	0.113578
NUP107	0.336948	0.113534
MCM3	0.336814	0.113444
KIF15	0.336698	0.113366
MRPL50	0.336627	0.113317
RP11.474G23.2	0.336619	0.113312
RACGAP1	0.336324	0.113114
CCT3	0.336195	0.113027
HPRT1	0.336162	0.113005
CBX1	0.335943	0.112858
ATAD2	0.335757	0.112733
ORC4	0.33572	0.112708
TMEM14B	0.335632	0.112649
LTV1	0.335367	0.112471
TIMM8A	0.33533	0.112446
HNRNPA3	0.334921	0.112172
MIS18A	0.334785	0.112081
RFC2	0.334749	0.112057
KIF4A	0.334682	0.112012
DTL	0.334343	0.111785
RPA2	0.334287	0.111748
C11orf82	0.334237	0.111715
SSX2IP	0.334208	0.111695

ARMC1	0.334051	0.11159
RFC3	0.333806	0.111427
GNAI3	0.333604	0.111292
DONSON	0.333517	0.111234
SLC25A33	0.333474	0.111205
ELAVL1	0.333473	0.111204
ASNSD1	0.333468	0.111201
TIMM23B	0.333405	0.111159
DARS2	0.333403	0.111158
CCNB2	0.333273	0.111071
MDH1	0.332893	0.110818
PSMG1	0.332739	0.110715
SMC3	0.332601	0.110623
DBF4	0.33258	0.11061
UBA2	0.33233	0.110443
DSN1	0.331952	0.110192
POLA1	0.330856	0.109465
DENR	0.330834	0.109451
NEDD1	0.330497	0.109228
EIF1AX	0.330395	0.109161
SKA3	0.330375	0.109148
UNG	0.330142	0.108994
DCAF13	0.329051	0.108275
AASDHPPT	0.328814	0.108119
HSPE1	0.328539	0.107938
MCMBP	0.328214	0.107725
ZCRB1	0.328203	0.107717
WDYHV1	0.328192	0.10771
GART	0.32817	0.107696
SNRPB	0.327741	0.107414
ANKRD32	0.327302	0.107127
UBXN2A	0.327272	0.107107

HNRNPA1	0.327186	0.10705
TMEM177	0.327034	0.106951
ETF1	0.326881	0.106851
MED20	0.326701	0.106734
SNRPG	0.326553	0.106637
NUP153	0.32655	0.106635
HAUS6	0.32647	0.106583
GIN51	0.325959	0.106249
FANCB	0.325432	0.105906
TAF1B	0.325284	0.10581
CENPL	0.32514	0.105716
ORC2	0.324867	0.105539
WDR75	0.324704	0.105433
MRT04	0.324466	0.105278
RBMXL1	0.324462	0.105275
MCUR1	0.324366	0.105213
MAGOHB	0.324209	0.105111
PPAT	0.324153	0.105075
CCT6A	0.323809	0.104852
UBE2V2	0.323629	0.104736
MRPS22	0.323407	0.104592
CTD.2256P15.4	0.323359	0.104561
SKP2	0.323256	0.104494
PHF13	0.323133	0.104415
TMPO	0.32291	0.104271
MRPL39	0.322906	0.104268
ZMYM1	0.322861	0.104239
ABCE1	0.322315	0.103887
CCZ1B	0.322297	0.103876
MRPL3	0.322283	0.103866
FAM104B	0.321855	0.10359
TUBB	0.321777	0.10354

CDKN2AIPNL	0.321331	0.103253
BAG4	0.321218	0.103181
CCNE2	0.321139	0.10313
SPAG5	0.321076	0.10309
ERAL1	0.320695	0.102845
CMSS1	0.320565	0.102762
TOMM22	0.320428	0.102674
NUFIP1	0.320371	0.102638
NEK2	0.320296	0.10259
RP11.144G7.2	0.319764	0.102249
NDC80	0.31949	0.102074
NDUFB4	0.319311	0.10196
EIF2S1	0.319205	0.101892
SKP1	0.319171	0.10187
MAGOH	0.318761	0.101609
PSMA4	0.3186	0.101506
WDR46	0.31839	0.101372
TIMM23	0.3182	0.101251
RRM2	0.318015	0.101133
DESI2	0.317959	0.101098
MRPS23	0.317947	0.101091
FARSB	0.317613	0.100878
EXO1	0.317582	0.100858
MRPS15	0.317457	0.100779
MRPL51	0.317446	0.100772
HAUS1	0.316431	0.100129
PRPF4	0.3163	0.100046
C4orf46	0.316241	0.100009

Appendix II

Gene correlates negatively with Glo1mRNA

Gene Name	Correlation	R squared
	Coffeinet (-)	
RASA4CP	0.31905	0.101791
KB.1027C11.4	0.32147	0.103342
CTB.134H23.2	0.33338	0.111141
TAPBPL	0.33516	0.11233
GNPTG	0.33612	0.11298
RP11.109L13.1	0.34757	0.120805
RP11.490O6.2	0.35131	0.12342
TRADD	0.35306	0.12465

Appendix III

Proteins in the cytoplasmic extract increased in abundance by treatment with methylglyoxal.

Uniprot accession no	Peptide count	Unique peptide	Confidence Score	P Value	Q value	Power analysis
Q9UKX7	2	2	88.49	0.042942	0.074824	0.572963
H3BNC9	3	0	110.49	0.049847	0.080881	0.537236
P10827	1	1	20.94	0.000449	0.01194	0.999871
A0A0G2JQ76	1	1	20.29	0.020731	0.051151	0.737904
H3BNT2	2	2	110.11	0.003257	0.023854	0.972966
H7C3A6	1	1	18.47	0.015038	0.043801	0.800756
H0YGR4	2	2	31.81	0.007458	0.032224	0.90642
A0A087X2I7	1	1	14.22	0.01482	0.043603	0.803415
H0YB67	1	1	18.67	0.033032	0.064512	0.634855
K7EM19	1	1	58.54	0.032581	0.064279	0.638038
H7C202	1	1	21.16	0.032736	0.064391	0.63694
Q03181	1	1	29.64	0.009896	0.036482	0.869417
P33552	2	2	151.7	0.034489	0.06598	0.624799
Q9BYD6	2	1	73.21	0.005625	0.028058	0.935688
Q3ZCX4	1	1	17.83	0.045807	0.077692	0.557516
P51587	1	1	15.44	0.043005	0.074878	0.572612
Q6ZR64	1	1	71.27	0.004716	0.026727	0.950336
H7BZL2	3	3	252.3	0.002133	0.020448	0.988079
A0A0A0MSD7	1	0	20.6	0.002372	0.021693	0.985165
F8W9Q7	1	0	17.09	0.002372	0.021693	0.985165
H0Y903	1	1	59.53	0.005179	0.02729	0.942886
H3BPB0	1	0	13.99	0.021678	0.051735	0.728558
D6RFM5	10	5	679.59	0.002892	0.02346	0.978225
A0A0B4J1Y4	1	1	69.13	0.039098	0.07078	0.595278

Q6KC79	1	1	14.5	0.041195	0.073184	0.582867
E7EQL8	1	1	20.04	0.046891	0.078534	0.551905
F5GYA2	1	1	19.91	0.04821	0.079762	0.545251
P53420	1	1	14.14	0.033393	0.065056	0.632329
A0A087WZY0	1	1	22.5	0.004606	0.026569	0.952091
H0Y390	1	1	19.64	0.002431	0.021894	0.984414
P29373	1	1	115.48	0.005095	0.027257	0.944242
P43897	2	2	123.56	0.004311	0.026216	0.956773
Q5T1U7	2	2	38.35	0.043271	0.075286	0.571141
P51608	1	1	52.04	0.008628	0.034953	0.888322
H3BQA6	2	2	93.36	0.022441	0.052734	0.721225
A0A087WT80	1	1	20.02	0.039578	0.071236	0.592382
P05543	1	1	25.09	0.030669	0.061737	0.65198
A0A087WWL5	1	1	22.24	0.023135	0.053354	0.714712
A0A1C7CYZ2	1	0	13.98	0.018018	0.047442	0.766341
Q9H0W5	1	0	20.92	0.018018	0.047442	0.766341
Q96ST2	2	2	54.61	0.005316	0.027446	0.940685
P02549	1	1	18.75	0.045543	0.077412	0.5589
J3KNP4	1	1	18.98	0.027759	0.05806	0.674619
A0A024R214	2	0	35.35	0.046281	0.078069	0.555046
A6PWM2	1	1	49.14	0.026027	0.055872	0.689007
A0A1B0GUS7	2	1	43.76	0.047508	0.079043	0.548773
K7ENL0	1	1	21.44	0.024939	0.054886	0.698414
P01023	2	2	145.01	0.02629	0.056379	0.68677
A0A087WWW8	1	1	18.6	0.039259	0.070879	0.594304
Q969S3	1	1	76.4	0.037146	0.068681	0.607382
H0YHS6	2	2	122.96	0.032981	0.064466	0.635213
Q96N66	1	1	43.03	0.02261	0.052867	0.719627
H0Y9N9	1	1	46.47	0.014819	0.043603	0.803428
E9PJ65	1	0	17.47	0.035051	0.066262	0.621018
Q5T2E8	1	0	15.18	0.035051	0.066262	0.621018
E9PJF9	2	0	95.97	0.040852	0.072768	0.584857

A0A087WUT0	1	1	14.82	0.046602	0.078198	0.553389
Q86T26	1	1	16.89	0.008656	0.034953	0.887895
Q14676	6	6	410.48	0.043405	0.075407	0.570402
H0YEZ9	1	1	49.13	0.006401	0.029496	0.923196
A0A0G2JQF3	1	0	19.04	0.023875	0.054112	0.707921
Q7Z698	1	1	17.45	0.025601	0.055616	0.692653
P41223	2	1	103.84	0.027084	0.057065	0.680141
A0A087WX24	1	0	17.42	0.024274	0.054385	0.704322
Q9BV73	1	0	17.15	0.005091	0.027257	0.944313
Q9C0J8	1	0	17.24	0.005091	0.027257	0.944313
Q99832	25	23	1731.02	0.027081	0.057065	0.680167
P08579	4	3	375.24	0.03413	0.065691	0.627245
A0A087WWT1	3	2	123.69	0.032948	0.064456	0.635442
Q9P1A2	1	1	22.59	0.044403	0.076465	0.564968
A0A087WZL3	1	1	18.94	0.02153	0.051735	0.730001
A0A0G2JS85	1	1	17.17	0.00481	0.026891	0.948823
Q9GZN8	3	3	216.45	0.020006	0.050626	0.745248
A8MUM1	1	1	31.52	0.013269	0.041518	0.822975
V9GYA7	3	3	213.94	0.011926	0.039829	0.840797
H0YL19	5	3	285.05	0.011621	0.039394	0.844968
H7C440	1	1	15.75	0.042217	0.073997	0.577028
J3QRD1	1	1	71.82	0.001899	0.018919	0.990729
P14921	1	1	18.61	0.042732	0.074622	0.574135
A0A0J9YYF7	1	1	26.17	0.023399	0.053497	0.712269
A0A087WYK2	1	1	15.43	0.044876	0.076943	0.562432
H3BPN4	1	0	16.74	0.034615	0.06598	0.623947
Q9NZ56	1	0	14.51	0.034615	0.06598	0.623947
P00390	8	5	521.58	0.044387	0.076465	0.565055
Q08E93	1	1	16.97	0.006811	0.030378	0.916642
P82933	2	2	104.75	0.040081	0.07191	0.589385
A0A0A0MQX8	1	0	15.41	0.030546	0.061595	0.6529
P02545	13	0	605.77	0.002746	0.022994	0.980237

Q9Y2W2	3	3	153.86	0.038464	0.070238	0.599145
Q86US8	2	2	60.97	0.041638	0.073489	0.580316
Q01469	6	3	340.21	0.049771	0.080869	0.537603
Q96PK6	6	6	391.38	0.013045	0.041268	0.825881
A0A075B7F8	2	2	43.43	0.026446	0.056465	0.685455
H7C537	3	2	150.99	0.036856	0.068359	0.609231
P15121	12	4	840.49	0.006556	0.029869	0.920724
P62995	6	3	339.66	0.0347	0.066021	0.623378
E9PNB5	8	1	405.61	0.005701	0.028198	0.934463

Proteins in the nuclear extract increased in abundance by treatment with methylglyoxal.

Uniprot accession no	Peptide count	Unique peptide	Confidence Score	P Value	Q value	Power analysis
A0A0C4DG26	1	1	14.31	0.027587	0.875668	0.718782
P02775	1	1	19.41	0.000196	0.409851	1
P01859	2	2	79.03	0.002727	0.42943	0.997125
P20366	3	1	72.54	0.001578	0.409851	0.999706
Q5T7N2	1	1	17.22	0.023	0.832407	0.764368
A0A0A0MR66	1	1	22.56	0.009714	0.681657	0.926565
P01042	11	10	576.13	0.000841	0.409851	0.999992
A0A0B4J2A4	5	5	127.76	0.00571	0.560698	0.975023
Q9BS19	2	2	50.5	0.008549	0.681657	0.94164
P04196	1	1	55.9	0.005851	0.560698	0.973554
P02776	1	1	26.33	0.047751	0.990711	0.56968
F8W696	6	6	270.14	0.001382	0.409851	0.999848
P01860	4	1	110.34	0.046522	0.986356	0.576933
P01023	6	5	197.8	0.01596	0.771084	0.845413
Q96M27	1	1	44.23	0.029133	0.876819	0.704601
Q13541	1	1	32.69	0.046278	0.986356	0.578398

P19878	1	0	29.07	0.022408	0.832407	0.770655
Q8TBY9	1	0	30.75	0.005118	0.560698	0.980859
Q9BT09	1	1	42.93	0.03377	0.884555	0.66522
X6R700	1	1	17.68	0.011656	0.681657	0.90096
E9PDQ8	2	2	68.67	0.01839	0.783856	0.815899
O14828	1	1	52.16	0.005617	0.560698	0.975967
Q5M9N0	1	1	23.33	0.02849	0.876819	0.710428
P30084	6	6	337.3	0.011195	0.681657	0.907049
O14745	2	2	65.39	0.006103	0.560698	0.970865
Q6S8J3	8	1	933.15	0.002964	0.435709	0.996153
Q9UMX5	2	2	65.68	0.031468	0.884555	0.684195
P60709	25	6	1970.86	0.017487	0.783856	0.826683
Q562R1	11	0	648.57	0.031221	0.884555	0.686294
P14735	1	0	33.56	0.04945	0.990711	0.559949
P52907	3	3	145.93	0.031976	0.884555	0.679919
P680325	16	2	1077.46	0.013613	0.733919	0.875298
B4DSN5	1	0	20.24	0.010977	0.681657	0.909941
A8K7Q2	16	1	967.97	0.045152	0.986356	0.585248
C9JIZ6	3	3	161.02	0.011252	0.681657	0.906299
O43923	1	1	17.68	0.023468	0.83462	0.759472
C9J8T6	1	1	76.51	0.04159	0.963765	0.608071
P10253	3	3	172.06	0.011708	0.681657	0.900277

Proteins in the nuclear extract decreased in abundance by treatment with methylglyoxal

Uniprot accession no	Peptide count	Unique peptide	Confidence Score	P Value	Q value	Power analysis
P13010+	25	25	1834.53	0.0071 4	0.6202 86	0.9590 46

A0A087WZR9	4	4	236.3	0.0414 31	0.9637 65	0.6091 3
F5H6P7	3	3	138.3	0.0184 31	0.7838 56	0.8154 11
Q10570	8	7	451.84	0.0238 68	0.8353 92	0.7553 22
A0A0A0MRA53	7	6	234.96	0.0271 13	0.8756 68	0.7232 47
Q14011	5	5	292.1	0.0385 91	0.9637 65	0.6287 56
P09661	14	14	865.61	0.0200 01	0.8227 57	0.7972 11
F8VZX2	7	5	267.99	0.0422 62	0.9637 65	0.6036 26
E7EQY1	1	1	55.92	0.0416 56	0.9637 65	0.6076 3
H0Y5B4	3	3	139.75	0.0273 25	0.8756 68	0.7212 51
Q96KR1	11	11	702.03	0.0211 22	0.8324 07	0.7846 48
A0A0A0MSI2	2	2	79.39	0.0417 34	0.9637 65	0.6071 12
J3QLW7	2	2	122.93	0.0306 63	0.8845 55	0.6910 92
Q9BXT5	2	0	61.17	0.0276 13	0.8756 68	0.7185 42
Q04760	4	4	148.73	0.0476 33	0.9907 11	0.5703 68
P62314	6	6	585.87	0.0157 66	0.7710 84	0.8478 34
A0A0U1RRM4	8	4	881.2	0.0490 2	0.9907 11	0.5623 82
P32322	6	6	482.89	0.0449 28	0.9863 56	0.5866 34
A0A087X1W2	4	4	200.28	0.0488 97	0.9907 11	0.5630 81
Q3SX64	1	0	14.67	0.0274 81	0.8756 68	0.7197 82

H0YKD8	5	5	227.67	0.0423 97	0.9637 65	0.6027 41
A0A087WWR2	2	2	174.35	0.0323 54	0.8845 55	0.6767 65
P53999	2	2	62.46	0.0045 76	0.5310 31	0.9856 76
F8WBM4	1	1	22.84	0.0277 99	0.8756 68	0.7168 07
F5H1S9	2	2	73.48	0.0017 85	0.4098 51	0.9994 77
O60832	9	8	430.27	0.0107 86	0.6816 57	0.9124 62
Q9H0A0	18	18	1069.26	0.0457 59	0.9863 56	0.5815 37
Q15427	1	0	23.51	0.0027	0.4294 3	0.9972 23
A0A0A0MSE2	3	3	190.21	0.0019 53	0.4098 51	0.9992 22
Q9Y2H1	7	6	461.93	0.0021 59	0.4098 51	0.9988 19
E7EVA0	1	1	32.16	0.0326 32	0.8845 55	0.6744 66
P21953	8	6	330.81	0.0340 99	0.8845 55	0.6625 98
P41208	1	1	21.25	0.0292 45	0.8768 19	0.7035 94
Q5JSZ5	3	3	131	0.0184 85	0.7838 56	0.8147 66
A0A024R341	2	0	69.64	0.0094 69	0.6816 57	0.9297 7
D6RAV8	2	2	80.34	0.0162 13	0.7710 84	0.8422 64
Q9UNZ5	1	1	19.3	0.0451 09	0.9863 56	0.5855 16
A0A0A0MRZ6	2	2	92.19	0.0315 86	0.8845 55	0.6832
Q8IXW0	1	1	17.1	0.0036 25	0.4701 46	0.9926 37

Q9NYB0	1	1	20.6	0.0168 29	0.7730 85	0.8346 76
Q9UII2;	2	2	45.94	0.0375 68	0.9632 19	0.6361 5
H0YMV8	2	2	116.01	0.0136 47	0.7339 19	0.8748 67
F5H2A4	3	1	178.67	0.0164 36	0.7710 84	0.8395 11
Q9UK45	1	1	90.64	0.0040 63	0.4976 77	0.9896 9
F8WAH1	2	2	58.67	0.0337 97	0.8845 55	0.665
P29084	1	0	33.27	0.0215 49	0.8324 07	0.7799 47
P13807	3	3	137.97	0.0021 41	0.4098 51	0.9988 57

Proteins of the mitochondrial matrix and intermembrane space increased by HEK293 cell treatment with methylglyoxal.

Uniprot accession no	Peptide count	Unique peptide	Confidence Score	P Value	Q value	Power analysis
A0A024R3B9	1	1	45.77	0.014208	0.534926	0.867613
Q15554	1	0	15.16	0.021296	0.534926	0.782729
A8MYB8	2	1	75.11	0.040235	0.534926	0.617241
P13647	5	1	193.05	0.017519	0.534926	0.826295
A0A1B0GVP8	1	1	14.26	0.030219	0.534926	0.694959
Q14151	5	1	260.52	0.027561	0.534926	0.719028
H0YBL3	1	1	22.05	0.047876	0.534926	0.568951
Q9NWZ3	1	1	24.12	0.001036	0.219198	0.99997
Q9NZT1	3	3	187.05	0.033451	0.534926	0.667784
P31944	1	1	53.7	0.046429	0.534926	0.577492

G3V1V0	12	12	591.82	0.046139	0.534926	0.579235
P46778	14	14	645.28	0.038272	0.534926	0.631044
G5E9G0	28	1	1846.28	0.044079	0.534926	0.591934
H3BMM9	3	3	92.96	0.026893	0.534926	0.72534
P39023	34	7	2199.3	0.046159	0.534926	0.579115
P00441	4	4	303.09	0.004101	0.286345	0.989408

Proteins of the mitochondrial matrix and intermembrane space decreased by HEK293 cell treatment with methylglyoxal.

Uniprot accession no	Peptide count	Unique peptide	Confidence		Q value	Power analysis
			e Score	P Value		
Q99733	6	4	412.84	0.048063	0.534926	0.567868
Q06124	5	5	268.71	0.0475	0.534926	0.571146
F8VQZ7	5	5	271.96	0.044498	0.534926	0.589306
P43487	6	6	305.33	0.039535	0.534926	0.622089
A0A087WY61	23	0	1139.19	0.046536	0.534926	0.576852
H0YIV4	11	1	659.78	0.001329	0.219198	0.999876
Q92688	10	5	586	0.032059	0.534926	0.679222
F8VV59	12	2	692.61	0.002455	0.286345	0.998046
Q14980	23	0	1130.12	0.025733	0.534926	0.736559
Q9GZL7	4	4	210.8	0.032495	0.534926	0.675599
Q13257	3	3	112.59	0.019125	0.534926	0.80728
A0A087WTB8	4	4	176.81	0.033558	0.534926	0.666919
Q6Y7W6	7	7	362.26	0.003798	0.286345	0.991528
M0R0Y2	3	3	110.61	0.032731	0.534926	0.673654
I3L397	6	6	585.41	0.027384	0.534926	0.720692
P50990	19	19	981.06	0.044299	0.534926	0.590555
O75792	1	1	36.31	0.042804	0.534926	0.600089
G3V1C3	6	6	358.31	0.034647	0.534926	0.658267
Q13564	9	9	423.51	0.045065	0.534926	0.585785

P18615	6	6	292.56	0.03632	0.534926	0.645412
Q9UJA5	3	3	260.16	0.048015	0.534926	0.568143
P13797	18	18	802.69	0.042826	0.534926	0.599949
M0R389	5	5	262.71	0.011189	0.534189	0.907129
C9JA08	4	4	189.02	0.025224	0.534926	0.741595
P22059	3	3	82.5	0.021998	0.534926	0.775073
P24666	2	2	109.09	0.045547	0.534926	0.582824
J3KTF8	5	5	187.34	0.018952	0.534926	0.809291
P17480	12	12	518.42	0.014855	0.534926	0.859338
P49770	5	5	273.66	0.018462	0.534926	0.815038
P78362	5	2	185.3	0.047497	0.534926	0.571159
A0A087WTP3	7	7	295.78	0.029125	0.534926	0.704666
B2WTI3	2	2	131.16	0.045533	0.534926	0.582912
P02647	21	19	1340.62	0.012107	0.534926	0.895007
Q92922	7	7	257.55	0.026187	0.534926	0.732134
Q9Y224	7	7	388.53	0.017384	0.534926	0.827926
Q5VYK3	13	13	576.35	0.043381	0.534926	0.596371
A0A0A0MTN3	5	4	200.64	0.01639	0.534926	0.840074
H0Y9N5	1	1	28.67	0.024053	0.534926	0.753428
I3L2B0	13	1	592.33	0.033703	0.534926	0.665757
G3V2E7	7	6	362.46	0.049555	0.546813	0.559359
Q96CT7	9	8	578.41	0.043907	0.534926	0.593022
Q86WV7	4	3	209.07	0.006893	0.403383	0.96196
P08670;	31	28	1670.35	0.003964	0.286345	0.990398
O14776;G3V220	5	5	235.93	0.037546	0.534926	0.636311
A0A087WY55	4	4	167.8	0.043234	0.534926	0.597313
Q96GX9	2	2	93.14	0.020118	0.534926	0.795881
Q8WU90	6	6	289.31	0.041648	0.534926	0.607682
Q99543;C9IZ83	11	11	588.25	0.009312	0.485137	0.931807
J3KPM9	3	3	148.47	0.018246	0.534926	0.817603
E7EVX8;	4	4	210.73	0.04496	0.534926	0.586436
O75153	14	1	637.43	0.045126	0.534926	0.585409
F5GZY1	2	2	100.36	0.021924	0.534926	0.77587
Q96KP4	3	2	118.69	0.022946	0.534926	0.764943
Q6P2E9	2	2	62.16	0.037817	0.534926	0.634329

Q15527	1	1	42.19	0.038537	0.534926	0.629141
Q9Y5X3	6	6	213.26	0.013097	0.534926	0.882024
F5H6C2	1	1	15.28	0.004262	0.286345	0.988201
C9JJP5	2	2	82.93	0.046455	0.534926	0.577335
F6TLX2	4	4	168.89	0.014995	0.534926	0.857556
Q96GX2	1	1	20.62	0.039038	0.534926	0.625579
A0A087X060	1	1	16.83	0.027509	0.534926	0.719515
Q16513	4	4	95.49	0.004224	0.286345	0.988489
Q14247	8	8	333.19	0.000741	0.219198	0.999997
O00178	7	7	424.16	0.032239	0.534926	0.677721
P0DN79	5	5	368.07	0.000806	0.219198	0.999994
Q5T4U8	1	1	34.28	0.011124	0.534189	0.907994
I3L2H7	1	1	69.84	0.006178	0.386467	0.970049
Q16762	3	3	155.3	0.027684	0.534926	0.717878
Q9BV57;	5	5	289.76	0.043424	0.534926	0.596096
Q8WUM0	2	2	56.83	0.045267	0.534926	0.584543
E7ER27	2	2	101.28	0.011639	0.534926	0.901182
F5H5U2	2	1	53.43	0.024065	0.534926	0.753305
A6NIR2	1	1	32.56	0.001646	0.229715	0.99964
Q14691	4	4	204.57	0.003288	0.286345	0.994577
Q9BRS2	3	3	112.52	0.032826	0.534926	0.672875
P15924	2	2	48.38	0.045152	0.534926	0.585249
P48147	3	3	147.44	0.035	0.534926	0.655508
A0A0C4DG62	1	1	49.25	0.028576	0.534926	0.709646
B4E1Z4	3	3	88.17	0.002541	0.286345	0.997775
O75794	9	9	429.32	0.003969	0.286345	0.990362

Proteins of the mitochondrial membrane of HEK 293 cells decreased by treatment with methylglyoxal.

Uniprot accession no	Peptide count	Unique peptide	Confidence Score	P Value	Q value	Power analysis
M0R0F0	2	2	191.72	0.08375	0.990182	0.43408
H0YIQ2	1	1	15.81	0.023877	0.828711	0.813109
H0YK64	1	1	16.46	0.033551	0.828711	0.717568
O15399	1	1	19.79	0.102047	0.990182	0.378051
D6RD47	1	1	58.93	0.153646	0.990182	0.275228
P02808	1	1	97.78	0.133391	0.990182	0.308579
O15303	1	1	21.59	0.017938	0.828711	0.879573
C9JW96	9	9	790.31	0.148825	0.990182	0.282543
Q6NVU6	1	1	16.74	0.087667	0.990182	0.420794